Design of a multifunctionalizable BODIPY platform for the facile elaboration of a large series of gold(I)-based optical theranostics

Jacques Pliquett,[a,b] Souheila Amor,[a] Miguel Ponce-Vargas,[a] Myriam Laly,[a] Cindy Racoeur,[b] Yoann Rousselin,[a] Franck Denat,[a] Ali Bettaïeb,[b] Paul Fleurat-Lessard,[a] Catherine Paul,*[b] Christine Goze,*[a] and Ewen Bodio*[a]

a. ICMUB UMR6302, CNRS, Univ. Bourgogne Franche-Comté, F-21000 Dijon, France. Tel: +33 (0)3 80 39 60 76; Email: ewen.bodio@u-bourgogne.fr; christine.goze@u-bourgogne.fr

b. Laboratoire d'Immunologie et Immunothérapie des Cancers, EPHE, PSL Research University, 75000, Paris, France; LIIC, EA7269, Université de Bourgogne Franche Comté, 21000, Dijon, France.

Content

General information

Unless stated otherwise reactions were carried out in technical grade solvents under normal atmosphere. Technical grade solvents were purchased from BioSolve. Dry solvents were non-stabilized, purchased from Carlo Erba and dried using a MB-SPS-800 (MBraun) or PureSolv-MD-5 (Inert®). All reagents were purchased from SigmaAldrich or ACROS Organics™ and used as received without further purification. Column chromatography was carried out using silica gel (SigmaAldrich; 40-63µm 230-400mesh 60Å). Analytical thin-layer chromatography was performed with Merck 60 F254 silica gel (precoated sheets, 0.2 mm thick). Reactions were monitored by thin-layer chromatography, RP-HPLC-MS and no-lock ^{31}P-NMR.

Synthetic procedure + NMR spectra

Gold(I)-amino-phosphine, BODIPY derivatives **1** and **2**, were synthesized thanks to reported procedures.[1-3]

NMR spectra: (^{1}H, ^{13}C, ^{11}B, ^{19}F) were recorded at 300K on Bruker 300 Avance III or 500 Avance III spectrometers. Chemical shifts are given relative to TMS (^{1}H, ^{13}C), BF_3*Et_2O (^{11}B), $CFCl_3$ (^{19}F) and H_3PO_4 (^{31}P) and were referenced to the residual solvent signal. High resolution mass spectra were recorded on a Thermo LTQ Orbitrap XL ESI-MS spectrometer. NMR and Mass-analyses were performed at the "Plateforme d'Analyse Chimique et de Synthèse Moléculaire de l'Université de Bourgogne" (PACSMUB).

Triphenylphosphonium-ethylammonium dibromide

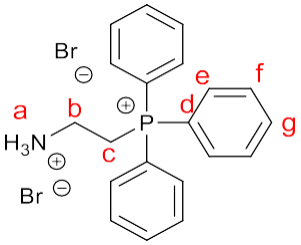

2g (7.63mmol, 1eq) PPh_3 and 1.562g (7.63mmol, 1eq) bromoethylamine hydrobromide were dissolved in 150 mL acetonitrile and refluxed for 72h. The reaction was stopped upon total consumption of PPh_3. Acetonitrile was evaporated and the crude product redissolved in 10 mL of MeOH. The product was crushed out with ice-cold Et_2O (300 mL). The solid was collected and the washing repeated twice to obtain 1.771g (3.82 mmol, yield = 50%) of the target compound as a white powder.

^{1}H NMR (500 MHz, DMSO-d_6) δ (ppm) = 3.13 – 3.07 (m, 2H), 4.05 – 3.97 (m, 2H), 7.80 (td, *J* = 7.8, 3.7 Hz, 6H), 7.86 (ddd, *J* = 13.0, 8.5, 1.4 Hz, 6H), 7.94 (td, *J* = 7.3, 1.8 Hz, 3H), 8.36 (s, 3H).

^{31}P NMR (202 MHz, DMSO-d_6) δ (ppm) = 21.39 (s).

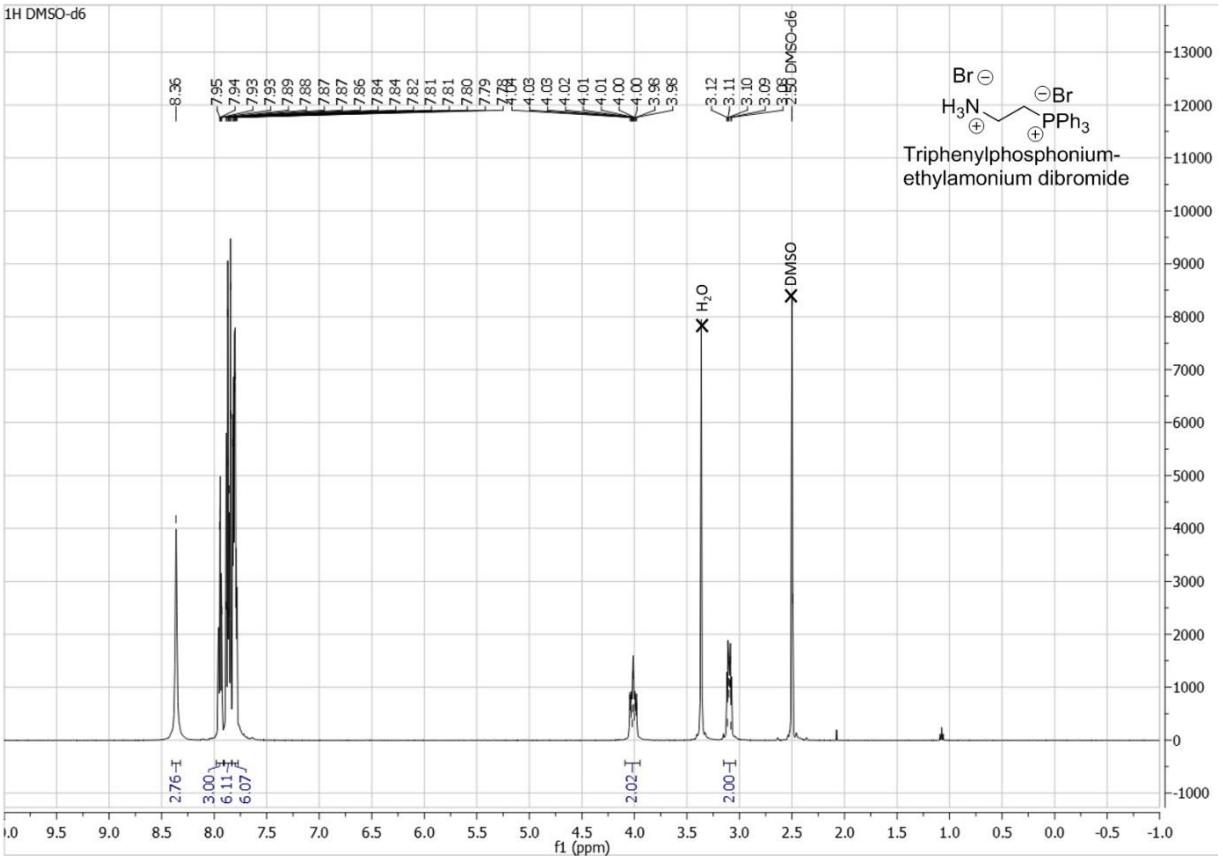

Figure S 1: ^{1}H NMR of 2-(Diphenylphosphino)ethylamine-aurichloride ($CDCl_3$, 126 MHZ, 300K)

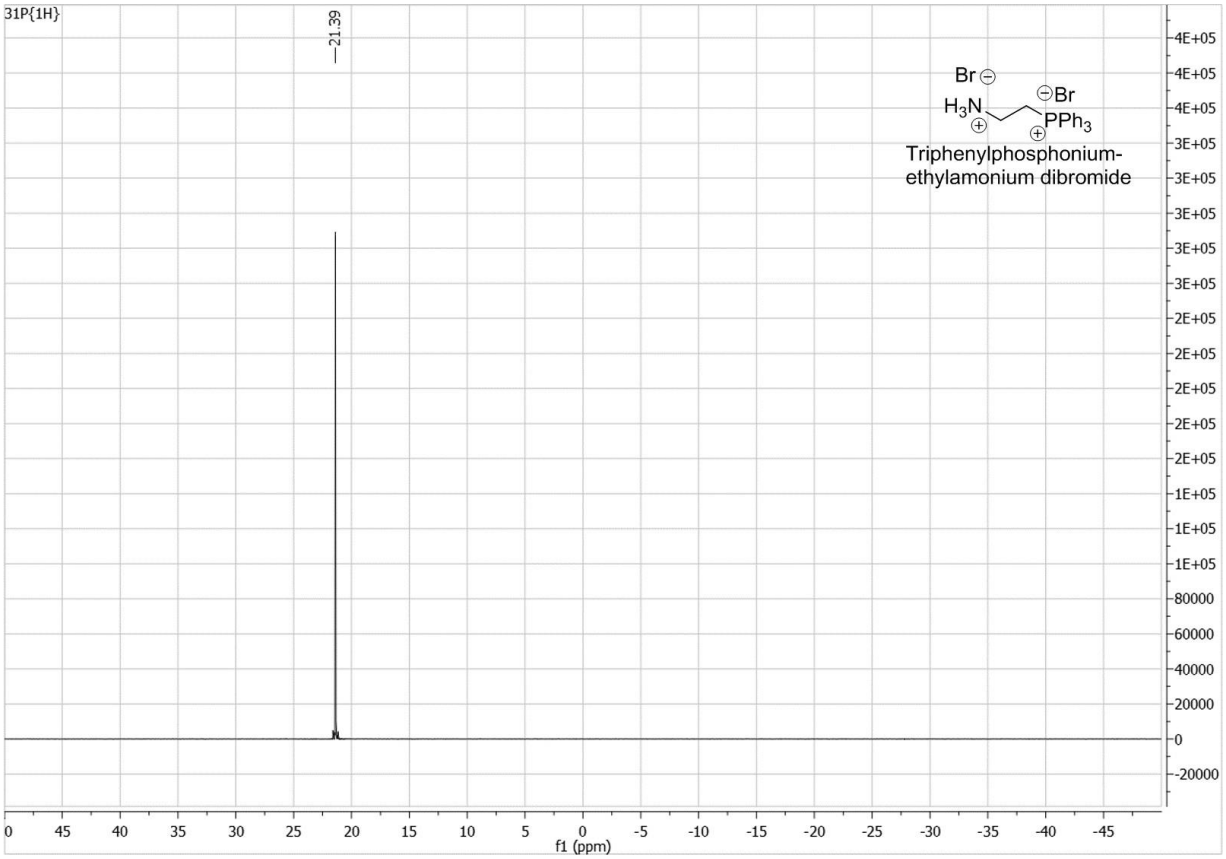

Figure S 2: ^{31}P NMR of 2-(Diphenylphosphino)ethylamine-aurichloride ($CDCl_3$, 202 MHZ, 300K)

BODIPY 3

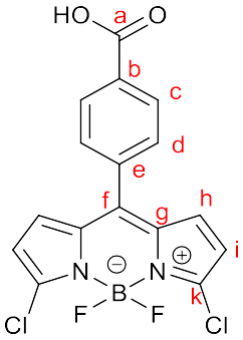

0.5 g (1.27 mmol) of BODIPY **2** were placed into a 100 mL round-bottom flask and dissolved in THF (20 mL). 20 mL of 3M HCl were added and the mixture refluxed for 60h. Upon completion of the reaction the solvents were removed under reduced pressure, and the crude product was purified by column chromatography on silica gel column (eluent: DCM → DCM/MeOH 95: 5). The resulting product was dissolved in a minimal amount of DCM and crushed out with Pentane to obtain 0.2603 g of the target compound as a dark red solid (0.686 mmol, yield = 54%).

^{1}H NMR (500 MHz, DMSO-D6) δ (ppm)= 6.80 (d, ^{3}J = 4.6 Hz, 2H, H_i), 7.08 (d, ^{3}J = 4.4 Hz, 2H, H_h), 7.76 (dt, ^{3}J = 8.5Hz, ^{4}J =3.5 Hz, 2H, H_d), 8.12 (dt, ^{3}J = 8.5Hz, ^{4}J =3.5 Hz, 2H, H_c).

^{13}C NMR(126 MHz, DMSO-D6) δ (ppm) = 119.7 (C_i), 129.2 (deprotonated form, C_d), 129.4 (C_d), 130.5 (deprotonated form, C_c), 131.0 (C_c), 132.8 (C_h), 133.0(C_g), 133.1(C_f), 135.4 (C_b), 143.1(C_e), 143.9(C_k), 166.7 (C_a), 167,1 (C_a, deprotonated form).

^{11}B NMR (160 MHz, DMSO-D6) δ (ppm)= 0.30 (t, $J_{B\text{-}F}$ = 28.1 Hz).

^{19}F NMR (470 MHz, DMSO-D6) δ (ppm)= -145.75 (dd, $J_{F\text{-}F}$ = 56.3, $J_{F\text{-}B}$ = 28.0 Hz).

HR-MS (ESI): *m/z* = calculated for $C_{16}H_9B_1Cl_2F_2N_2O_2Na$ $[M+Na]^+$ 402.99944; found 403.00080.

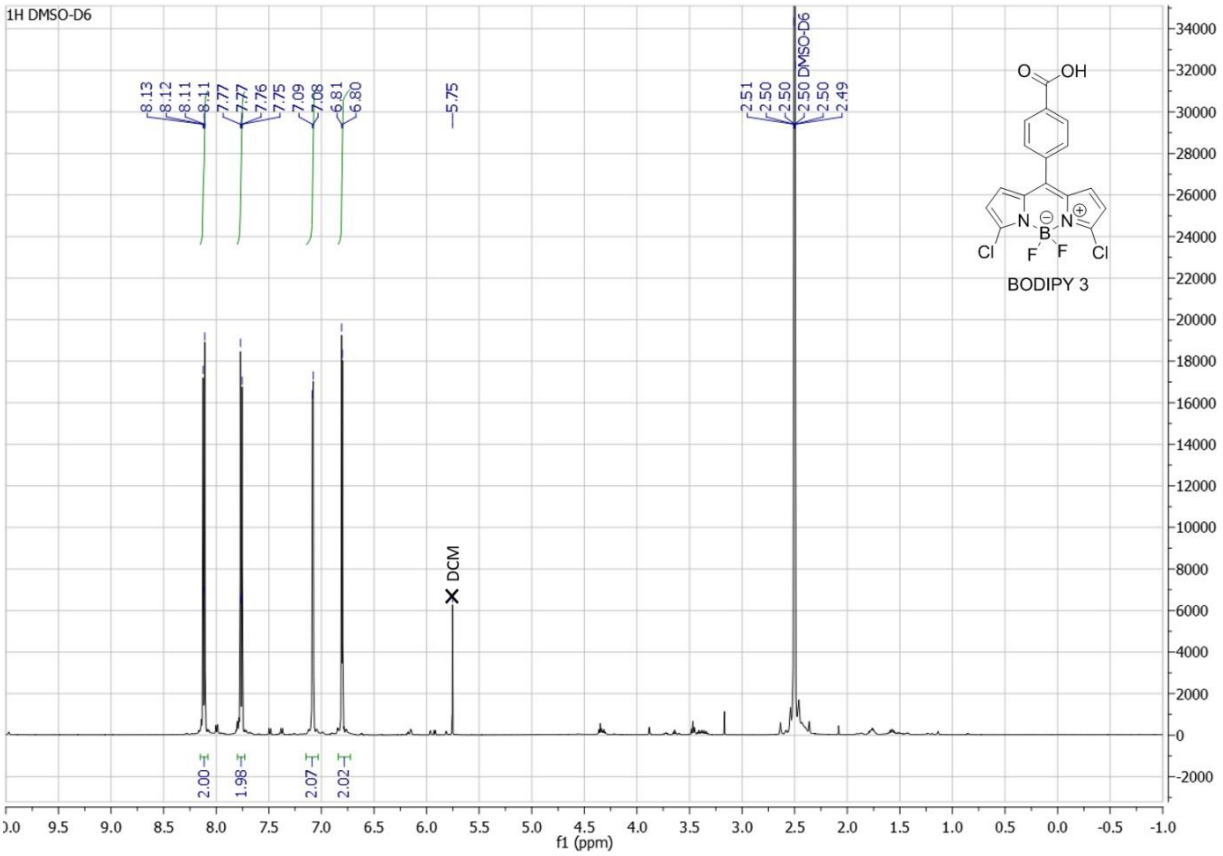

Figure S 3: ^{1}H NMR of BODIPY 3 (DMSO, 500 MHZ, 300K)

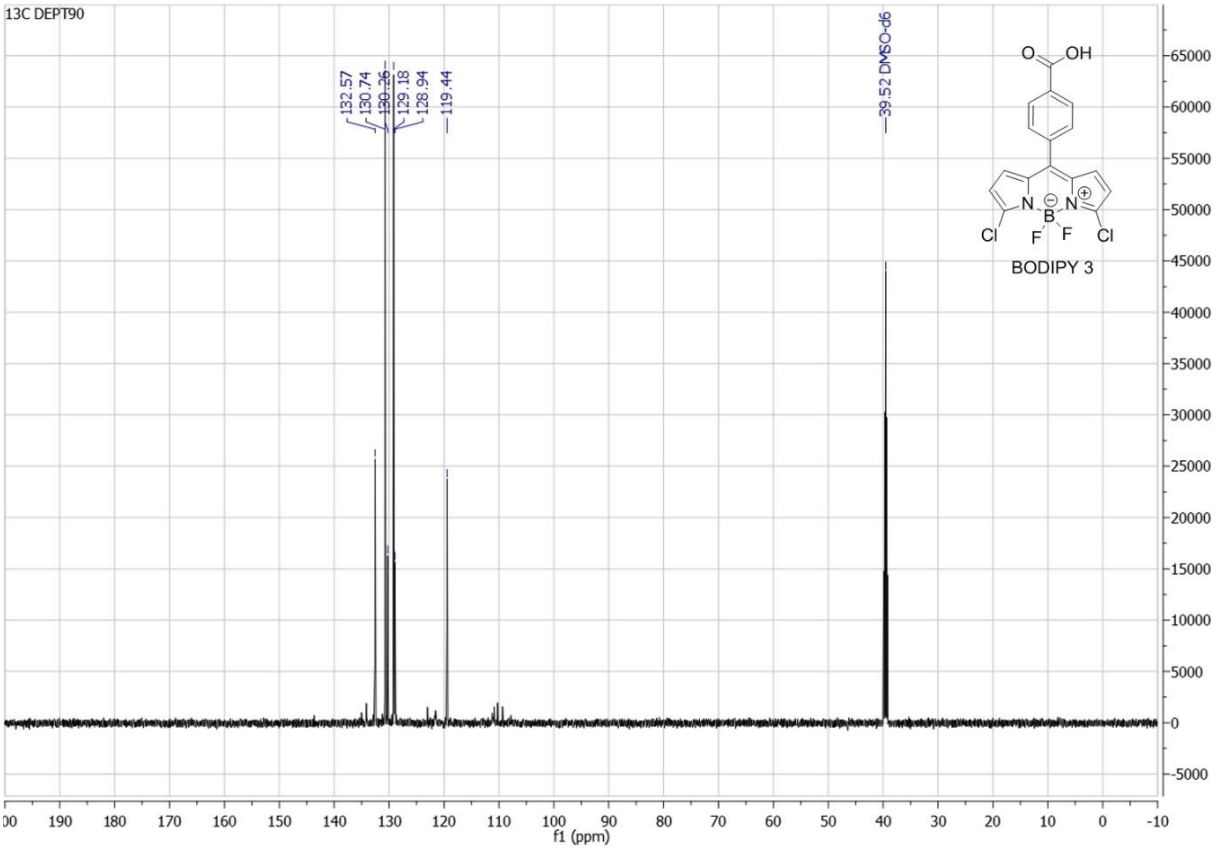

Figure S 4: ^{13}C NMR (DEPT90) of BODIPY **3** (DMSO, 126 MHZ, 300K)

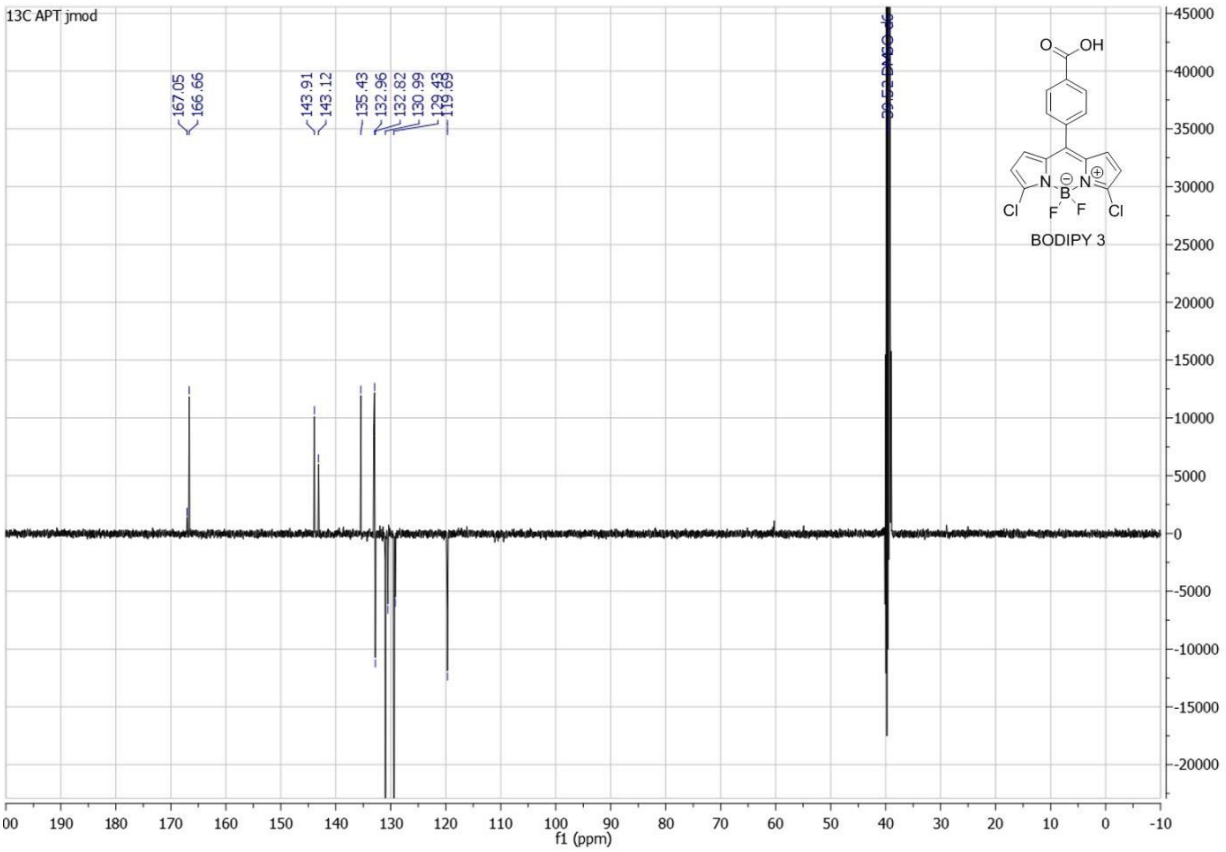

Figure S 5: ^{13}C NMR (APT jmod) of BODIPY **3** (DMSO, 126 MHZ, 300K)

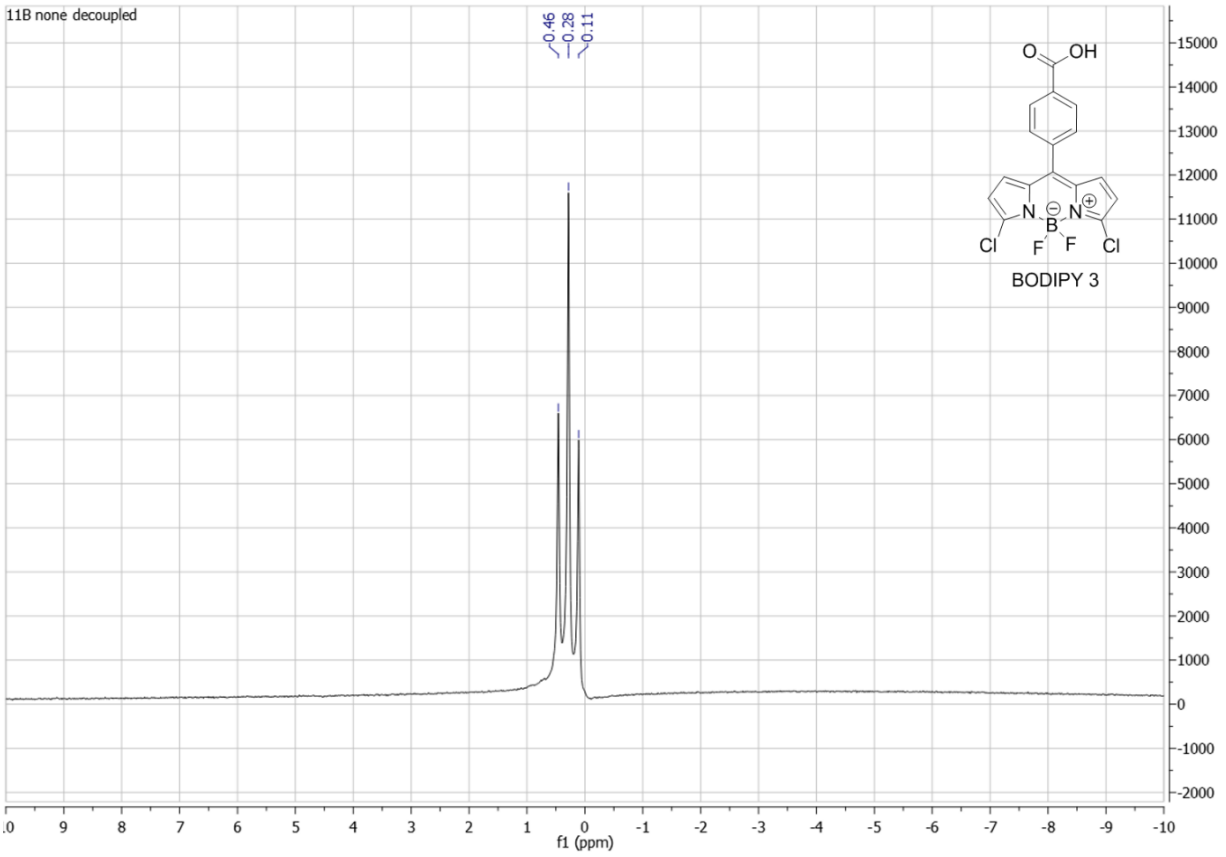

Figure S 6: ^{11}B NMR of BODIPY **3** (DMSO, 160 MHZ, 300K)

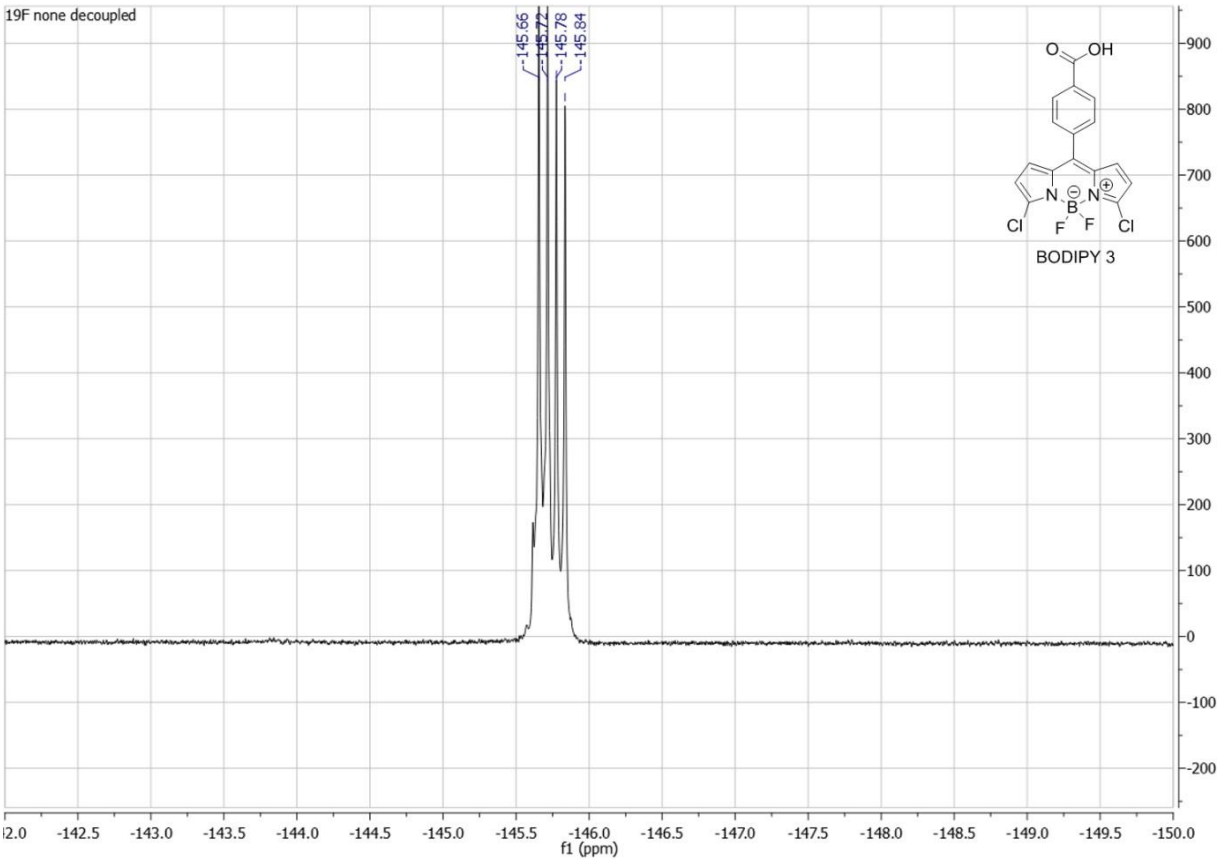

Figure S 7: ^{19}F NMR of BODIPY **3** (DMSO, 470 MHZ, 300K)

BODIPY 3-acid chloride

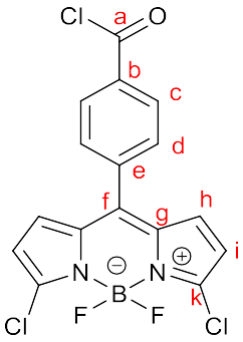

51mg (0.13mmol, 1eq) of BODIPY **3** and 73mg (50.3mmol, 4eq) of K_2CO_3 were placed into a 50 mL round bottom flask and dissolved in 30 mL DCM under argon. 23 µL (0.26mmol, 2eq) of oxalyl chloride were added, followed by a droplet of DMF. The reaction was stirred at room temperature for 45min. The solvents were evaporated under reduced pressure to yield the target compound quantitatively as a pink solid. The crude product was directly engaged in the next reaction without any further purification.

^{1}H NMR (300 MHz, $CDCl_3$) δ (ppm) = 6.47 (d, ^3J = 4.4 Hz, 2H, H_i), 6.77 (d, ^3J = 4.1 Hz, 2H, H_h), 7.66 (d, ^3J = 8.6 Hz, 2H, H_d), 8.28 (d, ^3J = 8.6 Hz, 2H, H_c).

^{11}B NMR (96 MHz, $CDCl_3$) δ (ppm) = 0.45 (t, J_{B-F} = 27.6 Hz).

^{19}F NMR (282 MHz, $CDCl_3$) δ (ppm) = -148.14 (dd, J_{F-F} = 55.2 Hz, J_{F-B} = 27.7 Hz).

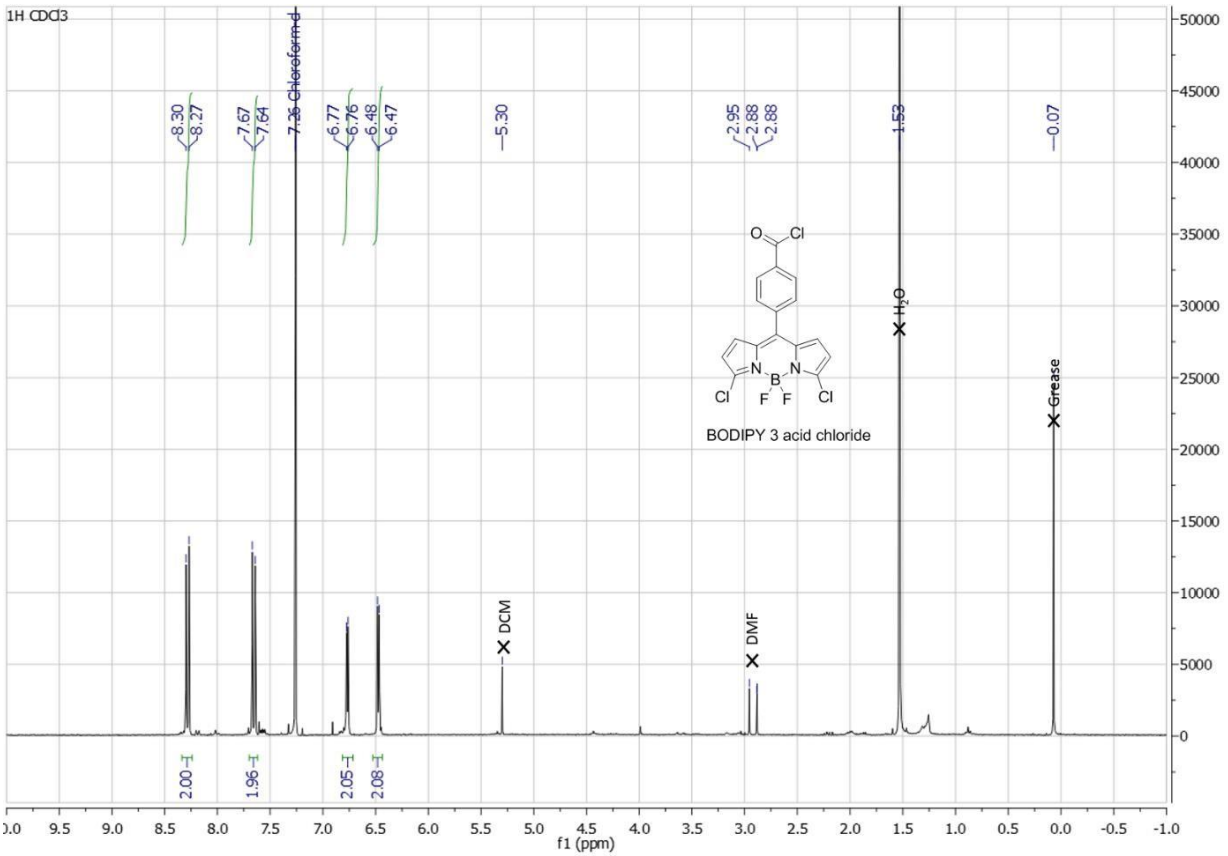

Figure S 8: ^{1}H NMR of BODIPY **3** acid chloride (CDCl3, 300 MHZ, 300K)

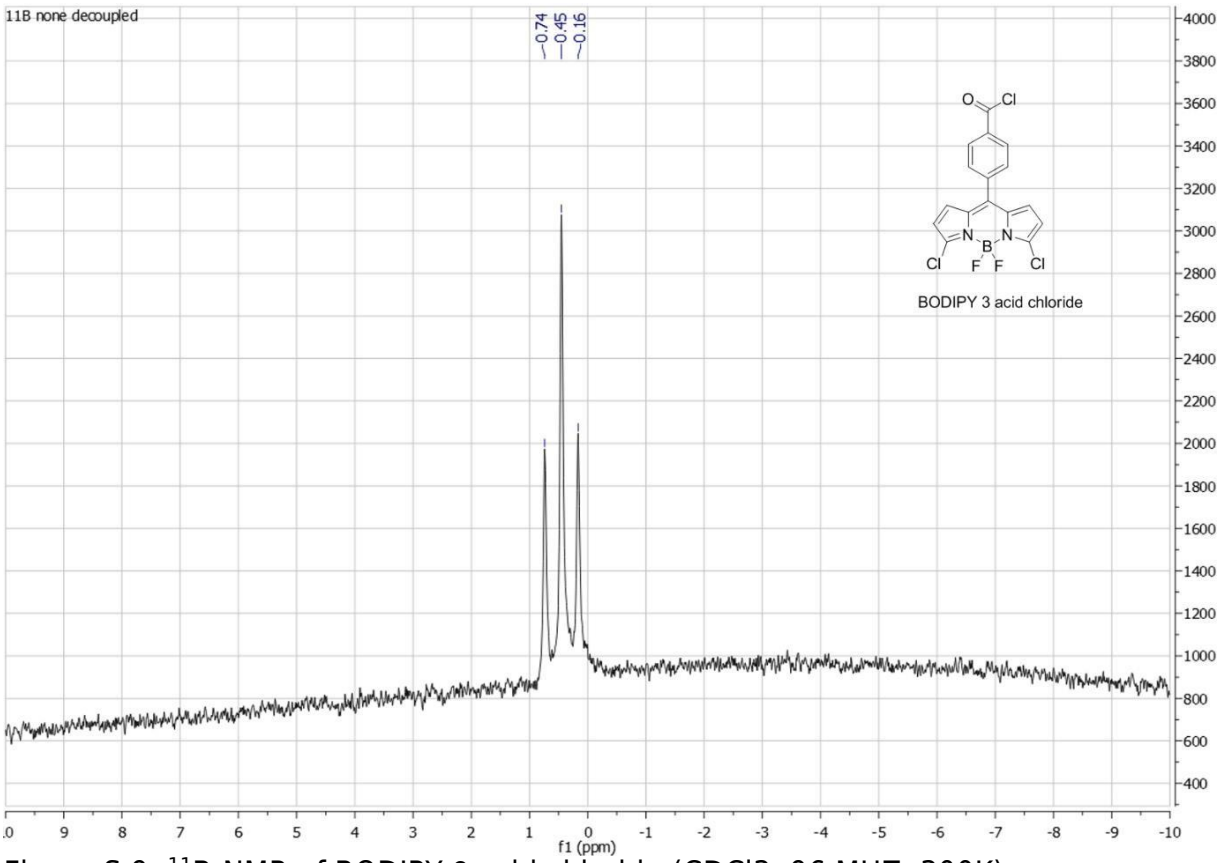

Figure S 9: ^{11}B-NMR of BODIPY **3** acid chloride (CDCl3, 96 MHZ, 300K)

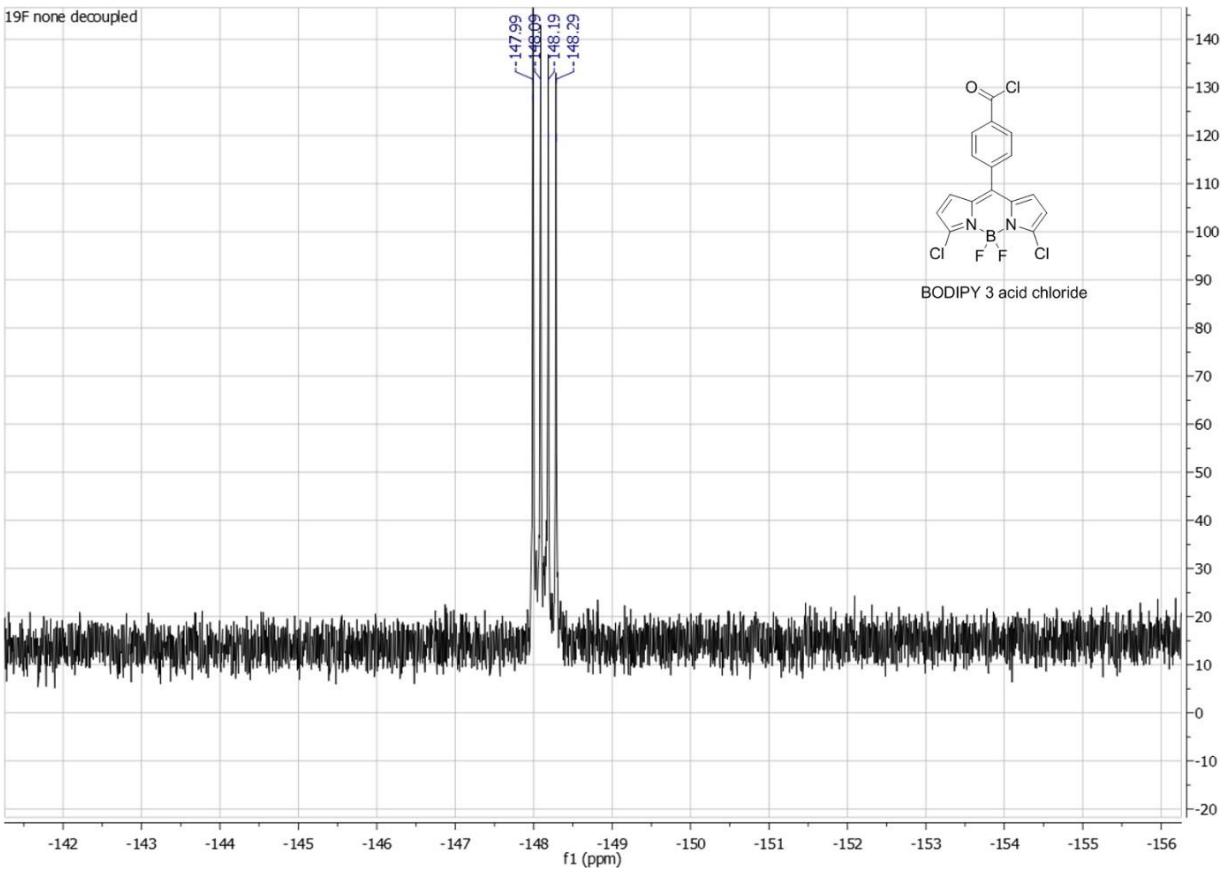

Figure S 10: ^{19}F NMR of BODIPY **3** acid chloride (CDCl3, 282 MHZ, 300K)

BODIPY 4

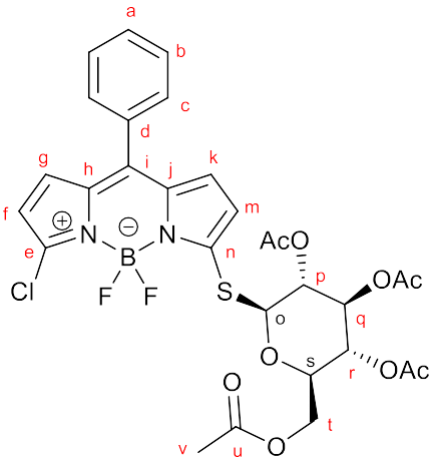

100mg of β-thioglucose-tetraacetate (0.274mmol, 0.95eq) were dissolved in acetone (2mL). 27.4 µL of 1M NaOH were added and the resulting solution stirred for 15min at room temperature. In a separate flask 97.5mg (0.289mmol, 1eq) BODIPY **1** and 48mg $NaHCO_3$ (0.578mmol, 2eq) were dissolved in acetone (10 mL). The thioglucose-tetraacetate solution was added over the course of 1h30 at room temperature, followed by stirring for another 90min at room temperature. The solvents were then evaporated and the crude product was purified by column chromatography on silica gel, using CH_2Cl_2 to CH_2Cl_2/MeOH 99:1 as eluent. Product fractions were evaporated to dryness. The resulting product was dissolved in a minimal amount of DCM and crushed out with Pentane to obtain 80.9mg (0.121 mmol, yield = 44%) of pure BODIPY **4** as a bright pink powder.

^{1}H NMR (500 MHz, DMSO-D6) δ (ppm)= 1.99 , 2.01, 2.02, 2.05 (4x s, 4x 3H, H_v), 4.08 (dd, J = 12.3, 2.0 Hz, 1H, H_t), 4.17 (dd, J = 12.4, 5.9 Hz, 1H, H_t), 4.30 (ddd, J = 10.0, 5.8, 2.2 Hz, 1H, H_s), 5.07 (t, J = 9.8 Hz, 1H, H_p), 5.15 (t, J = 9.7 Hz, 1H, H_r), 5.47 (t, J = 9.4 Hz, 1H, H_q), 5.83 (d, J = 10.1 Hz, 1H, H_o), 6.63 (d, J = 4.2 Hz, 1H, H_m), 6.83 (d, J = 4.1 Hz, 1H, H_k), 6.94 (d, J = 4.6 Hz, 1H, H_f), 7.16 (d, J = 4.5 Hz, 1H, H_g), 7.63 – 7.57 (m, 4H, H_b, H_c), 7.66 (m, 1H, H_a).

^{13}C NMR (126 MHz, DMSO-D6) δ (ppm) = 20.2 (C_v), 20.2 (C_v), 20.3 (C_v), 20.5 (C_v), 61.8 (C_t), 67.8 (C_r), 69.2 (C_q), 72.6 (C_p), 74.8 (C_s), 80.8 (C_o), 117.3 (C_f), 120.6 (C_m), 128.7 (C_g), 129.2 (C_k), 130.5 (C_a), 130.8 (C_b), 132.1 (C_h), 132.5(C_j), 133.2 (C_c), 135.7 (C_i), 138.7 (C_d), 141.1 (C_e), 157.0 (C_n), 169.1 (C_u), 169.3 (C_u), 169.6 (C_u), 170.0 (C_u).

^{11}B NMR (160 MHz, DMSO-D6) δ (ppm)= 0.37 (t, J = 30.3 Hz).

^{19}F NMR (470 MHz, DMSO-D6) δ (ppm)= -145.54 (dddd, J = 95.4, 91.6, 60.5, 30.2 Hz).

HR-MS (ESI): m/z = calculated for $C_{29}H_{28}B_1Cl_1F_2N_2O_9S_1Na_1$ [M+Na]$^+$ 687.11574; found 687.11699.

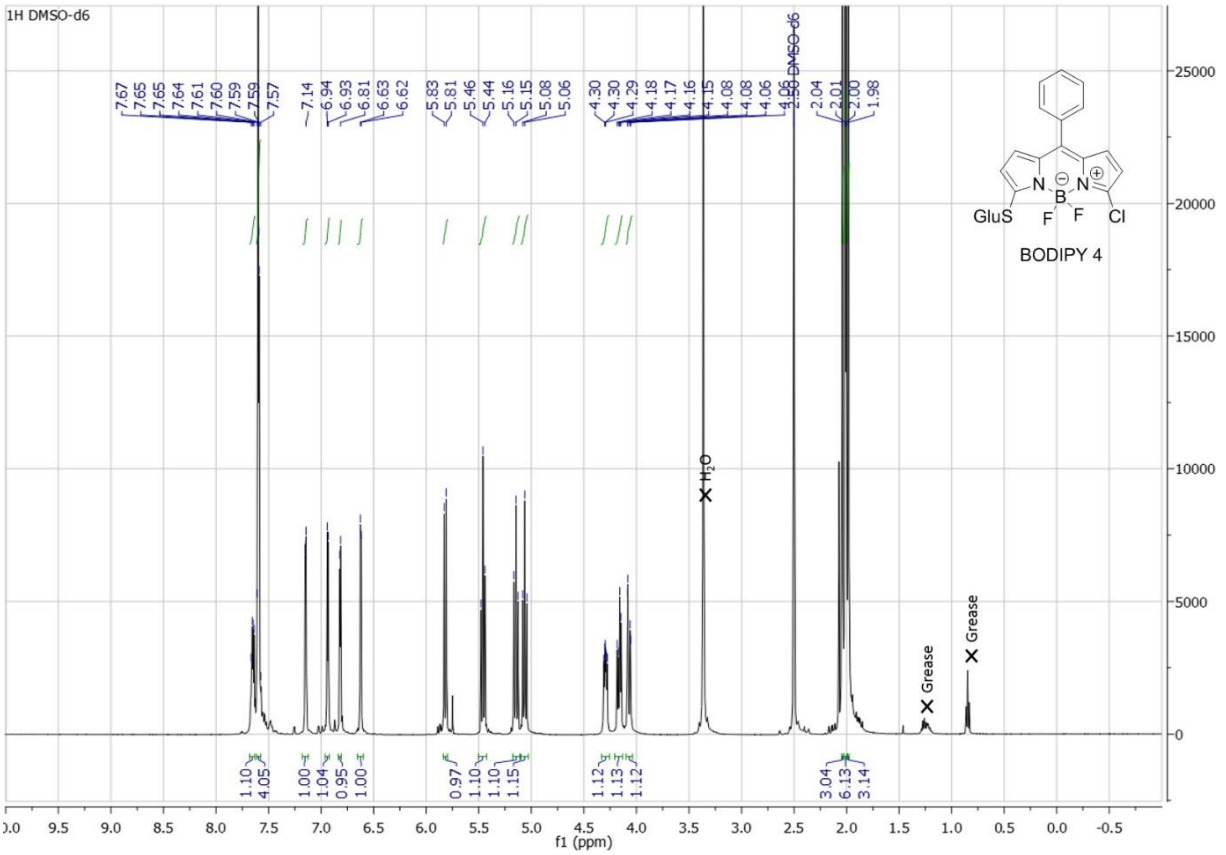

Figure S 11: ^{1}H NMR of BODIPY **4** (DMSO, 500 MHZ, 300K)

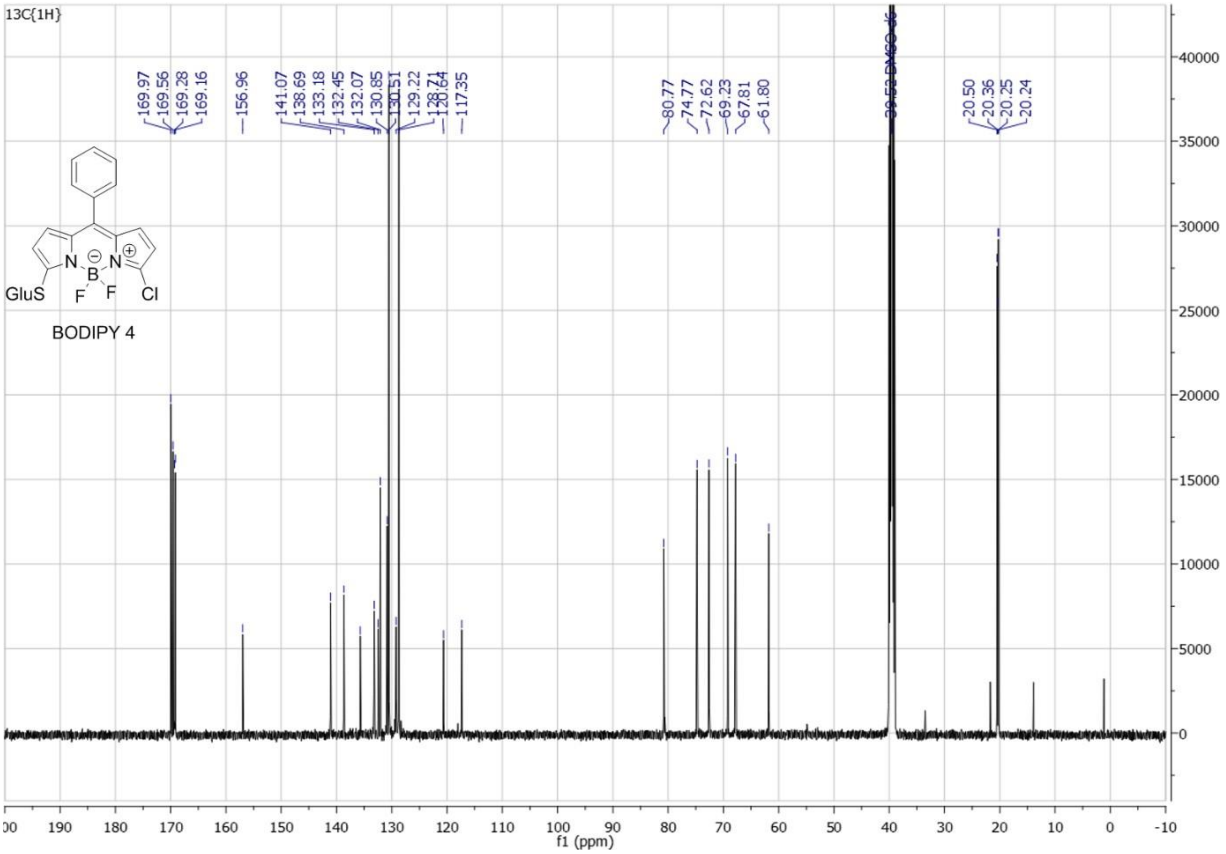

Figure S 12: ^{13}C NMR of BODIPY **4** (DMSO, 126 MHZ, 300K)

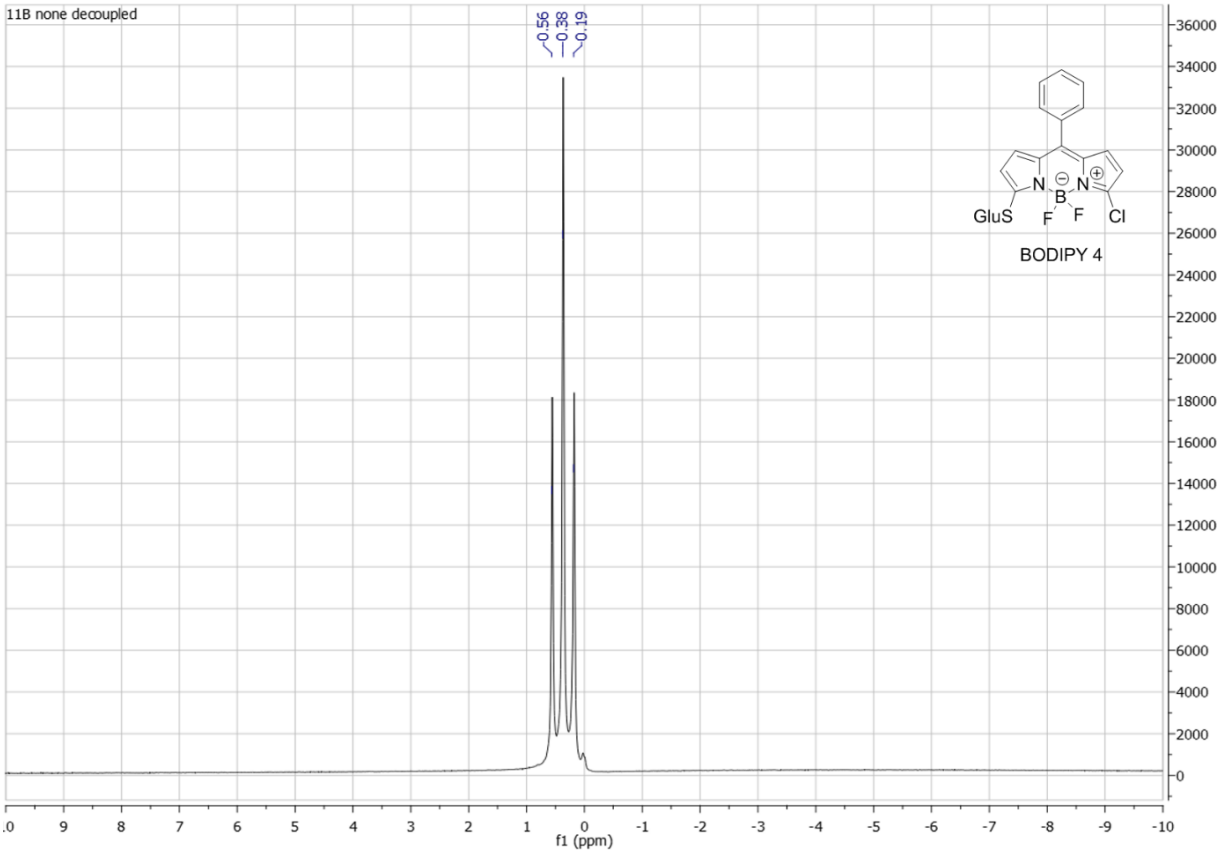

Figure S 13: ^{11}B NMR of BODIPY **4** (DMSO, 160 MHZ, 300K)

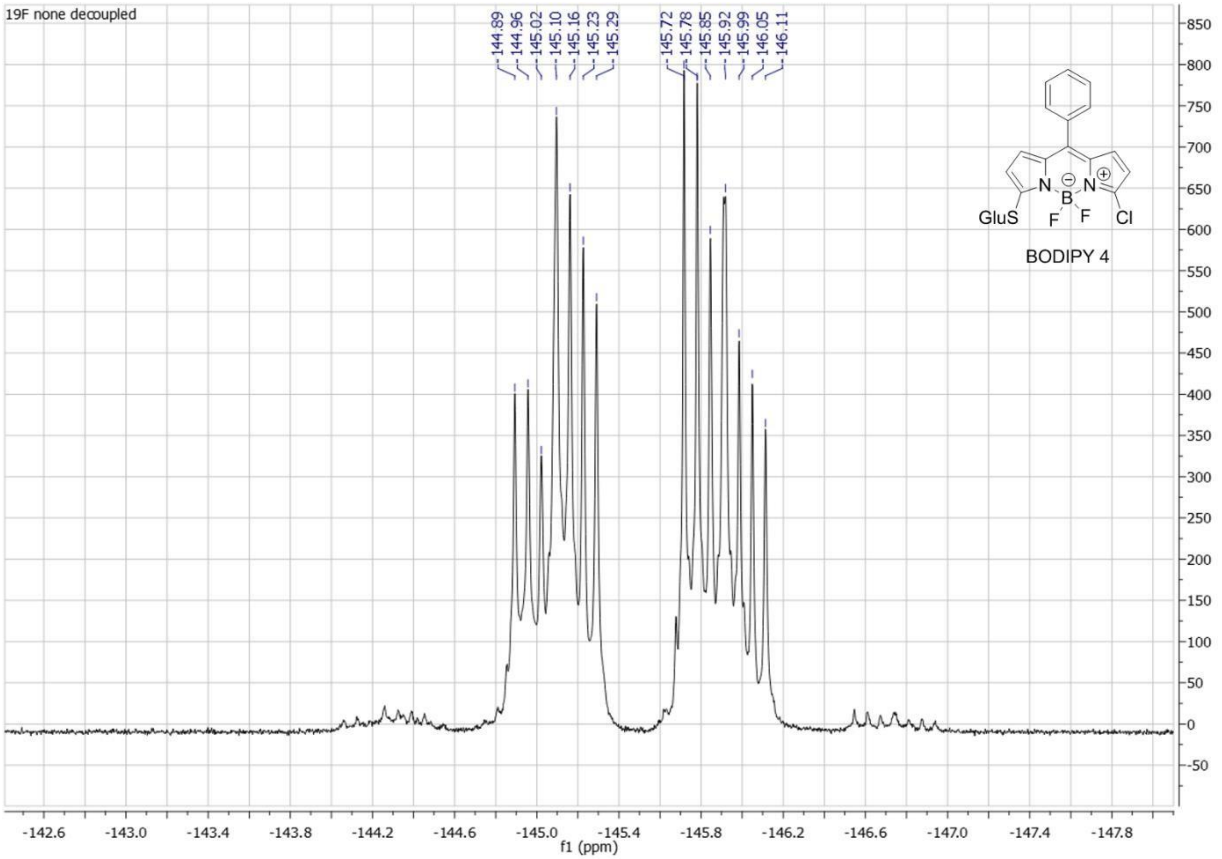

Figure S 14: ^{19}F NMR of BODIPY **4** (DMSO, 470 MHZ, 300K)

BODIPY 5

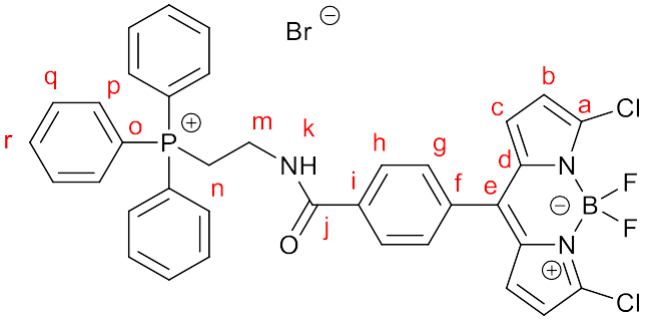

100mg (0.262mmol, 1eq) of BODIPY **3** were dissolved in 15 mL CH_2Cl_2. 45 µL (0.525mmol, 2eq) oxalyl chloride and a droplet of DMF were added (vigorous development of gas) and the solution stirred for 1h at room temperature. Solvents were then evaporated and the solid redissolved in 20 mL acetonitrile. 110mg (1.31mmol, 5eq) of $NaHCO_3$ and 122.6mg (0.262mmol, 1eq) of triphenylphosphonium-ethylammonium dibromide were added and the resulting mixture was refluxed for 1h. Upon completion of the reaction, the crude product was purified by column chromatography on silica gel, using CH_2Cl_2/MeOH (95:5) as eluent. The resulting product was dissolved in a minimal amount of DCM and crushed out with Pentane to yield pure BODIPY **5** (110mg, 0.147mmol, yield = 56%) as a pink powder.

^{1}H NMR (500 MHz, DMSO-D6) δ (ppm) = 3.70 – 3.60 (m, 2H, H_n), 3.95 – 3.86 (m, 2H, H_m), 6.83 (d, J = 4.4 Hz, 2H, H_b), 7.03 (d, J = 4.4 Hz, 2H, H_h), 7.81 – 7.73 (m, 8H, H_g, H_p), 7.95 – 7.86 (m, 11H, H_h, H_q, H_r), 9.12 (s 1H, H_k).

^{13}C NMR (126 MHz, DMSO-D6) δ (ppm) = 20.8 (d, J = 49.6 Hz, C_m), 33.4 (d, J = 12.6 Hz, C_n), 118.3 (dd, J = 86.1, 7.9 Hz, C_o), 119.7 (s, C_b), 127.4 (s, C_c), 130.2 (dd, J = 12.6, 3.2 Hz, C_r), 130.8 (s, C_h), 132.7 (s, C_g), 133.1 (s, C_i), 133.7 (d, J = 10.4 Hz, C_q), 134.3 (s, C_d), 135.0 (t, J = 3.8 Hz, C_p), 135.6 (s, C_e), 143.2 (s, C_f), 143.8 (s, C_a), 165.5 (s, C_j).

^{11}B NMR (160 MHz, DMSO-D6) δ (ppm) = 0.30 (t, J = 28.0 Hz).

^{19}F NMR (470 MHz, DMSO-D6) δ (ppm) = -145.77 (dd, J = 56.1, 28.0 Hz).

^{31}P NMR (202 MHz, DMSO-D6) δ (ppm) = 21.33 (s).

HR-MS (ESI): *m/z* = calculated for $C_{36}H_{28}B_1Cl_2F_2N_3O_1P_1$ $[M]^+$ 668.14027; found 668.13955.

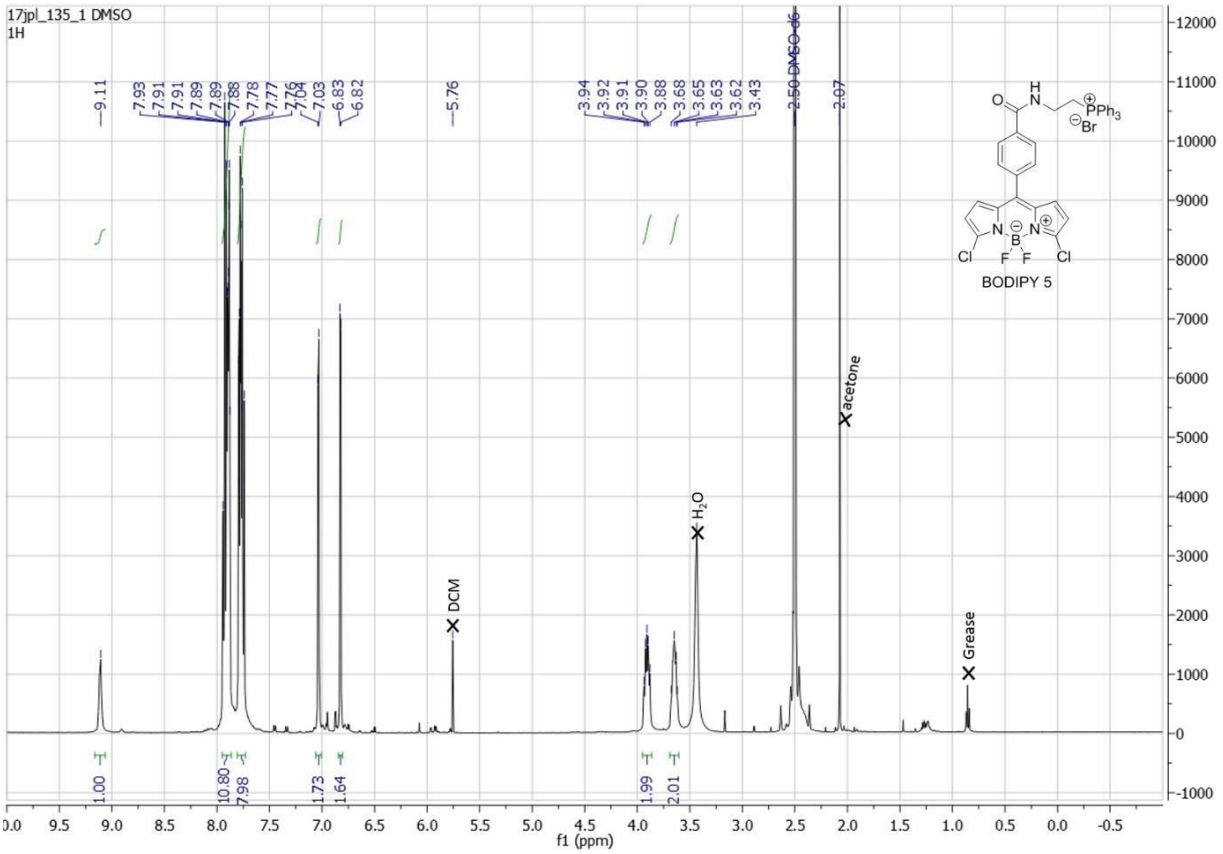

Figure S 15: ^{1}H NMR of BODIPY **5** (DMSO, 500 MHZ, 300K)

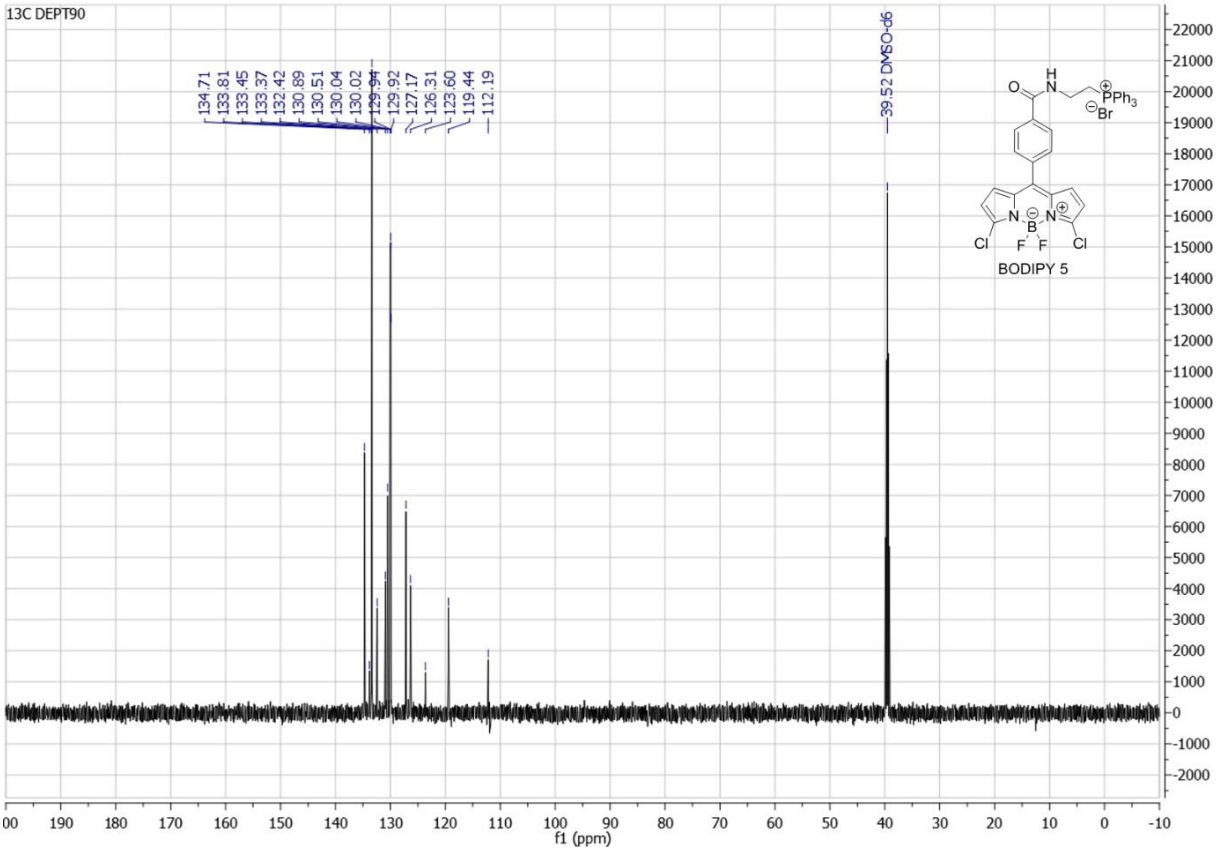

Figure S 16: ^{13}C NMR (DEPT90) of BODIPY **5** (DMSO, 126 MHZ, 300K)

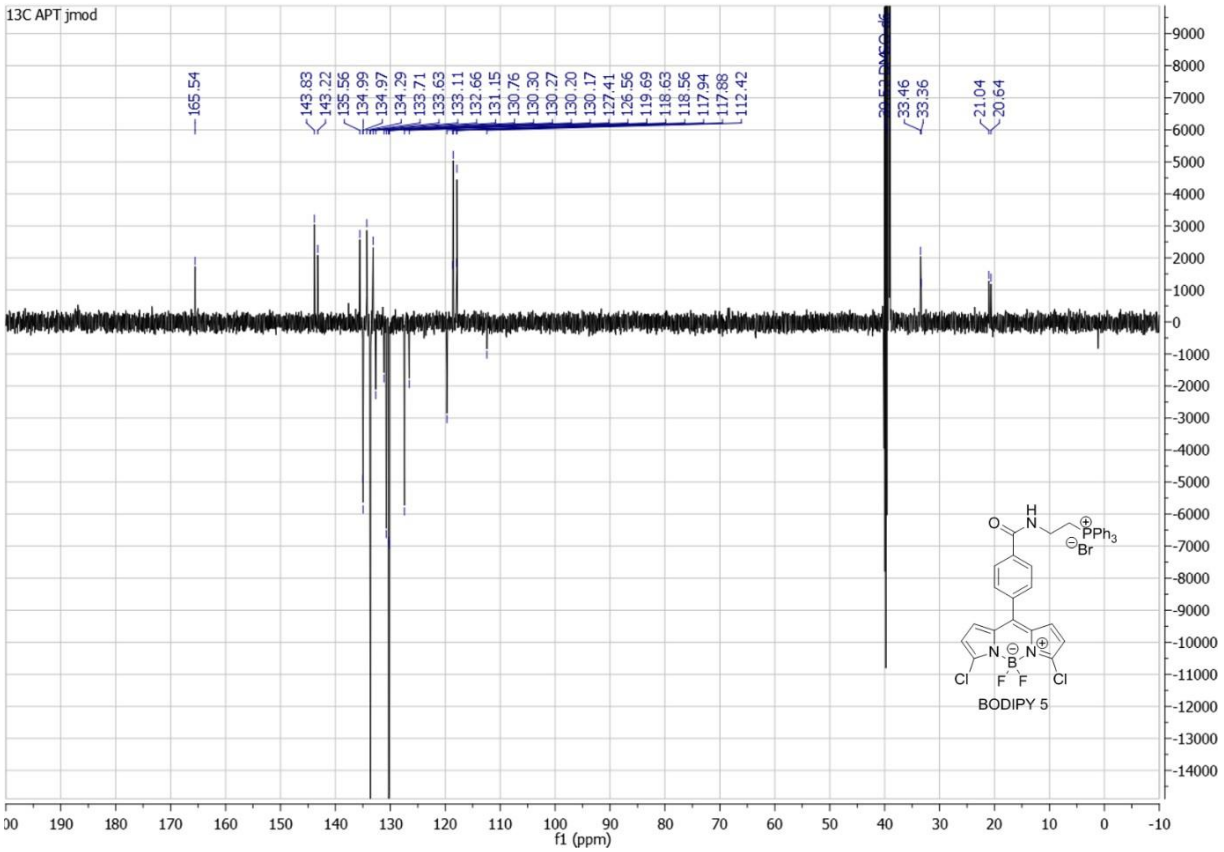

Figure S 17: ^{13}C NMR (APT jmod) of BODIPY **5** (DMSO, 126 MHZ, 300K)

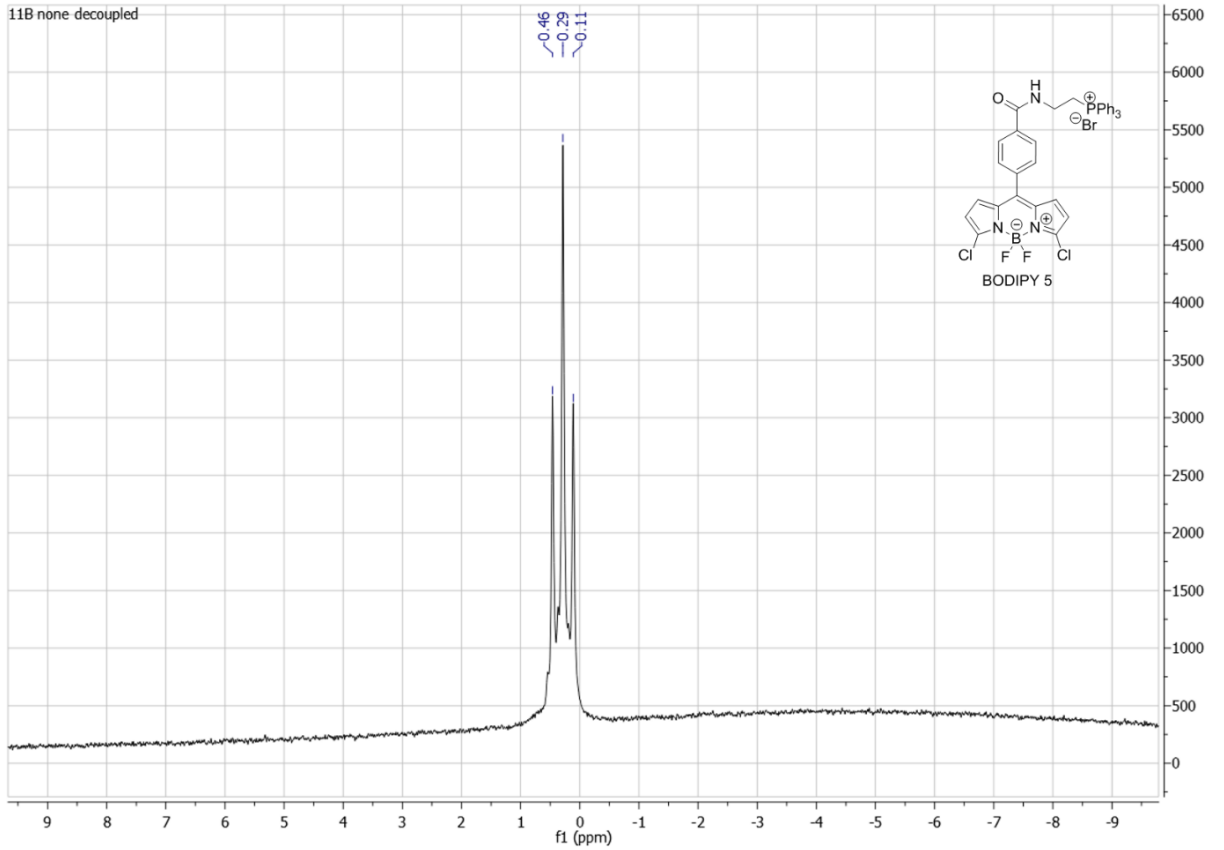

Figure S 18: ^{11}B NMR of BODIPY **5** (DMSO, 160 MHZ, 300K)

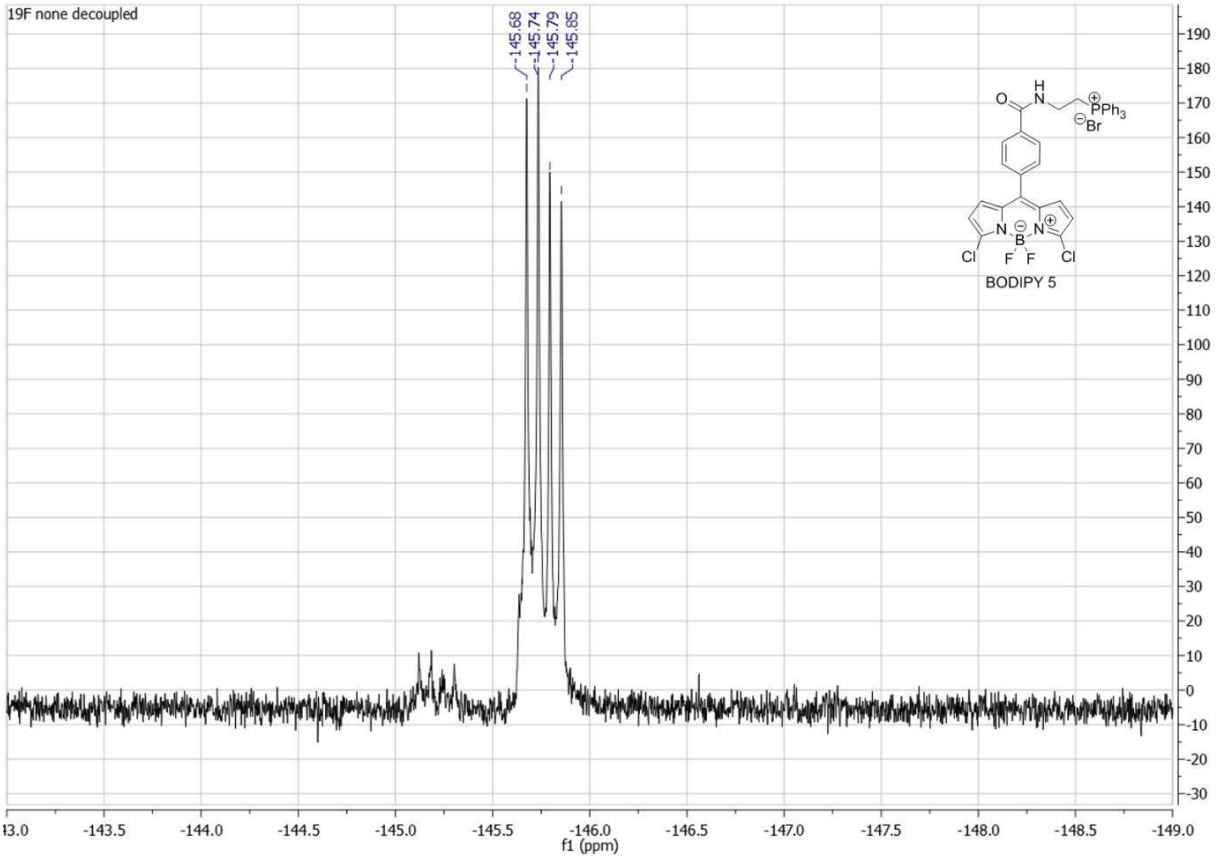

Figure S 19: ^{19}F NMR of BODIPY **5** (DMSO, 470 MHZ, 300K)

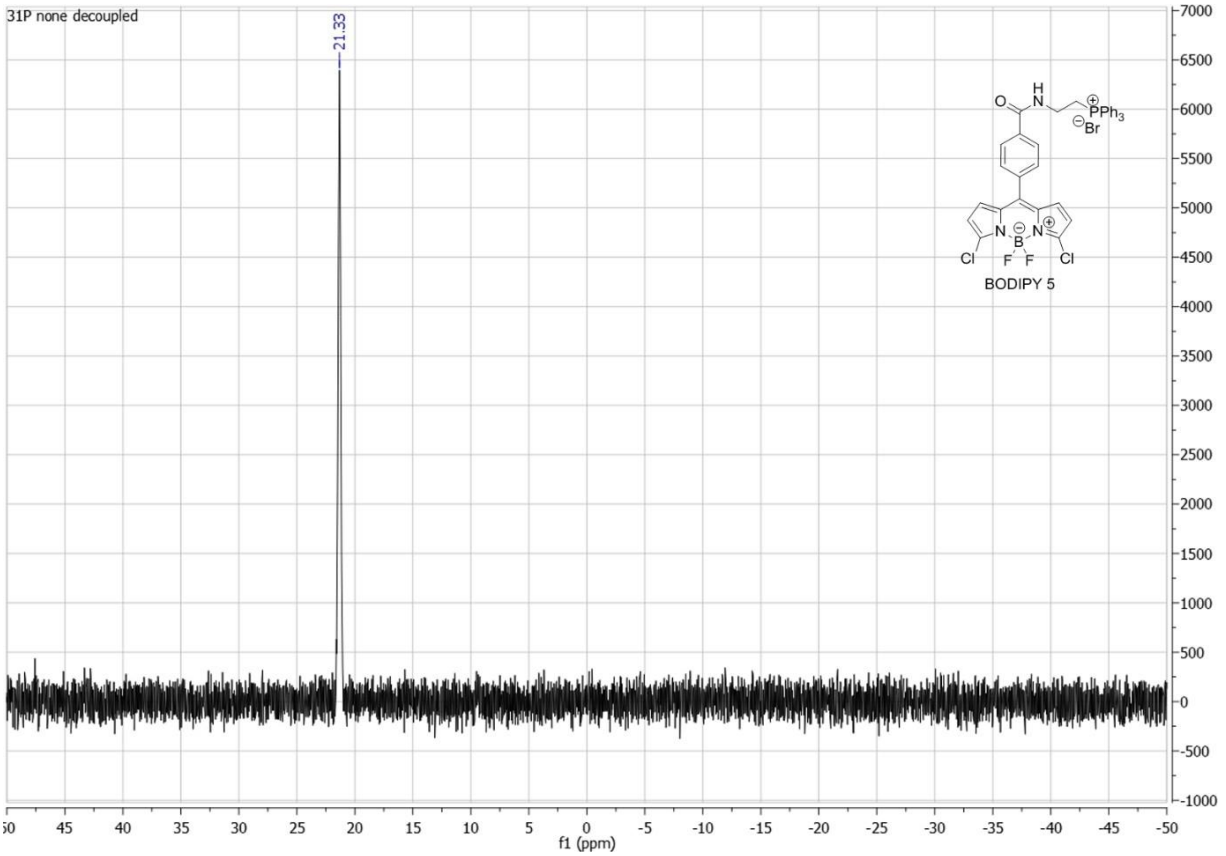

Figure S 20: ^{31}P NMR of BODIPY **5** (DMSO, 202 MHZ, 300K)

BODIPY 6

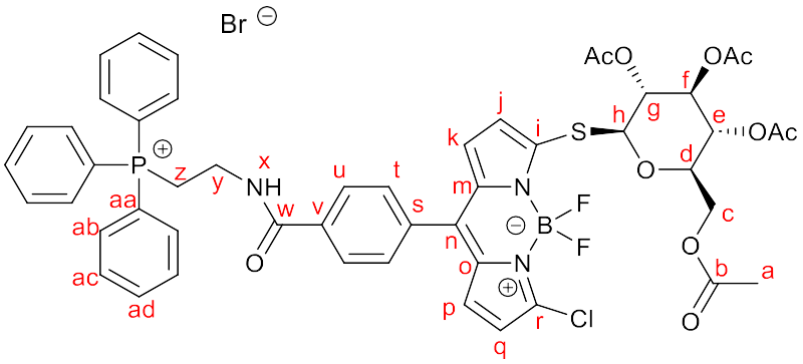

23.1mg (0.0634mmol, 0.95eq) of β-thioglucose-tetraacetate were dissolved in 4 mL of acetone. 63.4 µL of 1M NaOH were added, and the resulting mixture was stirred for 15min at room temperature. 50mg (0.066mmol, 1eq) BODIPY **5** and 17mg (0.2mmol, 3eq) $NaHCO_3$ were placed in a roundbottom flask and dissolved in 50 mL acetone. The thioglucose solution was added over the course of 1h30 and stirred for another hour at room temperature. The crude product was purified by column chromatography on silica gel, using CH_2Cl_2: MeOH (98:2 → 95:5+1% formic acid) as eluent. The resulting product was dissolved in a minimal amount of DCM and crushed out with Pentane to obtain 50mg (44.38 µmol, yield = 70%) of the pure BODIPY **6** as a bright pink powder.

^{1}H NMR (500 MHz, DMSO-D6) δ (ppm)= 1.98 (s, 3H, H_a), 2.01 (d, J = 4.3 Hz, 6H, H_a), 2.04 (s, 3H, H_a), 3.66 (t, J = 15.3 Hz, 2H, H_y), 3.93 (dt, J = 10.4, 4.8 Hz, 2H, H_z), 4.07 (dd, J = 12.3, 2.0 Hz, 1H, H_c), 4.16 (dd, J = 12.4, 5.8 Hz, 1H, H_c), 4.30 (ddd, J = 10.0, 5.7, 2.3 Hz, 1H, H_d), 5.06 (t, J = 9.8 Hz, 1H, H_g), 5.15 (t, J = 9.7 Hz, 1H, H_e), 5.46 (t, J = 9.4 Hz, 1H, H_f), 5.83 (d, J = 10.1 Hz, 1H, H_h), 6.66 (d, J = 4.3 Hz, 1H_j), 6.81 (d, J = 4.2 Hz, 1H, H_k), 6.97 (d, J = 4.7 Hz, 1H, H_q), 7.13 (d, J = 4.6 Hz, 1H, H_p), 7.70 (d, J = 8.5 Hz, 2H, H_t), 7.77 (td, J = 8.0, 3.5 Hz, 6H, H_{ab}), 7.90 (ddd, J = 8.4, 7.9, 4.0 Hz, 9H, H_{ac}, H_{ad}), 7.96 (d, J = 8.3 Hz, 2H, H_u), 9.28 (t, J = 5.5 Hz, 1H, H_x)

^{13}C NMR (126 MHz, DMSO-D6) δ (ppm)= 20.2 (s, C_a), 20.3 (s, C_a), 20.4 (s, C_a), 20.5 (s, C_a), 20.9 (d, J = 48.9 Hz, C_y), 33.4 (d, J = 7.4 Hz, C_z), 61.8 (s, C_c), 67.8 (s, C_e), 69.2 (s, C_f), 72.6 (s, C_g), 74.8 (s, C_d), 80.7 (s, C_h), 117.5 (s, C_q), 118.3 (dd, J = 86.0, 5.9 Hz, C_{aa}), 121.0 (s, C_j), 127.0 (s, C_p), 127.4 (s, C_k), 130.2 (d, J = 12.6 Hz, C_{ad}), 130.6 (s, C_u), 132.3 (s, C_v), 133.7 (d, J = 10.4 Hz, C_{ac}), 134.7 (s, C_m) 135.0 (d, J = 2.9 Hz, C_{ab}), 135.2 (s, C_n), 135.6 (s, C_o), 139.0 (s, C_r), 139.8 (s, C_s), 157.6 (s, C_i), 165.6 (s, C_w), 169.1 (s, C_b), 169.3 (s, C_b), 169.6 (s, C_b), 170.0 (s, C_b).

^{11}B NMR (160 MHz, DMSO-D6) δ (ppm)= 0.36 (t, J = 30.2 Hz).

^{19}F NMR (470 MHz, DMSO-D6) δ (ppm)= -145.51 (dddd, J = 125.5, 93.1, 78.3, 30.2 Hz).

^{31}P NMR (202 MHz, DMSO-D6) δ (ppm)= 21.33 (s).

HR-MS (ESI): *m/z* = calculated for $C_{50}H_{47}B_1Cl_1F_2N_3O_{10}P_1S_1$ [M]+ 996.24639; found 996.24908.

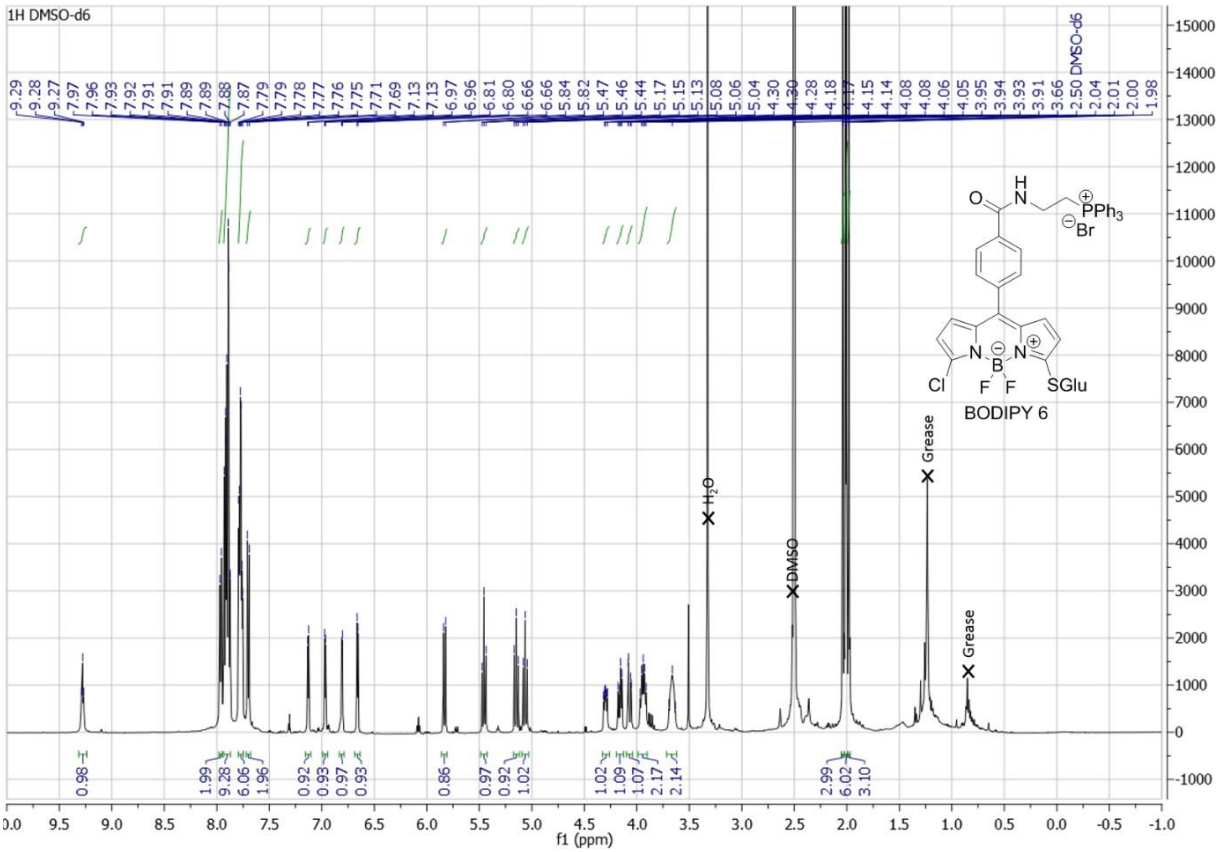

Figure S 21: ^{1}H NMR of BODIPY **6** (DMSO, 500 MHZ, 300K)

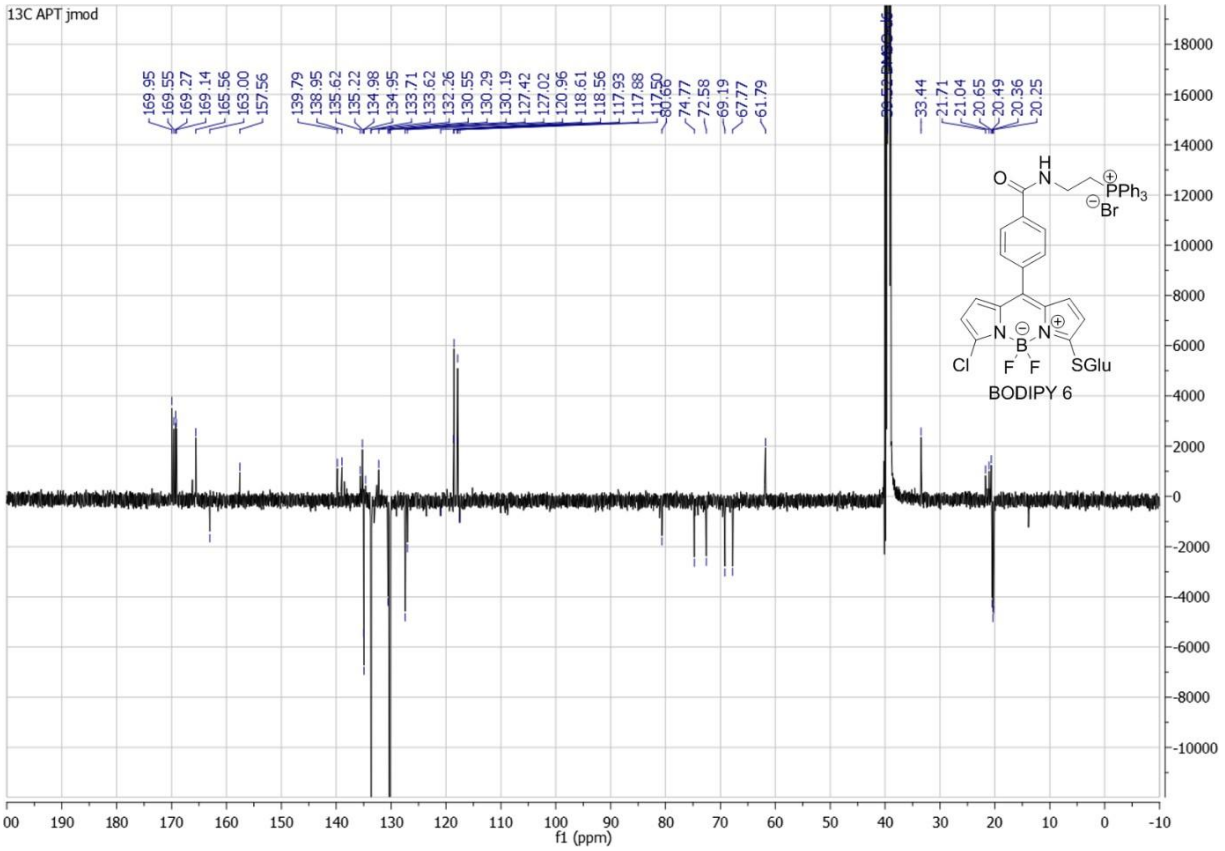

Figure S 22: ^{13}C NMR (APT jmod) of BODIPY **6** (DMSO, 126 MHZ, 300K)

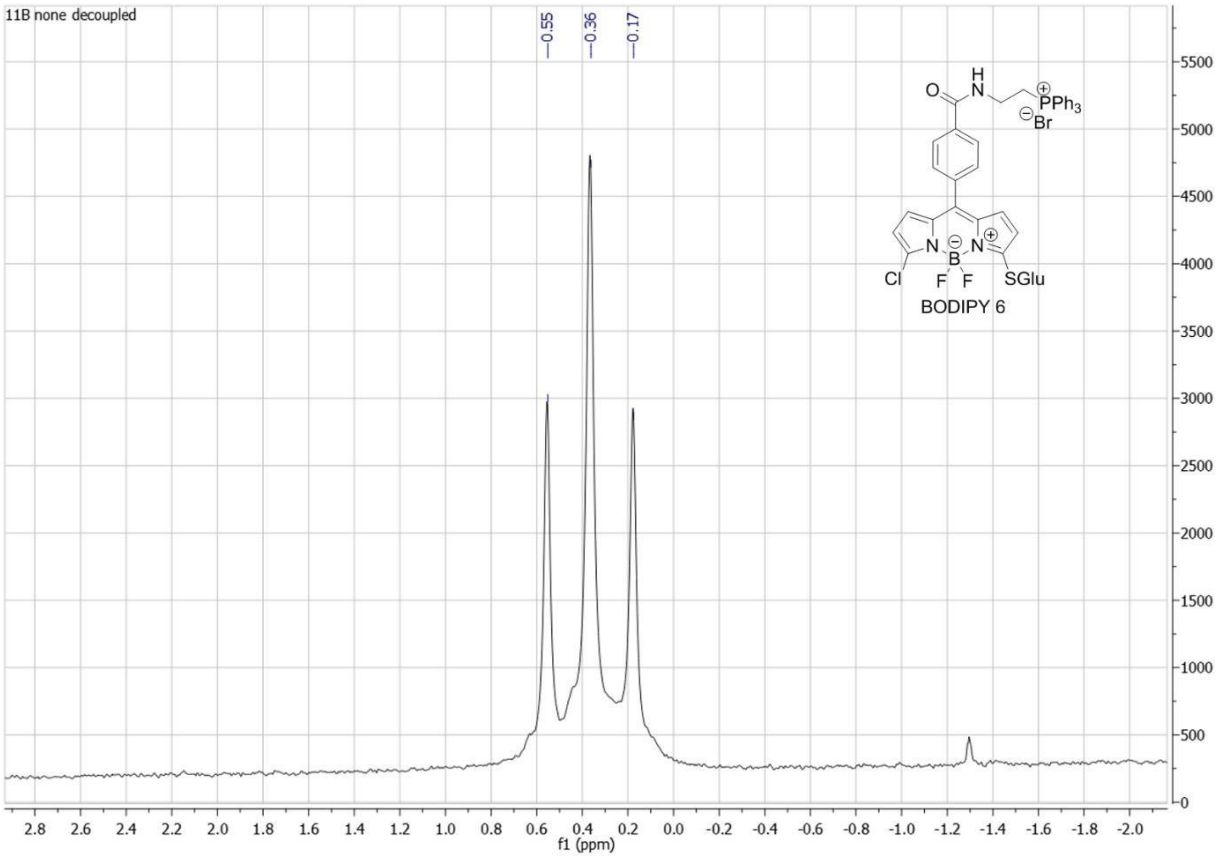

Figure S 23: ^{11}B NMR of BODIPY **6** (DMSO, 160 MHZ, 300K)

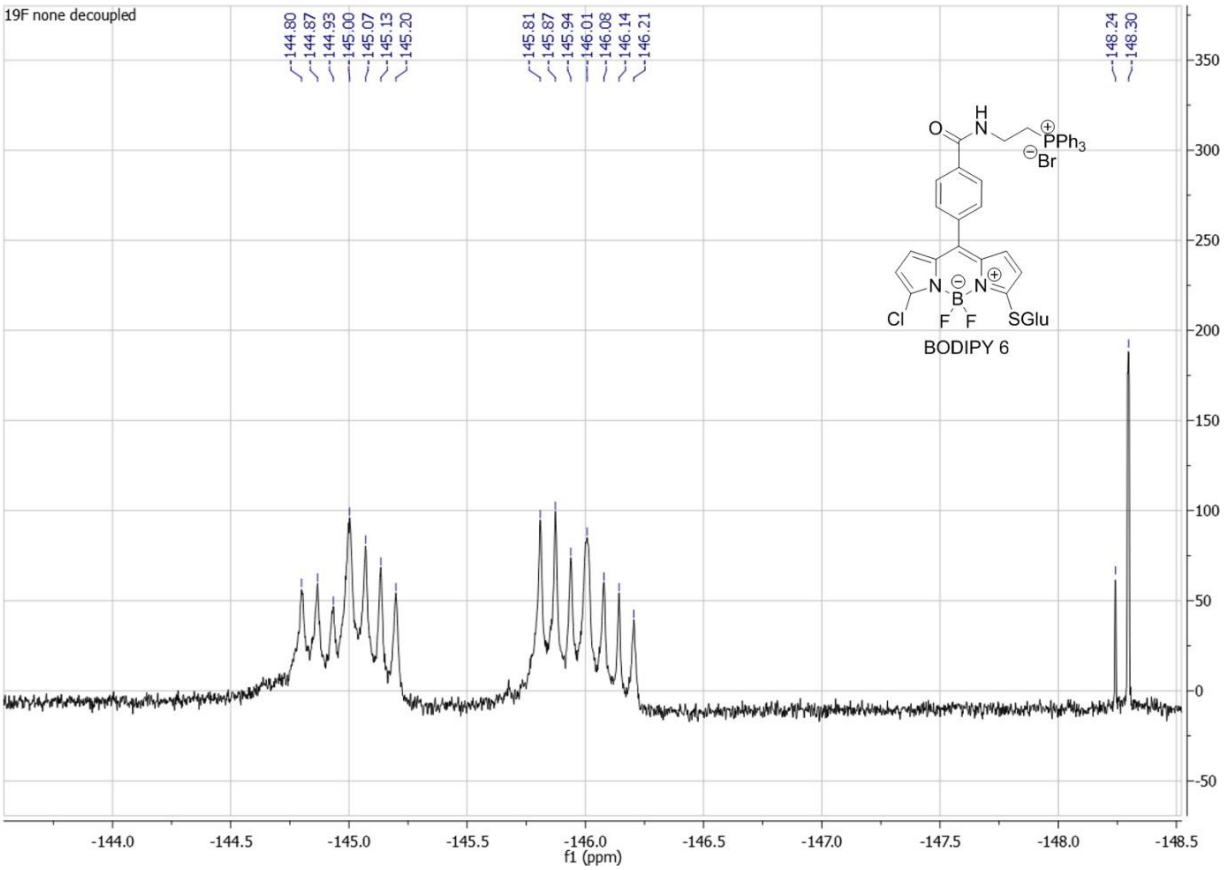

Figure S 24: ^{19}F NMR of BODIPY **6** (DMSO, 470 MHZ, 300K)

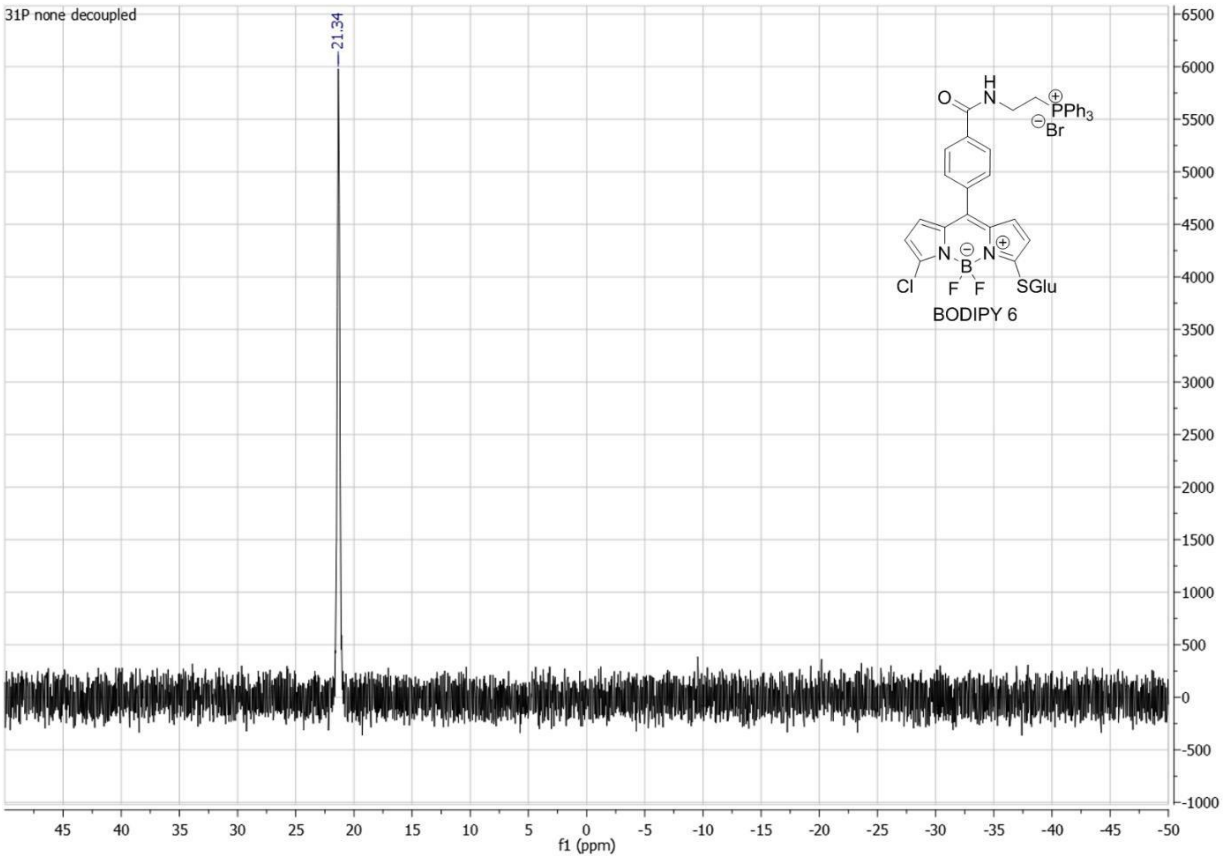

Figure S 25: ^{31}PNMR of BODIPY **6** (DMSO, 202 MHZ, 300K)

BODIPY 7

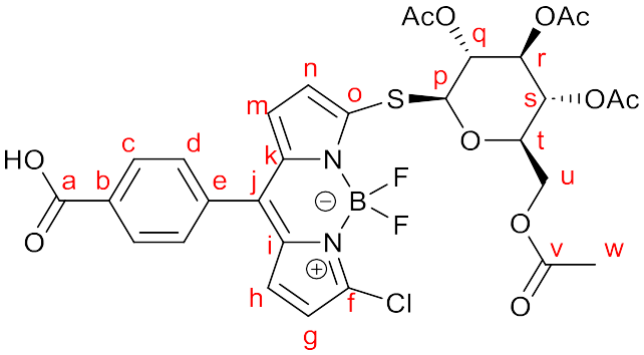

50 mg (0.13mmol, 1eq) of BODIPY **3** and 22 mg (0.26mmol, 2 eq) $NaHCO_3$ were placed in a round bottom flask and dissolved in acetone. In a separate vessel, 43 mg (0.124mmol, 0.9eq) of β-thioglucose-tetraacetate were dissolved in 2 mL acetone, 124 µL 1M NaOH were added and the mixture stirred at room temperature. After 10 min, the thioglucose-solution was drawn into a syringe and added slowly (30 min) to the solution of BODIPY **3**. The resulting solution was stirred at room temperature for another hour and then evaporated to dryness. The crude product was purified by column-chromatography on silica gel using CH_2Cl_2/formic acid (99:1) as eluent. The product fractions were collected, evaporated to dryness, dissolved in a minimal amount of DCM and crushed out with Pentane to yield 80mg (123.5 µmol, yield = 95%) of the targeted compound as a pink powder.

^{1}H NMR (500 MHz, DMSO-D6) δ (ppm)= 1.98 (s, 3H, H_w), 2.00 (s, 3H, H_w), 2.01 (s, 3H, H_w), 2.04 (s, 3H, H_w), 4.06 (dd, *J* = 12.4, 2.4 Hz, 1H, H_u), 4.15 (dd, *J* = 12.4, 5.8 Hz, 1H, H_u), 4.29 (ddd, *J* = 10.1, 5.8, 2.3 Hz, 1H, H_t), 5.06 (t, *J* = 9.8 Hz, 1H, H_q), 5.14 (t, *J* = 9.7 Hz, 1H, H_s), 5.45 (t, *J* = 9.5 Hz, 1H, H_r), 5.82 (d, *J* = 10.1 Hz, 1H, H_p), 6.64 (d, *J* = 4.2 Hz, 1H, H_n), 6.85 (d, *J* = 4.2 Hz, 1H, H_m), 6.94 (d, *J* = 4.7 Hz, 1H, H_g), 7.19 (d, *J* = 4.7 Hz, 1H, H_h), 7.73 (d, *J* = 8.2 Hz, 2H, H_d), 8.11 (d, *J* = 8.3 Hz, 2H, H_c).

^{13}C NMR (126 MHz, DMSO-D6) δ (ppm) = 20.2 (C_w), 20.2(C_w), 20.3(C_w), 20.5(C_w), 61.78(C_u), 67.8 (C_s), 69.2 (C_r), 72.6 (C_q), 74.8 (C_t), 80.7 (C_p), 117.5 (C_g), 120.9 (C_n), 129.2 (C_h), 129.4 (C_m), 130.8 (C_d), 132.2 (C_b), 132.6 (C_f), 133.2 (C_c), 135.6 (C_i), 136.1 (C_j), 139.0 (C_k), 139.7(C_e), 157.7 (C_o), 166.7 (C_a), 169.1 (C_u), 169.2 (C_u), 169.5 (C_u), 169.9 (C_u).

^{11}B NMR (160 MHz, DMSO-D6) δ (ppm)= 0.37 (t, *J* = 30.2 Hz).

^{19}F NMR (470 MHz, DMSO-D6) δ (ppm)= -145.50 (dddd, *J* = 125.7, 90.1, 60.3, 29.9 Hz).

HR-MS (ESI): *m/z* = calculated for $C_{30}H_{28}B_1Cl_1F_2N_2O_{11}S_1Na_1$ $[M+Na]^+$ 731.10557; found 731.10681,

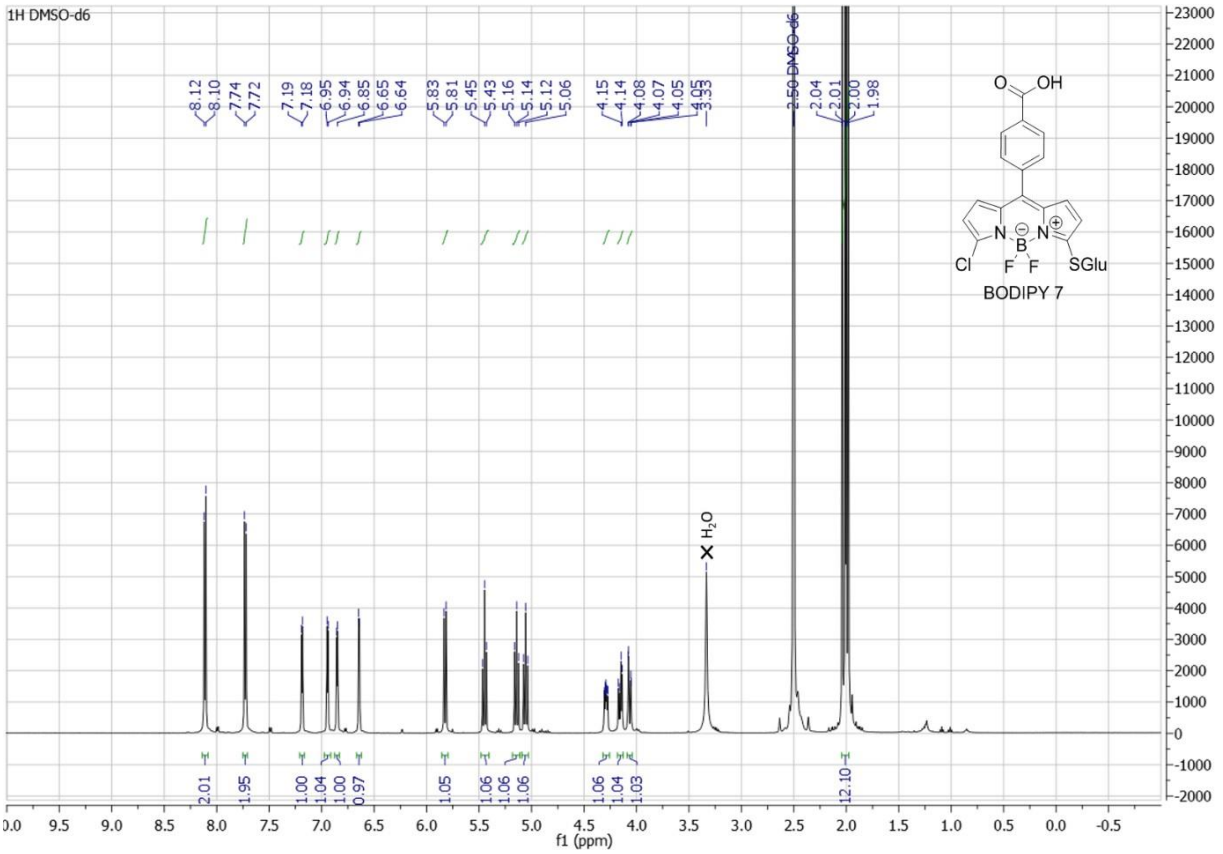

Figure S 26: ^{1}H NMR of BODIPY **7** (DMSO, 500 MHZ, 300K)

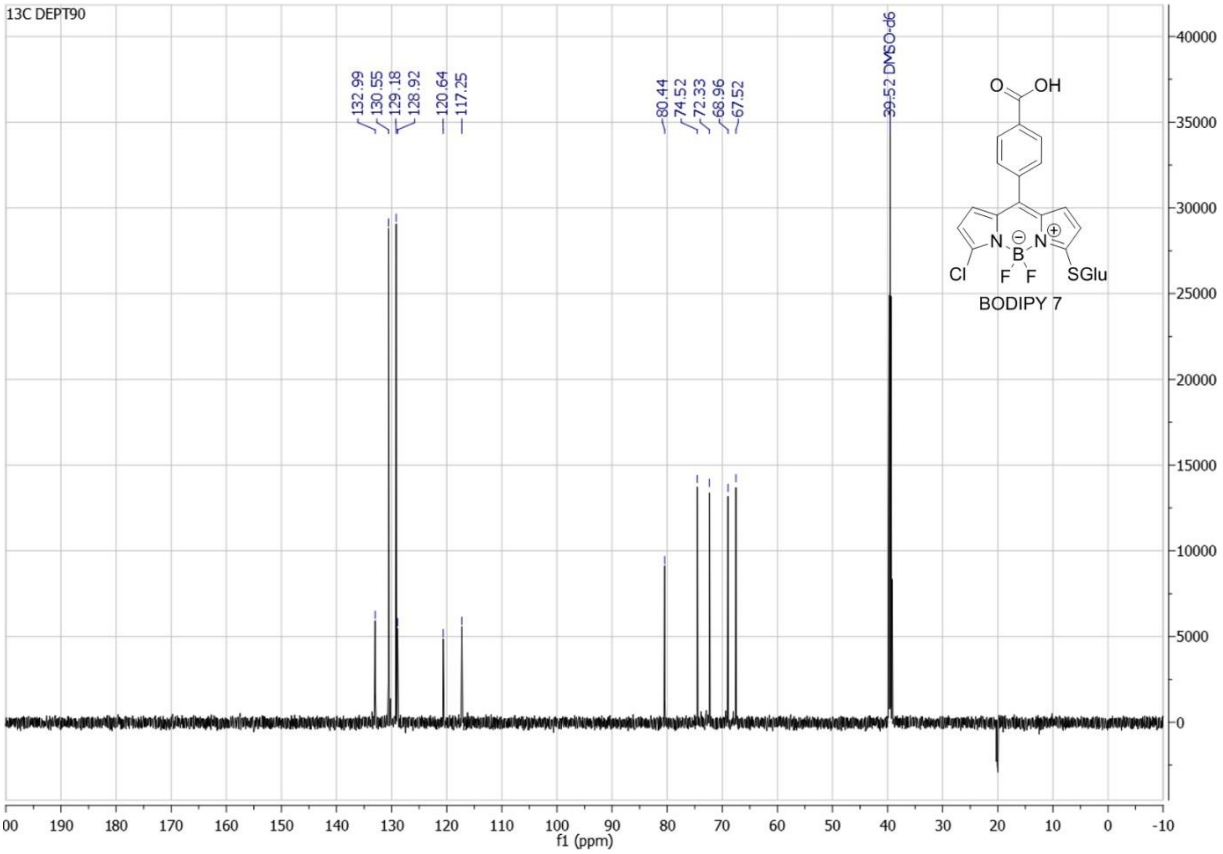

Figure S 27: ^{13}C NMR (DEPT90) of BODIPY **7** (DMSO, 126 MHZ, 300K)

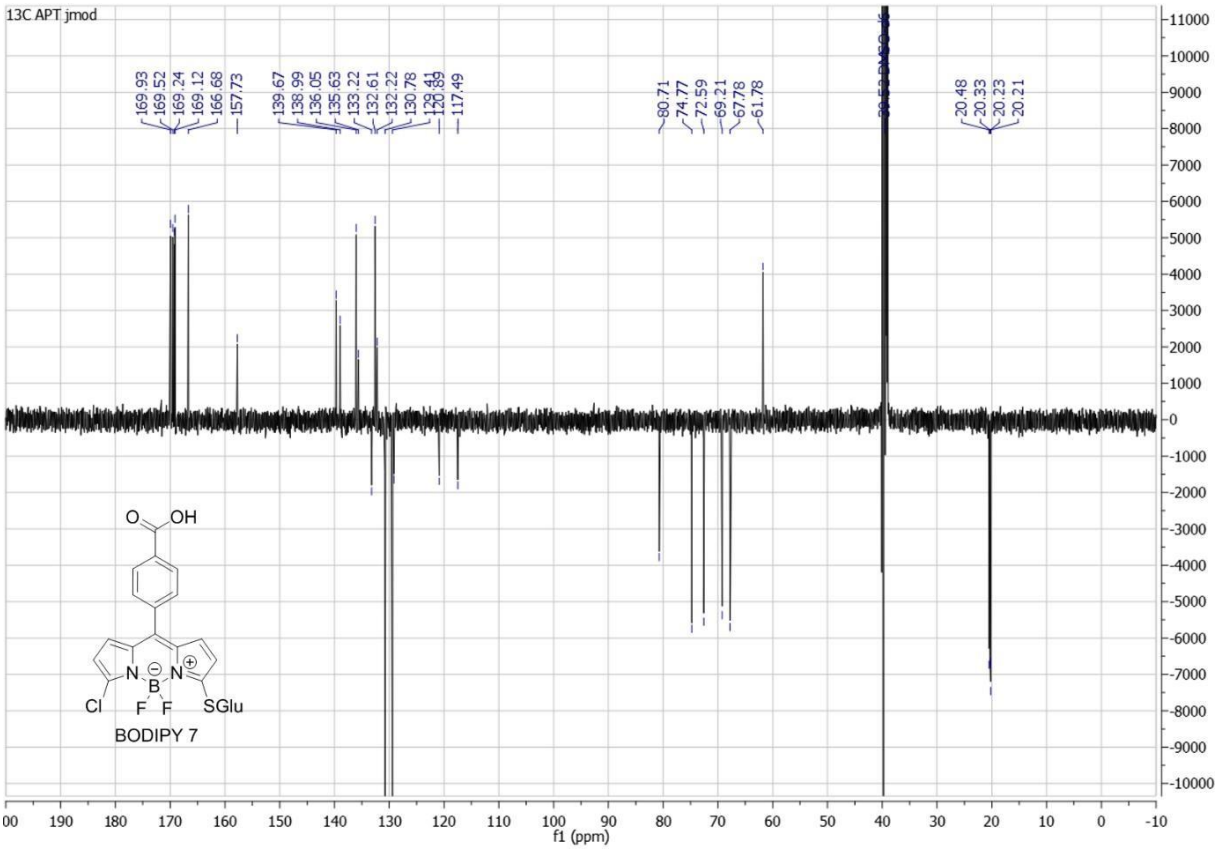

Figure S 28: ^{13}C NMR (APT jmod) of BODIPY **7** (DMSO, 126 MHZ, 300K)

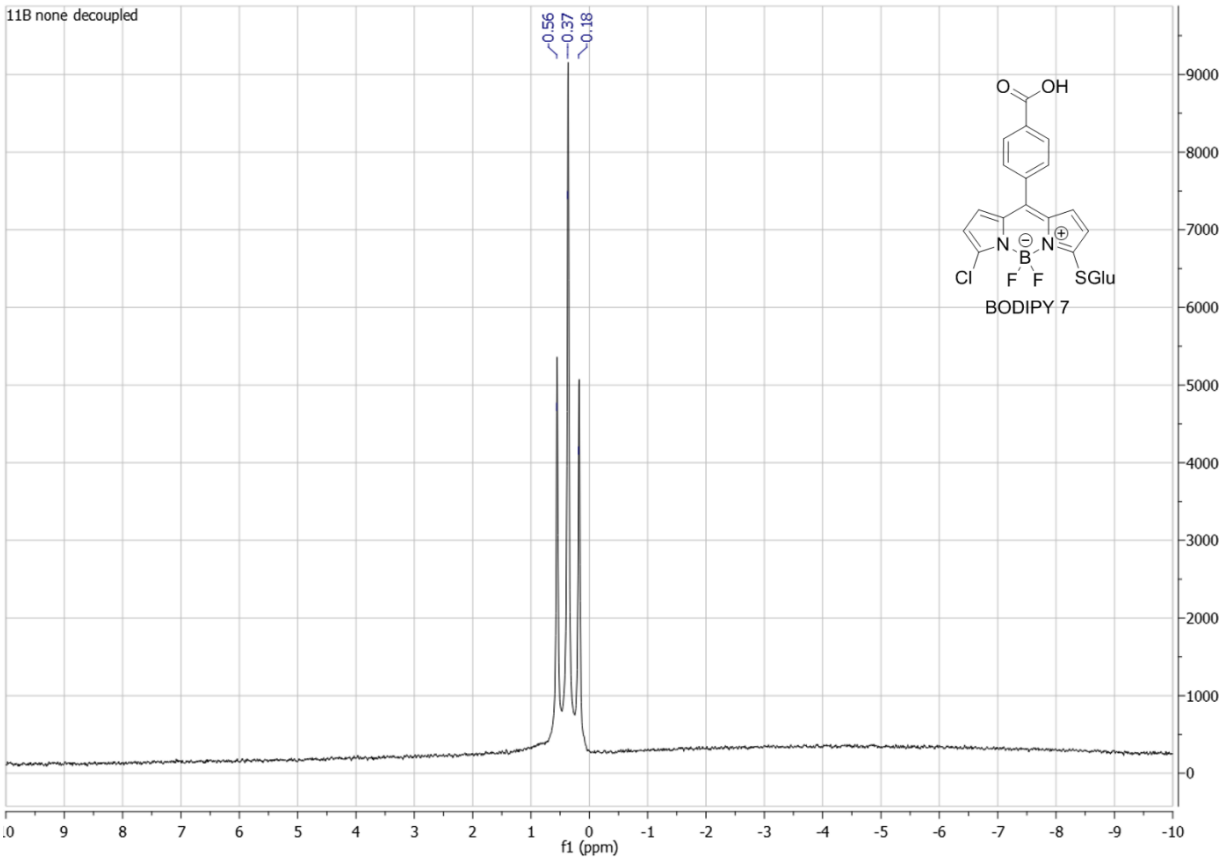

Figure S 29: ^{11}B NMR of BODIPY **7** (DMSO, 160 MHZ, 300K)

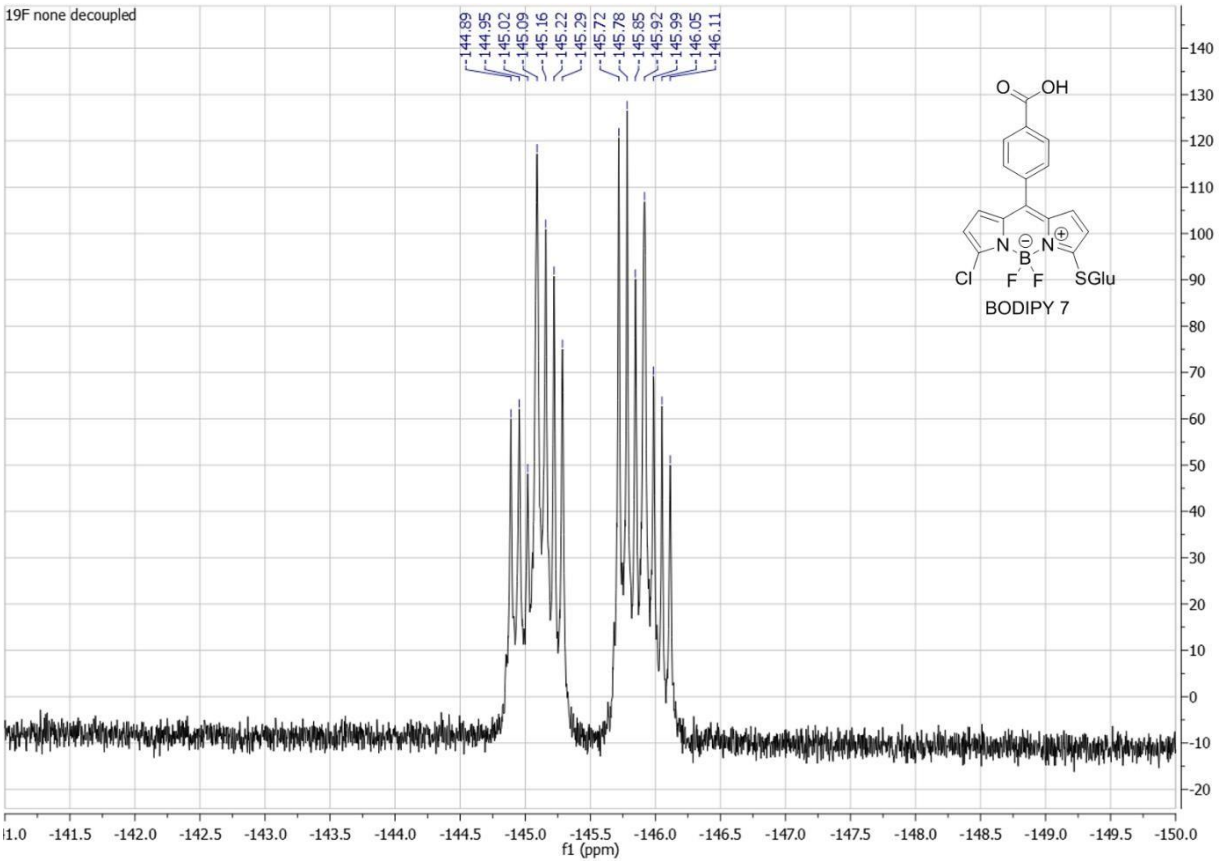

Figure S 30: ^{19}F NMR of BODIPY **7** (DMSO, 470 MHZ, 300K)

BODIPY 8

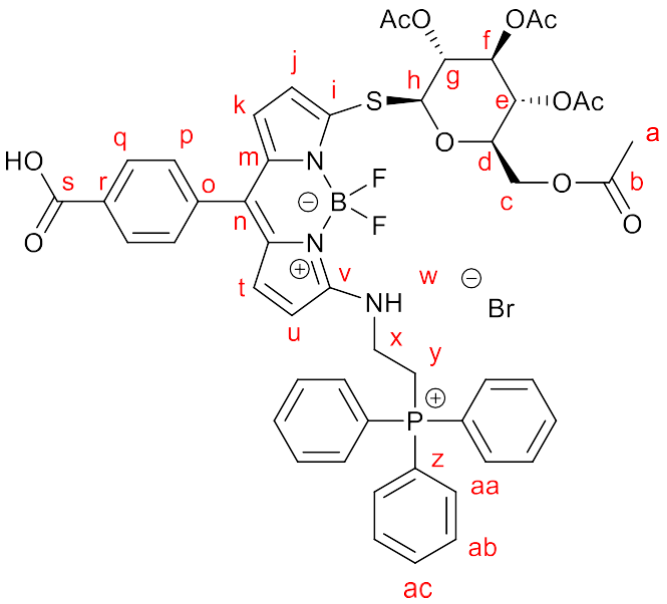

150.4mg (0.21 mmol, 1eq) of BODIPY **7** were placed in a roundbottom flask and dissolved in acetonitrile. Triphenylphosphonium-ethylamonium dibromide (148 mg, 0.32 mmol, 1.5eq) and $NaHCO_3$ (89mg, 1.06mmol, 5eq) were added and the resulting mixture was refluxed for 70 min. The solvent was then evaporated and the crude product purified by column chromatography on silica gel, using as eluent CH_2Cl_2/MeOH/formic acid (99:1:1 to 90:10:1). The product fractions were evaporated, dissolved in a minimal amount of MeOH and precipitated with Et_2O. The procedure is repeated with CH_2Cl_2 and pentane to obtain 135mg (126 µmol, yield = 60%) of the target compound as a pink-orange powder.

^{1}H NMR (500 MHz, DMSO-D6) δ (ppm)= 1.95 (s, 3H, H_a), 2.00 (ps-d, 9H, H_a), 3.76 (d, J = 6.0 Hz, 2H, H_y), 4.09 – 3.95 (m, 3H, H_c, H_x), 4.23 – 4.13 (m, 2H, $H_{c'}$, H_d), 4.96 (ps-td, J = 9.7, 2.9 Hz, 2H, H_g, H_e), 5.36 (d, J = 10.1 Hz, 1H, H_h), 5.41 (t, J = 9.4 Hz, 1H, H_f), 6.34 (d, J = 3.8 Hz, 1H, H_u), 6.41 (d, J = 5.0 Hz, 1H, H_t), 6.44 (d, J = 3.8 Hz, 1H, H_j), 6.97 (d, J = 5.0 Hz, 1H, H_k), 7.52 (d, J = 7.8 Hz, 2H, H_p), 7.77 (ddd, J = 14.9, 7.4, 2.9 Hz, 6H, H_{aa}), 7.85 (dd, J = 12.9, 7.5 Hz, 6H, H_{ab}), 7.92 (t, J = 7.3 Hz, 3H, H_{ac}), 8.05 (d, J = 7.8 Hz, 2H, H_q), 8.24 (s, 1H, H_w).

^{13}C NMR (126 MHz, DMSO-D6) δ (ppm)= 20.4 (s, C_a), 20.4 (s, C_a), 20.4 (s, C_a), 20.5 (s, C_a), 22.1 (d, J = 48.4 Hz, C_x), 38.6 (s, C_y), 61.9 (s, C_c), 68.0 (s, C_e), 69.3 (s, C_f), 72.9 (s, C_g), 74.3 (s, C_d), 83.0 (s, C_h), 113.0 (s, C_u), 114.9 (s, C_j), 118.0 (d, J = 86.3Hz, C_z), 119.1 (s, C_t), 128.5 (s, C_n), 129.3 (s, C_k), 130.1 (d, J = 12.9 Hz, C_q), 130.3 (d, J = 12.7 Hz, C_{ac}), 132.4 (s, C_m, C_n), 133.0 (s, C_i, C_v), 133.2 (d, J = 10.7 Hz, C_p), 133.7 (d, J = 10.5 Hz, C_{ab}), 134.6 (s, C_o), 135.1 (d, J = 1.6Hz, C_{aa}), 161.0 (s, C_s), 169.0 (s, C_b), 169.3 (s, C_b), 169.5 (s, C_b), 170.0 (s, C_b)

^{11}B NMR (160 MHz, DMSO-D6) δ (ppm)= 0.70 (t, J = 32.7 Hz)

^{19}F NMR (470 MHz, DMSO-D6) δ (ppm) = -143.45. (vbr)

^{31}P NMR (202 MHz, DMSO-D6) δ (ppm) = 21.46

HR-MS (ESI): *m/z* = calculated for $C_{50}H_{48}B_1F_2N_3O_{11}P_1S_1$ $[M]^+$ 978.28028; found 978.28403.

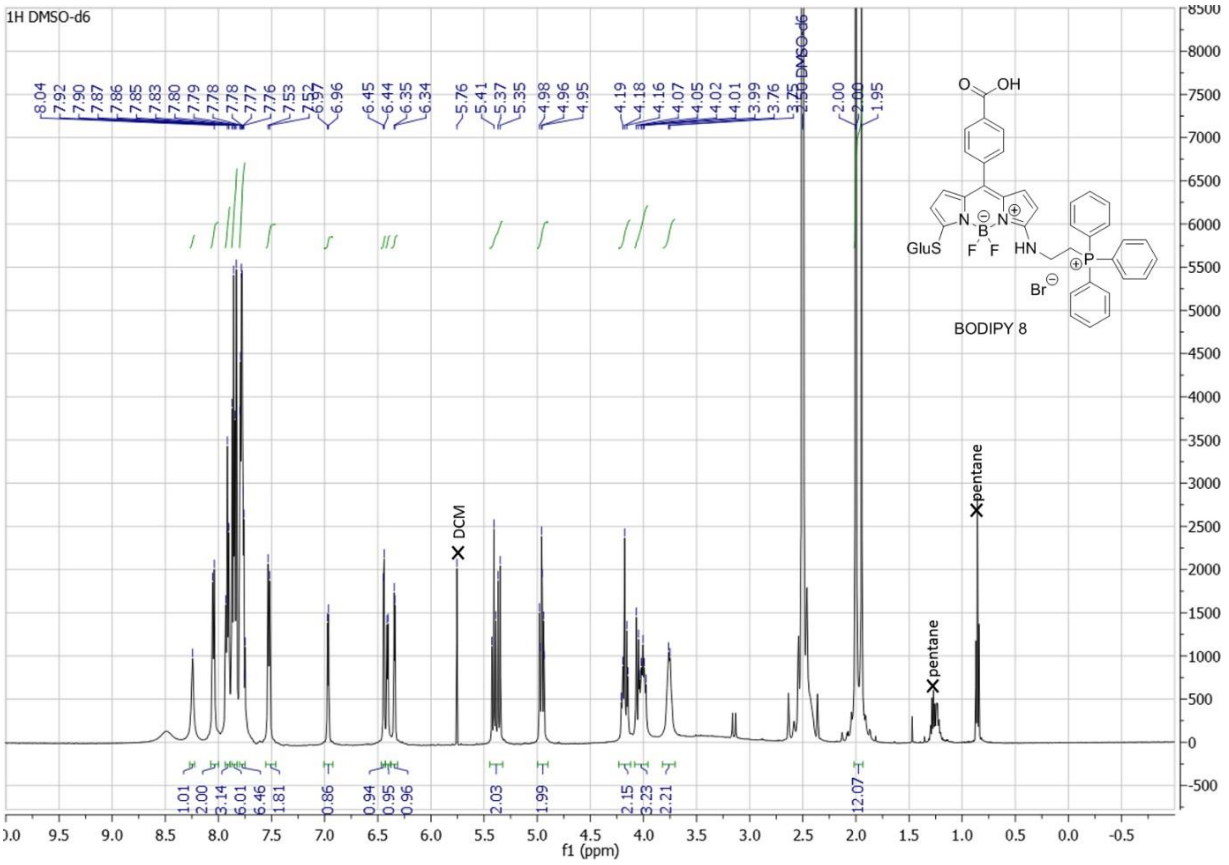

Figure S 31: ^{1}H NMR of BODIPY **8** (DMSO, 500 MHZ, 300K)

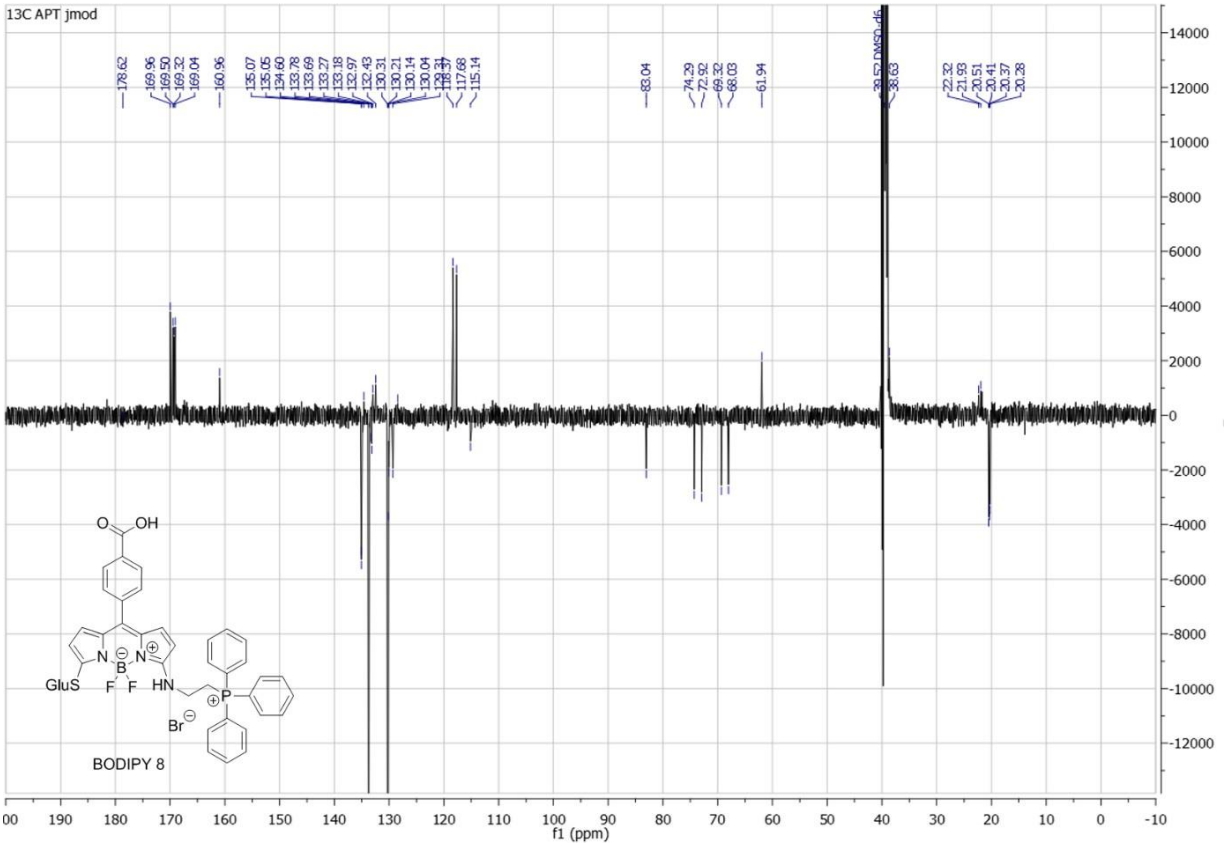

Figure S 32: ^{13}C NMR (APT jmod) of BODIPY **8** (DMSO, 126 MHZ, 300K)

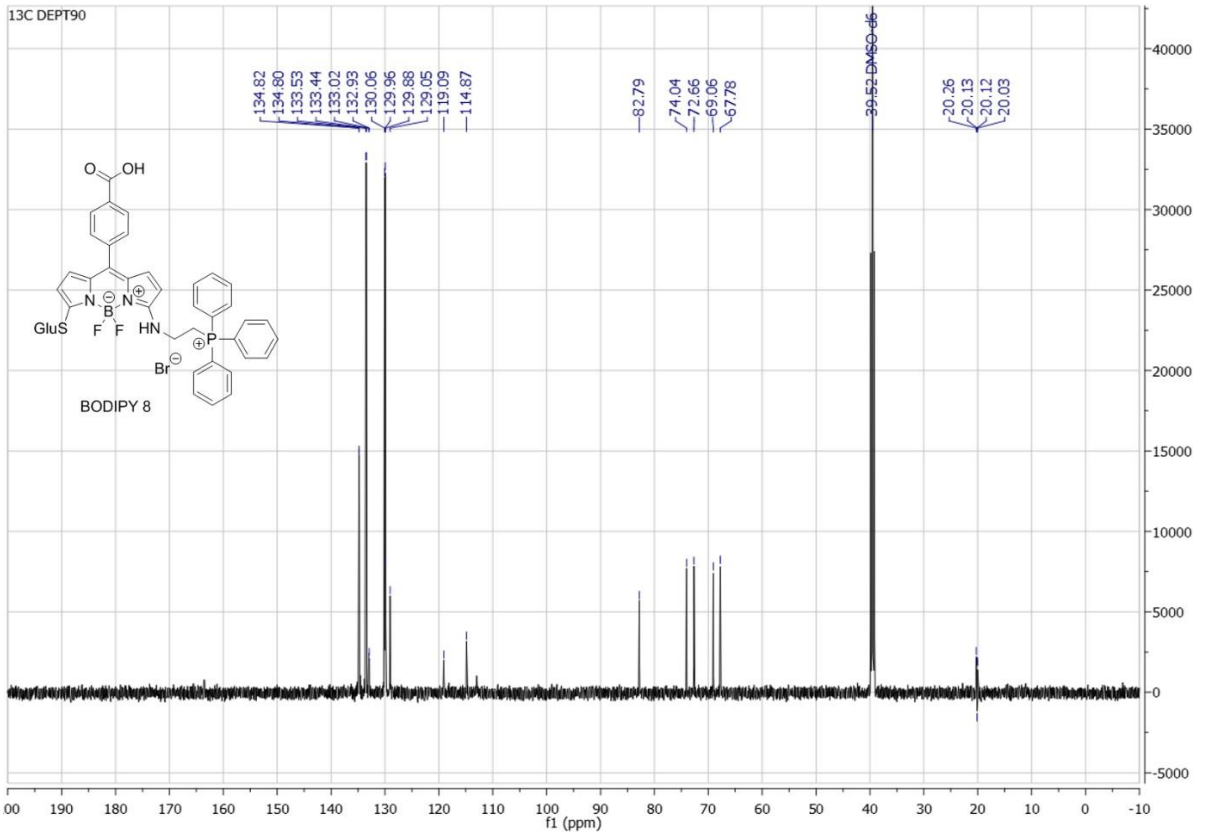

Figure S 33: ^{13}C NMR (DEPT90) of BODIPY **8** (DMSO, 126 MHZ, 300K)

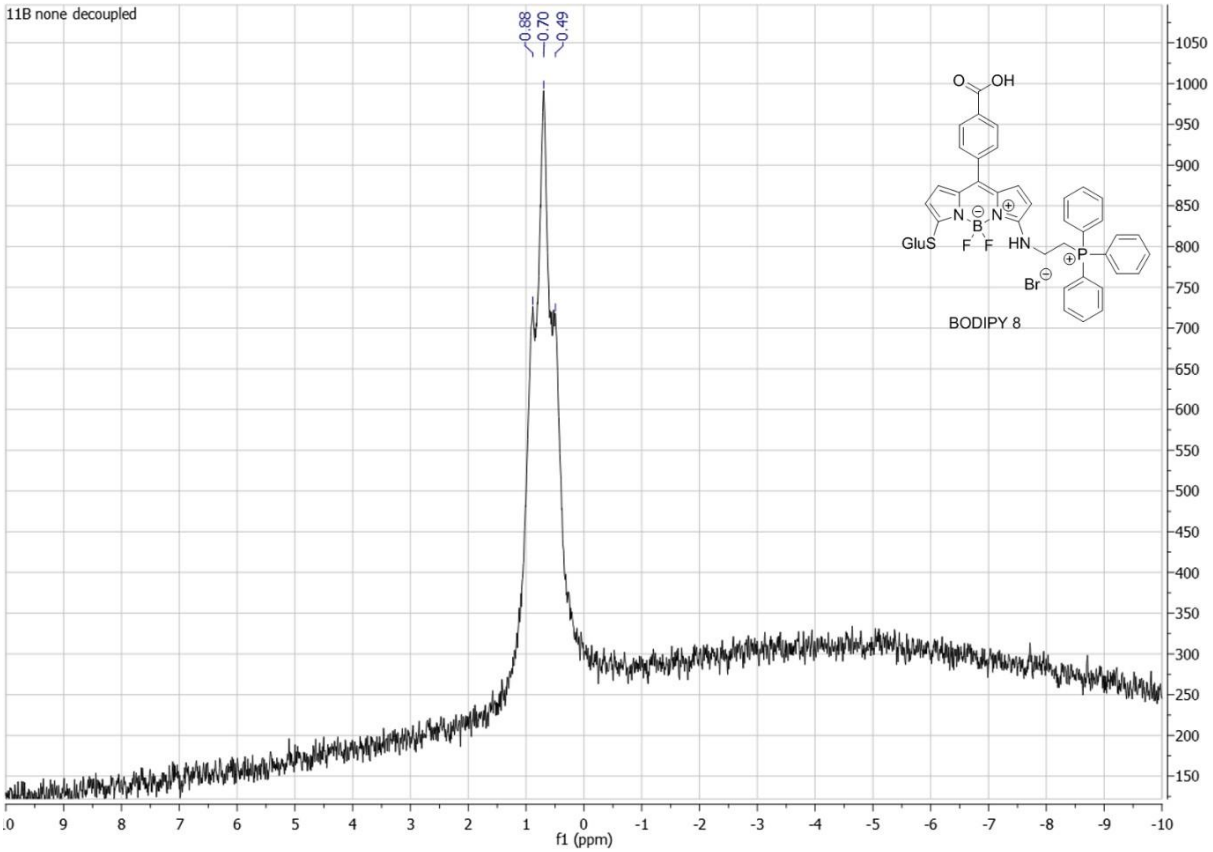

Figure S 34: ^{11}B NMR of BODIPY **8** (DMSO, 160 MHZ, 300K)

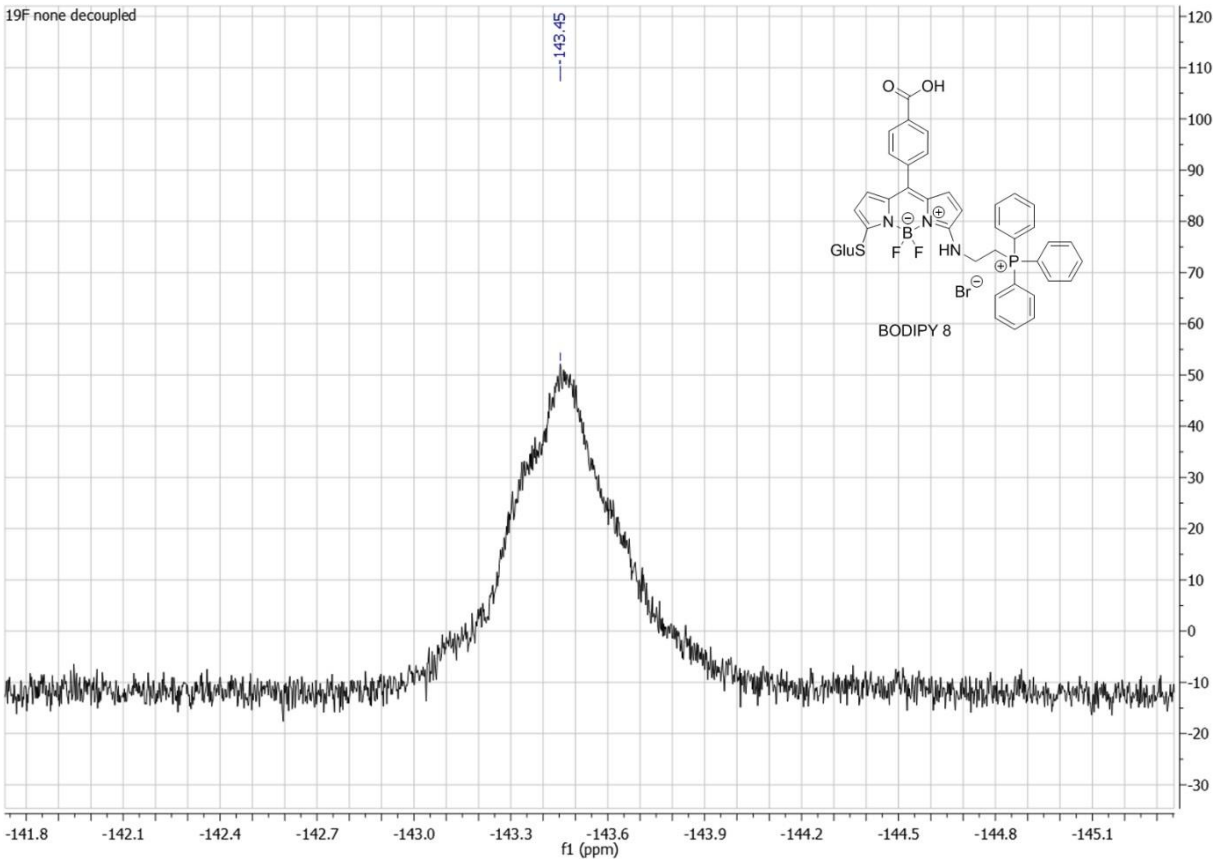

Figure S 35: ^{19}F NMR of BODIPY **8** (DMSO, 470 MHZ, 300K)

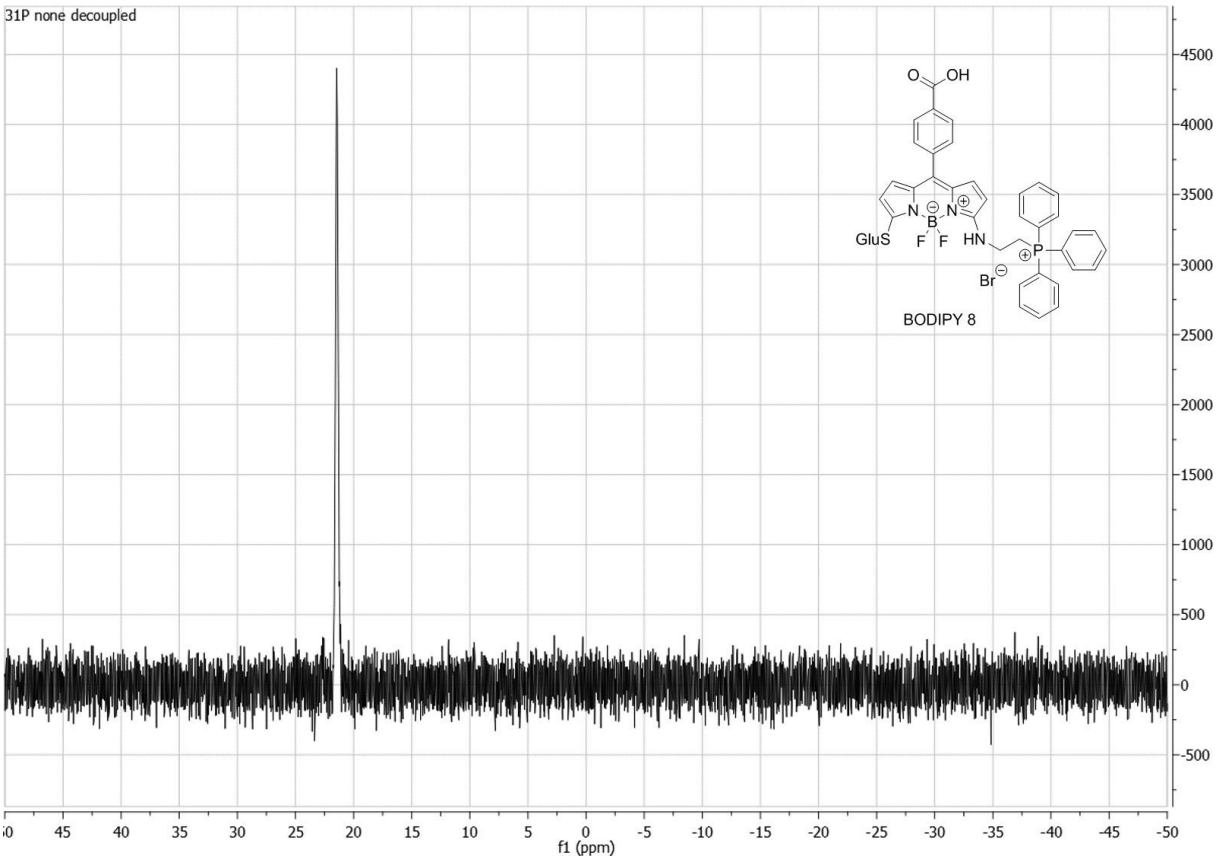

Figure S 36: ^{31}P NMR of BODIPY **8** (DMSO, 202 MHZ, 300K)

BODI-Au-7

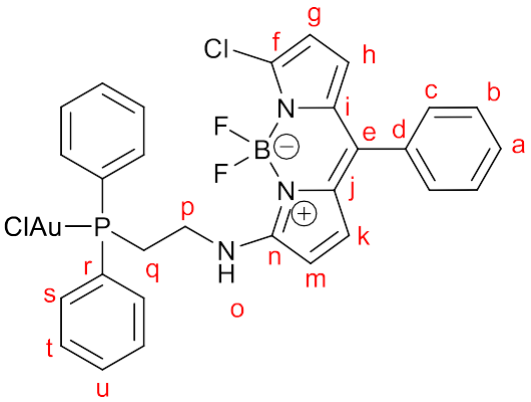

173mg (0.376mmol,1.2eq) of 2-(diphenylphosphino)-ethylamine-aurichloride, 106mg (0.314mmol, 1eq) of BODIPY **1** and 203mg (1.47mmol, 5eq) K_2CO_3 were placed in a 50 mL round bottom flask and put under argon. 15 mL dry THF were added and the reaction was refluxed for 70 minutes. The solvents were evaporated and the crude product was purified by column chromatography on silica gel using hexane/EtOAc/NEt_3 (90/10/3 to 70/30/3) as eluent. After evaporation of the solvents under reduced pressure the crude product was dissolved in CH_2Cl_2 and crushed out with pentane to yield 218mg (285.74 mmol, yield = 91%) of **BODI-Au-7** as an orange solid.

^{1}H NMR (500 MHz, DMSO-D6) δ (ppm)= 3.17 (ddd, *J* = 11.7, 7.8, 5.1 Hz, 2H, H_q), 3.71 (s, 2H, H_p), 6.19 (d, *J* = 3.8 Hz, 1H, H_m), 6.24 (d, *J* = 3.8 Hz, 1H, H_k), 6.57 (d, *J* = 5.1 Hz, 1H, H_g), 6.96 (d, *J* = 5.1 Hz, 1H, H_h), 7.47 – 7.43 (m, 2H, H_c), 7.54 – 7.50 (m, 3H, H_b, H_a), 7.63 – 7.55 (m, 6H, H_{at}, H_u), 7.84 – 7.78 (m, 4H, H_s), 8.58 (t, *J* = 5.9 Hz, 1H, H_o).

^{13}C NMR (126 MHz, DMSO-D6) δ (ppm)= 27.4 (d, *J* = 36.1 Hz, C_p), 41.2 (d, *J* = 9.7 Hz, C_q), 111.8 (s, C_g), 114.4 (s, C_m), 117.5 (s, C_h), 126.0 (s, C_i, C_j), 128.4 (s, C_e), 128.5 (s, C_k), 128.9 (d, *J* = 60.7 Hz, C_r), 129.2 (s, C_a), 129.4 (d, *J* = 11.6 Hz, Cu), 130.1 (s, C_b), 131.1 (s, C_d), 132.1 (d, *J* = 2.3 Hz, C_t), 133.2 (d, *J* = 13.5 Hz, C_s), 133.3 (s, C_f), 133.7 (s, C_n), 135.8 (s, C_c).

^{11}B NMR (160 MHz, DMSO-D6) δ (ppm)= 0.64 (t, *J* = 32.7 Hz).

^{19}F NMR (470 MHz, DMSO-D6) δ (ppm)= -144.48 (dd, *J* = 64.1, 31.5 Hz).

^{31}P NMR (202 MHz, DMSO-D6) δ (ppm)= 24.32 (s).

HR-MS (ESI): m/z = calculated for $C_{29}H_{24}Au_1B_1Cl_2F_2N_3P_1Na_1$ $[M+Na]^+$ 784.07037; found 784.07020.

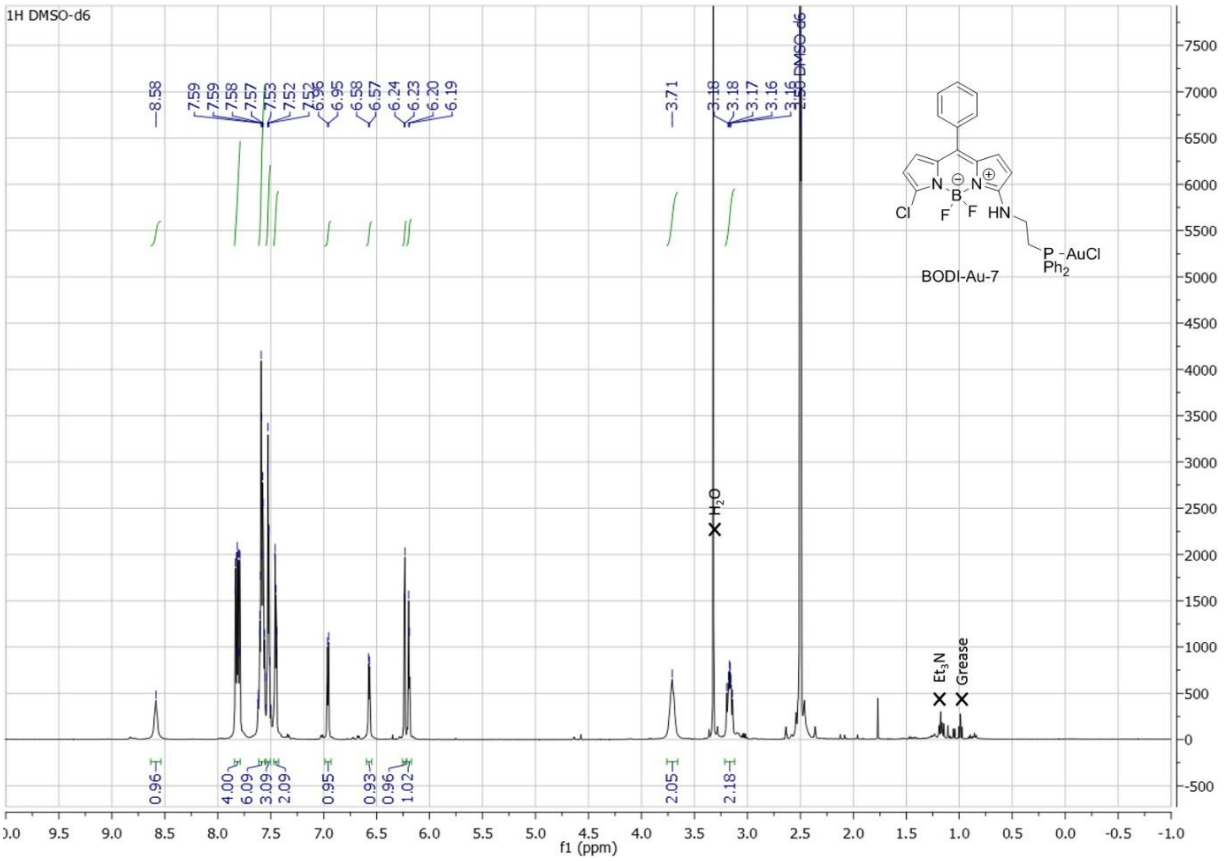

Figure S 37: ^{1}H NMR of **BODI-Au-7** (DMSO, 500 MHZ, 300K)

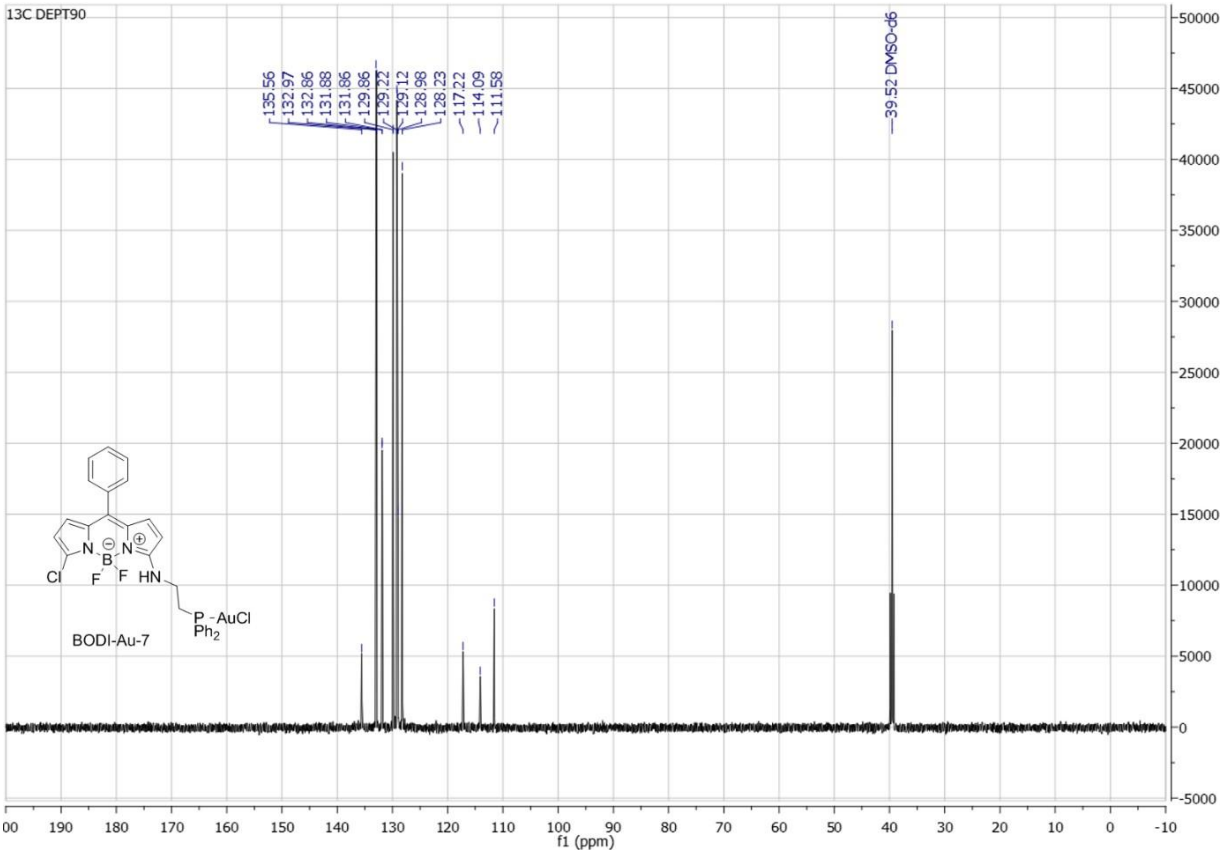

Figure S 38: ^{13}C NMR (DEPT90) of **BODI-Au-7** (DMSO, 126 MHZ, 300K)

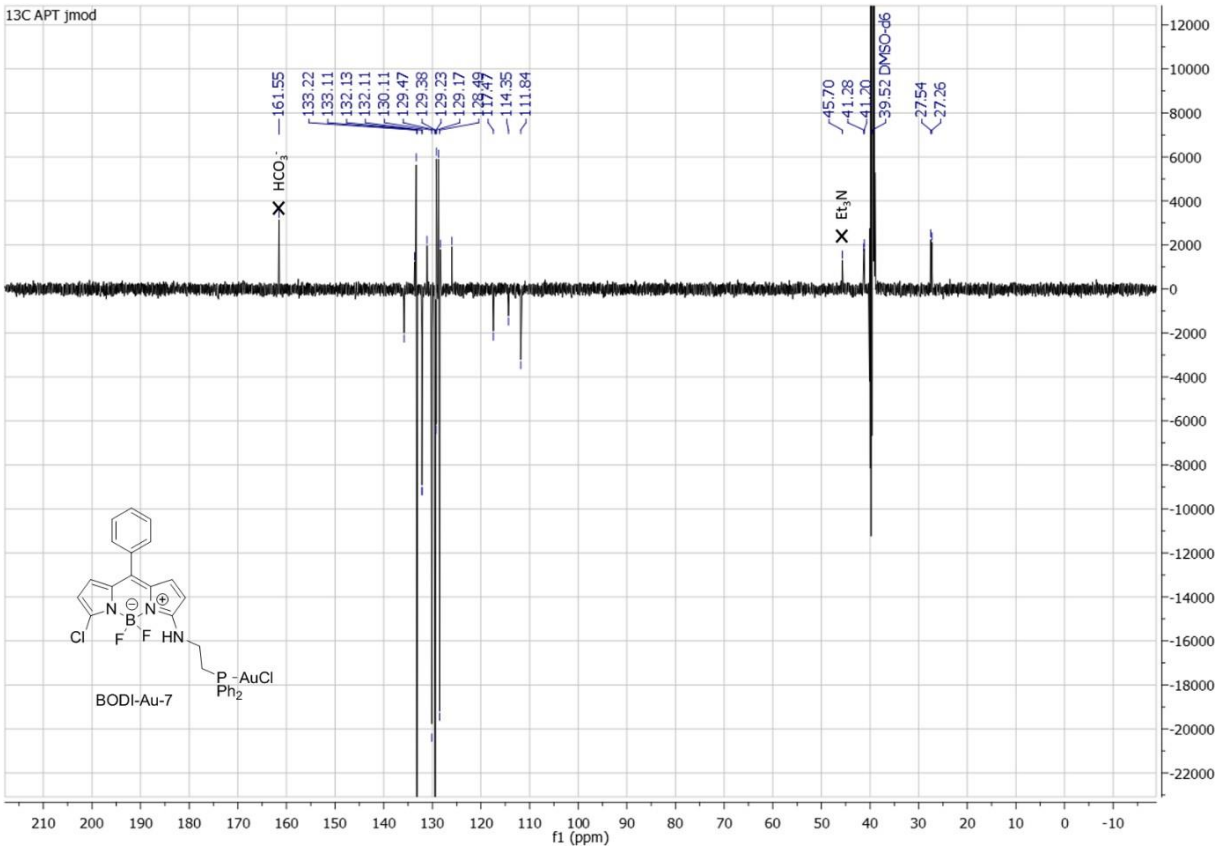

Figure S 39: ^{13}C NMR (APT jmod) of **BODI-Au-7** (DMSO, 126 MHZ, 300K)

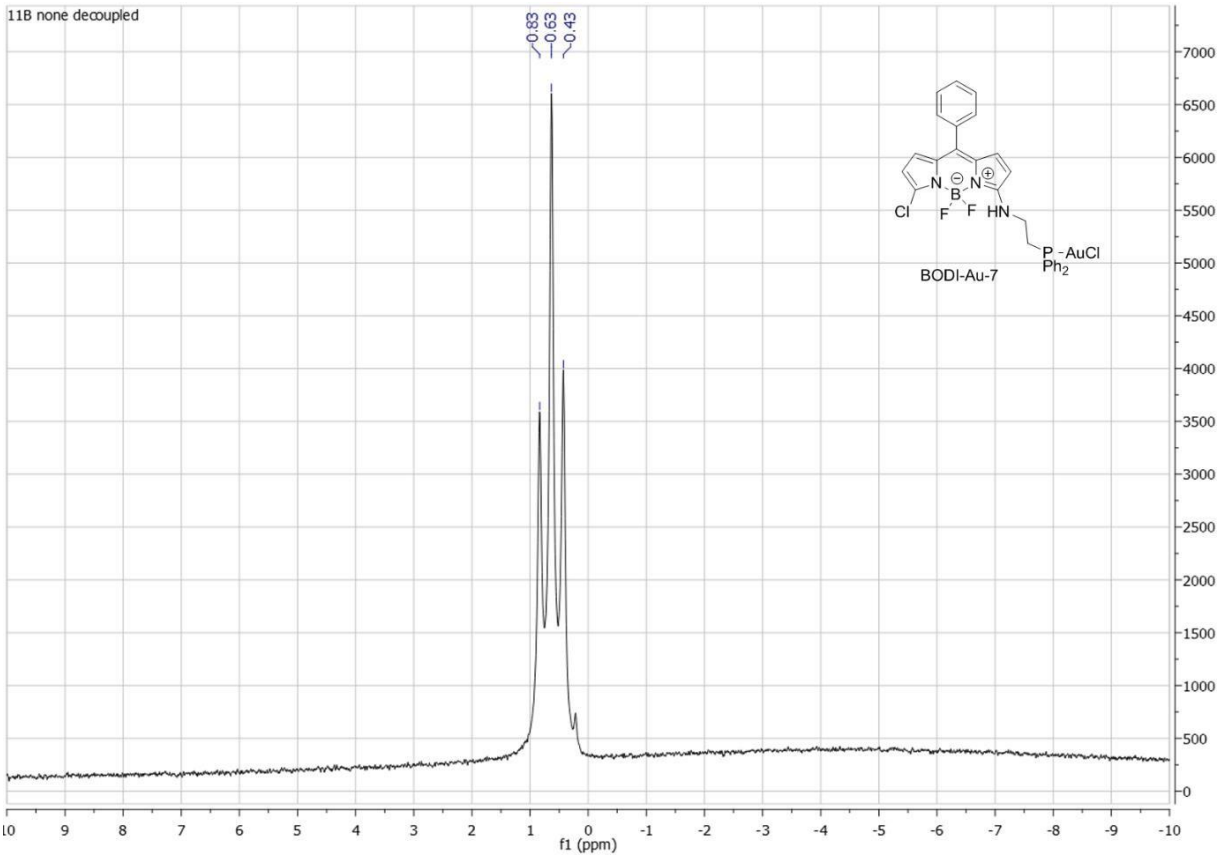

Figure S 40: ^{11}B NMR of **BODI-Au-7** (DMSO, 160 MHZ, 300K)

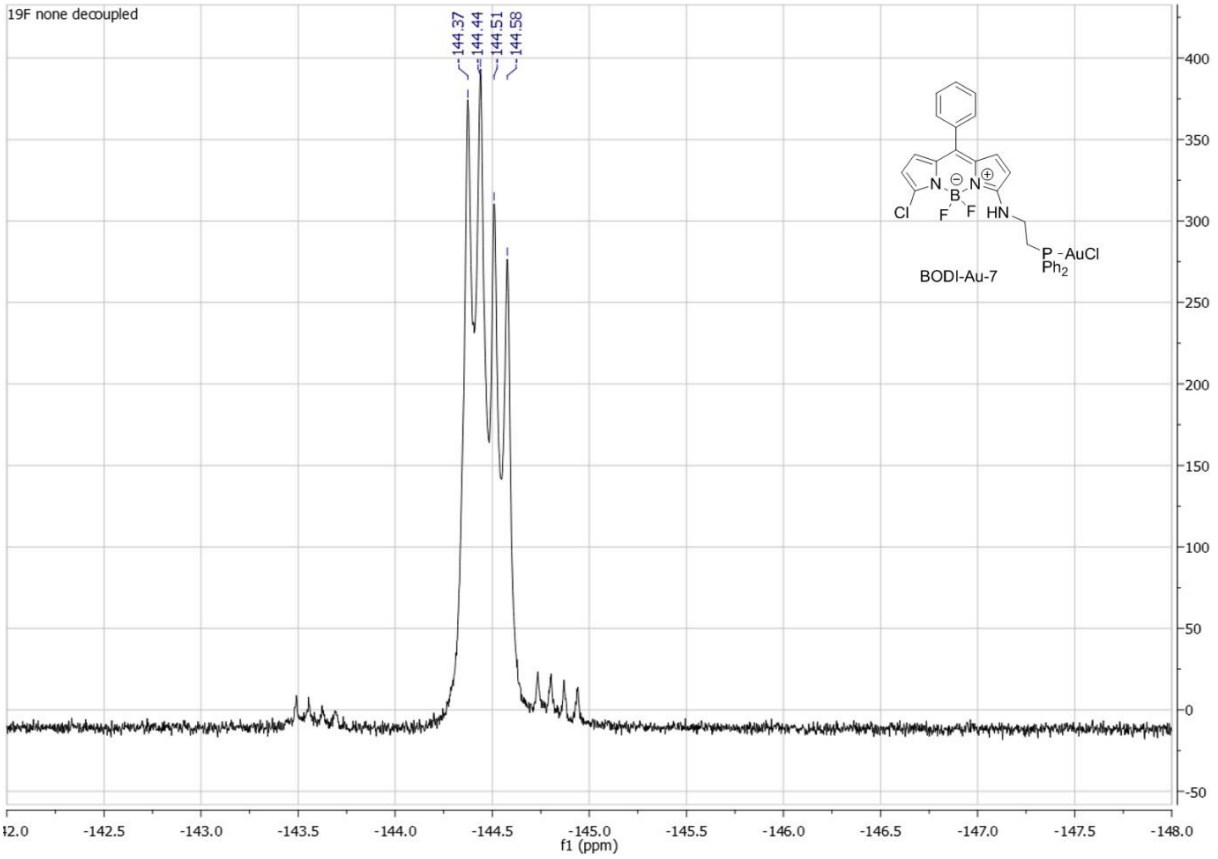

Figure S 41: ^{19}F NMR of **BODI-Au-7** (DMSO, 470 MHZ, 300K)

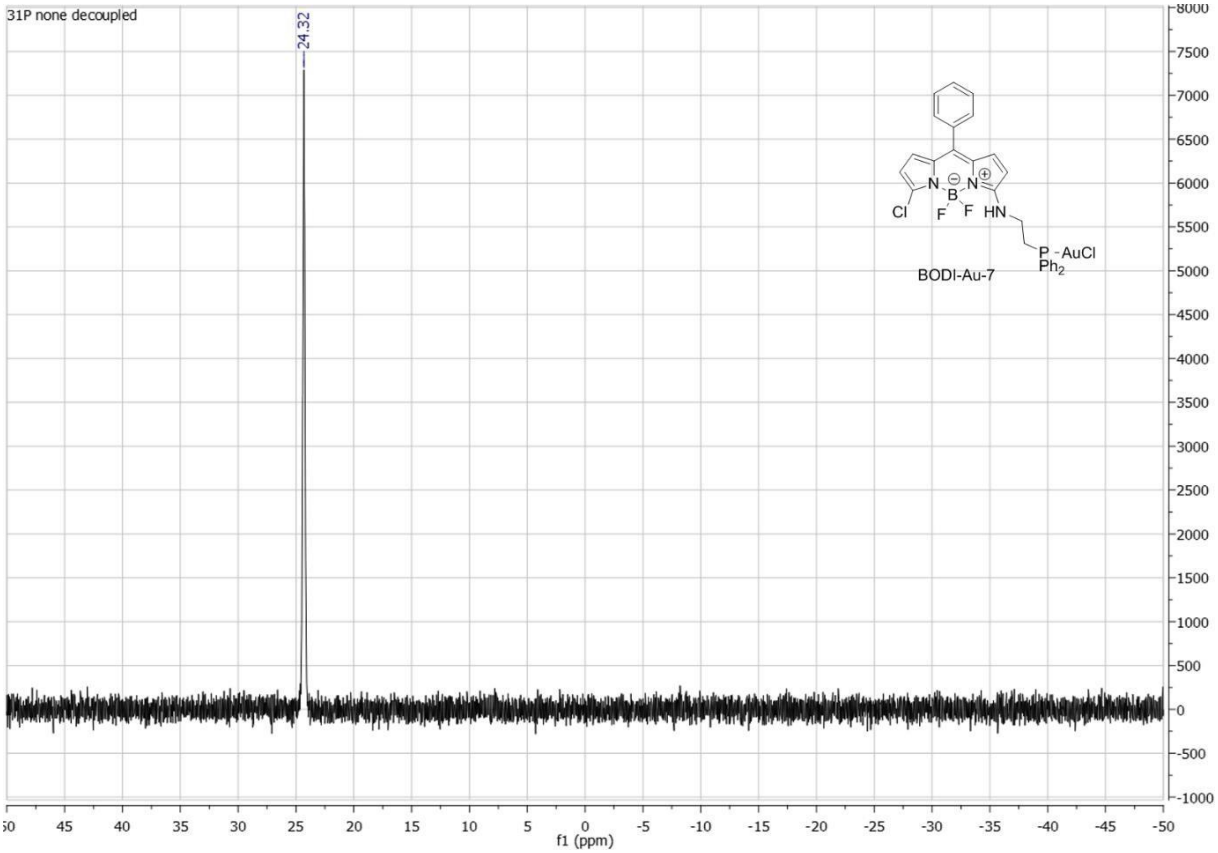

Figure S 42: ^{31}P NMR of **BODI-Au-7** (DMSO, 202 MHZ, 300K)

BODI-Au-8

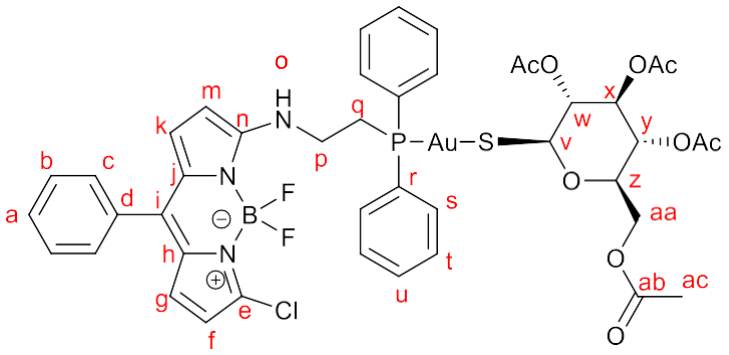

19.1mg (52.4µmol) of β-Thioglucose tetraacetate was dissolved in acetone (1 mL). 52.4µl of 1M NaOH (1 eq) was added and the resulting solution stirred for 15 min. 40mg (52.4µmol) of **BODI-Au-7** was placed in a separate roundbottom flask and dissolved in acetone (5 mL). The thioglucose solution was added at once and the reaction stirred for 30 min at room temperature. The solvents were evaporated, CH_2Cl_2 (10 mL) was added, and the supernatant separated and evaporated. The resulting crude product was dissolved in a minimal amount of CH_2Cl_2 and precipitated with pentane to obtain the pure target compound as a flaky orange powder. Yield: 56mg (96%).

^{1}H NMR (500 MHz, DMSO-D6) δ (ppm)= 1.85 (s, 6H, H_{ac}), 2.00 – 1.94 (m, 6H, H_{ac}), 3.19 – 3.07 (m, 2H, H_q), 3.74 (ddd, *J* = 15.3, 12.5, 7.5 Hz, 2H, H_p), 4.03 – 3.96 (m, 2H, H_{aa}, H_z), 4.08 (dd, *J* = 12.7, 5.8 Hz, 1H, H_{aa}), 4.90 (ps-dt, *J* = 13.2, 9.6 Hz, 2H, H_w, H_y), 5.18 (t, *J* = 9.5 Hz, 1H, H_x), 5.33 (d, *J* = 9.4 Hz, 1H, H_v), 6.20 (d, *J* = 3.8 Hz, 1H, H_m), 6.24 (d, *J* = 3.8 Hz, 1H, H_k), 6.59 (d, *J* = 5.1 Hz, 1H, H_f), 6.96 (d, *J* = 5.1 Hz, 1H, H_g), 7.47 – 7.44 (m, 2H, H_c), 7.54 – 7.48 (m, 3H, H_b, H_a), 7.62 – 7.55 (m, 6H, H_{at}, H_u), 7.92 – 7.80 (m, 4H, H_s), 8.58 (t, *J* = 6.2 Hz, 1H, H_o).

^{13}C NMR (126 MHz, DMSO-D6) δ (ppm)= 20.3 (s, C_{ac}), 20.3 (s, C_{ac}), 20.4 (s, C_{ac}), 20.8 (s, C_{ac}), 27.5 (d, *J* = 32.6 Hz, C_p), 41.3 (d, *J* = 12.1 Hz, C_q), 62.4 (s, C_{aa}), 68.6 (s, C_y), 73.2 (s, C_x), 74.3 (s, C_w), 77.5 (s, C_z), 81.8 (s, C_v), 111.8 (s, C_f), 114.1 (s, C_m), 117.5 (s, C_g), 126.0 (s, C_h, C_j), 128.4 (s, C_i), 128.4 (s, C_k), 129.2 (s, C_a), 129.3 (d, *J* = 11.3 Hz, C_u), 129.8 (dd, J = 55.0, 26.9 Hz, C_r), 130.1 (s, C_b)131.1 (s, C_d), 131.9 (dd, J = 9.4, 0.9 Hz, C_t) 133.2 (dd, *J* = 23.9, 13.7 Hz, C_s), 133.3 (s, C_e), 133.6 (s, C_n), 135.8 (s, C_c), 169.2 (s, C_{ab}), 169.3 (s, C_{ab}), 169.4 (s, C_{ab}), 170.0 (s, C_{ab}).

^{11}B NMR (160 MHz, DMSO-D6) δ (ppm)= 0.63 (t, *J* = 32.6 Hz).

^{19}F NMR (470 MHz, DMSO-D6) δ (ppm)= -144.52 (dd, *J* = 65.1, 30.2 Hz).

^{31}P NMR (202 MHz, DMSO-D6) δ (ppm) = 29.67.

HR-MS (ESI): *m/z* = calculated for $C_{43}H_{43}Au_1B_1Cl_1F_2N_3O_9P_1S_1Na_1$ $[M+Na]^+$ 1112.1765; found 1112.17971.

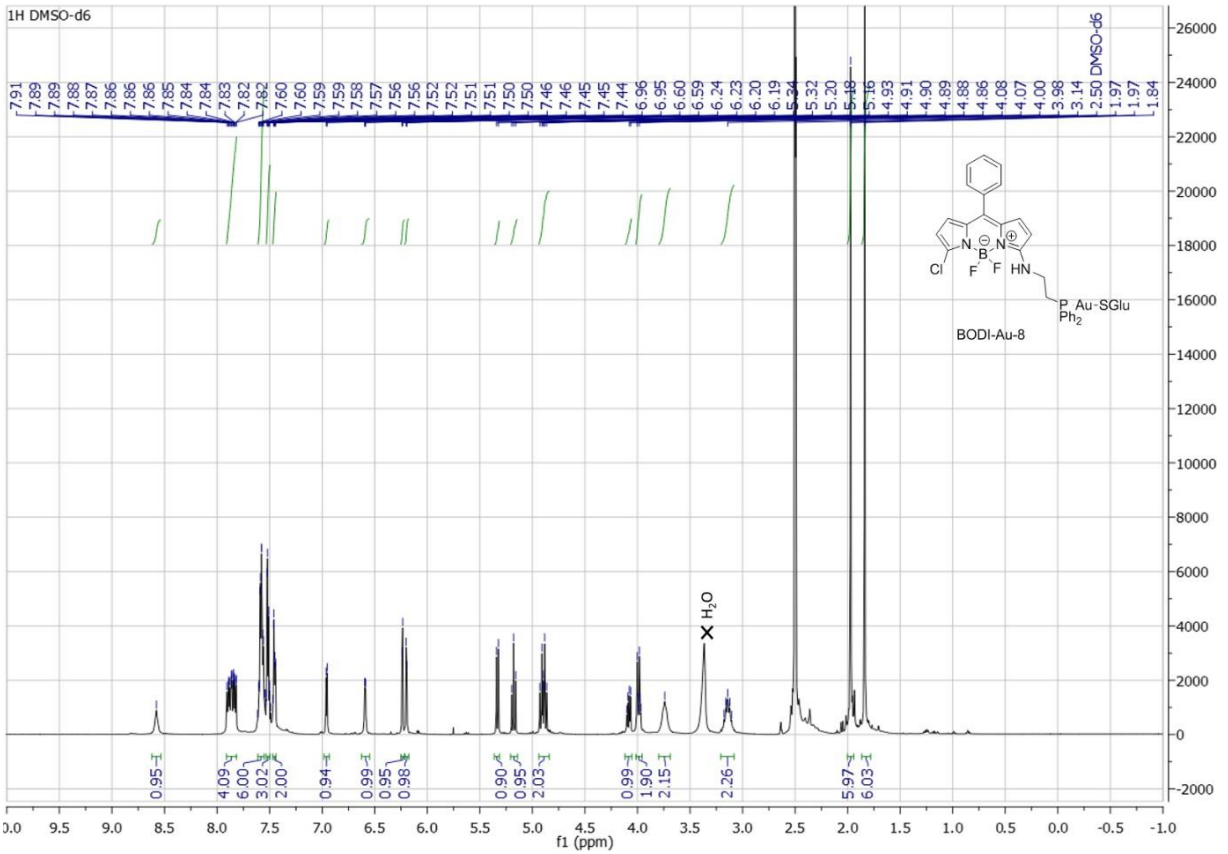

Figure S 43: ^{1}H NMR of **BODI-Au-8** (DMSO, 500 MHZ, 300K)

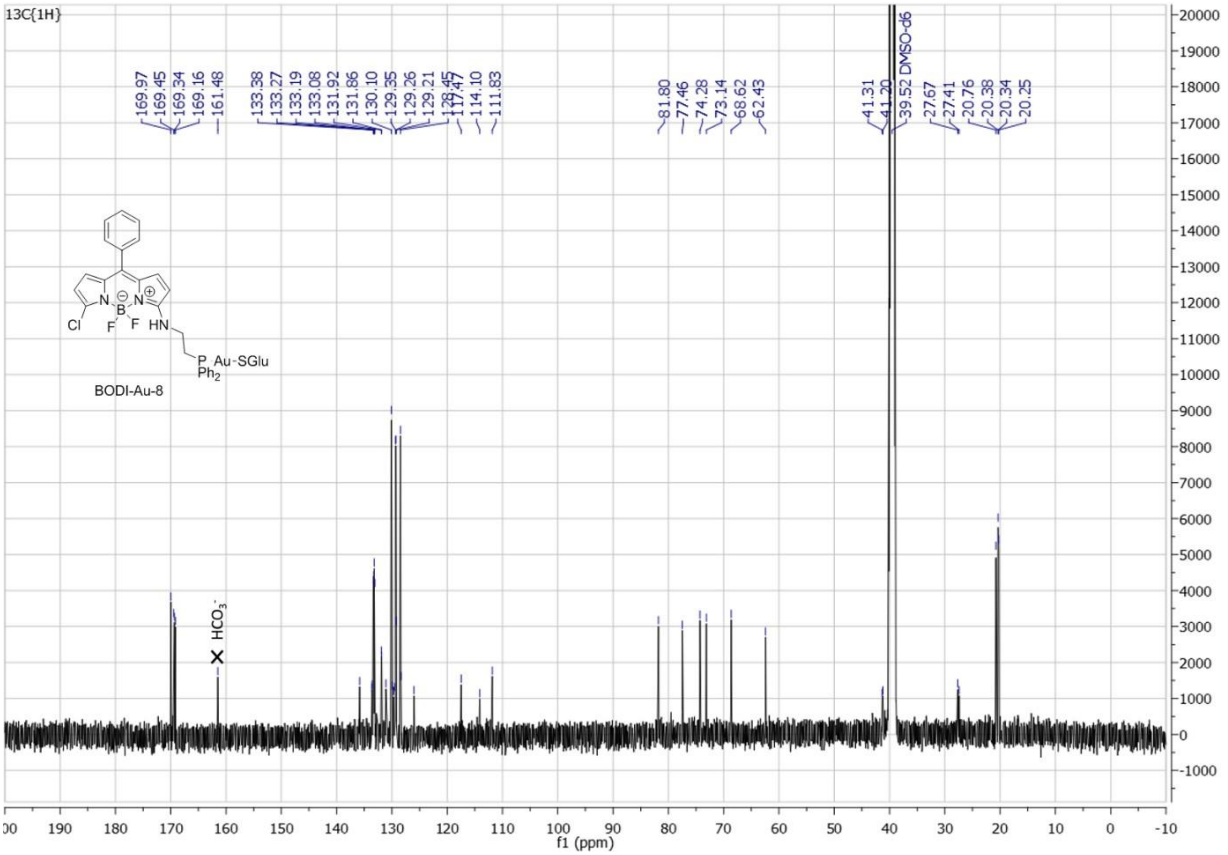

Figure S 44: ^{13}C NMR of **BODI-Au-8** (DMSO, 126 MHZ, 300K)

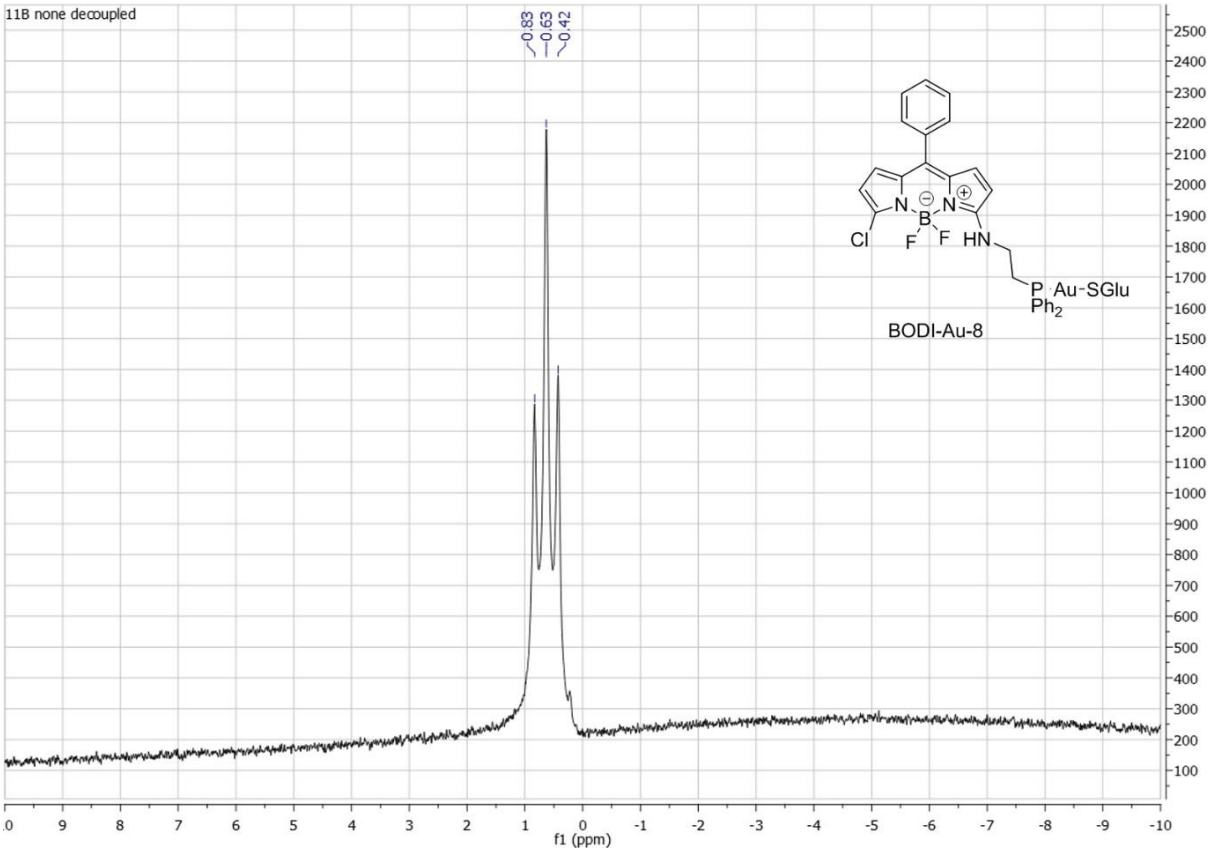

Figure S 45: ^{11}B NMR of **BODI-Au-8** (DMSO, 160 MHZ, 300K)

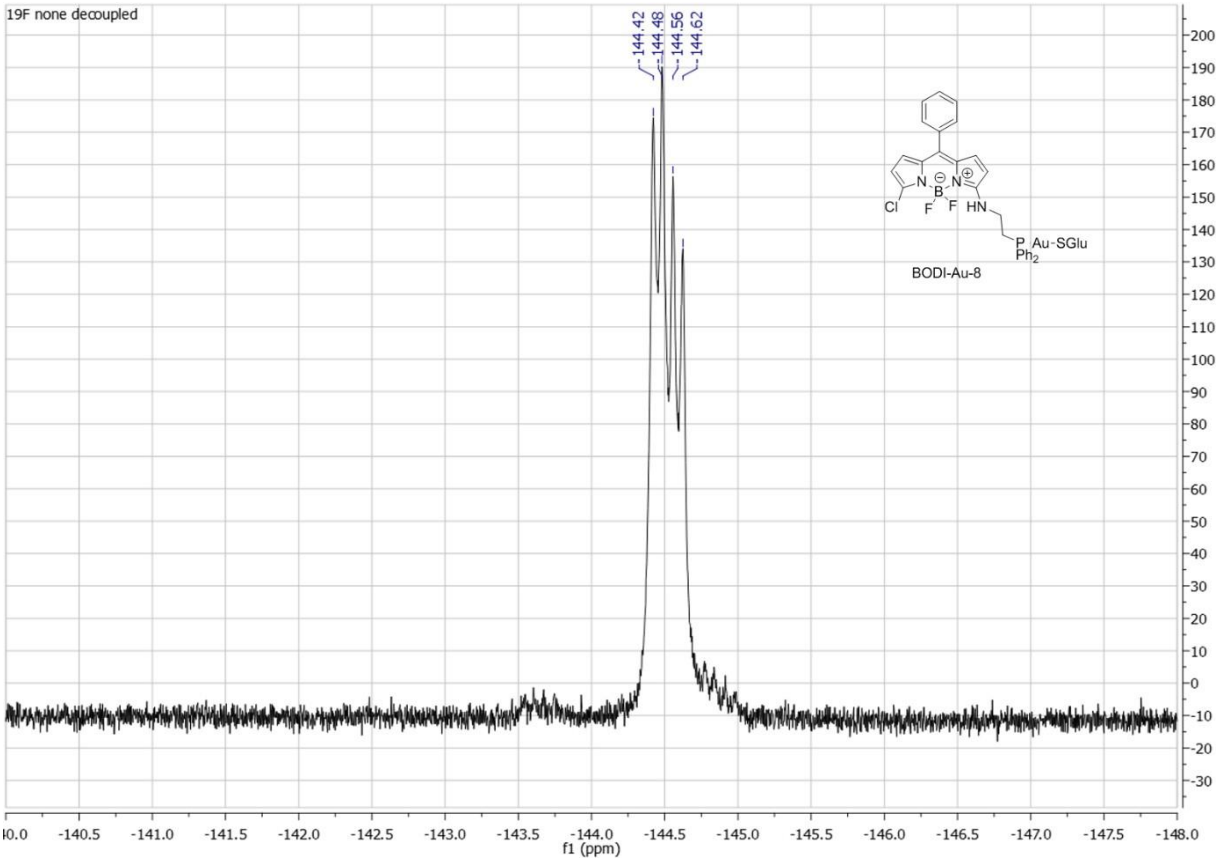

Figure S 46: ^{19}F NMR of **BODI-Au-8** (DMSO, 470 MHZ, 300K)

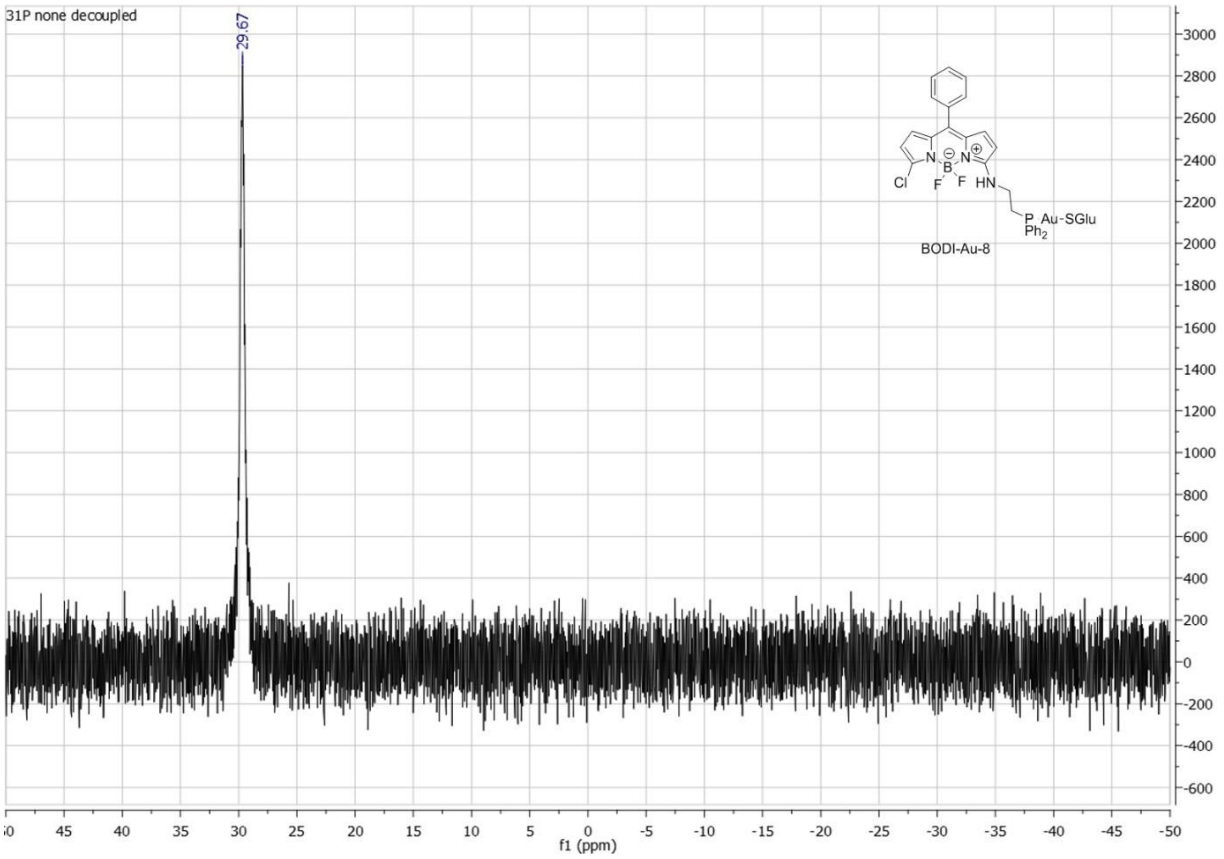

Figure S 47: ^{31}P NMR of **BODI-Au-8** (DMSO, 202 MHZ, 300K)

BODI-Au-9

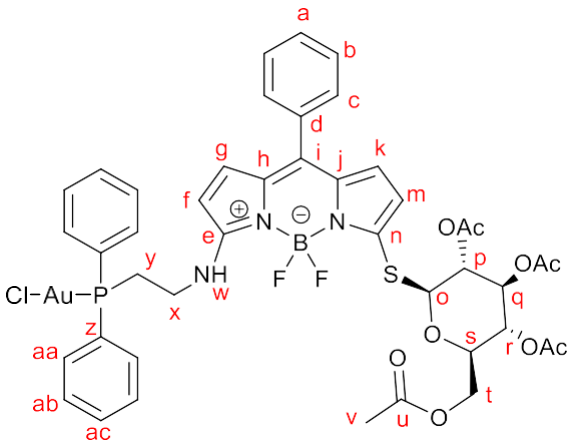

20mg (0.03mmol, 1eq) of BODIPY **4** were placed in a roundbottom flask and suspended in 10 mL of dry THF. 2-(Diphenylphosphino) ethylamine-aurichloride (15.3m, 0.033mmol, 1.1eq) and $NaHCO_3$ (10.1mg, 0.12mmol, 4eq) were added, and the reaction was refluxed for 1h. Upon total consumption of the starting BODIPY the solvents were evaporated and the crude product was purified by column chromatography on silica gel, using CH_2Cl_2 as eluent. The product fractions were evaporated to dryness, dissolved in CH_2Cl_2 and precipitated by addition of pentane twice to obtain **BODI-Au-9** (31mg, 28.5µmol 95% yield) as an orange-pink powder.

^{1}H NMR (500 MHz, DMSO-D6) δ (ppm)= 1.94 (s, 3H, H_v), 1.99 (s, 3H, H_v), 2.01 (s, 6H, H_v), 3.15 (ddd, J = 11.0, 8.4, 5.2 Hz, 2H, H_y), 3.68 (dt, J = 21.4, 7.8 Hz, 2H, H_x), 4.05 (dd, J = 14.8, 5.2 Hz, 1H, H_s), 4.16 (q, J = 5.3 Hz, 2H, H_t), 4.94 (ps-tt, J = 9.6, 2.0 Hz, 2H, H_r, H_p), 5.32 (d, J = 10.1 Hz, 1H, H_o), 5.40 (t, J = 9.4 Hz, 1H, H_q), 6.28 (d, J = 3.8 Hz, 1H, H_f), 6.42 (d, J = 3.8 Hz, 1H, H_g), 6.48 (d, J = 5.1 Hz, 1H, H_m), 6.90 (d, J = 5.1 Hz, 1H, H_k), 7.46 – 7.43 (m, 2H, H_c), 7.54 – 7.50 (m, 3H, H_a, H_b), 7.62 – 7.55 (m, 6H, H_{ab}, H_{ac}), 7.84 – 7.78 (m, 4H, H_{aa}), 8.40 (s, 1H, H_w).

^{13}C NMR (126 MHz, DMSO-D6) δ (ppm) = 20.3 (s, Cv), 20.4 (s, C_v), 20.4 (s, C_v), 20.5 (s, C_v), 27.4 (d, J = 35.6 Hz, C_x), 41.2 (d, J = 10.8 Hz, C_y), 61.9 (s, C_t), 68.1 (s, C_r), 69.3 (s, C_q), 73.0 (s, C_p), 74.3 (s, C_s), 83.3 (s, C_o), 113.0 (s, C_f) 115.2 (s, C_m), 118.7 (s, C_g), 128.5 (s, C_a), 128.7 (s, C_h), 129.0 (d, J = 60.6 Hz, C_z), 129.2 (s, C_k), 129.2 (s, C_i), 129.4 (d, J = 11.7 Hz, C_{ac}), 130.1 (s, C_b), 132.1 (d, J = 2.2 Hz, C_{ab}), 132.8 (s, C_j), 133.2 (d, J = 13.6 Hz, C_{aa}), 133.6 (s, C_d), 133.8 (s, C_e), 135.2 (s, C_c), 161.0 (s, C_n), 169.1 (s, C_u), 169.3 (s, C_u), 169.5 (s, C_u), 170.0 (s, C_u)

^{11}B NMR (160 MHz, DMSO-D6) δ (ppm) = 0.72 (t, J = 33.7 Hz).

^{19}F NMR (470 MHz, DMSO-D6) δ (ppm) = -143.29 (dd, J = 194.7, 81.2 Hz).

^{31}P NMR (202 MHz, DMSO-D6) δ (ppm) = 24.40.

HR-MS (ESI): m/z = calculated for $C_{43}H_{43}Au_1B_1Cl_1F_2N_3O_9P_1S_1Na_1$ $[M+Na]^+$ 1112.17650; found 1112.17964.

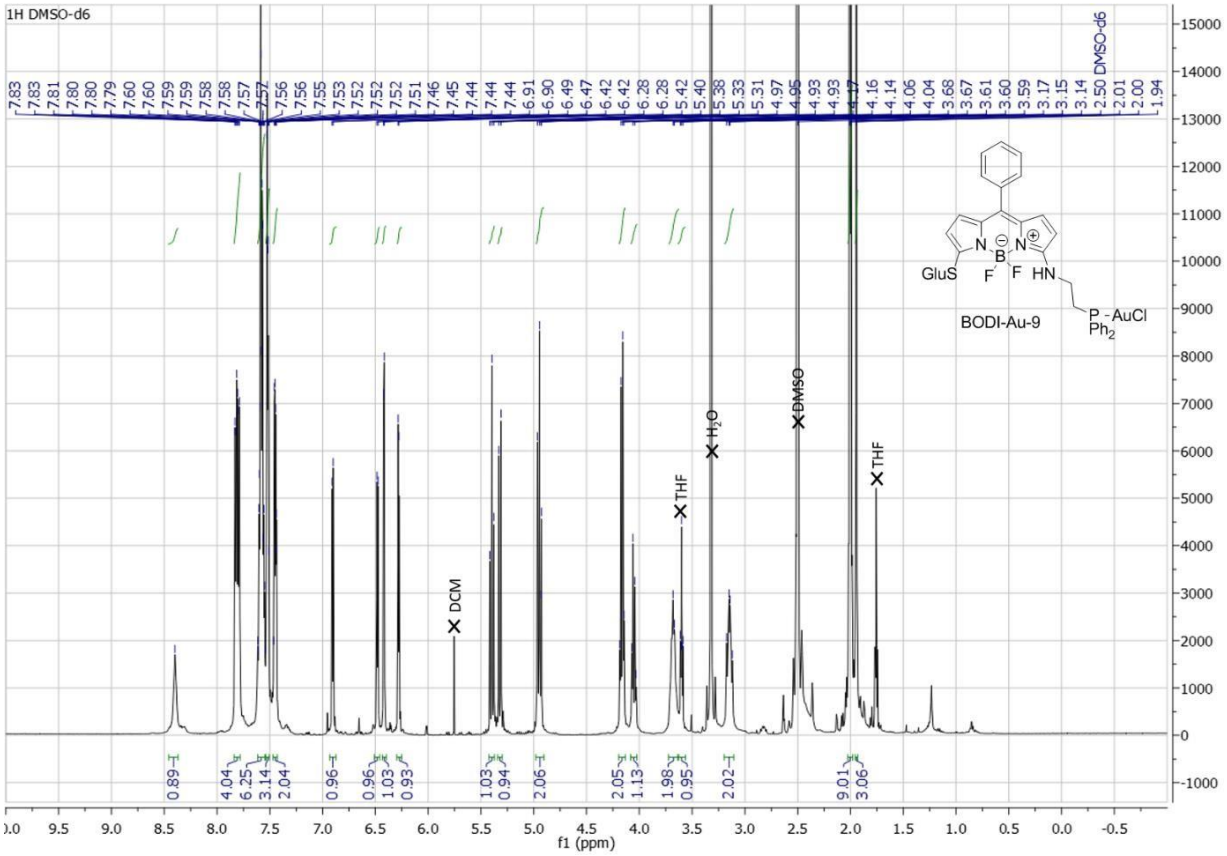

Figure S 48: ^{1}H NMR of **BODI-Au-9** (DMSO, 500 MHZ, 300K)

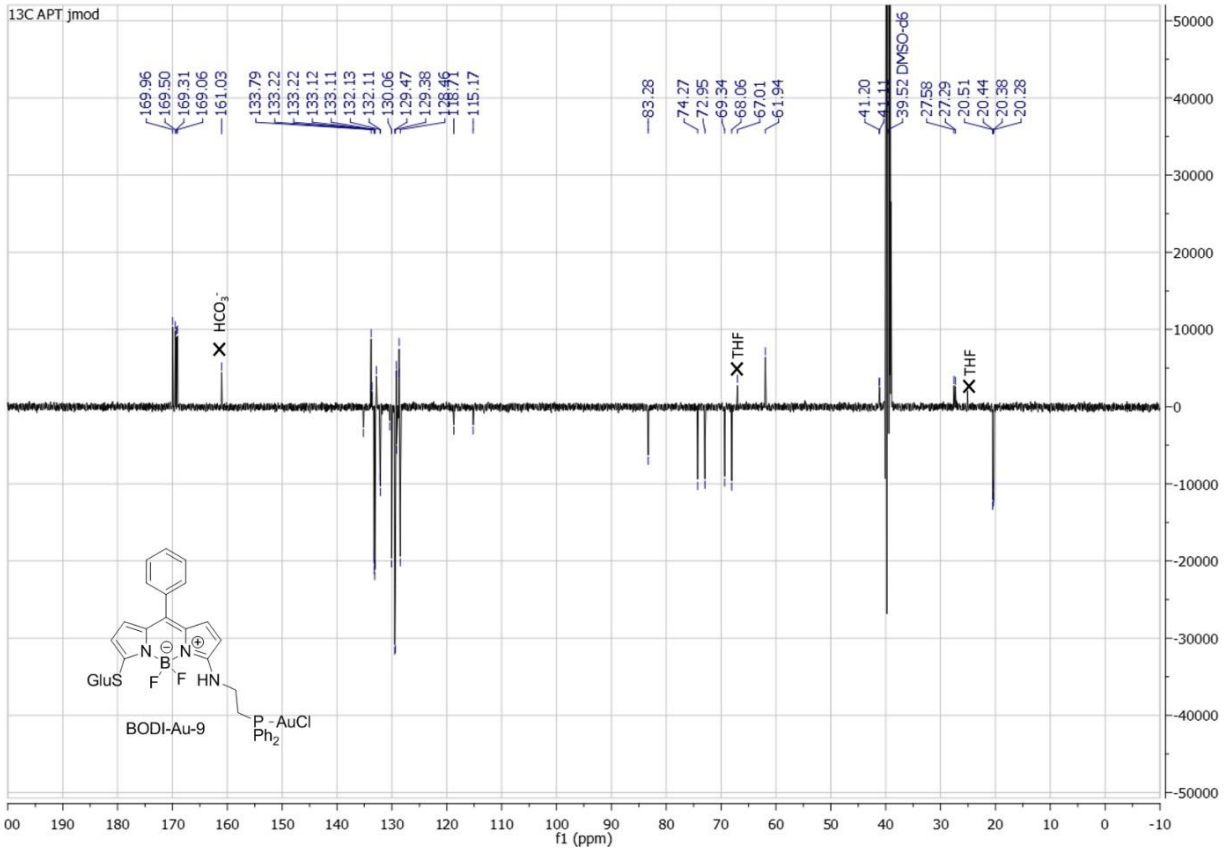

Figure S 49: ^{13}C NMR (APT jmod) of **BODI-Au-9** (DMSO, 126 MHZ, 300K)

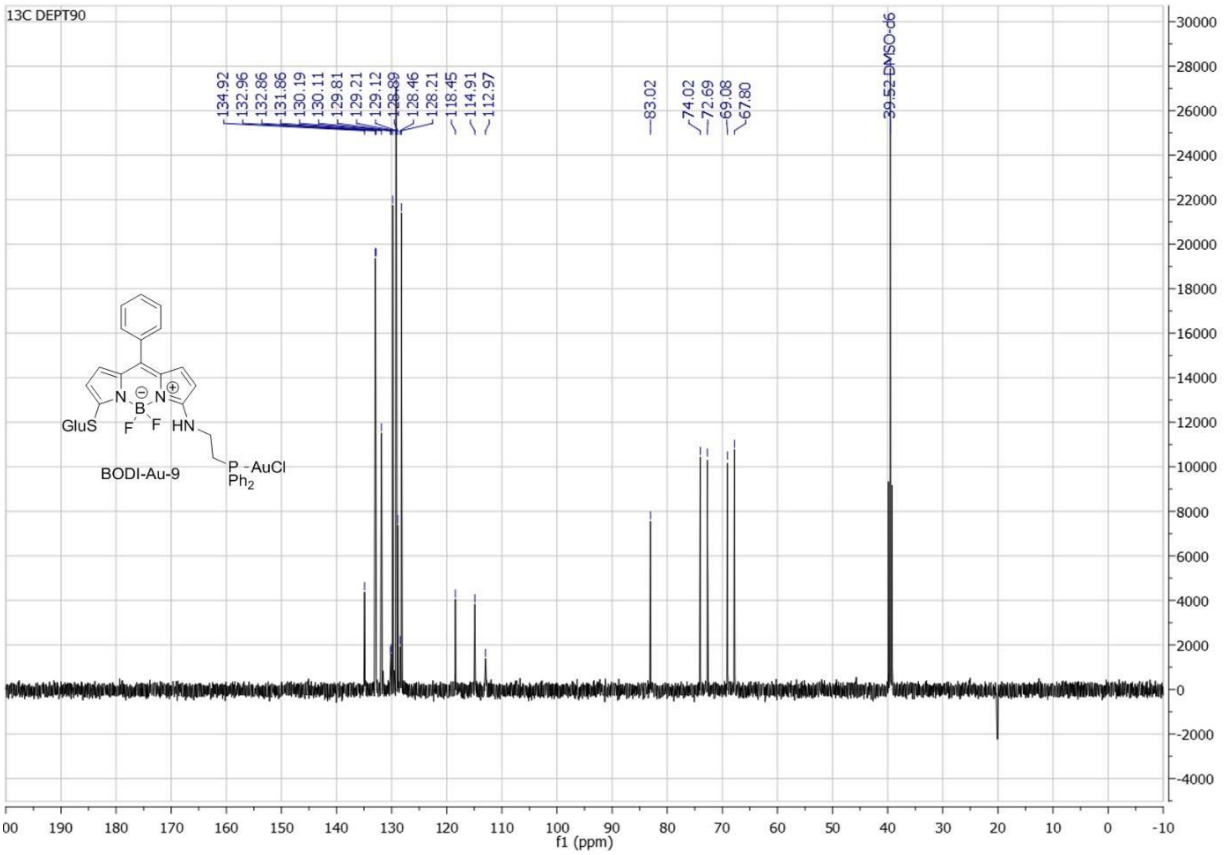

Figure S 50: ^{13}C NMR (DEPT90) of **BODI-Au-9** (DMSO, 126 MHZ, 300K)

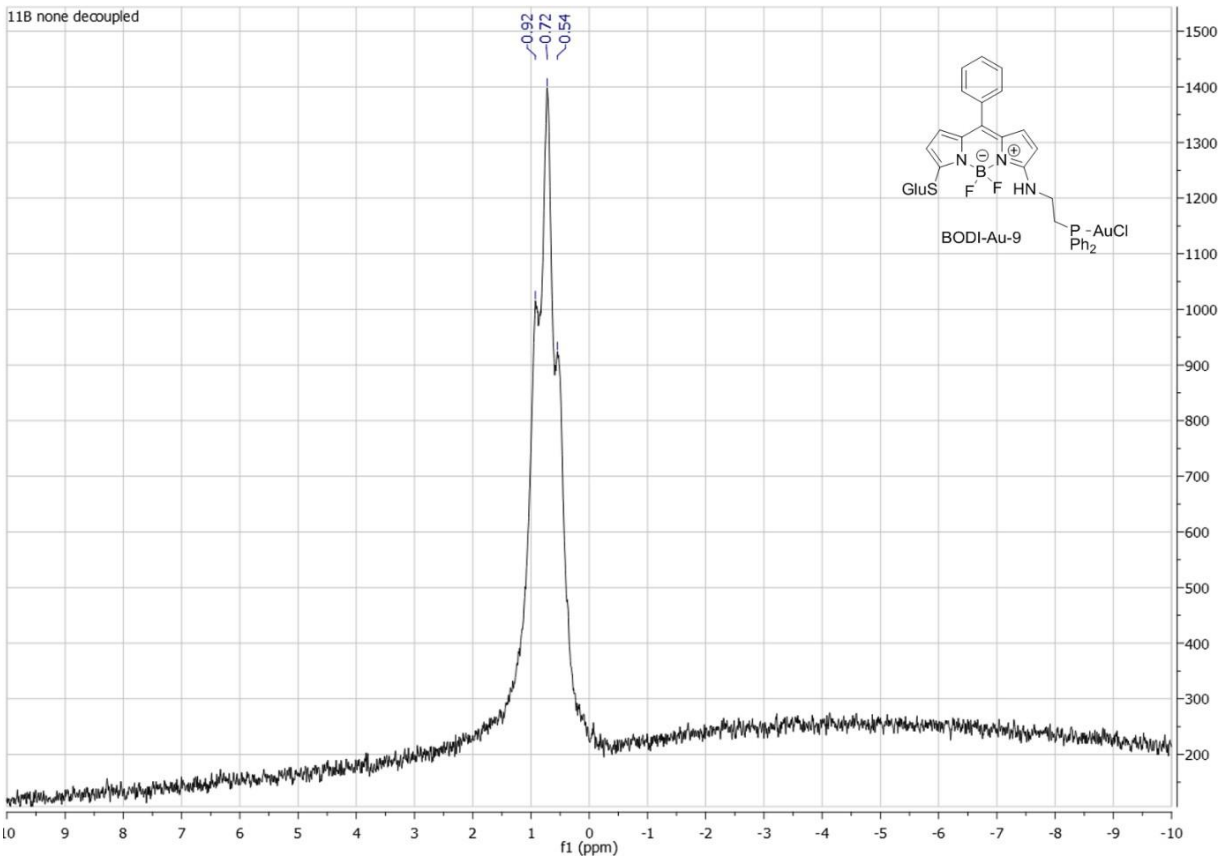

Figure S 51: ^{11}B NMR of **BODI-Au-9** (DMSO, 160 MHZ, 300K)

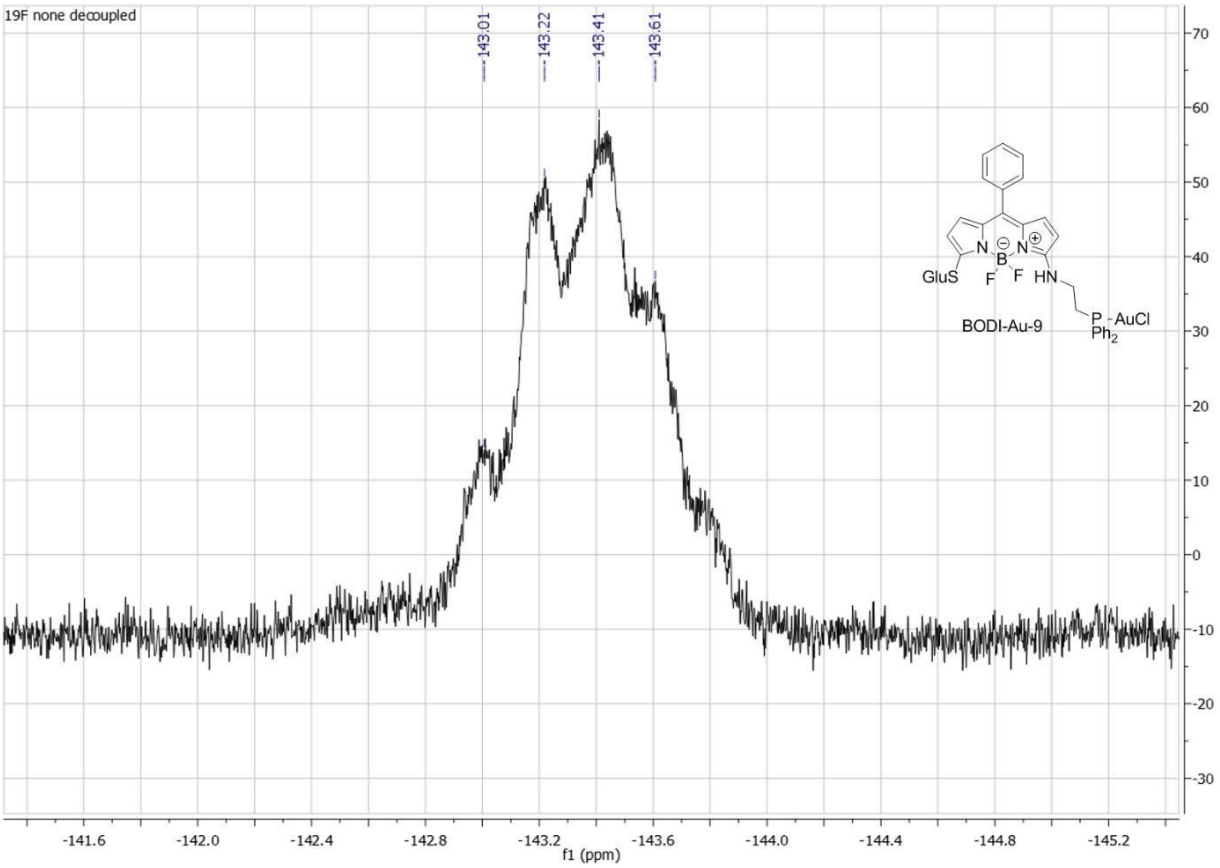

Figure S 52: ^{19}F NMR of **BODI-Au-9** (DMSO, 470 MHZ, 300K)

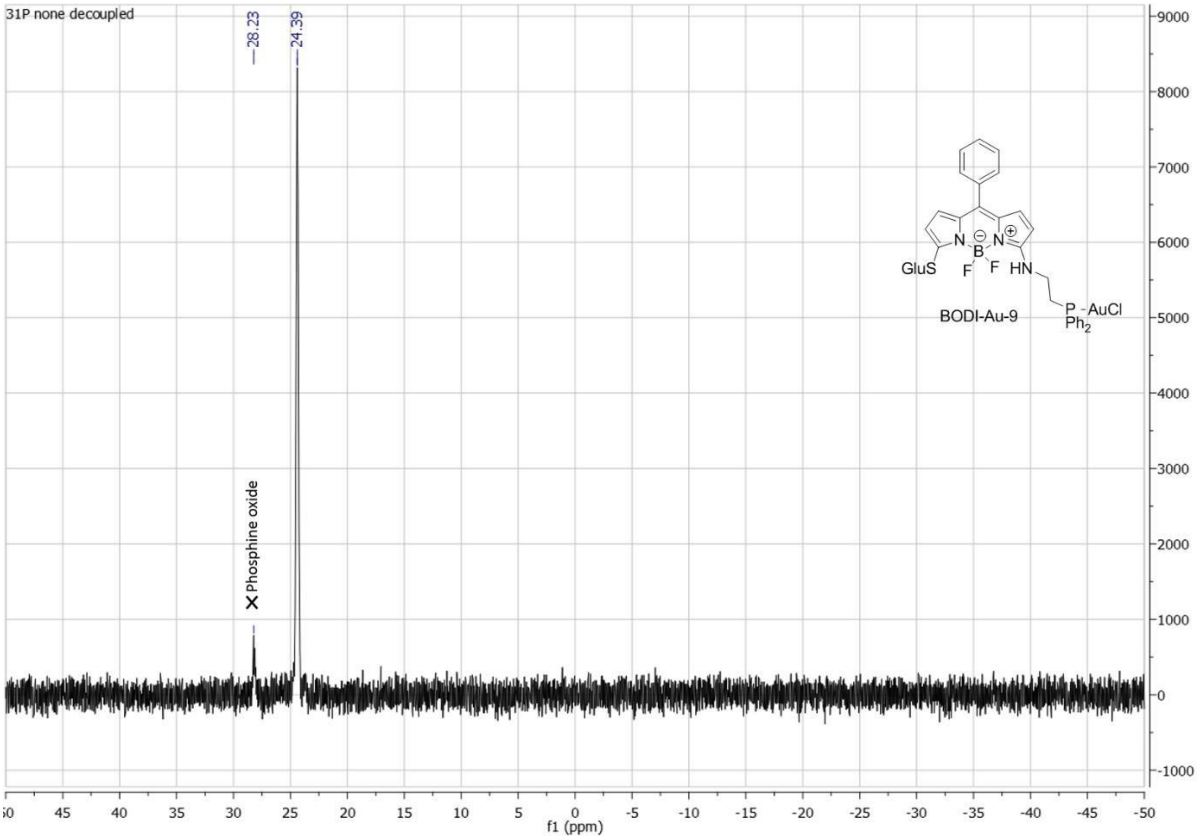

Figure S 53: ^{31}P NMR of **BODI-Au-9** (DMSO, 202 MHZ, 300K)

BODI-Au-10

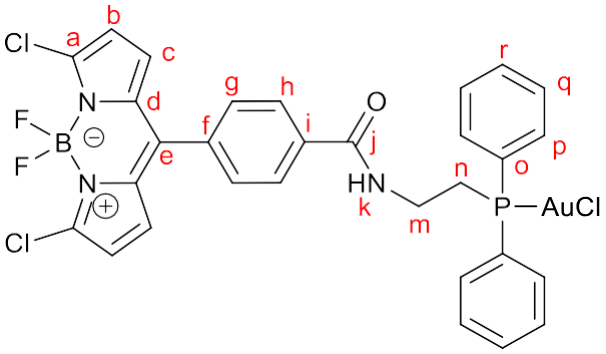

51mg (0.13mmol, 1eq) of BODIPY **3** and 73 mg (50.3mmol, 4eq) of K_2CO_3 were placed in a 50 mL round bottom flask and dissolved in 30 mL dry DCM under argon. 23 µL (0.26mmol, 2eq) of oxalyl chloride were added, followed by a droplet of DMF. The resulting mixture was stirred at room temperature for 45min and then evaporated to dryness. The crude acid chloride was redissolved in 10 mL CH_2Cl_2 and 60.4 mg (0.131 mmol, 1eq) of 2-(diphenylphosphino)ethylamine-aurichloride was added. The resulting solution was stirred for 100 min at room temperature, the solvents were evaporated and the crude product purified by column chromatography on silica gel, using CH_2Cl_2/MeOH (100:0 to 99.2:0.8) as eluent. The solvents were removed under reduced pressure and the product dissolved in a minimal amount of CH_2Cl_2, followed by precipitation with pentane to yield pure **BODI-Au-10** (60.1mg, 71.5µmol, yield = 55%) as a pink-orange solid.

^{1}H NMR (500 MHz, $CDCl_3$) δ (ppm)= 2.96 (dt, ^3J = 10.6, ^4J = 6.5 Hz, 2H, H_n), 3.81 (dq, ^3J = 17.2, ^3J = 6.4 Hz, 2H, H_m), 6.45 (d, ^3J = 4.4 Hz, 2H, H_b), 6.80 (d, ^3J = 4.3 Hz, 2H, H_c), 6.96 (t, ^3J = 5.8 Hz, 1H, H_k), 7.55 – 7.46 (m, 8H, H_g, H_q, H_r), 7.71 (ddd, J = 13.2, 8.0, 1.5 Hz, 4H, H_p), 7.90 (d, ^3J = 8.3 Hz, 2H, H_h).

^{13}C NMR (126 MHz, $CDCl_3$) δ (ppm)= 28.48 (d, J = 38.5 Hz, C_m), 36.60 (d, J = 3.5 Hz, C_n), 119.44 (s, (C_b), 127.47 (s, C_c), 128.59 (d, J = 61.4 Hz, C_o), 129.67 (d, J = 11.8 Hz, C_r), 130.66 (s, C), 130.81 (s, C_g), 131.63 (s, C_h), 132.48 (d, J = 2.6 Hz, C_q), 133.36 (d, J = 13.3 Hz, C_p), 133.69 (s, Cd, C_e), 135.70 (s, C_i), 142.44 (s, C_f), 145.75 (s, C_a), 166.72 (s, C_j).

^{11}B NMR (160 MHz, $CDCl_3$) δ (ppm)= 0.46 (t, $J_{B\text{-}F}$ = 27.7 Hz).

^{19}F NMR (470 MHz, $CDCl_3$) δ (ppm)= -148.10 (dd, J = 55.6, 27.8 Hz).

^{31}P NMR (202 MHz, $CDCl_3$) δ (ppm) = 23.47.

HR-MS (ESI): *m/z* = calculated for $C_{30}H_{23}Au_1B_1Cl_3F_2N_3O_1P_1Na_1$ $[M+Na]^+$ 848.02337; found 828.02495.

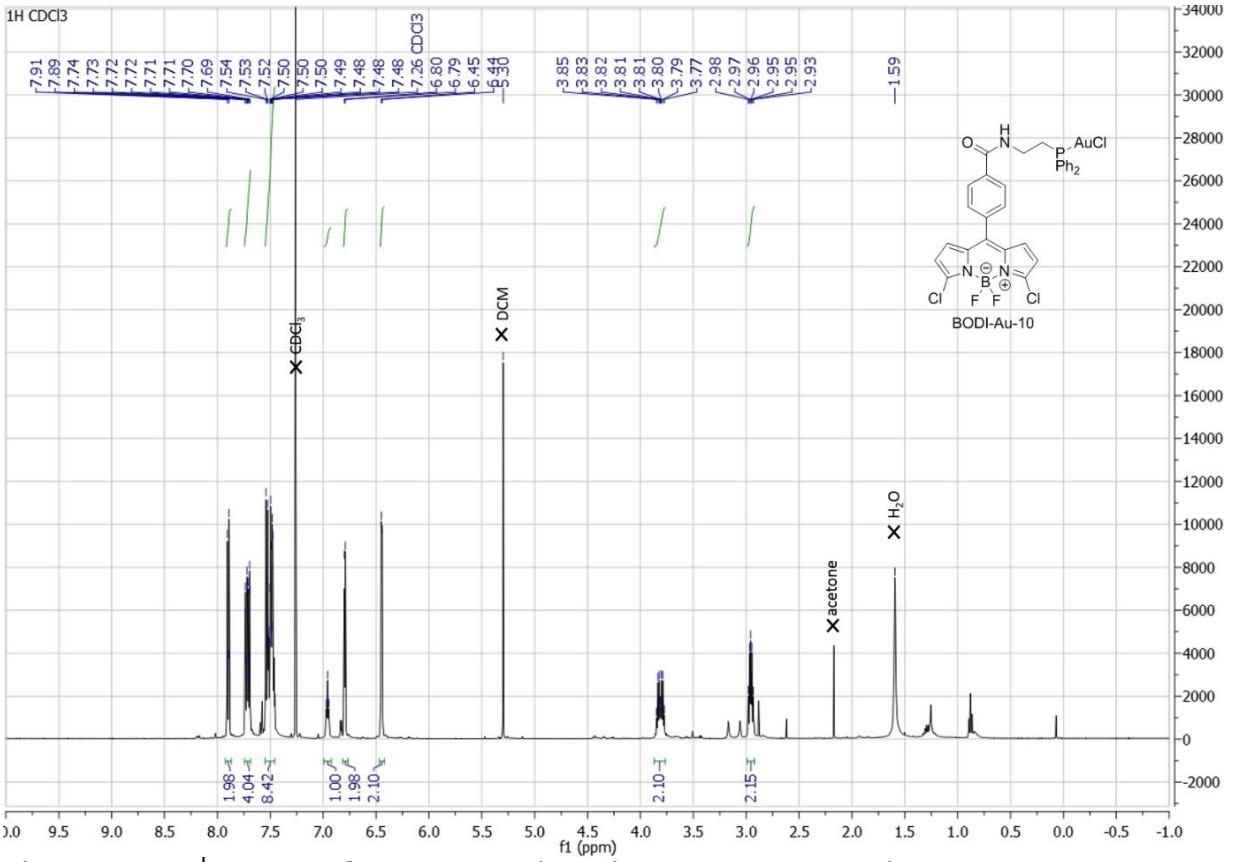

Figure S 54: ^{1}H NMR of **BODI-Au-10** ($CDCl_3$, 500 MHZ, 300K)

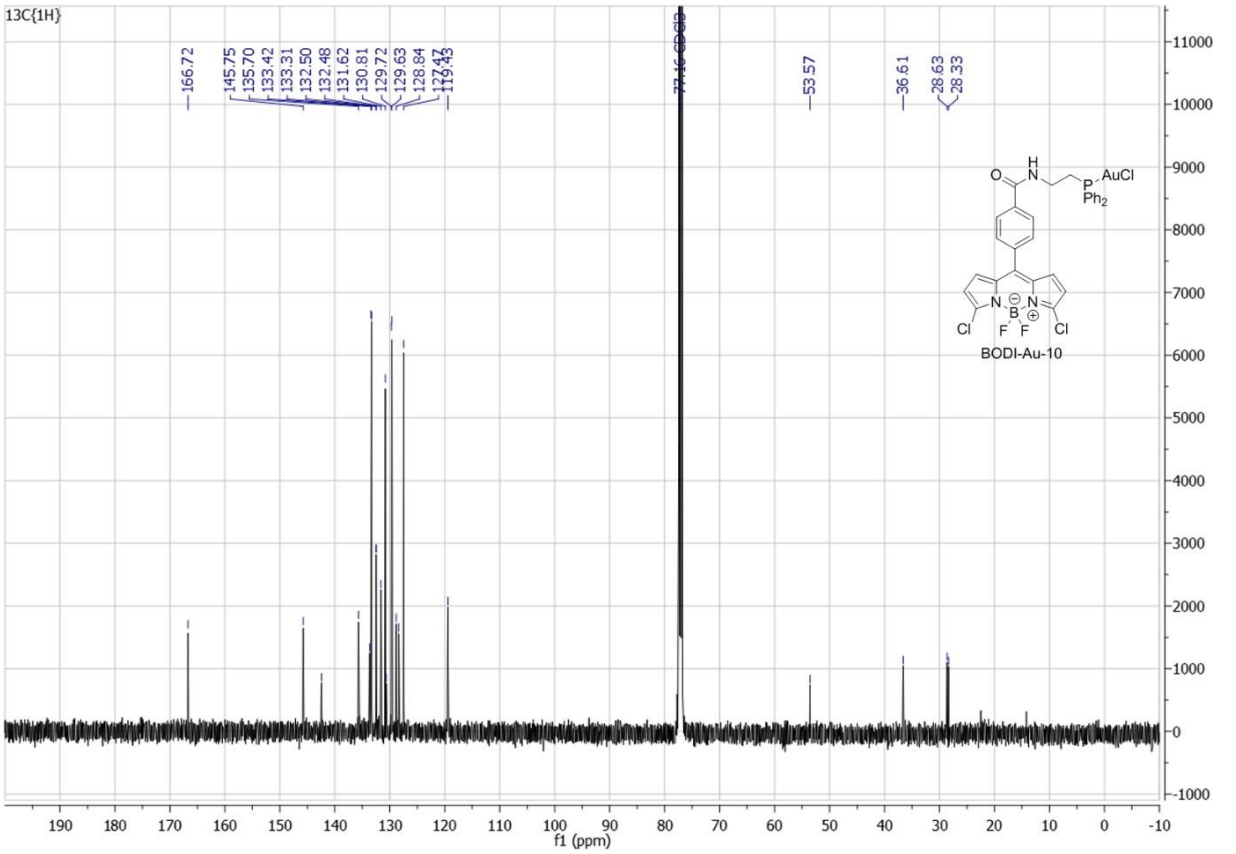

Figure S 55: ^{13}C NMR of **BODI-Au-10** ($CDCl_3$, 126 MHZ, 300K)

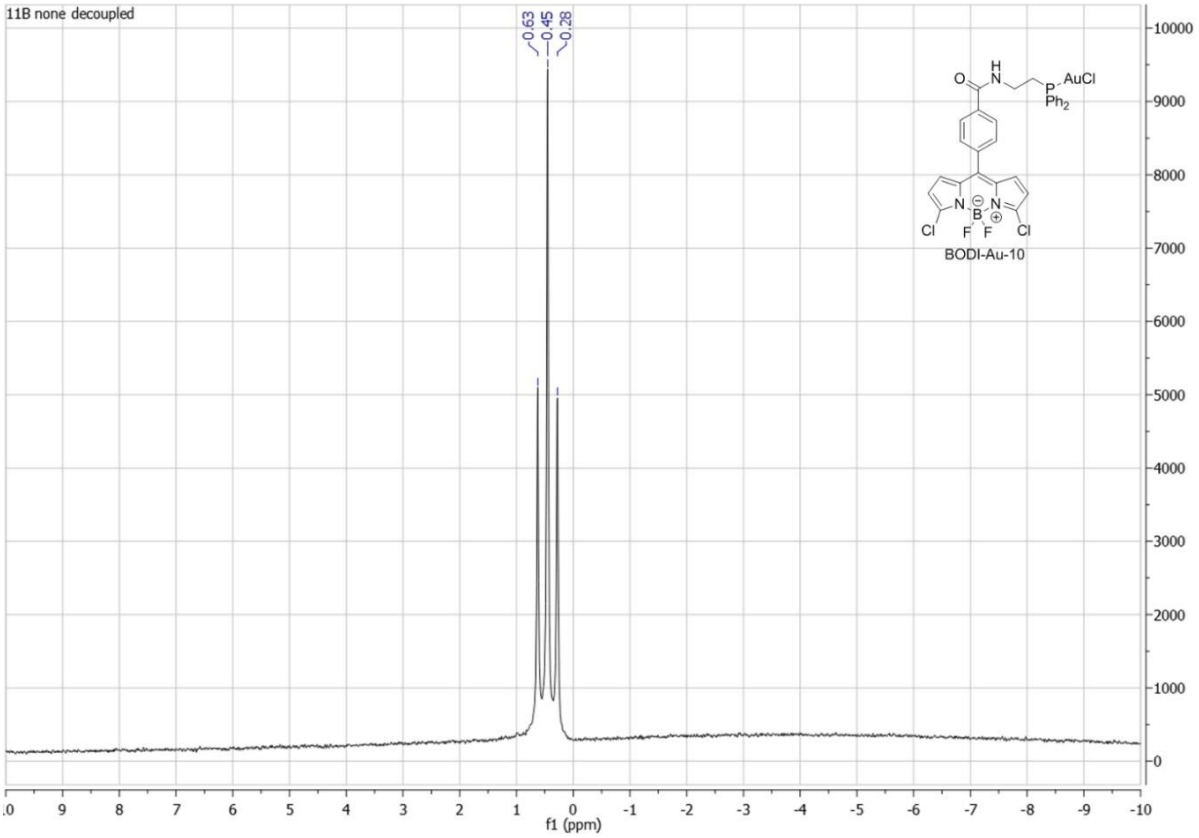

Figure S 56: ^{11}B NMR of **BODI-Au-10** ($CDCl_3$, 160 MHZ, 300K)

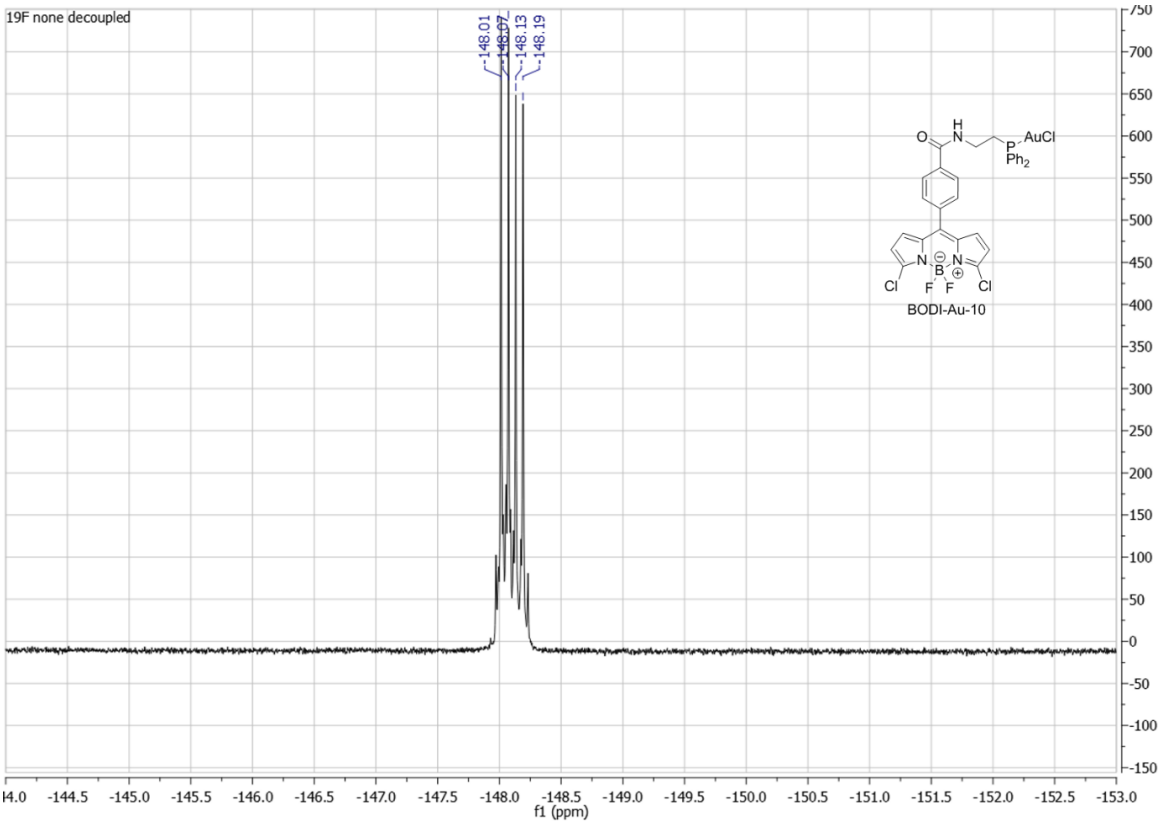

Figure S 57: ^{19}F NMR of **BODI-Au-10** ($CDCl_3$, 470 MHZ, 300K)

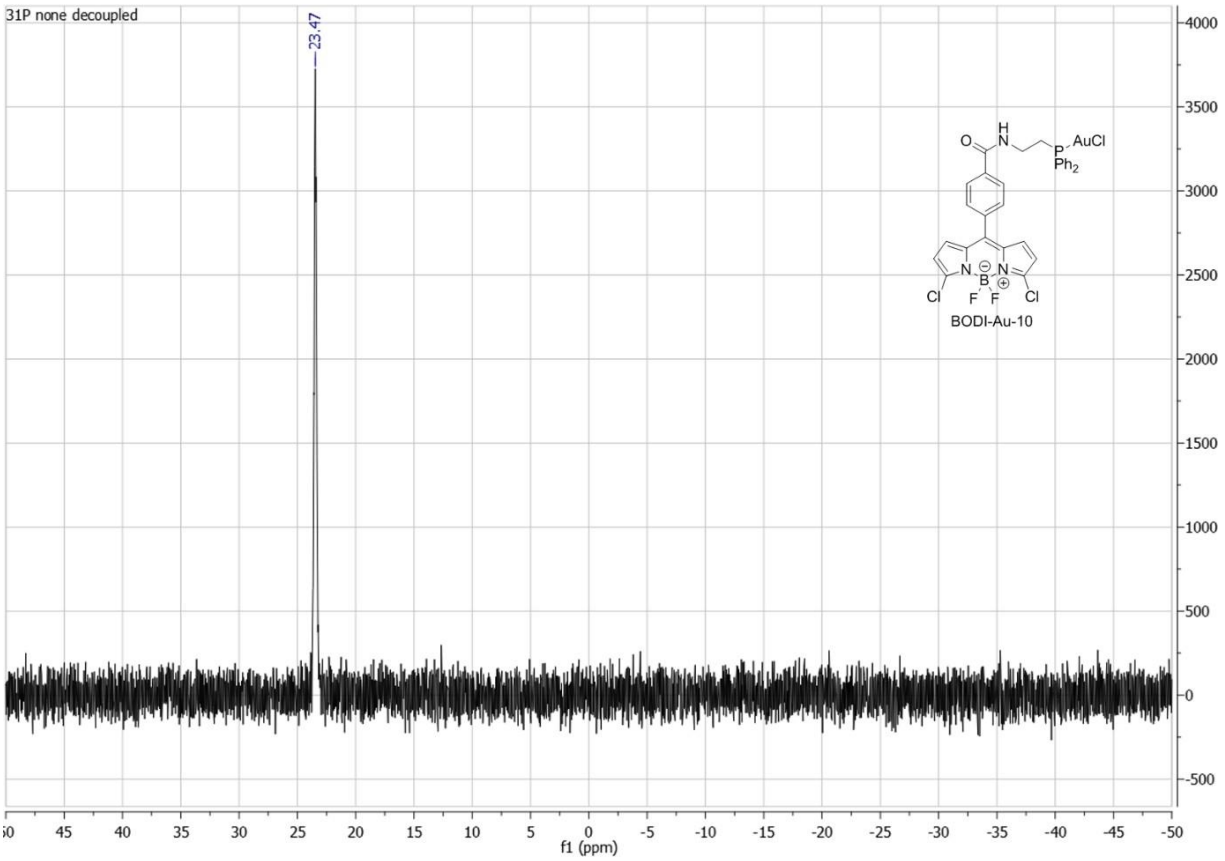

Figure S 58: ^{31}P NMR of **BODI-Au-10** ($CDCl_3$, 202 MHZ, 300K

BODI-Au-11

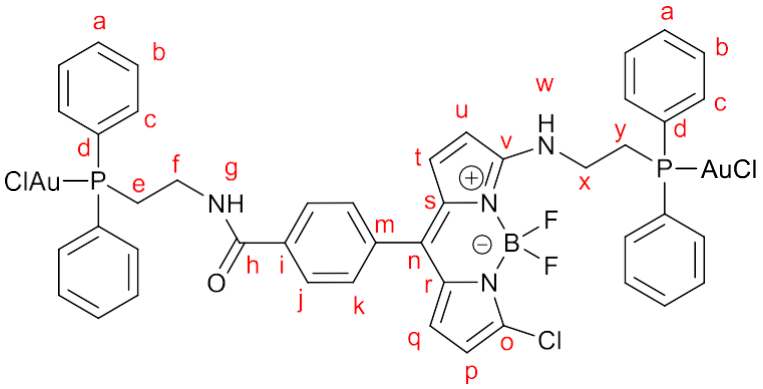

100 mg (0.262mmol, 1 eq) of BODIPY **3** were placed in a round bottom flask and dissolved in 10 mL DCM. 45 µL (0.524mmol, 2 eq) oxalylchloride were added, followed by a droplet of DMF. The reaction was stirred at room temperature for 1h before evaporation to dryness. The solid was redissolved in 10 mL THF. 181mg (1.31mmol, 5eq) of K_2CO_3 and 254mg (0.551mmol, 2.1eq) of 2-(diphenylphosphino)ethylamine-aurichloride were added and the reaction refluxed for 80 min. Upon total consumption of the BODIPY starting material the solvents were evaporated and the product was purified by column chromatography on silica gel, using as eluent CH_2Cl_2/MeOH (99:1). The product fractions were collected, and evaporated to dryness. The product was dissolved in a minimal amount of CH_2Cl_2 and crushed out with pentane twice to yield **BODI-Au-11** (305mg, 243.66 µmol, yield = 93%) as an orange powder.

^{1}H NMR (500 MHz, DMSO-D6) δ (ppm)= 3.09 (dt, *J* = 11.0, 7.0 Hz, 2H, H_y), 3.17 (dd, *J* = 15.9, 11.4 Hz, 2H, H_e), 3.58 (dt, *J* = 20.3, 6.7 Hz, 2H, H_x), 3.80 – 3.65 (m, 2H, H_f), 6.20 (d, *J* = 3.9 Hz, 1H, H_u), 6.26 (d, *J* = 3.8 Hz, 1H, H_t), 6.65 – 6.59 (m, 1H, H_p), 6.96 (t, *J* = 5.6 Hz, 1H, H_q), 7.50 (d, *J* = 8.3 Hz, 2H, H_k), 7.63 – 7.53 (m, 12H, $H_{a,b}$), 7.85 – 7.77 (m, 8H, H_c), 7.89 (d, *J* = 8.3 Hz, 2H, H_j), 8.70 – 8.62 (m, 1H, H_w), 8.86 (t, *J* = 5.6 Hz, 1H, H_g).

^{13}C NMR (126 MHz, DMSO-D6) δ (ppm)= 26.4 (d, *J* = 37.7 Hz, C_f), 27.4 (d, *J* = 39.3 Hz, C_x), 35.8 (d, *J* = 6.2 Hz, C_e), 41.3 (d, *J* = 10.6 Hz, C_y), 111.9 (s, C_p), 114.8 (s, C_u), 117.3 (s, C_q), 126.1 (s, C_r, C_s), 127.4 (s, C_j), 128.9 (d, *J* = 60.8 Hz, C_d), 129.0 (s, C_n), 129.7 (s, C_t), 129.4 (dd, *J* = 11.7, 3.5 Hz, C_a), 130.0 (s, C_k), 130.8 (s, C_i), 132.1 (dd, *J* = 15.5, 2.1 Hz, C_b), 133.2 (dd, *J* = 13.4, 3.5 Hz, C_c), 133.8 (s, C_m), 134.4 (s, C_o), 136.1 (s, C_v), 161.7 (s, C_h).

^{11}B NMR (160 MHz, DMSO-D6) δ (ppm)= 0.66 (t, *J* = 32.5 Hz).

^{19}F NMR (470 MHz, DMSO-D6) δ (ppm)= -144.40 (dd, *J* = 64.4, 31.2 Hz).

^{31}P NMR (202 MHz, DMSO-D6) δ (ppm)= 24.52 – 24.13 (m), 25.35 – 24.84 (m).

^{31}P {^{1}H} NMR (1H decoupled) (202 MHz, DMSO-D6) δ (ppm) = 24.33, 25.09.

HR-MS (ESI): *m/z* = calculated for $C_{44}H_{38}Au_2B_1Cl_3F_2N_4O_1P_2Na_1$ $[M+Na]^+$ 1273.08413; found 1273.08874.

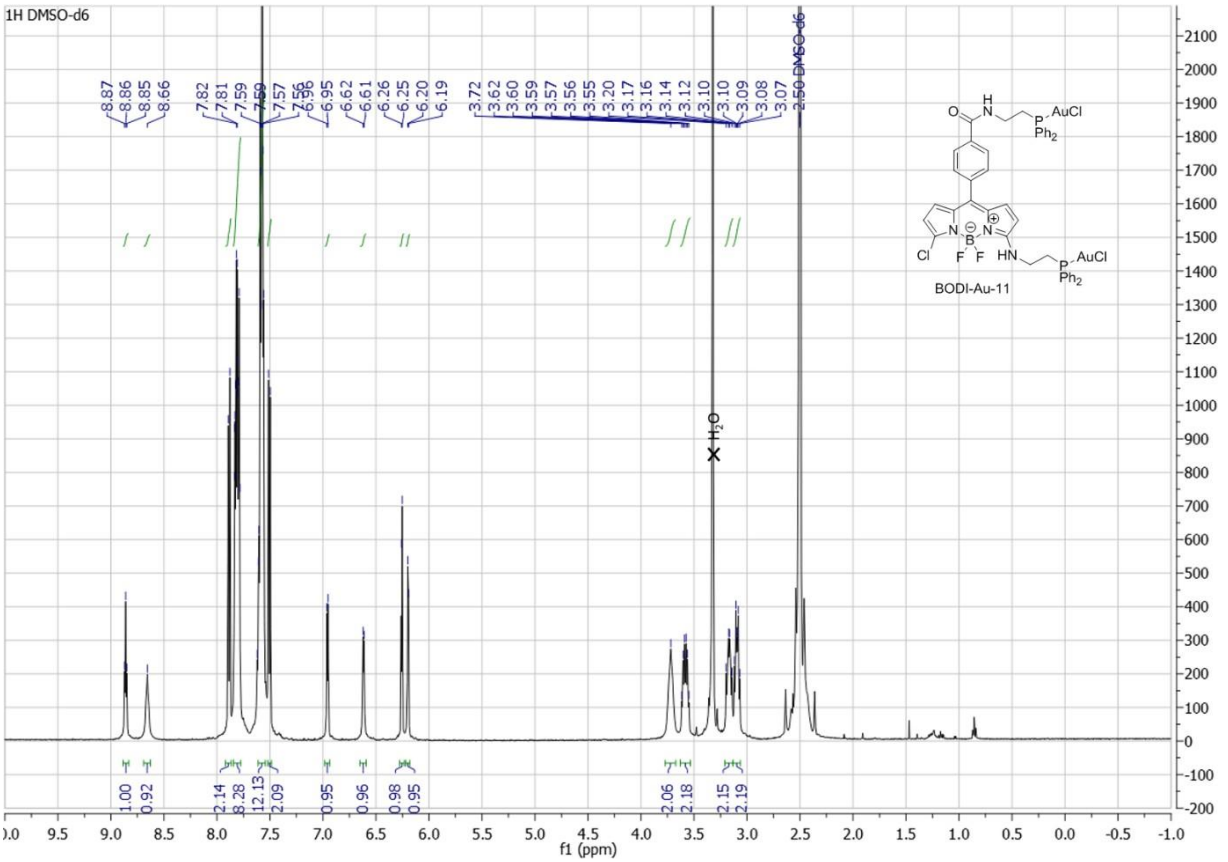

Figure S 59: ^{1}H NMR of **BODI-Au-11** (DMSO, 500 MHZ, 300K)

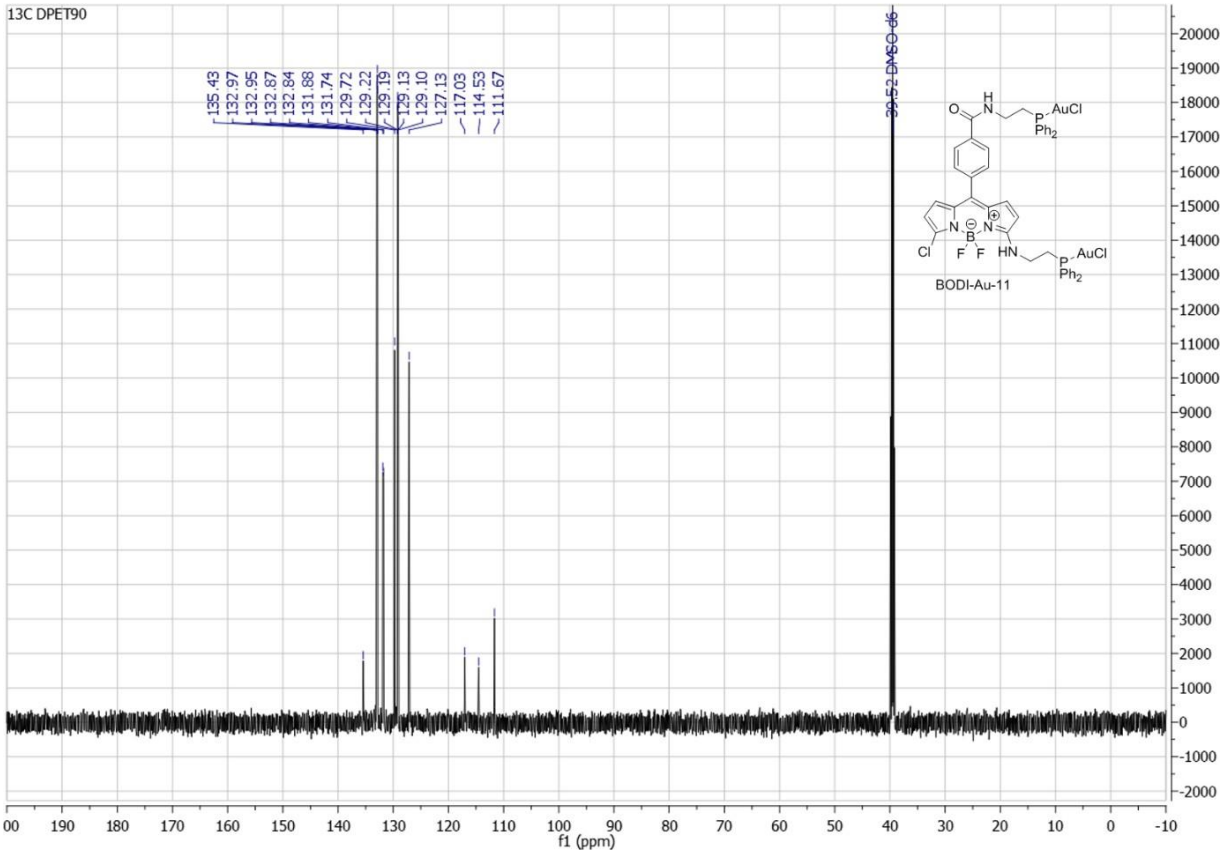

Figure S 60: ^{13}C NMR (DEPT90) of BODI-Au-11 (DMSO, 126 MHZ, 300K)

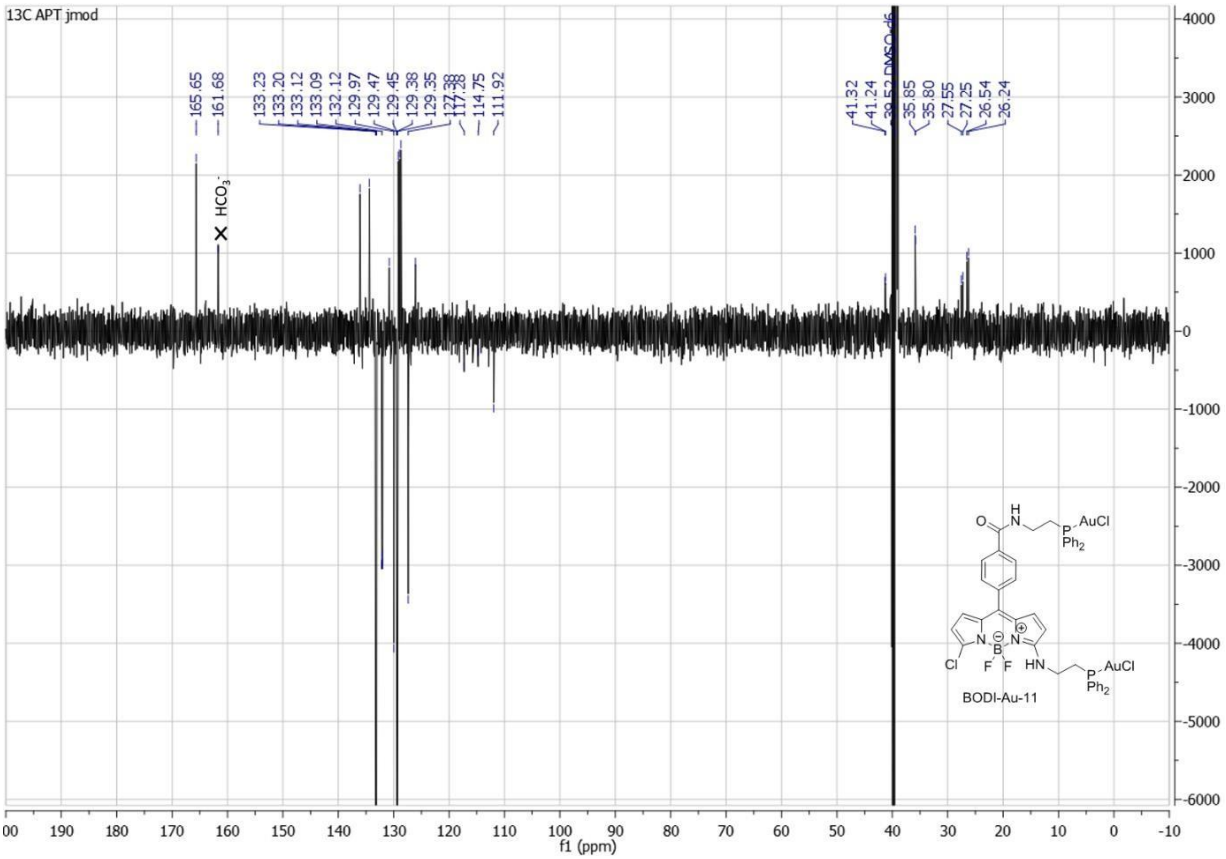

Figure S 61: ^{13}C NMR (APT jmod) of **BODI-Au-11** (DMSO, 126 MHZ, 300K)

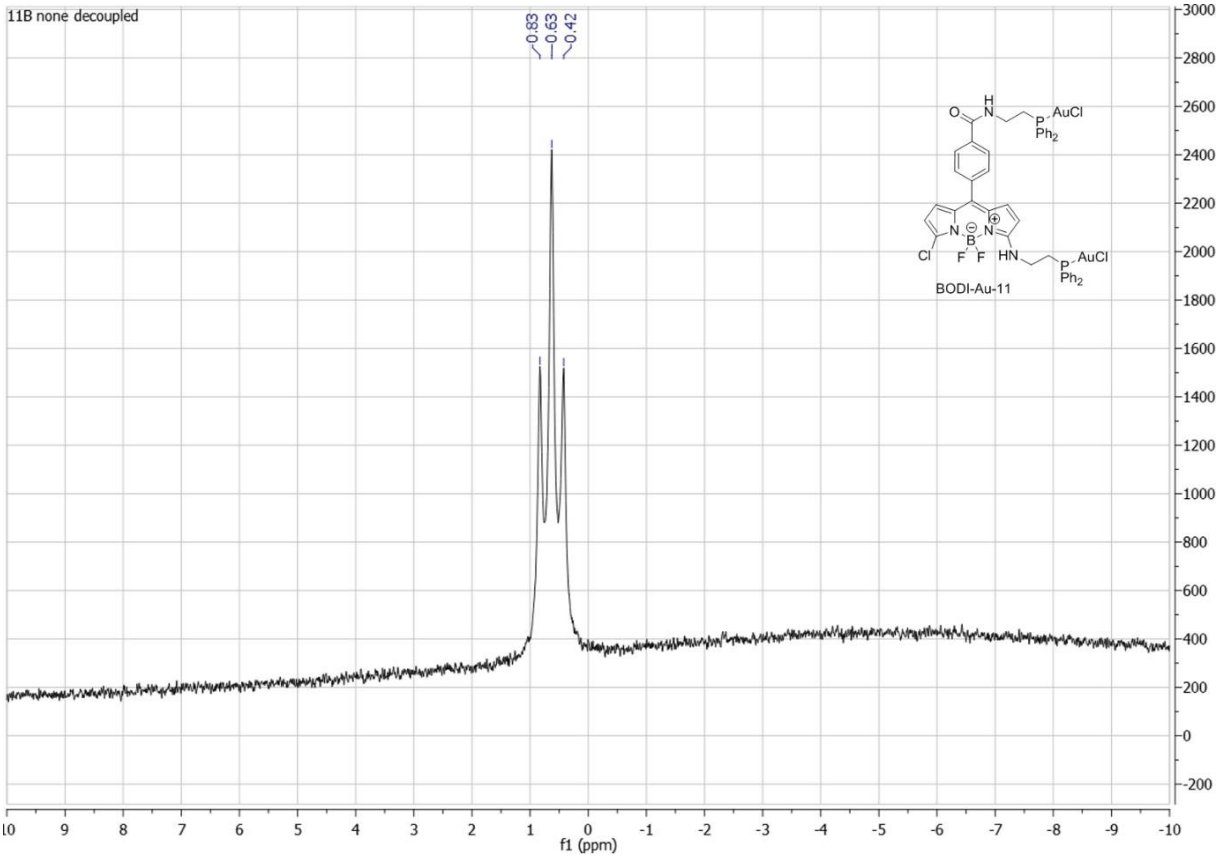

Figure S 62: ^{11}B NMR of **BODI-Au-11** (DMSO, 160 MHZ, 300K)

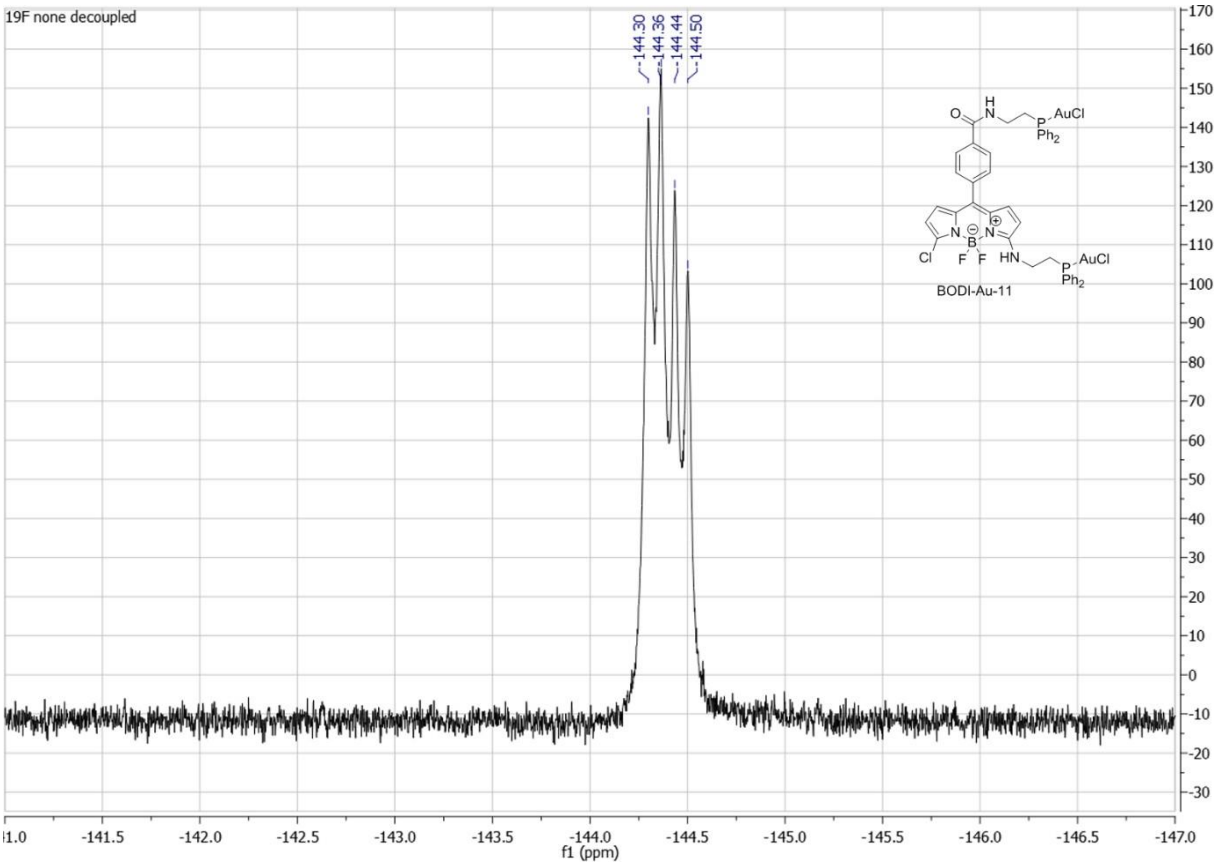

Figure S 63: ^{19}F NMR of **BODI-Au-11** (DMSO, 470 MHZ, 300K)

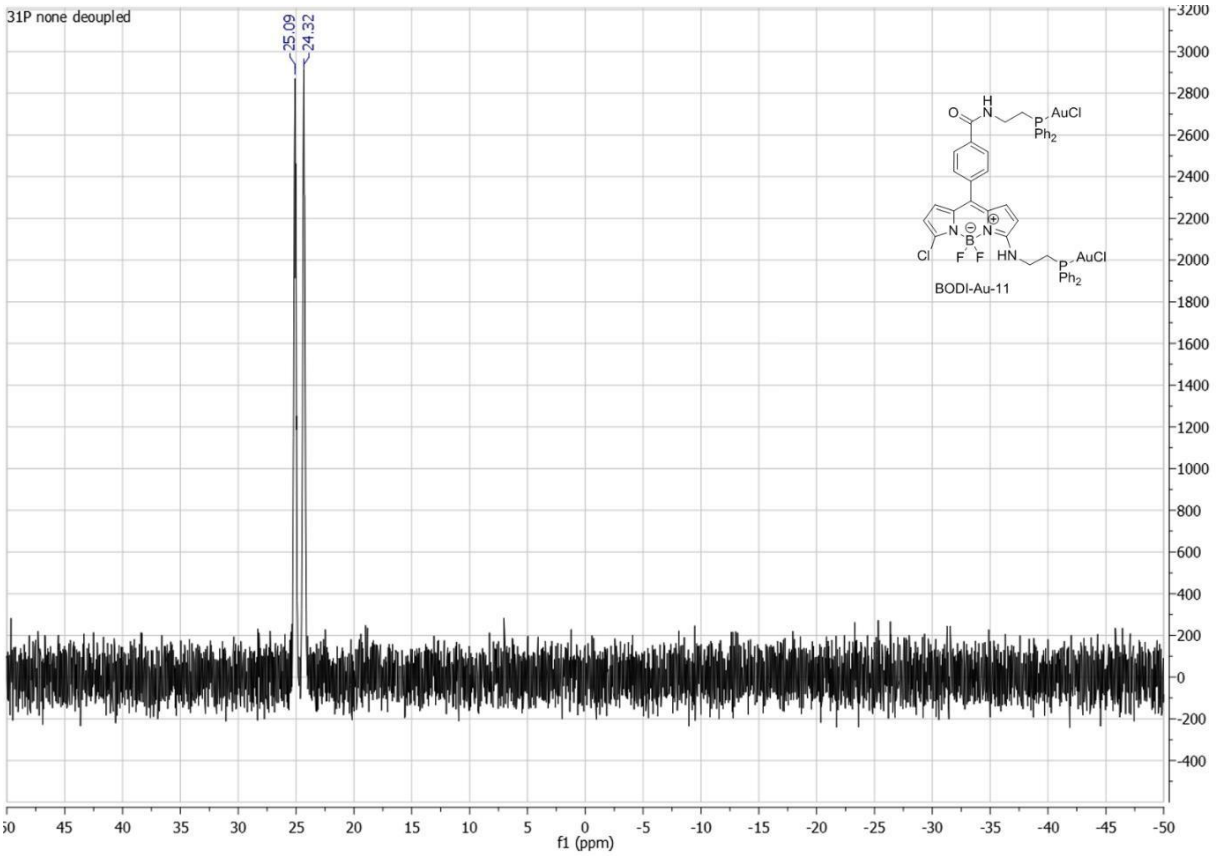

Figure S 64: ^{31}P NMR of **BODI-Au-11** (DMSO, 202 MHZ, 300K)

BODI-Au-12

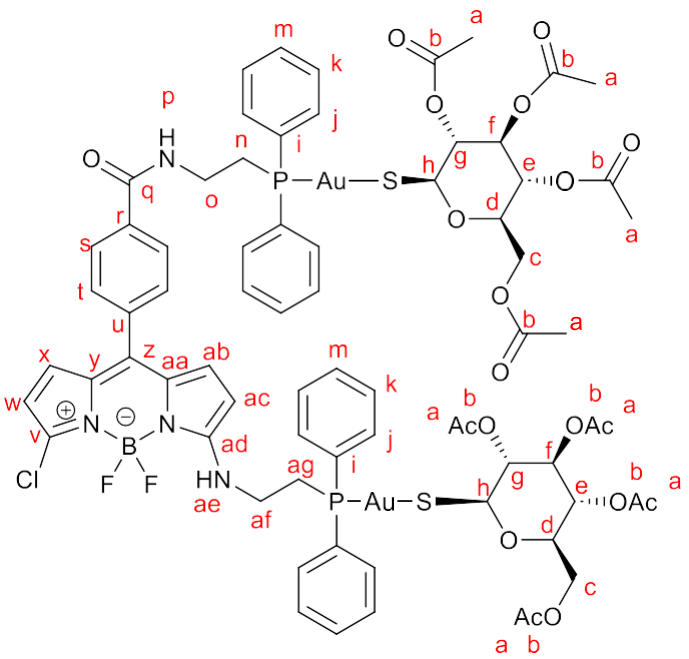

26,2mg (72µmol) β-thioglucose-tetraacetate (1 eq) was dissolved in acetone (1 mL). 72µL 1M NaOH 1M NaOH (1 eq) was added and the resulting solution stirred for 15 min. 45mg (36µmol) of **BODI-Au-11** was placed in a separate roundbottom flask and dissolved in acetone (5 mL). The thioglucose solution was added at once and the reaction stirred for 30 min at room temperature. The solvents were evaporated, CH_2Cl_2 (10 mL) was added, and the supernatant separated and evaporated. The resulting crude product was dissolved in a minimal amount of CH_2Cl_2 and precipitated with pentane to obtain the pure target compound as an orange powder (62mg, 32.4 µmol, yield = 90%).

^{1}H NMR (500 MHz, DMSO-D6) δ (ppm)= 1.84 (s, 6H, H_a), 1.88 (s, 6H, H_a), 1.96 (s, 6H, H_a), 1.97 (s, 6H, H_a), 3.20 – 2.99 (m, 4H, H_{ag}, H_n), 3.60 (dt, *J* = 12.7, 6.9 Hz, 2H, H_o), 3.76 (s, 2H, H_{af}), 3.99 (dt, *J* = 5.6, 2.6 Hz, 4H, H_c, H_d), 4.08 (dd, *J* = 12.7, 5.7 Hz, 2H, H_c), 4.90 (dt, *J* = 18.8, 9.6 Hz, 4H, H_g, H_e), 5.19 (t, *J* = 9.5 Hz, 2H, H_f), 5.33 (d, *J* = 9.4 Hz, 2H, H_h), 6.21 (d, *J* = 3.8 Hz, 1H, H_{ac}), 6.26 (d, *J* = 3.8 Hz, 1H, H_{ab}), 6.63 (d, *J* = 5.1 Hz, 1H, H_w), 6.97 (d, *J* = 5.1 Hz, 1H, H_x), 7.50 (d, J = 8.3Hz, 2H, H_s), 7.61 – 7.54 (m, 12H, $H_{k,m}$), 7.92 – 7.81 (m, 10H, H_j, H_s), 8.65 (t, *J* = 6.4 Hz, 1H, H_{ae}), 8.81 (t, *J* = 5.5 Hz, 1H, H_p).

^{13}C NMR (126 MHz, DMSO-D6) δ (ppm)= 20.3 (s, C_a), 20.3 (s C_a), 20.4 (s C_a), 20.8 (s C_a), 26.5 (d, *J* = 34.1 Hz, C_o) 27.4 (s, C_{af}), 35.8 (d, *J* = 8.0 Hz, C_n), 41.3 (d, *J* = 10.2 Hz, C_{ag}), 62.4 (s, C_c), 68.6 (s, C_e), 73.2 (s, C_f), 74.3 (s, C_g), 77.4 (s, C_d), 81.8 (s, C_h), 111.9 (s, C_w), 114.5 (s, C_{ac}), 117.3 (s, C_x) 126.1 (s, C_y,C_{aa}), 127.3 (s, C_{ab}), 127.4 (s, C_r), 129.3 (d, *J* = 11.1 Hz, C_m), 129.9 (d, J = 56.6 Hz, C_i), 130.0 (s, C_s), 130.8 (s, C_z), 132.0 – 131.5 (m, C_k), 133.3 – 133.0 (m, C_j), 133.4 (s, C_t) 133.7 (s, C_u), 134.4 (s, C_v), 136.1 (s, C_{ad}), 161.6 (s, C_q), 165.6 (s, CHCO3-), 169.1 (s, C_b), 169.3 (s, C_b), 169.5 (s, C_b), 170.0 (s, C_b).

^{11}B NMR (160 MHz, DMSO-D6) δ (ppm)= 0.62 (t, *J* = 32.4 Hz).

^{19}F NMR (470 MHz, DMSO-D6) δ (ppm)= -144.45 (dd, *J* = 64.6, 30.5 Hz).

^{31}P NMR (202 MHz, DMSO-D6) δ (ppm) = 29.66.

HR-MS (ESI): *m/z* = calculated for $C_{72}H_{76}Au_2B_1Cl_1F_2N_4O_{19}P_2S_2Na_1$ $[M+Na]^+$ 1927.30049; found 1927.30492.

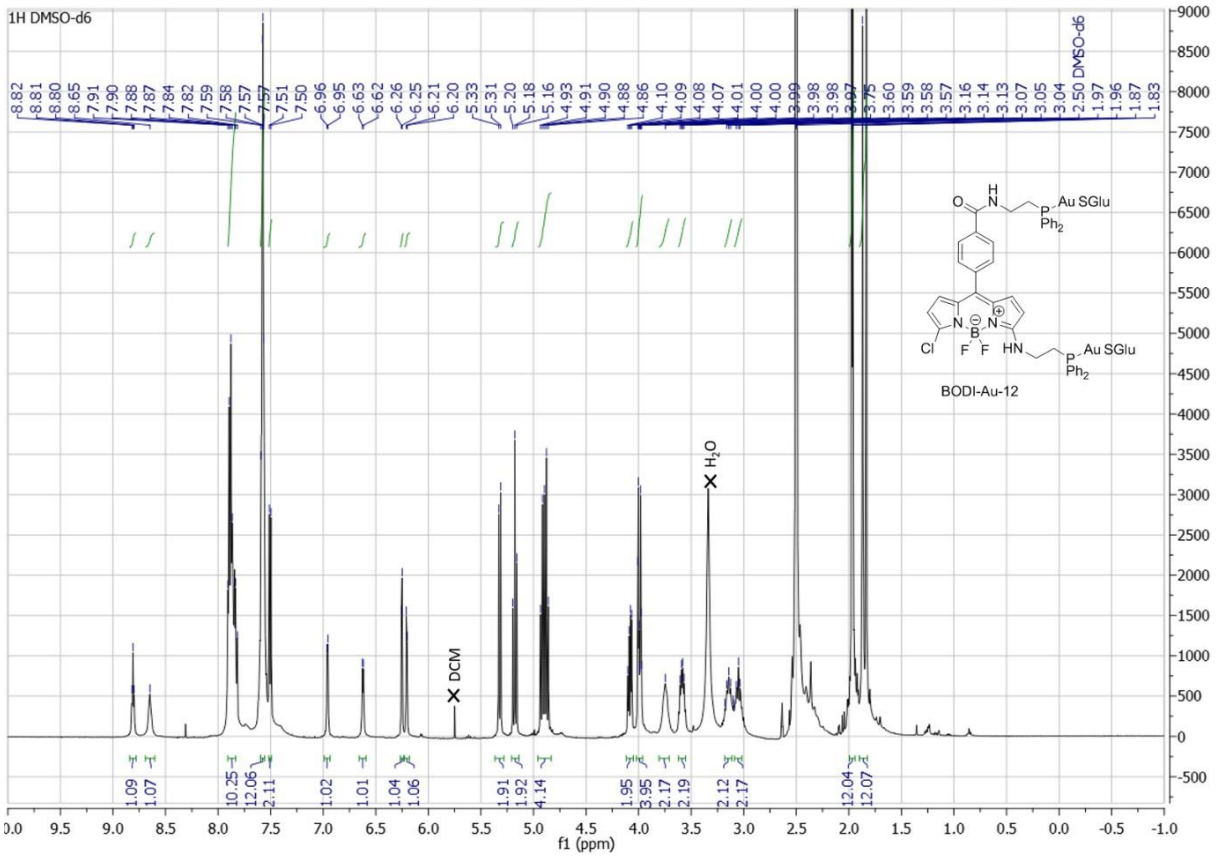

Figure S 65: ^{1}H NMR of **BODI-Au-12** (DMSO, 500 MHZ, 300K)

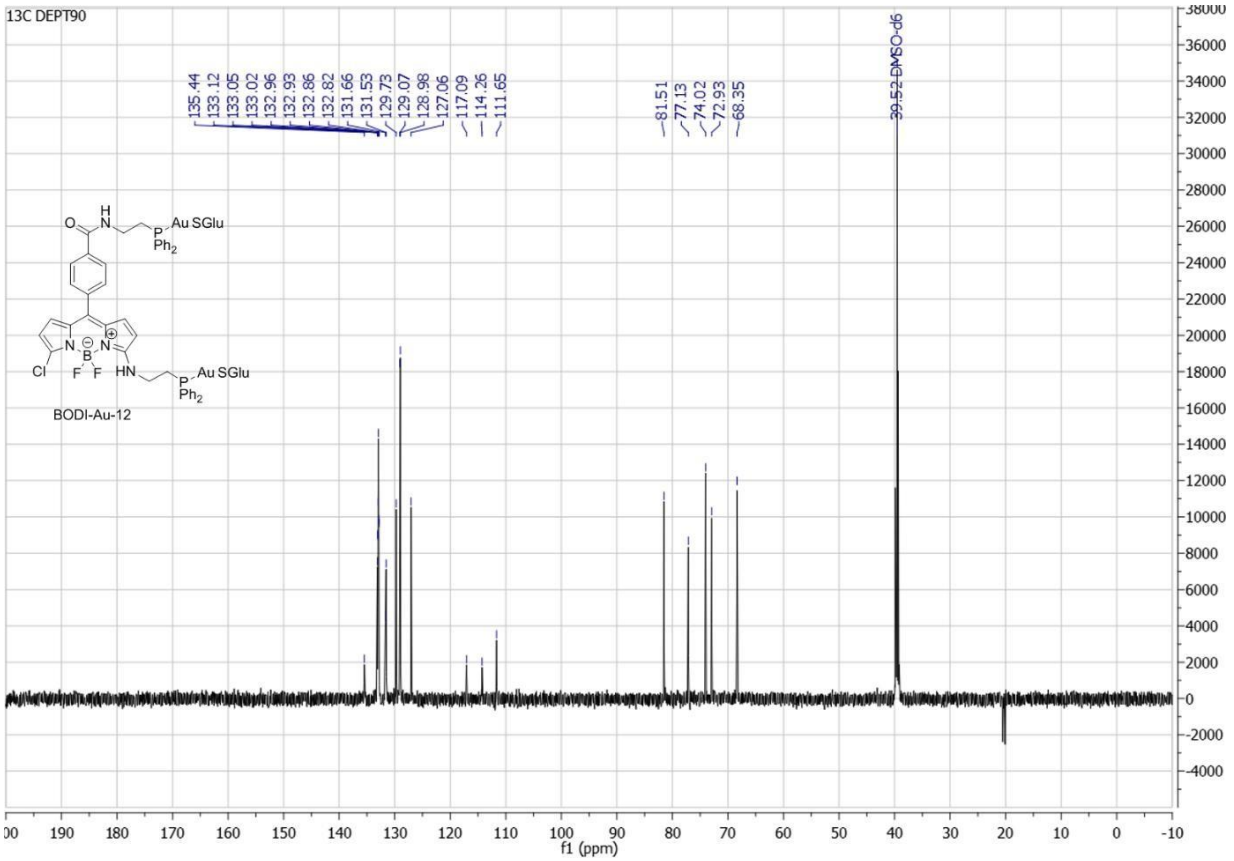

Figure S 66: ^{13}C NMR (DEPT90) of **BODI-Au-12** (DMSO, 126 MHZ, 300K)

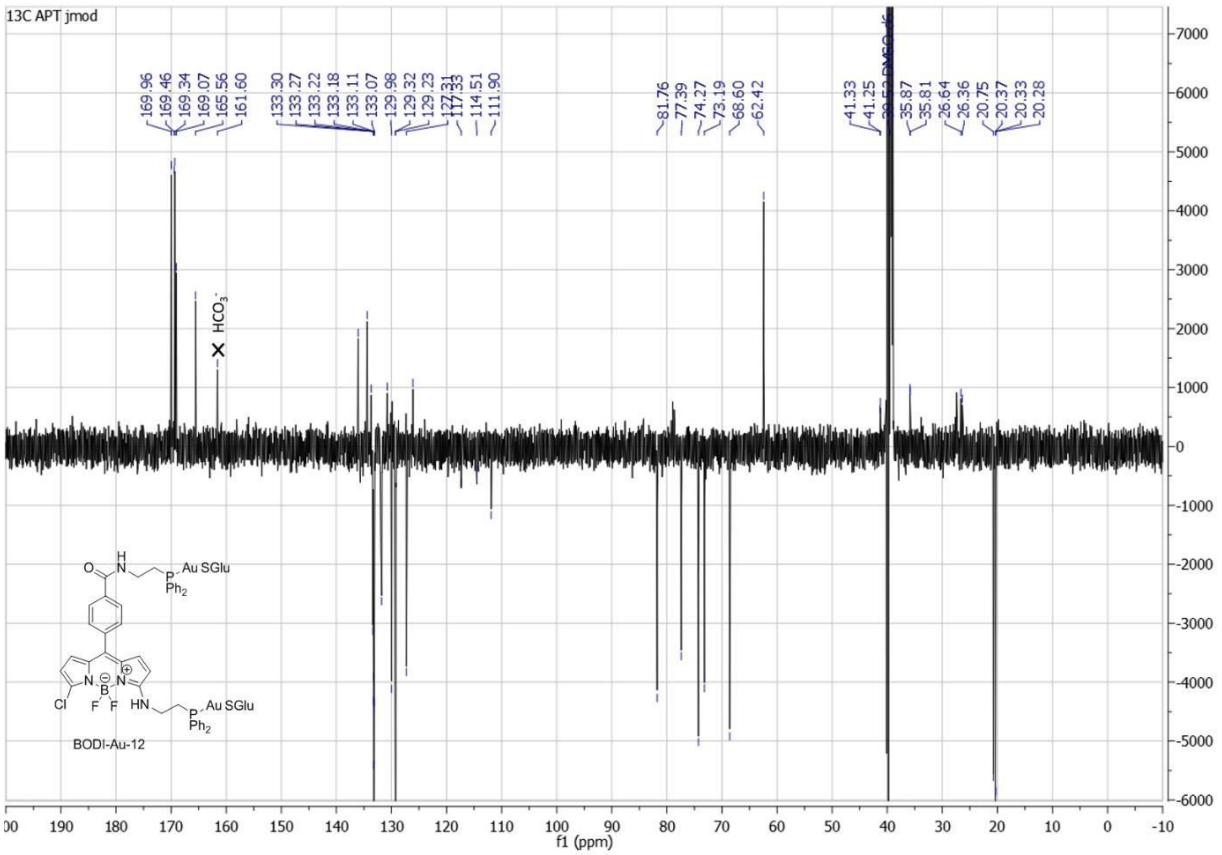

Figure S 67: ^{13}C NMR (APT jmod) of **BODI-Au-12** (DMSO, 126 MHZ, 300K)

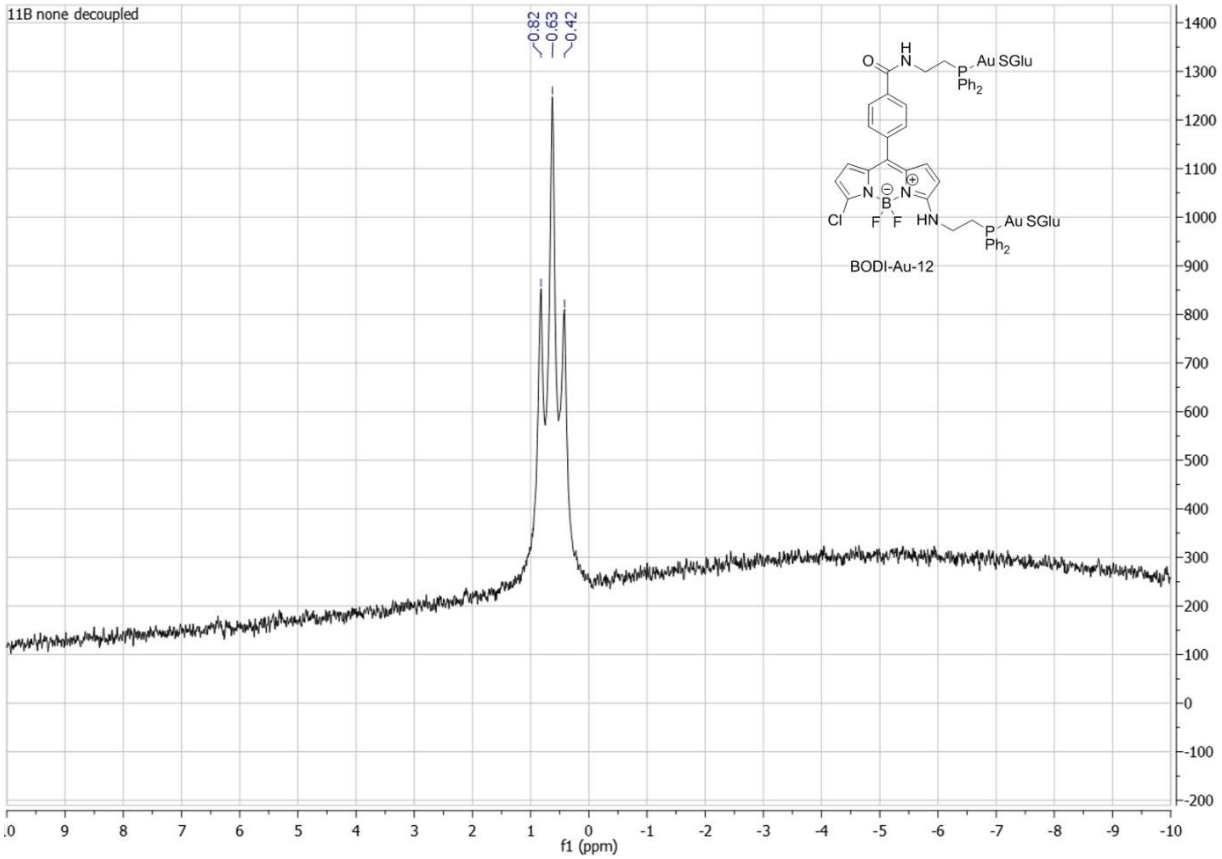

Figure S 68: ^{11}B NMR of **BODI-Au-12** (DMSO, 160 MHZ, 300K)

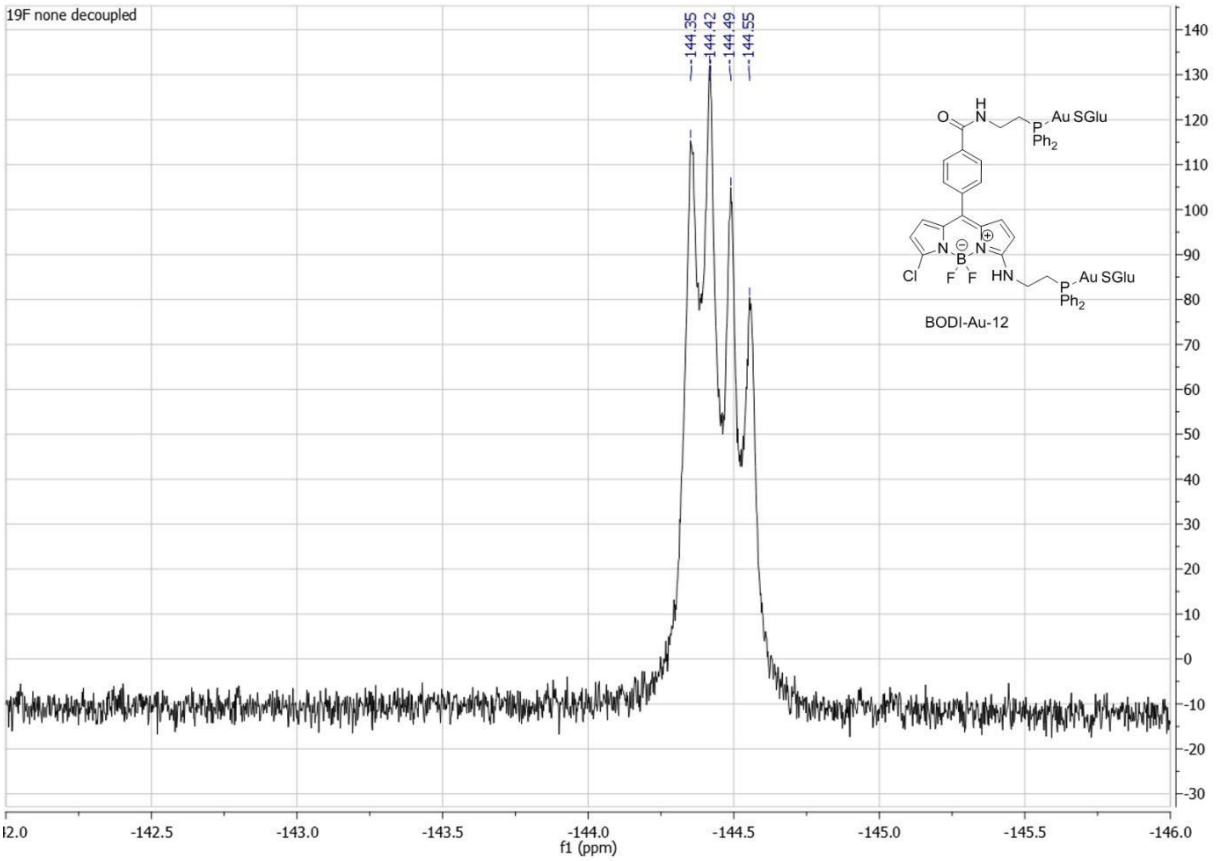

Figure S 69: ^{19}F NMR of **BODI-Au-12** (DMSO, 470 MHZ, 300K)

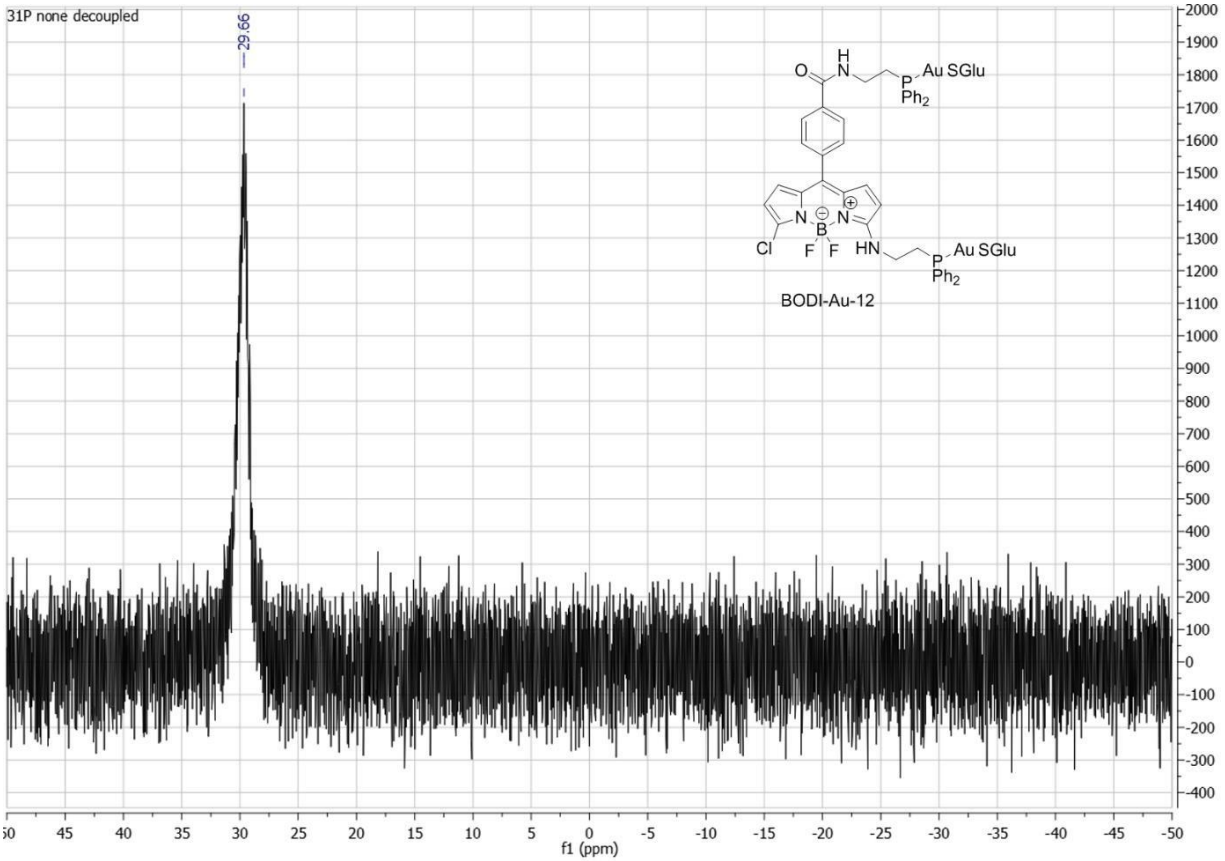

Figure S 70: ^{31}P NMR of **BODI-Au-12** (DMSO, 202 MHZ, 300K)

BODI-Au-13

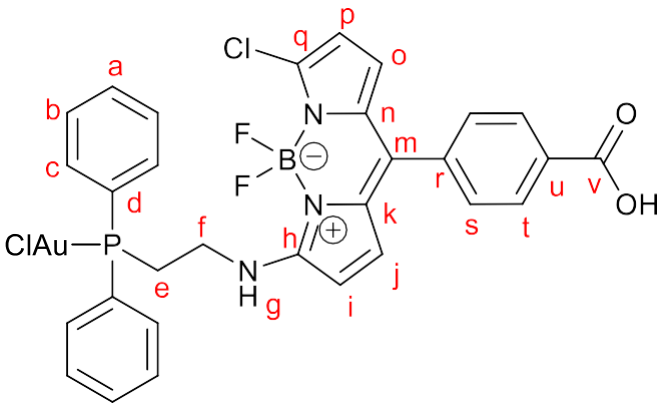

2-(Diphenylphosphino) ethylamine-aurichloride (145mg, 0.315mmol,1,2eq), BODIPY **3** (100mg, 0.26mmol, 1eq) and K_2CO_3 (181mg, 1.96mmol, 5eq) were placed in a 20 mL round bottom flask and put under argon. 15 mL dry THF were added and the reaction refluxed overnight. The solvents were evaporated and the crude product was purified by column chromatography using CH_2Cl_2/MeOH (100:0 to 80:20) as eluent. After evaporation of solvents under reduced pressure the product was dissolved in a minimal amount of CH_2Cl_2 and precipitated by addition of pentane to obtain 202.2mg (208 µmol; yield = 80%) of **BODI-Au-13** as a red-orange solid.

^{1}H NMR (500 MHz, DMSO-D6) δ (ppm)= 3.21 – 3.13 (m, 2H, H_e), 3.78 – 3.65 (m, 2H, H_f), 6.21 (d, J = 3.8 Hz, 1H, H_i), 6.25 (d, J = 3.8 Hz, 1H, H_j), 6.61 (d, J = 5.1 Hz, 1H, H_p), 7.01 (d, J = 5.2 Hz, 1H, H_o), 7.63 – 7.53 (m, 8H, $H_{a,b}$, H_s), 7.81 (ddd, J = 13.2, 7.8, 1.5 Hz, 4H, H_c), 8.06 (d, J = 8.3 Hz, 2H, H_t), 8.67 (s, 1H, H_g).

^{13}C NMR (126 MHz, DMSO-D6) δ (ppm)= 27.4 (d, J = 35.6 Hz, C_f), 41.3 (d, J = 11.0 Hz, C_e), 111.9 (s, Cp), 114.9 (s, C_i), 117.3 (s, C_o), 126.1 (s, Cn, C_k), 127.1 (s, C_m), 128.9 (d, J = 60.7 Hz, C_d), 129.3 (s, C_j), 129.4 (d, J = 11.5 Hz, C_a), 130.4 (s, C_s), 130.7 (s, C_u), 131.3 (s, C_r), 132.1 (d, J = 2.3 Hz, C_b), 133.2 (d, J = 13.5 Hz, C_c), 133.8 (s, C_q), 135.8 (s, C_t), 137.6 (s, C_h), 161.7 (s, C_v).

^{11}B NMR (160 MHz, DMSO-D6) δ (ppm)= 0.64 (t, J = 32.4 Hz).

^{19}F NMR (470 MHz, DMSO-D6) δ (ppm)= -144.38 (dd, $J_{F\text{-}F}$ = 64.5, $J_{F\text{-}B}$ = 31.3 Hz).

^{31}P NMR (202 MHz, DMSO-D6) δ (ppm) = 24.33.

HR-MS (ESI): *m/z* = calculated for $C_{30}H_{24}Au_1B_1Cl_2F_2N_3O_2P_1Na_1$ $[M+Na]^+$ 828.06020; found 828.06136.

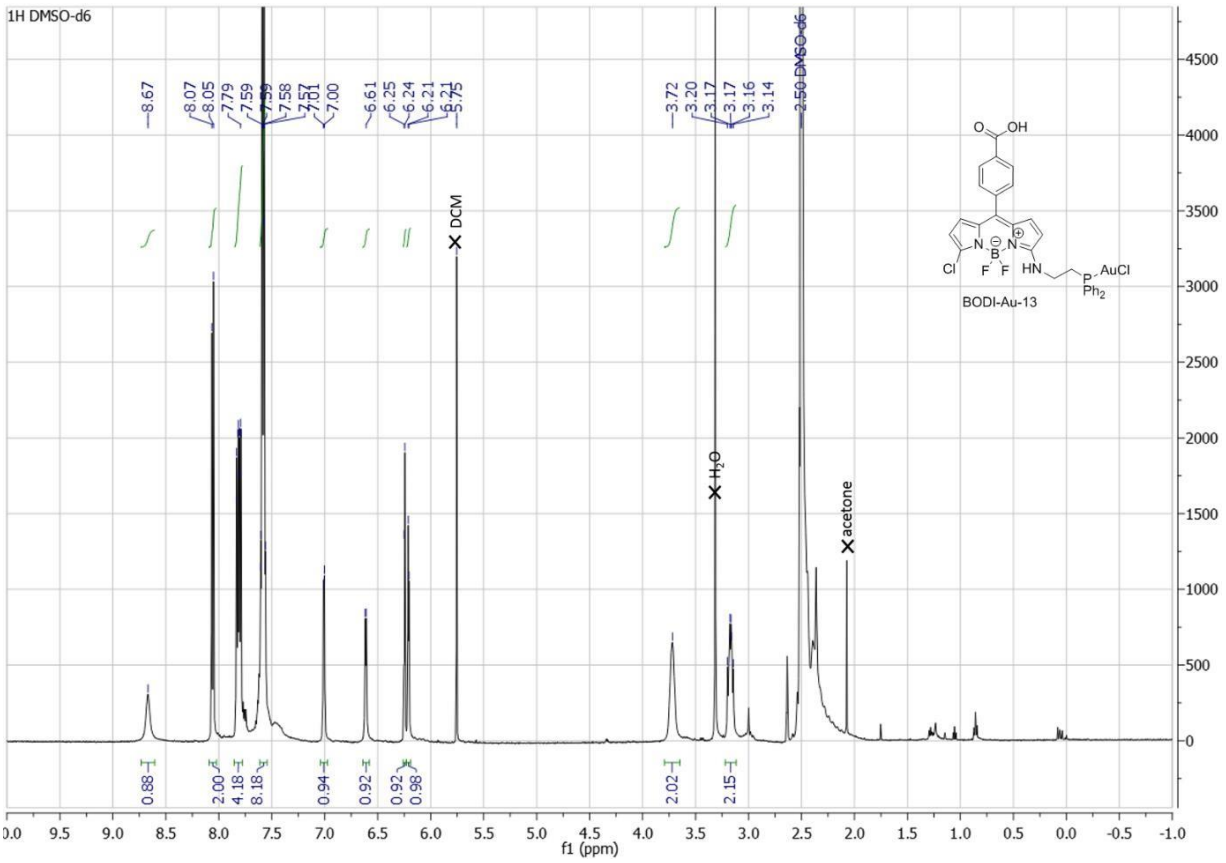

Figure S 71: ^{1}H NMR of **BODI-Au-13** (DMSO, 500 MHZ, 300K)

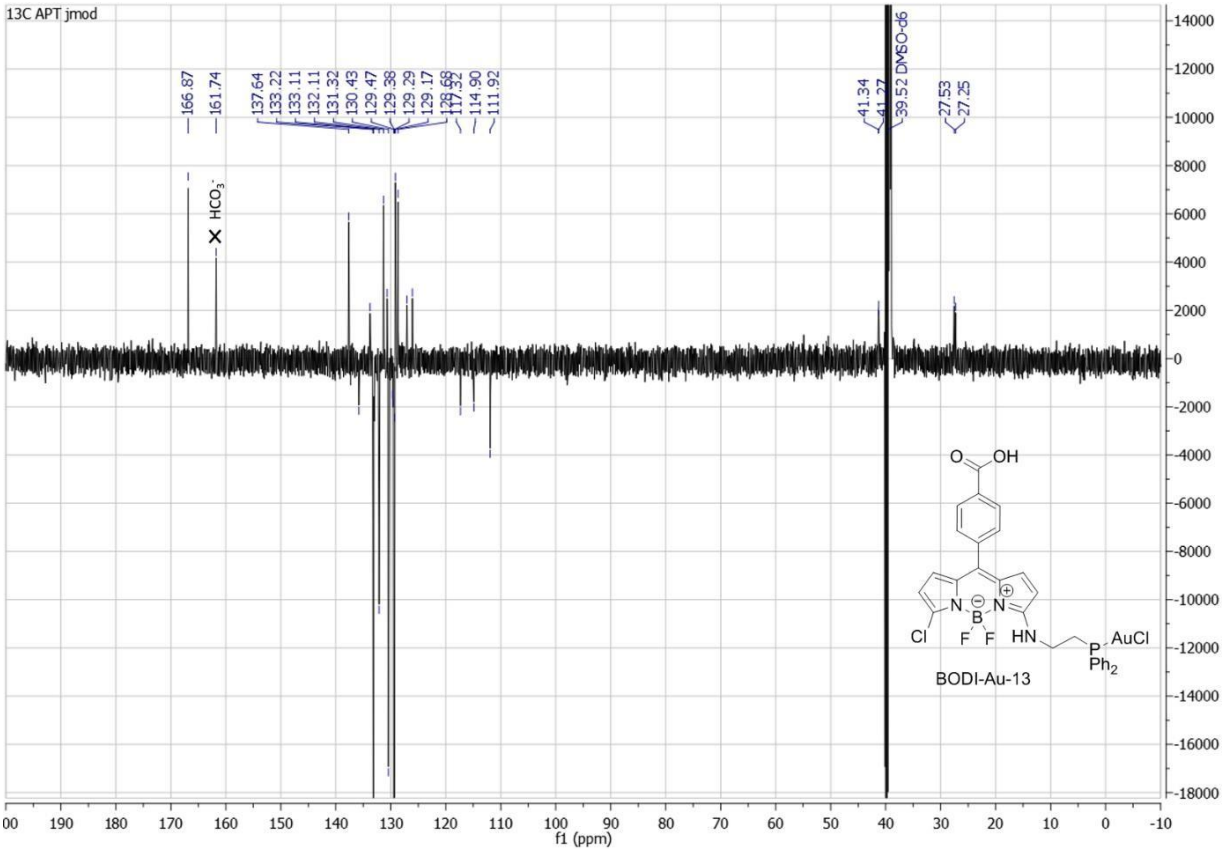

Figure S 72: ^{13}C NMR (APT jmod) of **BODI-Au-13** (DMSO, 126 MHZ, 300K)

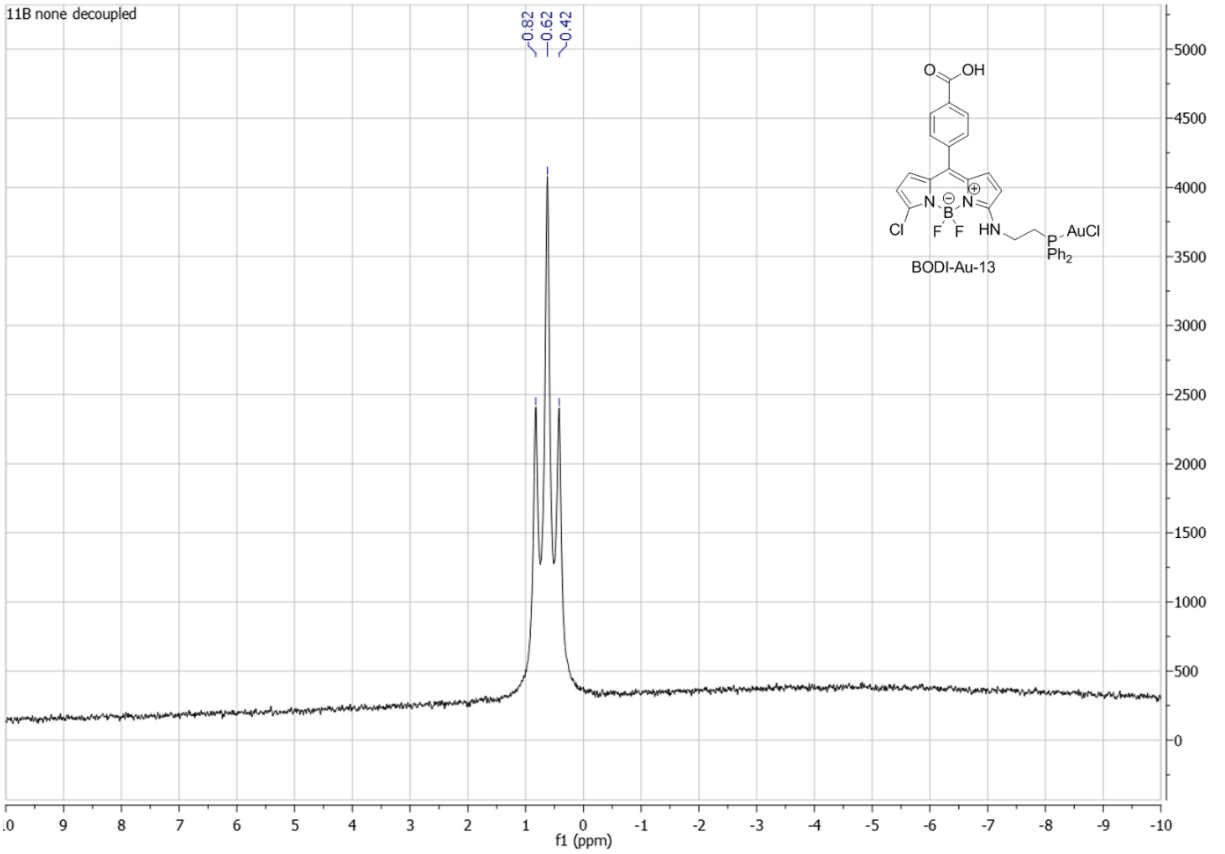

Figure S 73: ^{11}B NMR of **BODI-Au-13** (DMSO, 160 MHZ, 300K)

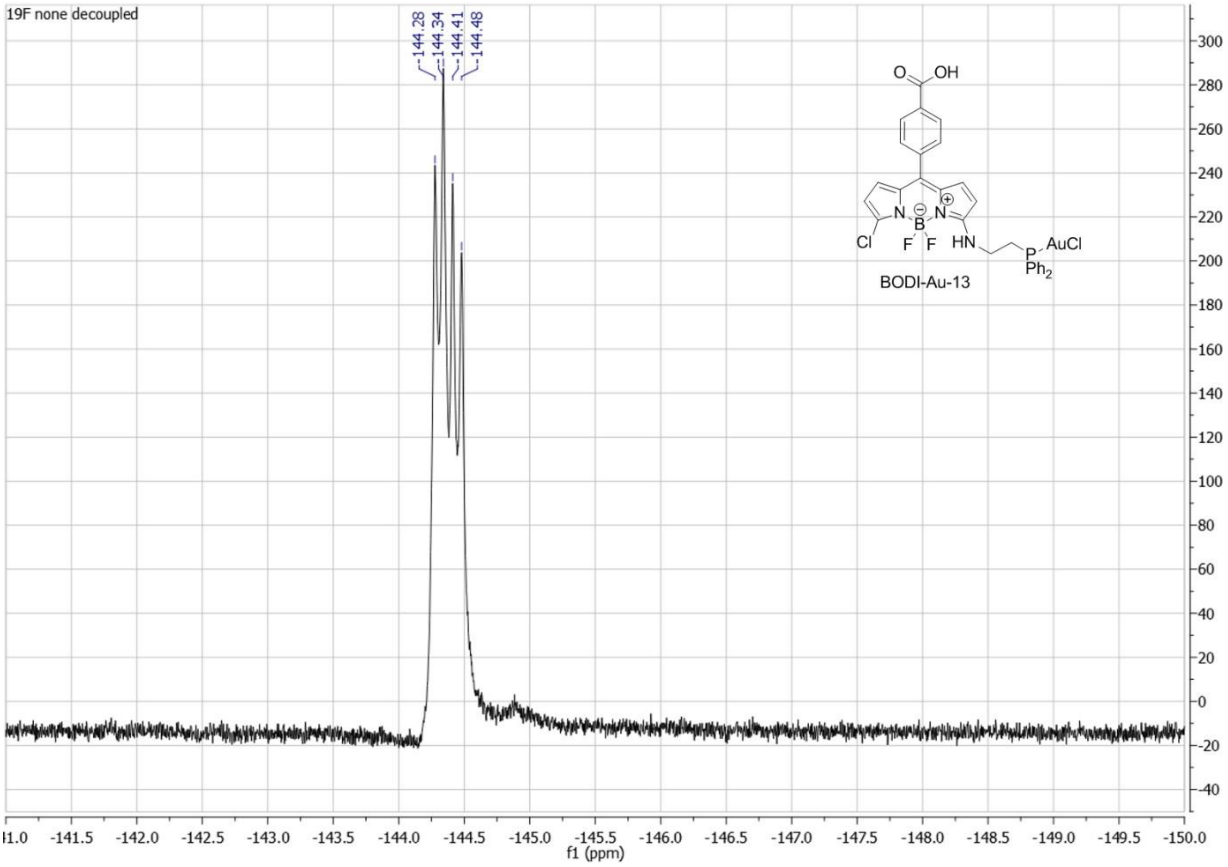

Figure S 74: ^{19}F NMR of **BODI-Au-13** (DMSO, 470 MHZ, 300K)

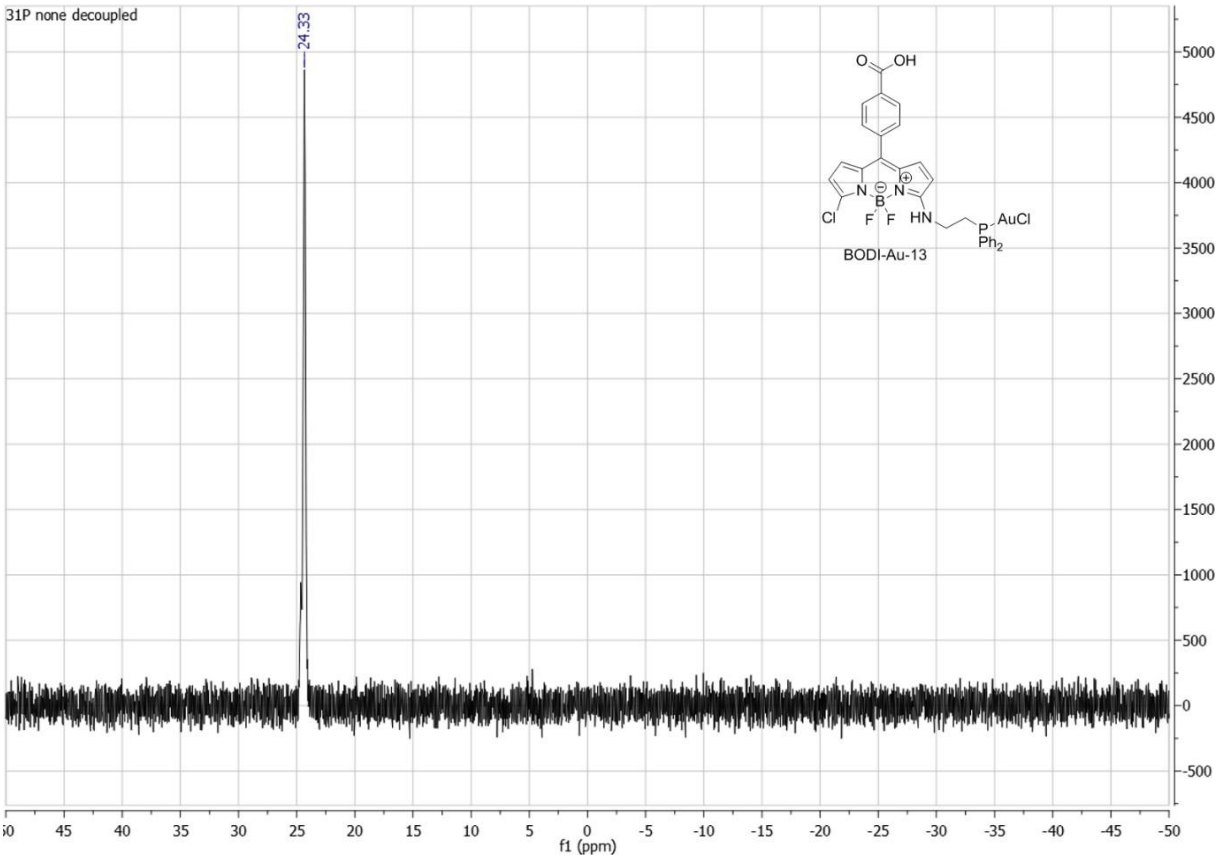

Figure S 75: ^{31}P NMR of **BODI-Au-13** (DMSO, 202 MHZ, 300K)

BODI-Au-14

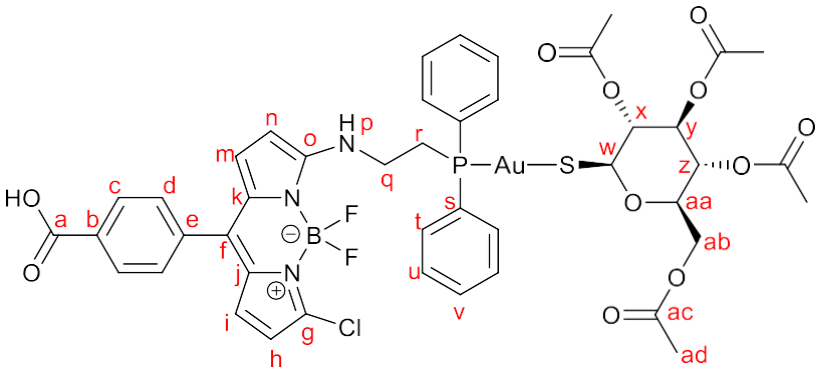

18 mg (49.6µmol) β-thioglucose-tetraacetate (1 eq) was dissolved in acetone (1 mL). 49.6µl 1M NaOH (1 eq) was added and the resulting solution stirred for 15 min. 40mg (49.6µmol) **BODI-Au-13** was placed in a separate roundbottom flask and dissolved in acetone (5 mL). The thioglucose solution was added at once and the reaction stirred for 30 min at room temperature. The solvents were evaporated, CH_2Cl_2 (10 mL) was added, and the supernatant separated and evaporated. The resulting crude product was dissolved in a minimal amount of CH_2Cl_2 and precipitated with pentane to obtain the pure target compound as a flaky orange powder 51mg (45.14 µmol, 91%).

^{1}H NMR (500 MHz, $CDCl_3$) δ (ppm)= 1.94 (s, 3H, H_{ad}), 1.96 (s, 3H, H_{ad}), 2.02 (s, 3H, H_{ad}), 2.11 (s, 3H, H_{ad}), 2.91 (tdd, *J* = 10.2, 6.6, 3.3 Hz, 2H, H_r), 3.77 (ddd, *J* = 9.4, 4.9, 2.4 Hz, 1H, H_{ab}), 3.83 (dt, *J* = 16.1, 7.7 Hz, 2H, H_q), 4.13 (dd, *J* = 12.2, 2.2 Hz, 1H, $H_{ab'}$), 4.24 (dd, *J* = 12.2, 5.0 Hz, 1H, H_z), 5.17 – 5.05 (m, 3H, H_x,H_y, H_{aa}), 5.22 (d, *J* = 8.7 Hz, 1H_w), 6.19 (d, *J* = 3.8 Hz, 1H, H_n), 6.26 (d, *J* = 4.9 Hz, 1H, H_m), 6.31 (d, *J* = 3.7 Hz, 1H, H_h), 6.83 (d, *J* = 4.8 Hz, 1H, H_i), 6.90 (s, 1H, H_p), 7.62 – 7.37 (m, 8H, $H_{u,v}$, H_d), 7.84 – 7.67 (m, 4H, H_t), 8.18 (d, *J* = 8.0 Hz, 2H, H_c).

^{13}C NMR (126 MHz, $CDCl_3$) δ (ppm)= 20.8 (s, C_{ad}), 20.8 (s, C_{ad}), 20.9 (s, C_{ad}), 21.3 (s, C_{ad}), 29.9 (d, *J* = 31.7 Hz, C_q), 41.3 (d, *J* = 12.3 Hz, C_r), 63.0 (s, C_{ab}), 69.1 (s, C_z), 74.3 (s, C_y), 76.0 (s, C_x), 78.3 (s, C_{aa}), 83.6 (s, C_w), 111.4 (s, C_h), 113.3 (s, C_n), 120.7 (s, C_i), 129.0 (dd, *J* = 55.4, 8.0 Hz, C_s), 129.8 (dd, *J* = 11.4, 6.5 Hz, C_v), 130.2 (s, C_m), 130.3 (s, C_k, C_j), 130.6 (s, C_d), 130.9 (s, C_f), 131.5 (s, C_e), 132.4 (dd, *J* = 8.3, 2.2 Hz, C_u), 133.4 (t, *J* = 13.9 Hz, C_t), 135.8 (s, C_c), 139.2 (s, C_g, C_o), 161.6 (s, C_a), 169.9 (s, C_{ac}), 170.5 (s, C_{ac}), 170.6 (s, C_{ac}), 171.0 (s, C_{ac}).

^{11}B NMR (160 MHz, $CDCl_3$) δ (ppm)= 0.83 (t, *J* = 32.7 Hz).

^{19}F NMR (470 MHz, $CDCl_3$) δ (ppm)= -147.78 (s, br).

^{31}P NMR (202 MHz, $CDCl_3$) δ (ppm) = 29.39. (s, br).

HR-MS (ESI): *m/z* = calculated for $C_{44}H_{43}Au_1B_1Cl_1F_2N_3O_{11}P_1S_1Na_1$ $[M+Na]^+$ 1156.16633; found 1156.16962.

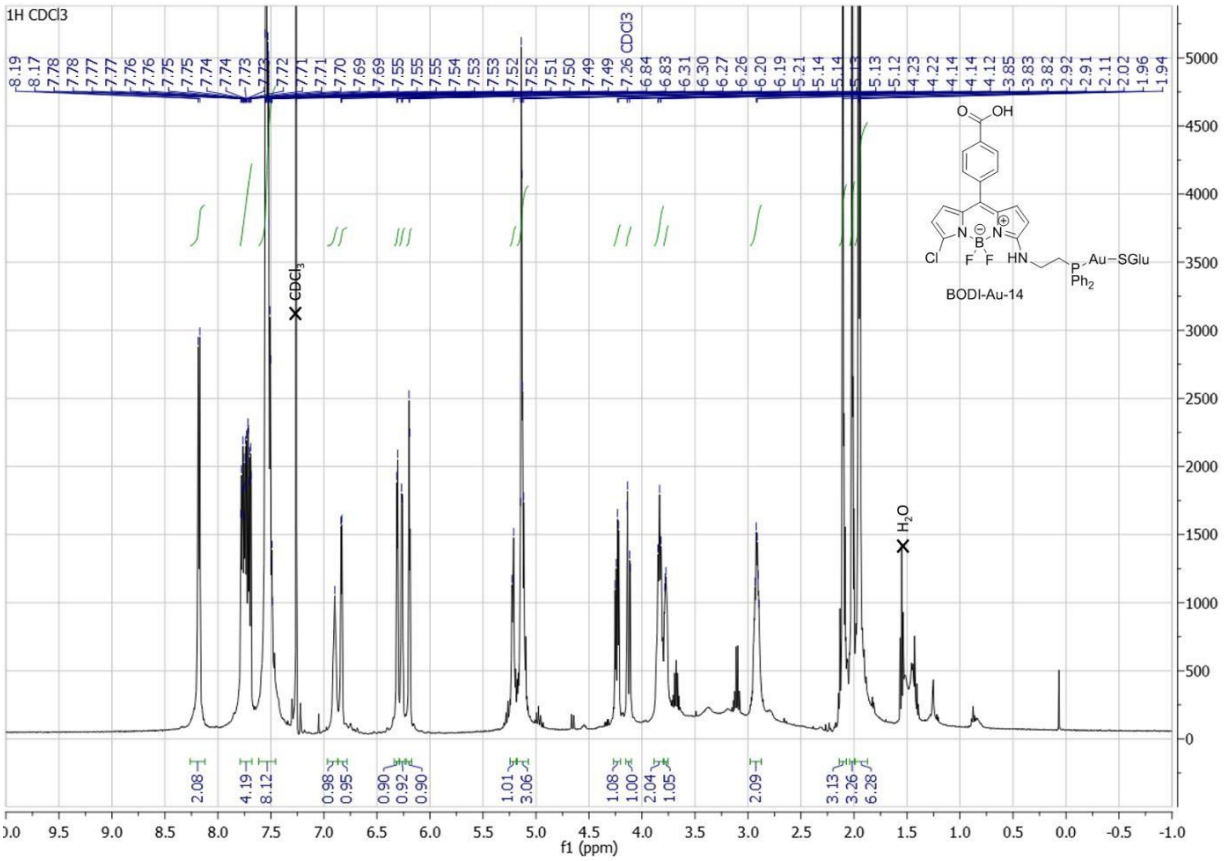

Figure S 76: ^{1}H NMR of **BODI-Au-14** ($CDCl_3$, 500 MHZ, 300K)

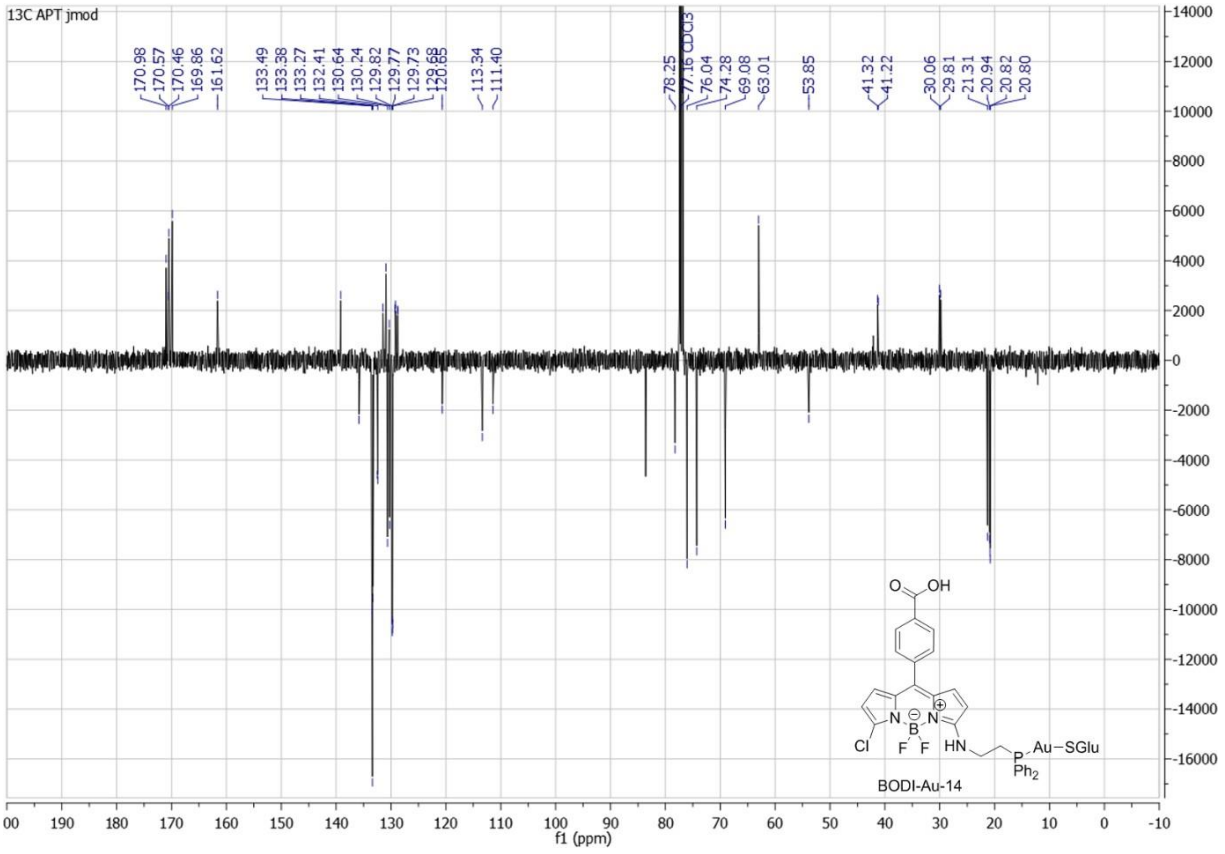

Figure S 77: ^{13}C NMR (APT jmod) of **BODI-Au-14** ($CDCl_3$, 126 MHZ, 300K)

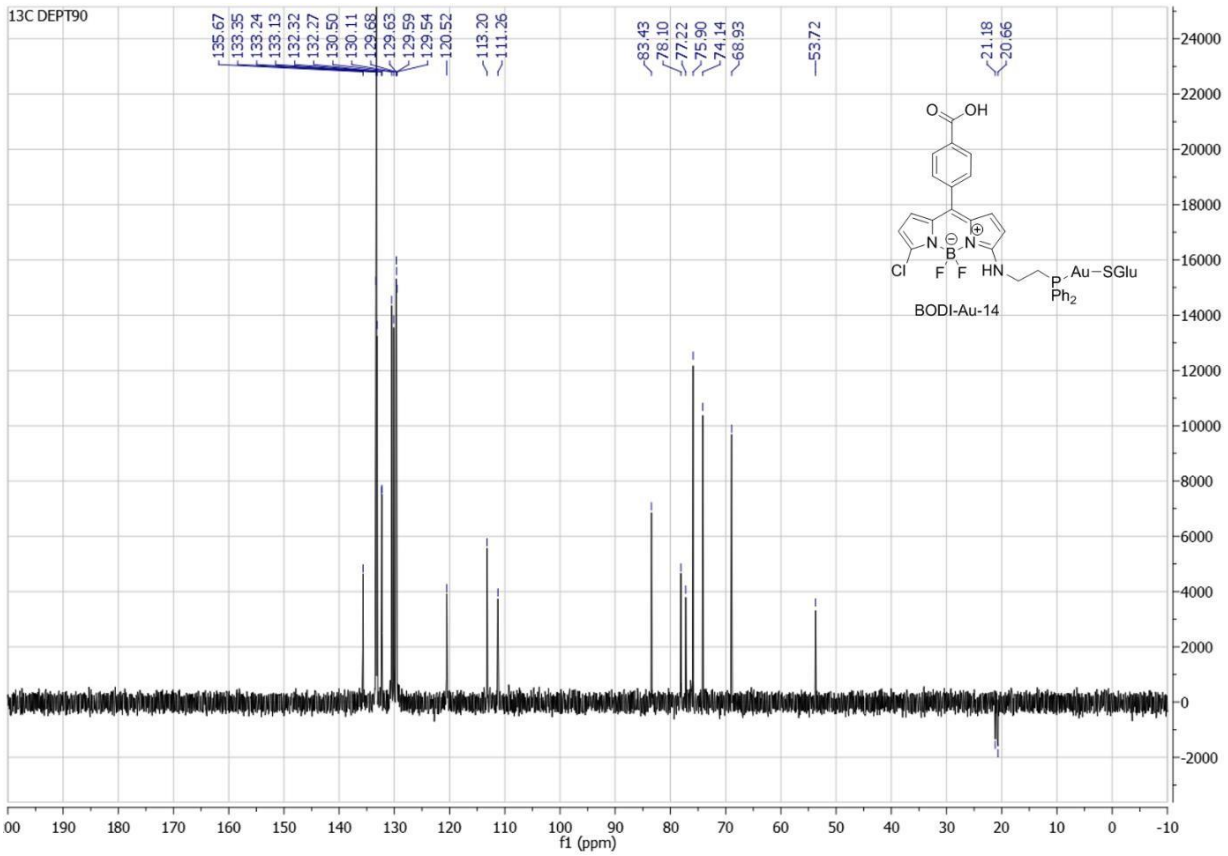

Figure S 78: ^{13}C NMR (DEPT90) of **BODI-Au-14** ($CDCl_3$, 126 MHZ, 300K)

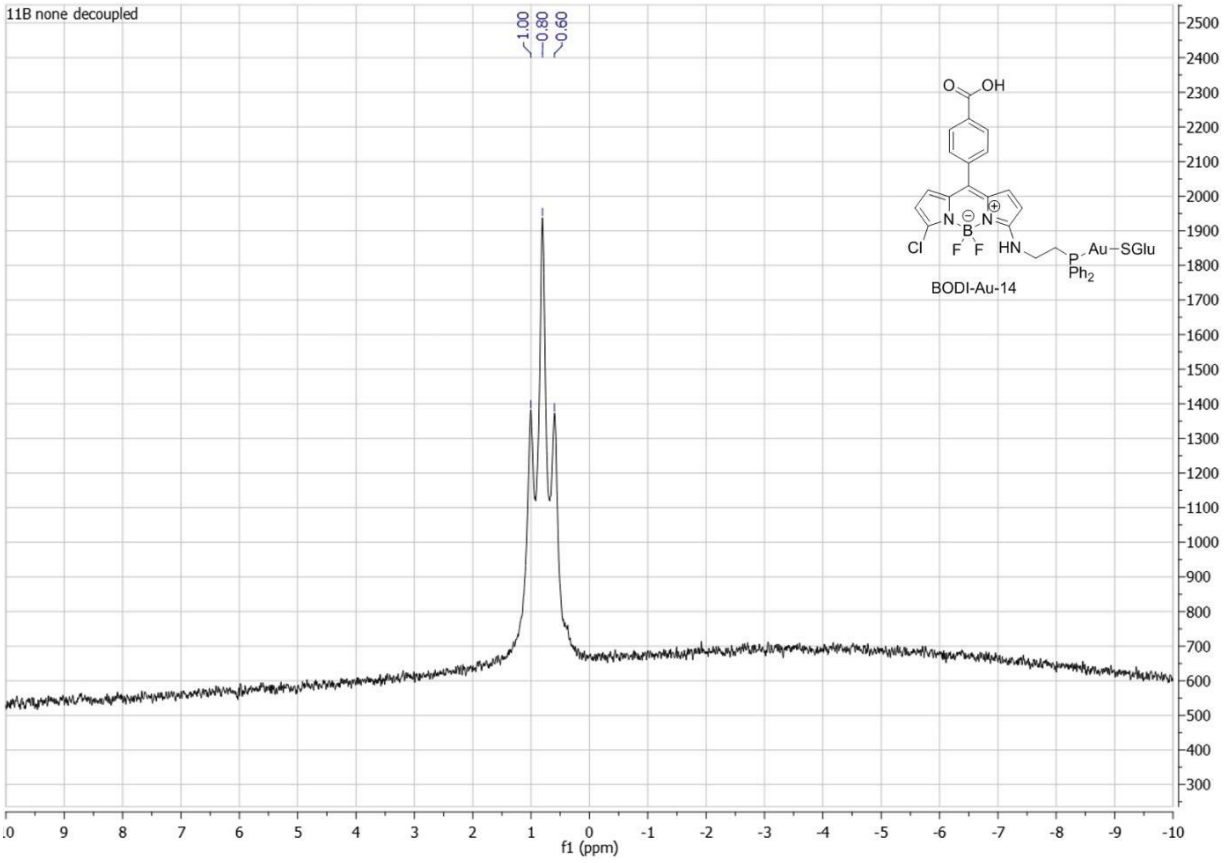

Figure S 79: ^{11}B NMR of **BODI-Au-14** ($CDCl_3$, 160 MHZ, 300K)

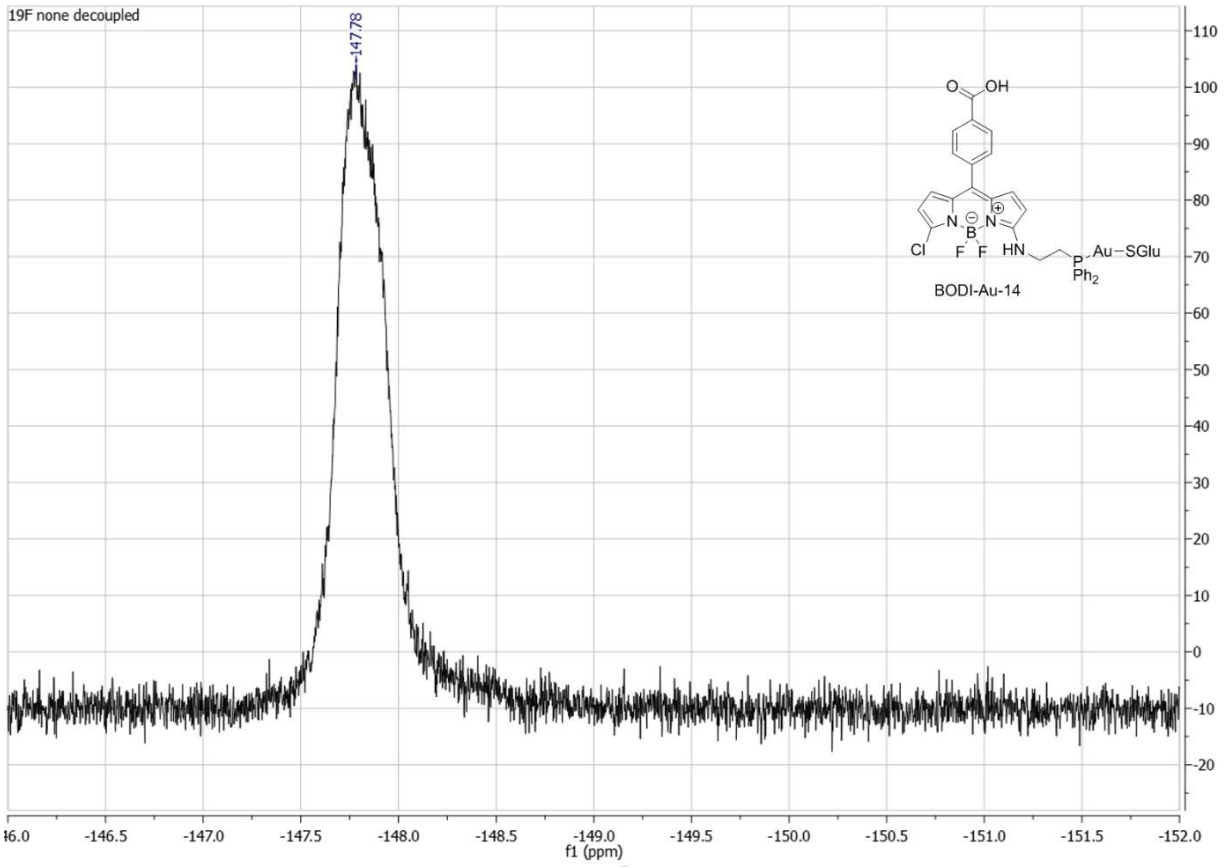

Figure S 80: ^{19}F NMR of **BODI-Au-14** ($CDCl_3$, 470 MHZ, 300K)

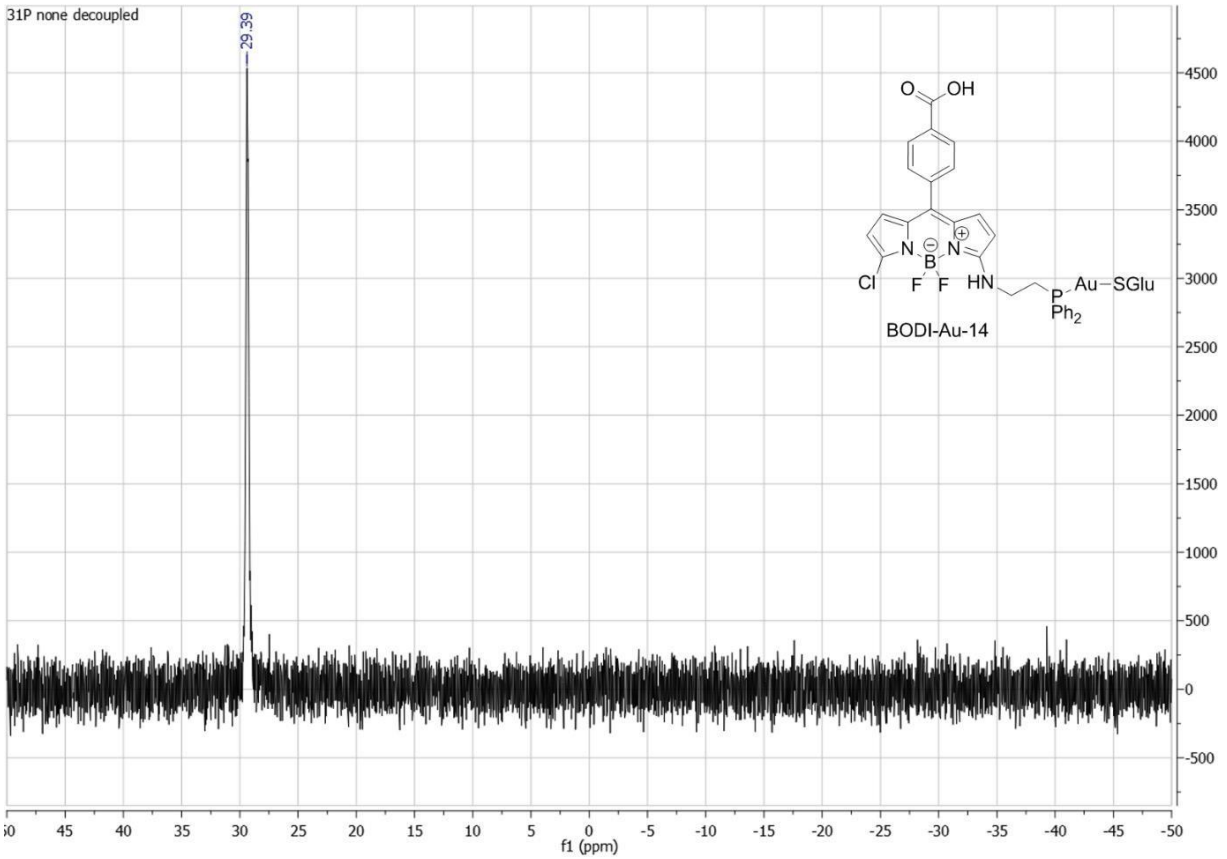

Figure S 81: ^{31}P NMR of **BODI-Au-14** ($CDCl_3$, 202 MHZ, 300K)

BODI-Au-15

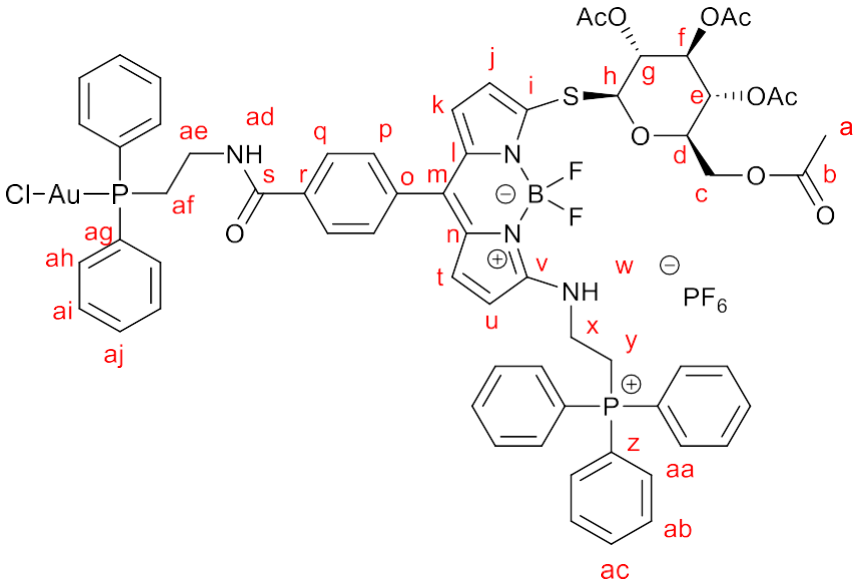

BODIPY **8** (50mg, 0.047mmol, 1eq) was placed in a dried round bottom flask and dissolved in 5 mL dry DMF. 0.1 mL of DIPEA and 27mg (0.071mmol, 1.5eq) of HBTU were added and the reaction stirred for 40 min at 30°C. 2-(Diphenylphosphino)-ethylamine-aurichloride (32.7mg, 0.071mmol, 1.5eq) was dissolved in 1 mL dry DMF and added to the solution. The reaction was stirred for 4h at 30°C. The solvent was then evaporated and the crude product purified by column chromatography on silica gel using CH_2Cl_2/MeOH/Formic acid (99:1:1 to 97:3:1) as eluent, was dissolved in a minimal amount of CH_2Cl_2 and precipitated by addition of pentane to obtain **BODI-Au-15** at a purity of ≈ 85% (69.9mg of a mixture containing ≈ 60 mg of **BODI-Au-15**, 38.3 µmol, equivalent to 81% yield) as an orange-pink solid. *The impurities are salts coming from coupling agents. Additional column chromatography or preparative HPLC did not succeeded in improving the purity of the compound.*

^{1}H NMR (500 MHz, DMSO) δ [ppm]= 2.09 – 1.84 (m, 12H, H_a), 3.15 – 3.01 (m, 2H, H_{af}), 3.58 (qd, J = 13.9, 7.3 Hz, 2H, H_{ae}), 3.82 – 3.68 (m, 2H, H_y), 4.04 – 3.94 (m 2H, 2 H_x), 4.06 (d, J = 10.2 Hz, 1H, H_c), 4.17 (m, 2H, H_c, H_d), 4.96 (m, 2H, H_g, H_e), 5.36 (d, J = 10.1 Hz, 1H, H_h), 5.41 (t, J = 9.4 Hz, 1H, H_f), 6.33 (d, J = 3.8 Hz, 1H, H_u), 6.42 (d, J = 5.1 Hz, 1H, H_j), 6.45 (d, J = 3.8 Hz, 1H, H_t), 6.93 (d, J = 5.0 Hz, 1H, H_k), 7.49 (d, J = 8.2 Hz, 2H, H_p), 7.68 – 7.52 (m, 10H, H_{ah}, H_{aa}), 8.01 – 7.68 (m, 17H, $H_{ai, aj, ab, ac}$, H_q), 8.50 (s, 1H, H_w), 8.87 (t, J = 5.3 Hz, 1H, H_{ad}).

^{13}C NMR (126 MHz, DMSO-D6) δ (ppm)= 20.28 (s, Ca), 20.38 (s, C_a), 20.41 (s, C_a), 20.52 (s, C_a), 26.71 (d, J = 36.7 Hz, C_{ae}), 35.63 (d, J = 3.9 Hz, C_x), 38.62 (s, C_{af}), 40.57 (d, J = 10.0 Hz, C_y), 61.97 (s, C_c), 68.05 (s, C_e), 69.32 (s, C_f), 72.91 (s, C_g), 74.31 (s, C_d), 82.99 (s, C_h), 113.16 (s, C_u), 115.12 (s, C_j), 118.02 (d, J = 86.2 Hz, C_z), 118.93 (s, C_t), 127.45 (s, C_k), 128.49 (s, C_n), 128.78 (d, J = 60.7 Hz, C_{ag}), 129.03 (s, C_i), 129.41 (d, J = 11.5 Hz, C_{aj}), 129.56 (d, J = 11.6 Hz, C_{aj}), 129.90 (s, C_q), 130.26 (d, J = 12.7 Hz, C_{ac}), 132.34 (s, C_p), 132.48 (s, C_m), 132.97 (s, C_o), 133.15 (dd, J = 13.4, 2.4 Hz, C_{ah}), 133.74 (d, J = 10.6 Hz, C_{ab}), 134.37 (s, C_v), 135.07 (d, J = 2.7 Hz, C_{aa}), 136.38 (s, C_i), 165.61 (s, C_s), 169.04 (s, C_b), 169.32 (s, C_b), 169.50 (s, C_b), 169.94 (s, C_b).

^{11}B NMR (160 MHz, DMSO-D6) δ (ppm)= 0.69 (t, J = 33.3 Hz).

^{19}F NMR (470 MHz, DMSO-D6) δ (ppm)= -143.49 (s, 2F), -70.15 (d, J_{F-P} = 711.2 $_6$Hz, 6F, PF^-).

^{31}P NMR (202 MHz, DMSO-D6) δ (ppm)= -144.19 (hept, J_{P-F} = 711.3 Hz, 1P, PF_6^-), 21.43 (s, 1P), 25.68 (s, br, 1P).

HR-MS (ESI): m/z = calculated for $C_{64}H_{62}Au_1B_1Cl_1F_2N_4O_{10}P_2S_1$ $[M]^+$ 1421.30716; found 1421.31370.

Chromatogram and Results

Injection Details

Injection Name:	**BODI-Au-15**	*Run Time (min):*	**8.51**
Vial Number:	**GA2**	*Injection Volume:*	**10.00**
Injection Type:	**Unknown**	*Channel:*	**UV_VIS_1**
Calibration Level:		*Wavelength:*	**220.0**
Instrument Method:	**Standard-Kinetex**	*Bandwidth:*	**4**
Processing Method:	**no integration**	*Dilution Factor:*	**1.0000**
Injection Date/Time:	**02/Aug/17 18:05**	*Sample Weight:*	**1.0000**

Chromatogram

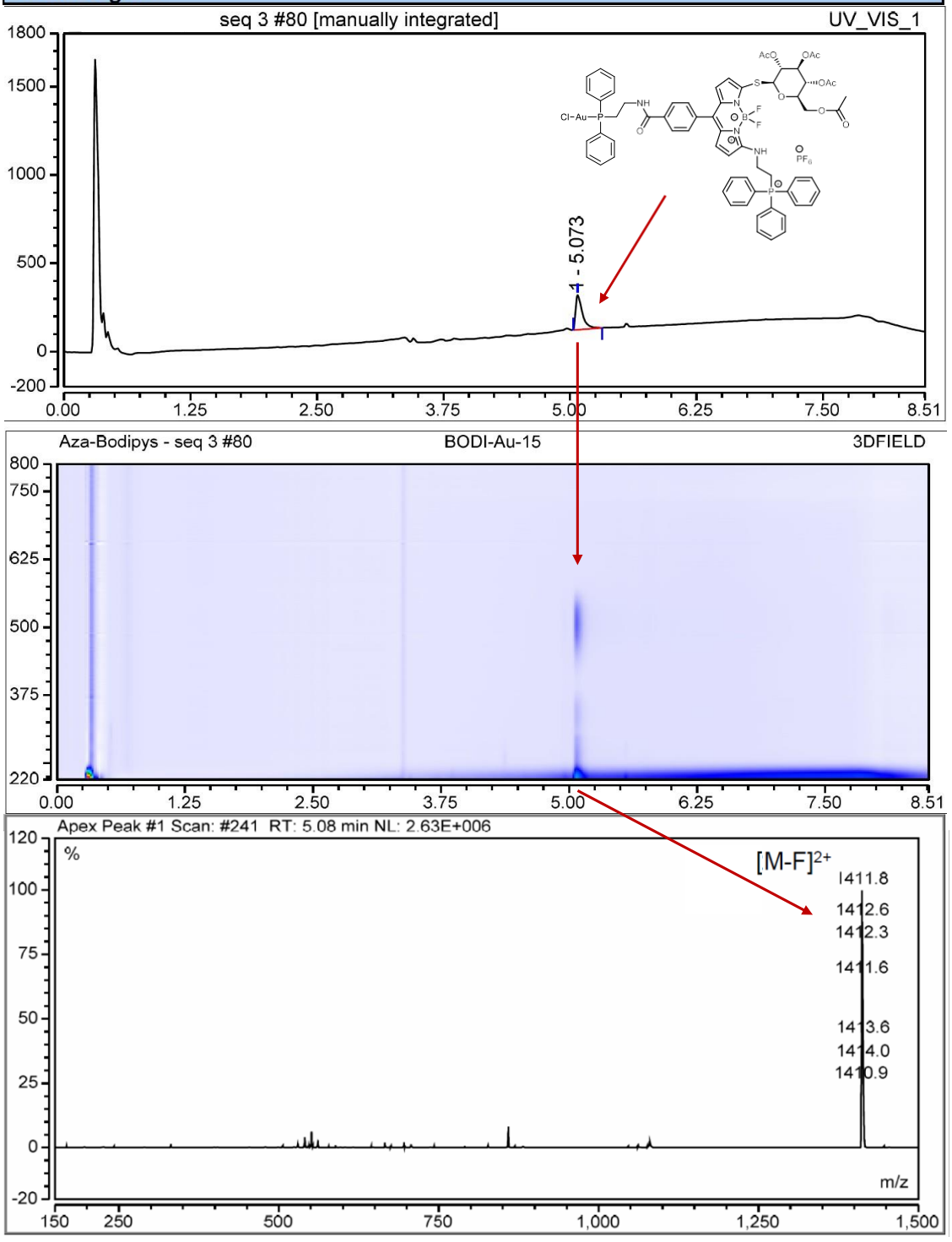

Figure S 82: HPLC chromatogram of **BODI-Au-15** (UV-detection at 220 nm + MS analysis)

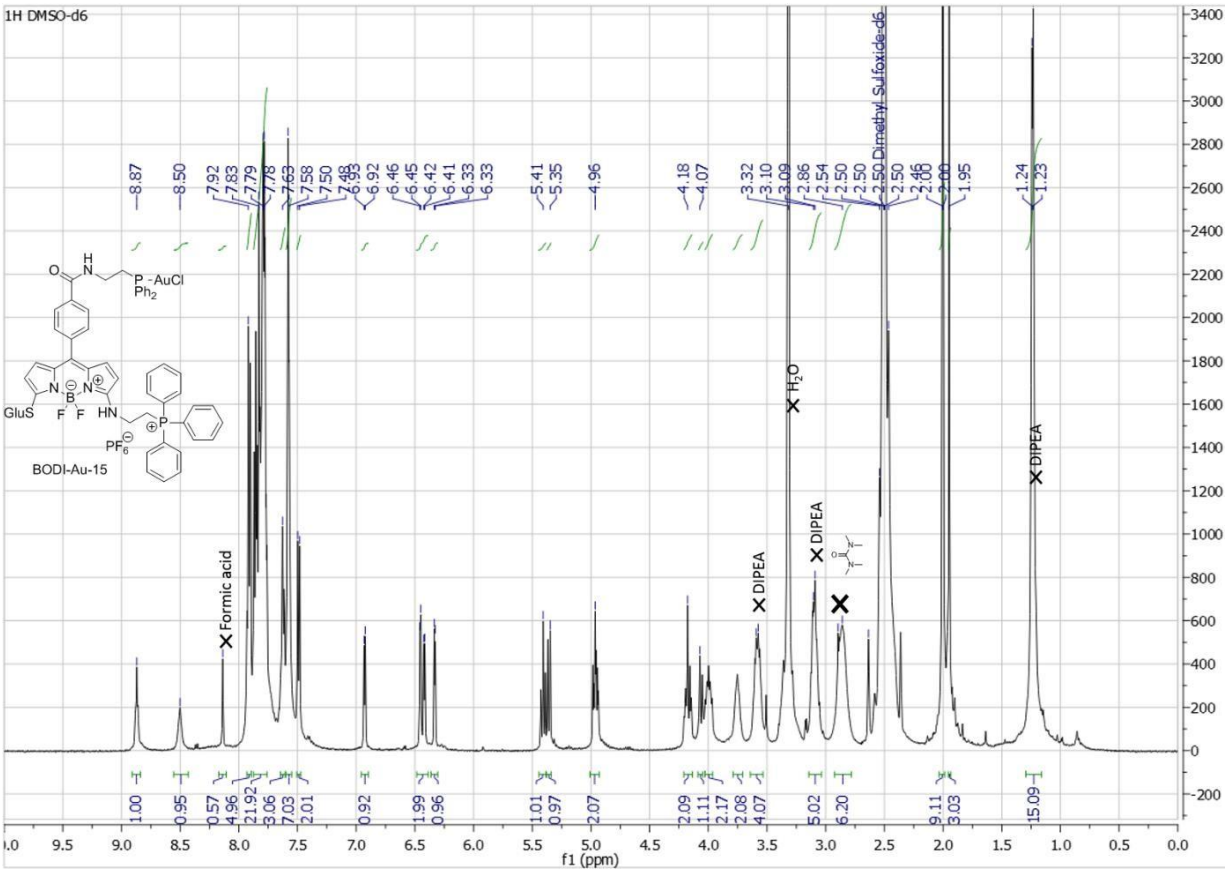

Figure S 83: ^{1}H NMR of **BODI-Au-15** (DMSO, 500 MHZ, 300K)

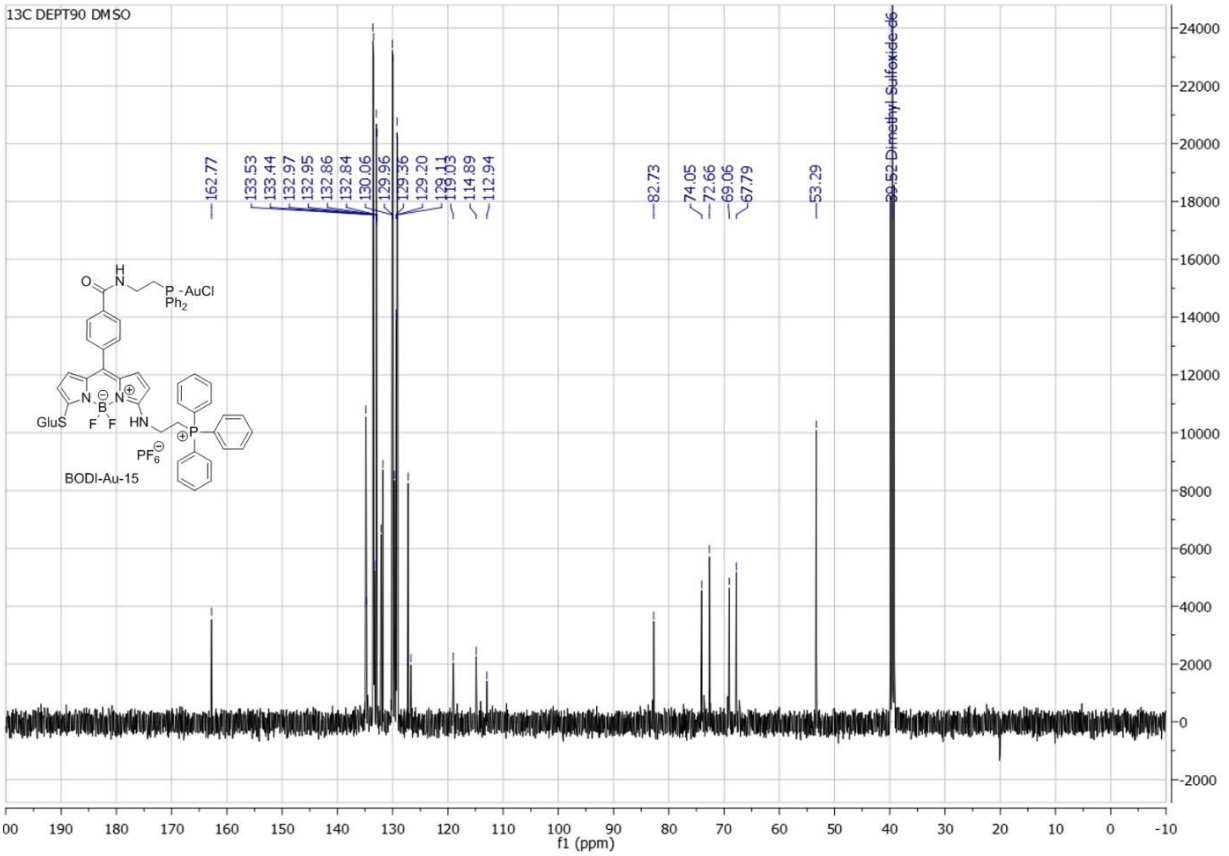

Figure S 84: ^{13}C NMR (DEPT90) of **BODI-Au-15** (DMSO, 126 MHZ, 300K)

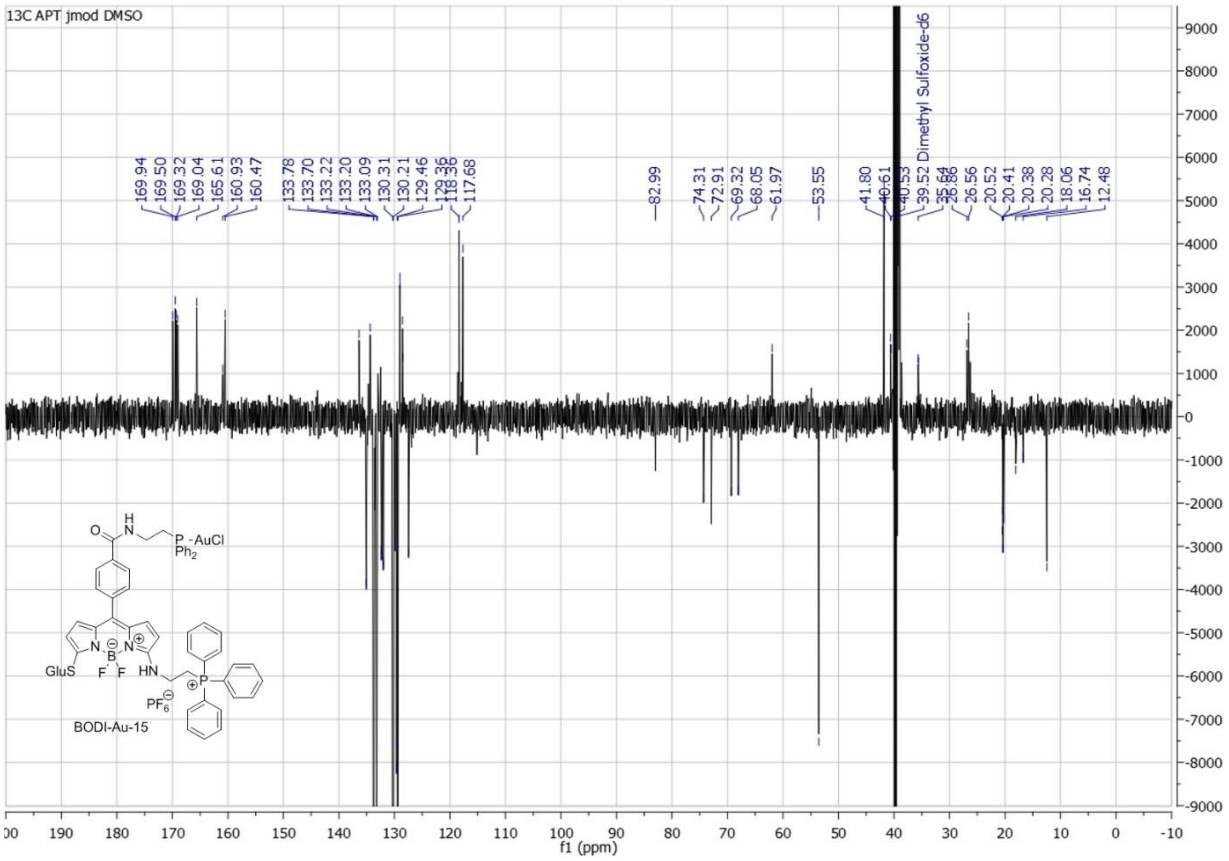

Figure S 85: ^{13}C NMR (APT jmod) of **BODI-Au-15** (DMSO, 126 MHZ, 300K)

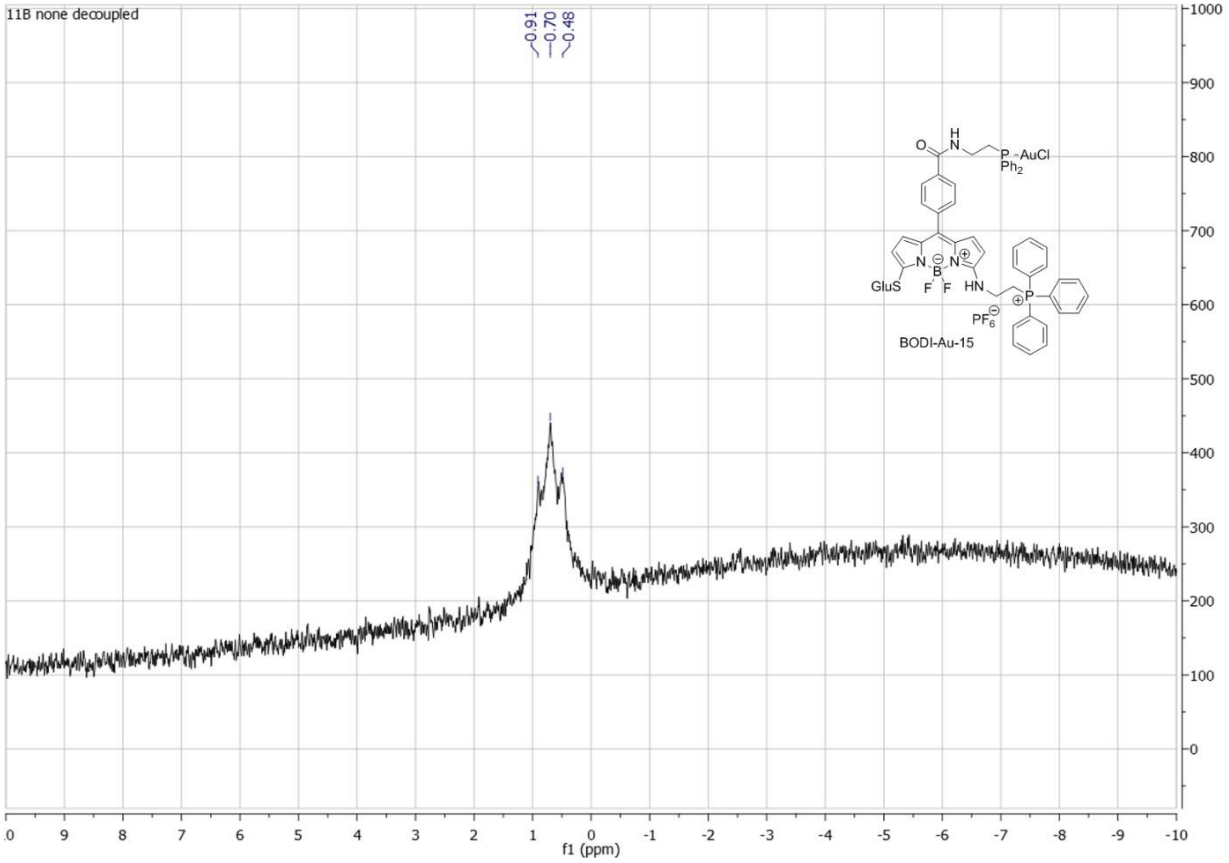

Figure S 86: ^{11}B NMR of **BODI-Au-15** (DMSO, 160 MHZ, 300K)

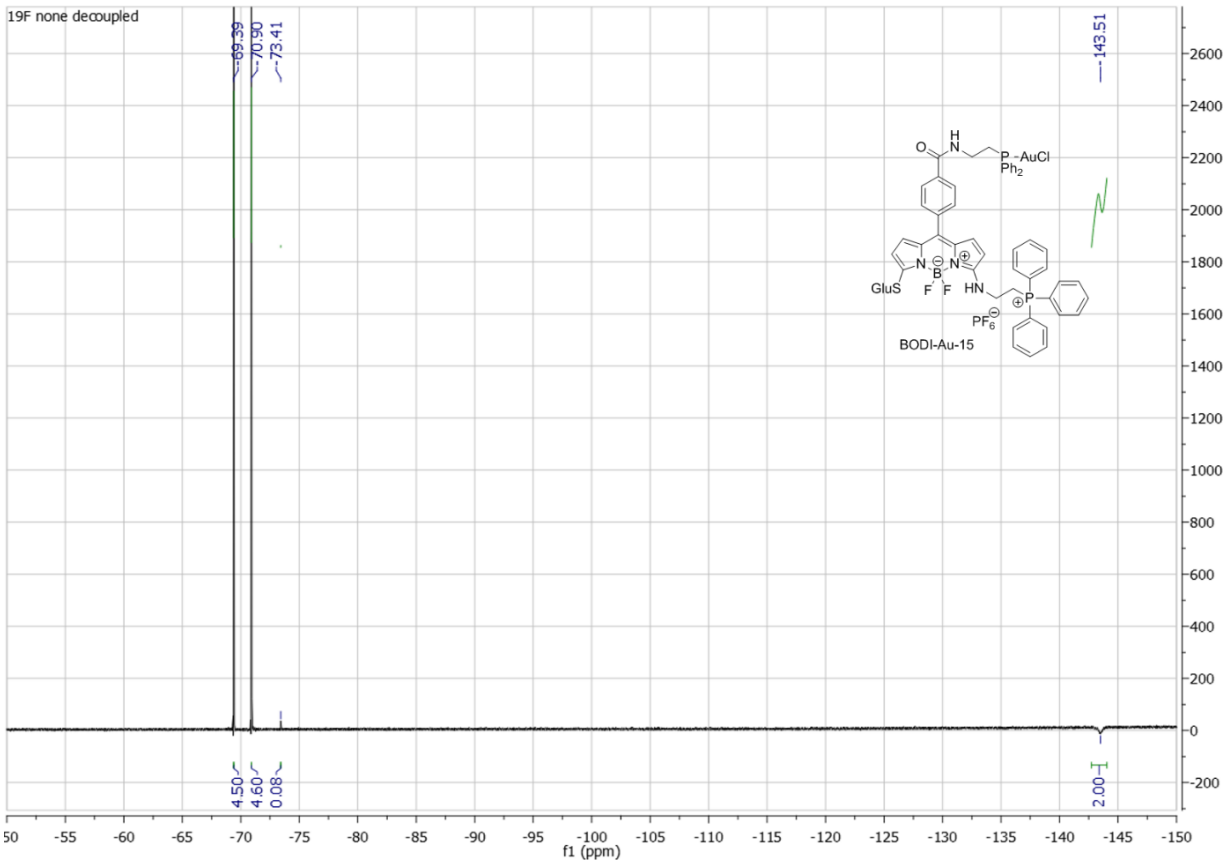

Figure S 87: ^{19}F NMR of **BODI-Au-15** (DMSO, 470 MHZ, 300K)

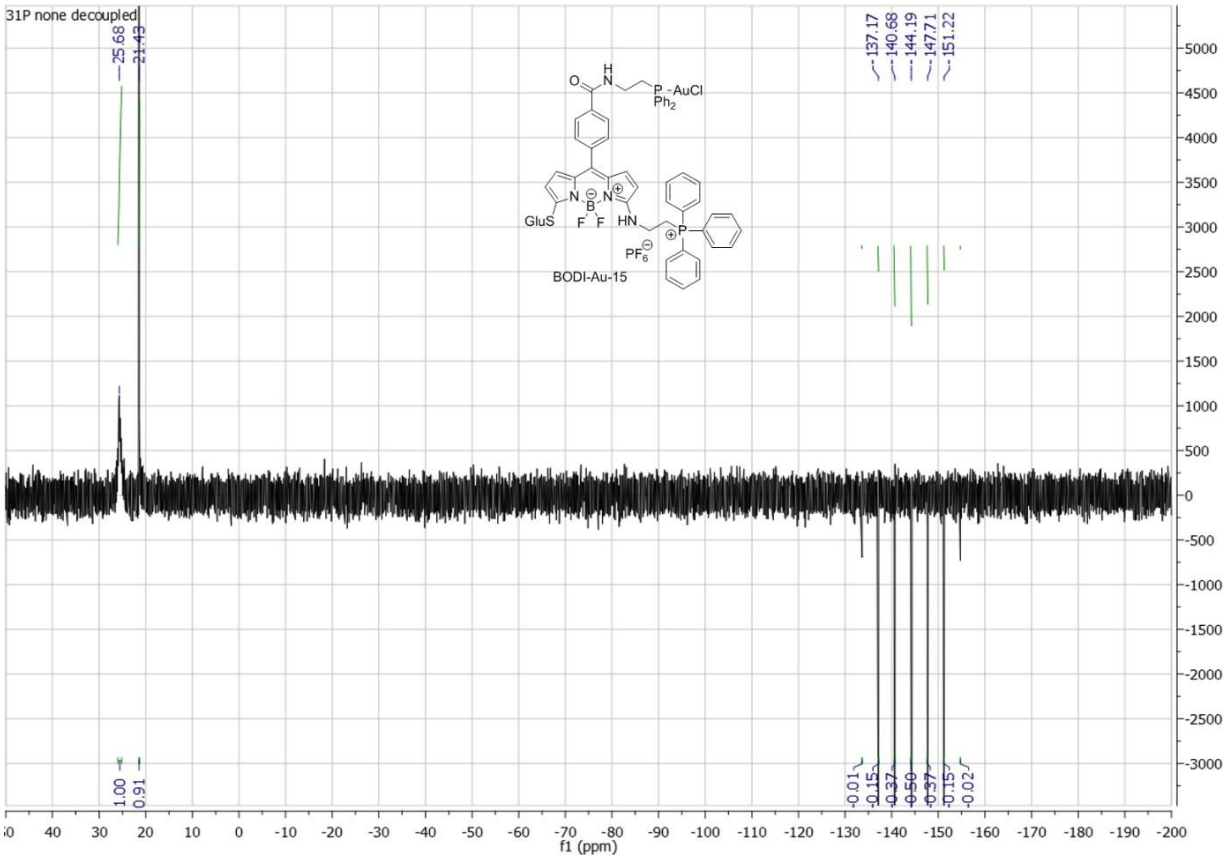

Figure S 88: ^{31}P NMR of **BODI-Au-15** (DMSO, 202 MHZ, 300K)

BODI-Au-16

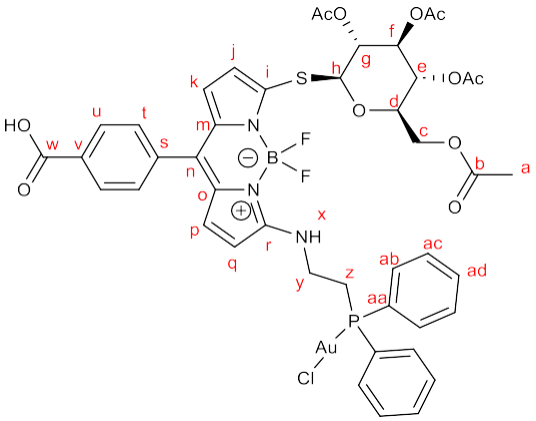

32.2mg (0.045mmol, 1eq) of BODIPY **7** were dissolved in 8 mL dry THF. 25.2mg (0.054mmol, 1.2eq) of 2-(diphenylphosphino)-ethylamine-aurichloride and 31.4mg (0.227mmol, 5eq) of K_2CO_3 were added, and the reaction was refluxed for 60min. The solvent was evaporated, and the crude product was purified by column chromatography on silica gel, using CH_2Cl_2/MeOH (100:0 to 90:10) as eluent. Product fractions were collected and evaporated to dryness. After dissolution in a minimal amount of CH_2Cl_2 the product is crushed out by addition of pentane (twice) to yield pure **BODI-Au-16** (42mg, 36.9 µmol, 82% yield) as a red-pink powder.

^{1}H NMR (500 MHz, DMSO-D6) δ (ppm)= 1.94, 1.99, 2.00 (3s, 12H, H_a), 3.22 – 3.07 (m, 2H, H_z), 3.68 (s, 2H, H_y), 4.05 (dd, J = 14.7, 5.2 Hz, 1H, H_d), 4.16 (q, J = 5.3 Hz, 2H, H_c), 4.95 (t, J = 9.7 Hz, 2H, H_g, H_e), 5.32 (d, J = 10.1 Hz, 1H, H_h), 5.39 (t, J = 9.4 Hz, 1H, H_f), 6.30 (d, J = 3.8 Hz, 1H, H_q), 6.43 (d, J = 3.8 Hz, 1H, H_p), 6.51 (d, J = 5.1 Hz, 1H, H_j), 6.94 (d, J = 5.1 Hz, 1H, H_k), 7.53 (d, J = 8.1Hz, H_{at}), 7.60 – 7.55 (m, 6H, H_{ac}, H_{ad}), 7.86 – 7.76 (m, 4H, H_{ab}), 8.06 (d, J = 7.9 Hz, 2H, H_u), 8.46 (s, 1H, H_x).

^{13}C NMR (126 MHz, DMSO-D6) δ (ppm)= 20.3 (s, C_a), 20.4 (s, C_a), 20.4 (s, C_a), 20.5 (s, C_a), 27.5 (d, J = 35.5 Hz, C_y), 41.2 (d, J = 10.5 Hz, C_z), 61.9 (s, C_c), 68.1 (s, C_e), 69.3 (s, C_f), 73.0 (s, C_g), 74.3 (s, C_d), 83.3 (s, C_h), 113.3 (s, C_q), 115.0 (s, C_j), 118.6 (s, C_p), 127.5 (s, C_r), 128.7 (ps-d, J = 3.5 Hz, C_{aa}, C_o, C_m), 129.2 (ps-d, J = 3.5 Hz, C_n, C_v), 129.3 (s, C_k), 129.4 (d, J = 11.7 Hz, C_{ad}), 130.1 (s, C_t), 132.1 (d, J=1.8Hz, C_{ac}), 132.5 (s, C_r, C_n), 133.2 (d, J = 12.6 Hz, C_{ab}), 133.7 (s, br, C_i, C_s), 135.2 (s, C_u), 161.2 (s, C_w), 169.1 (s, C_b), 169.3 (s, C_b), 169.5 (s, C_b), 170.0 (s, C_b).

^{11}B NMR (160 MHz, DMSO-D6) δ (ppm)= 0.69 (t, J = 34.0 Hz).

^{19}F NMR (470 MHz, DMSO-D6) δ (ppm)= -142.81 – -143.79 (m).

^{31}P NMR (202 MHz, DMSO-D6) δ (ppm) = 24.40 (s, br).

HR-MS (ESI): *m/z* = calculated for $C_{44}H_{43}Au_1B_1Cl_1F_2N_3O_{11}P_1S_1Na_1$ $[M+Na]^+$ 1156.16633; found 1156.17033.

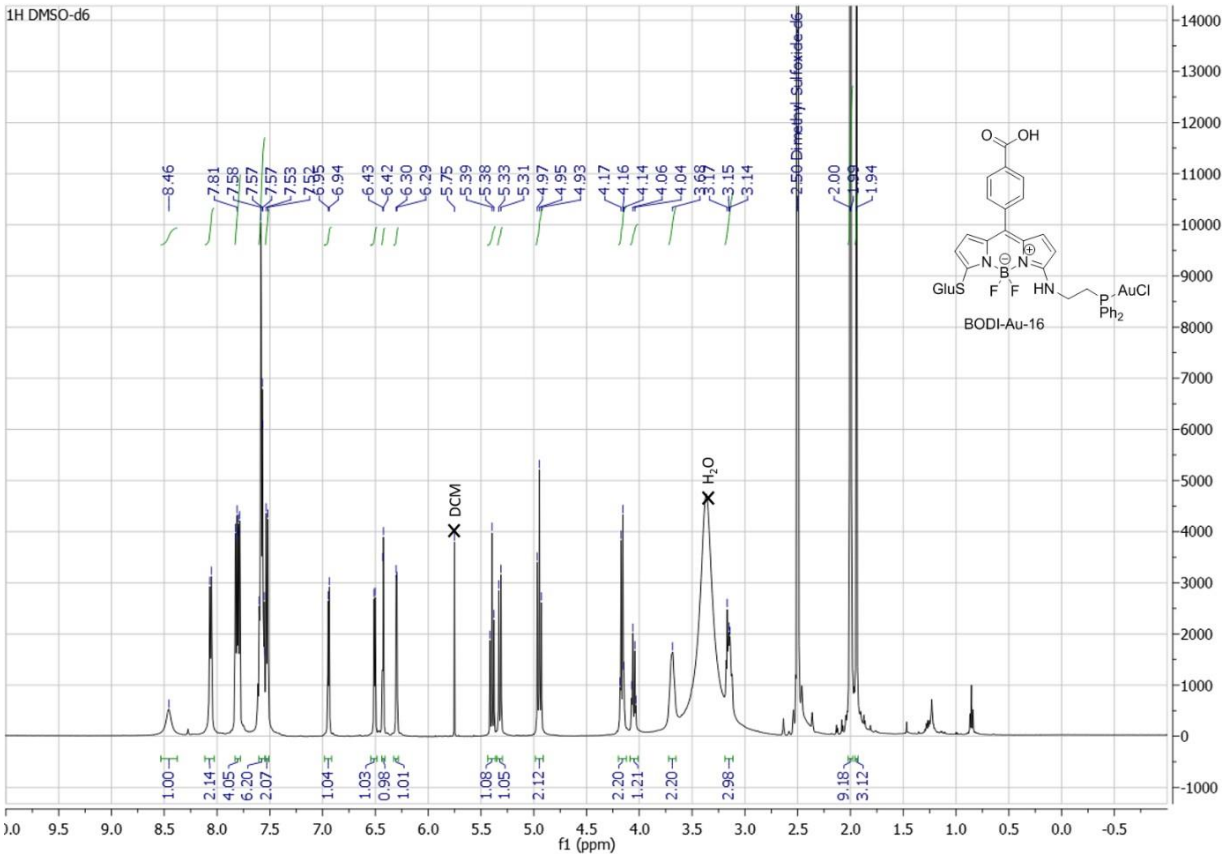

Figure S 89: ^{1}H NMR of **BODI-Au-16** (DMSO, 500 MHZ, 300K)

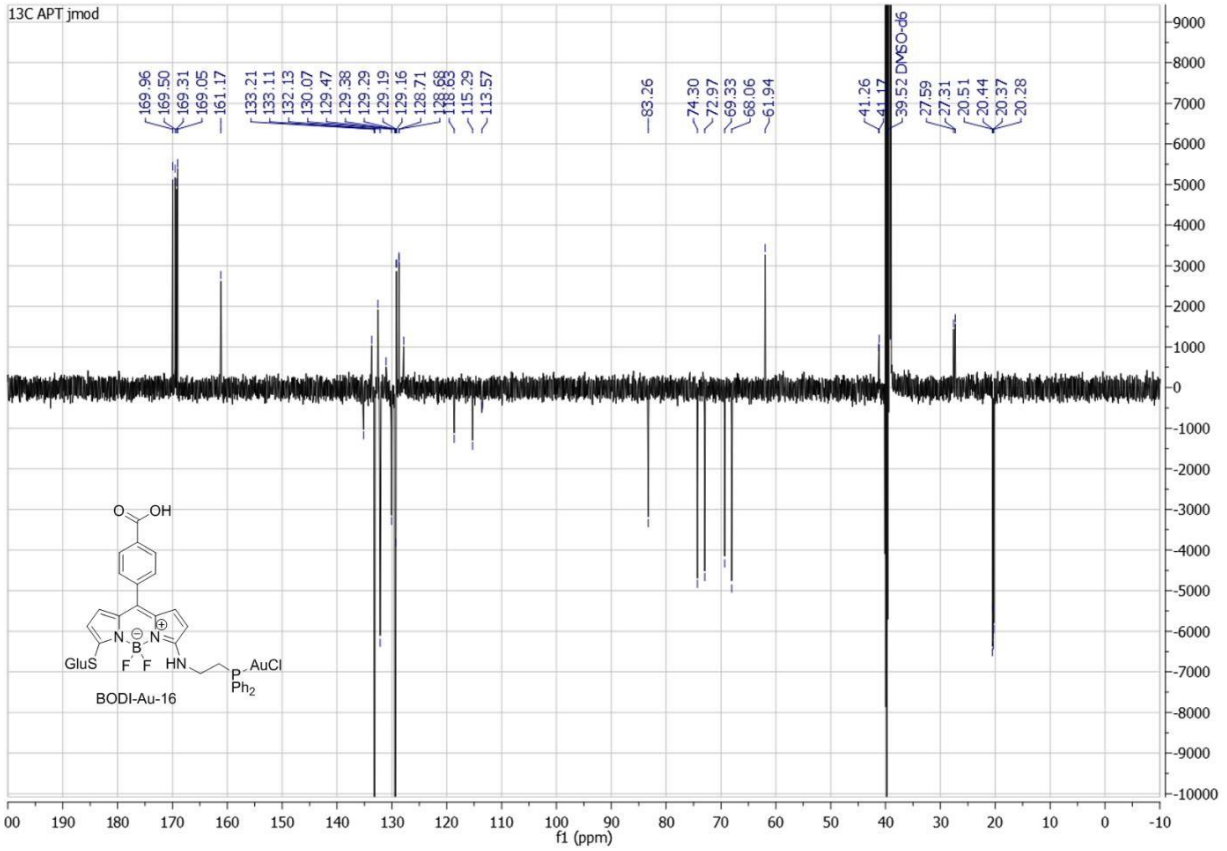

Figure S 90: ^{13}C NMR (APT jmod) of BODI-Au-16 (DMSO, 126 MHZ, 300K)

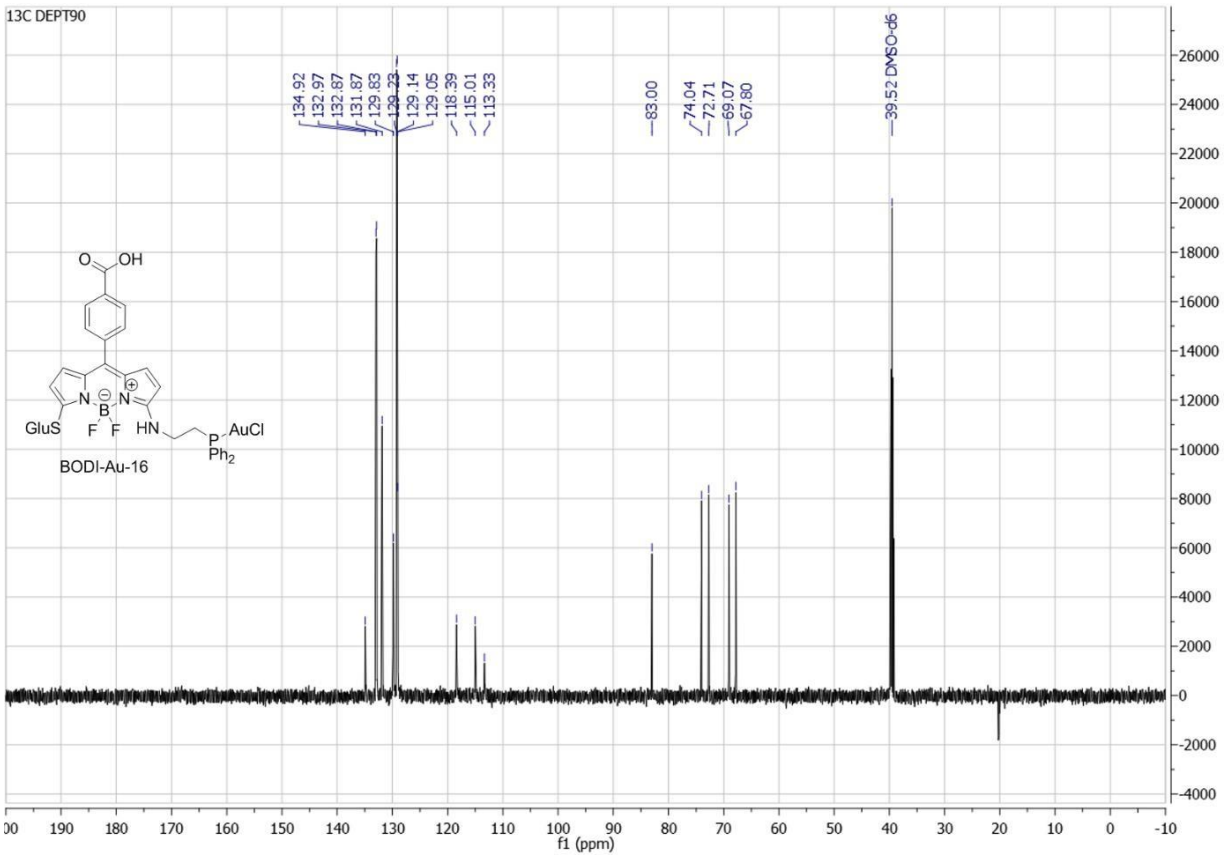

Figure S 91: ^{13}C NMR (DEPT90) of **BODI-Au-16** (DMSO, 126 MHZ, 300K)

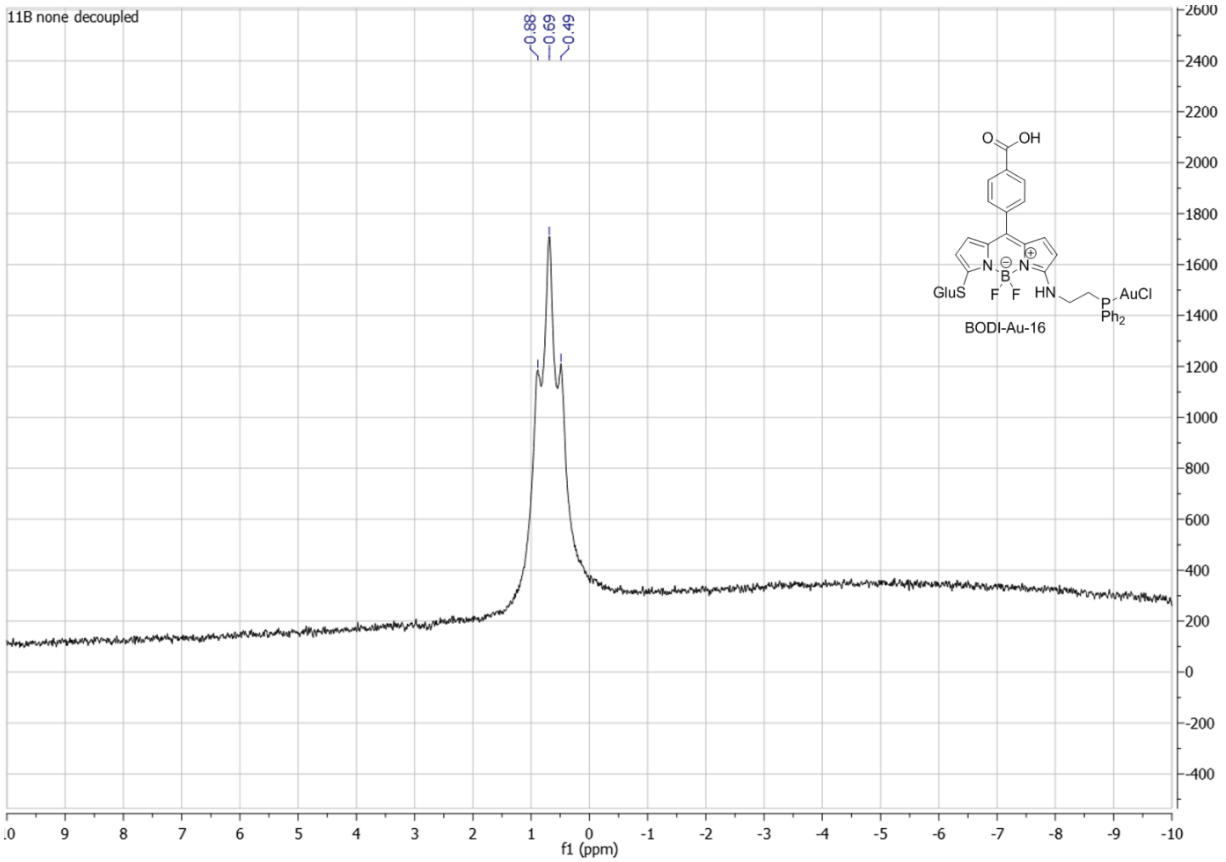

Figure S 92: ^{11}B NMR of **BODI-Au-16** (DMSO, 160 MHZ, 300K)

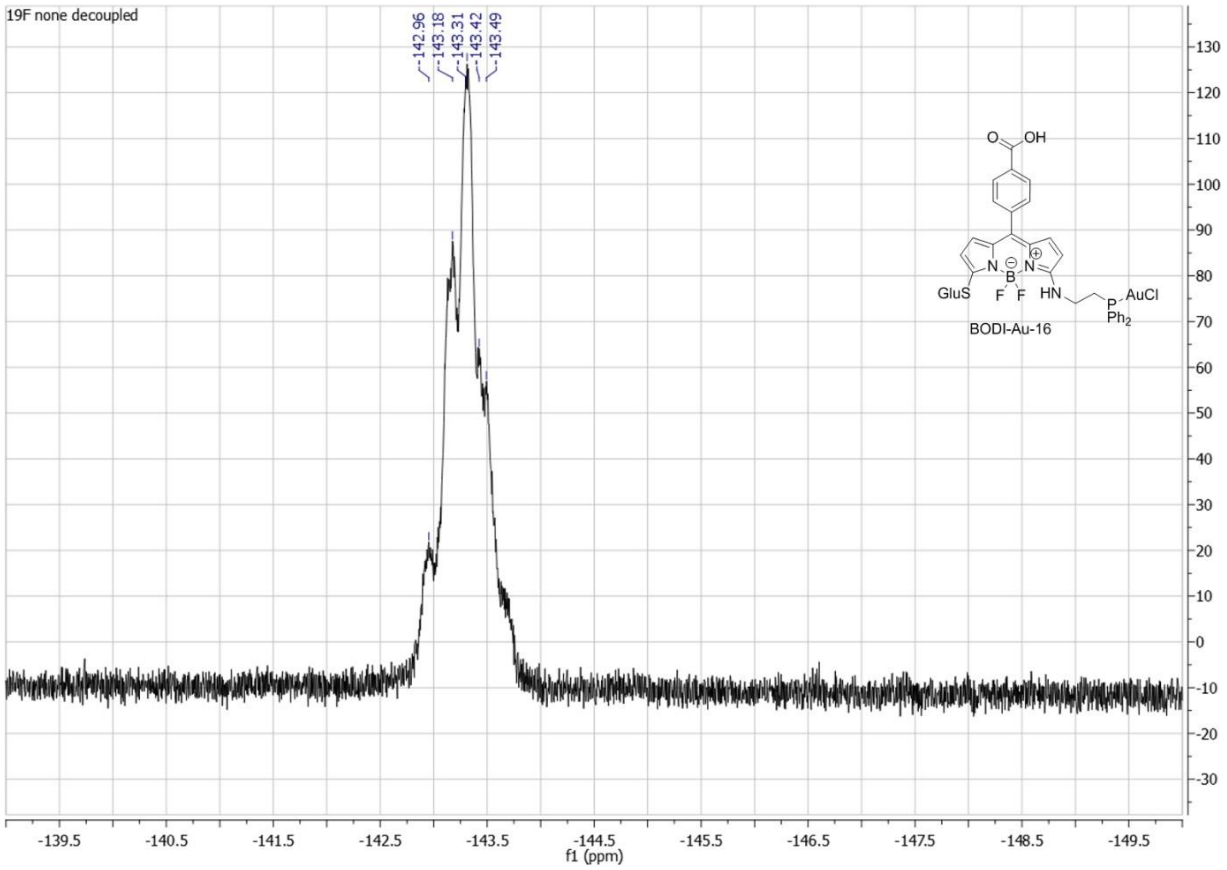

Figure S 93: ^{19}F NMR of **BODI-Au-16** (DMSO, 470 MHZ, 300K)

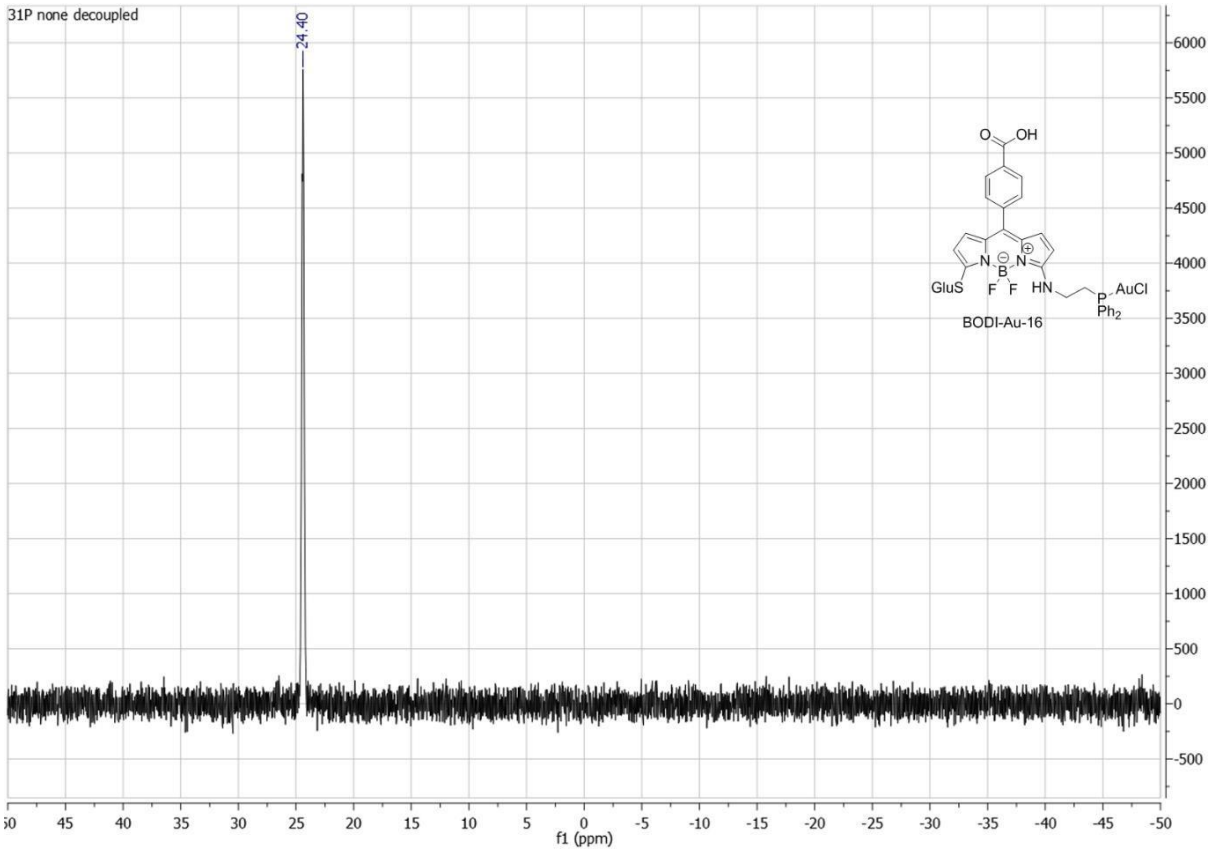

Figure S 94: ^{31}P NMR of **BODI-Au-16** (DMSO, 202 MHZ, 300K)

BODI-Au-17

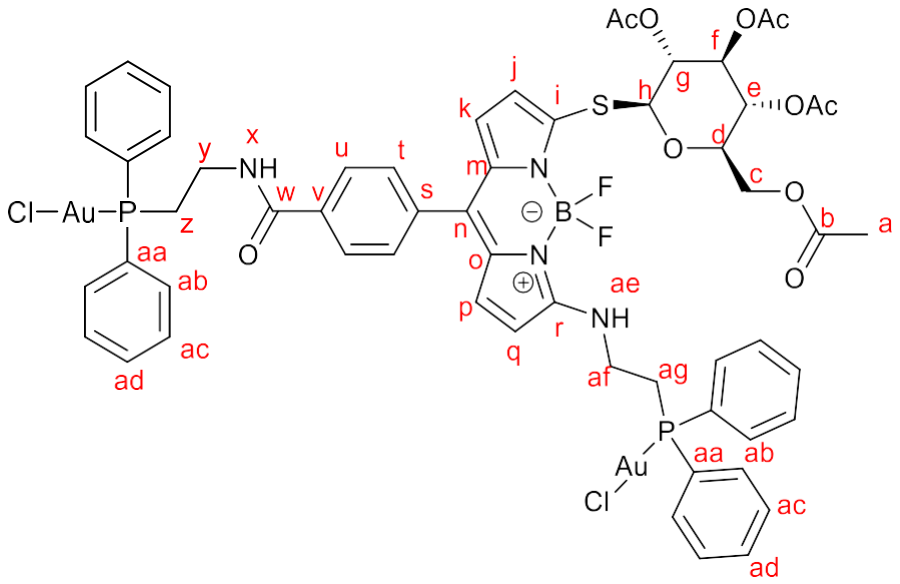

50mg (0.071mmol, 1eq) of BODIPY **7** were dissolved in 5 mL CH_2Cl_2. 30 µL (0.35mmol, 5eq) of $(COCl)_2$ and a droplet of DMF were added and the reaction was stirred at room temperature. After 45min the solvents were evaporated and the resulting solid was redissolved in 15 mL CH_3CN. 2-(Diphenylphosphino) ethylamine-aurichloride (78mg, 0.169mmol, 2.4eq) and $NaHCO_3$ (30mg, 0.35mmol, 5eq) were added and the reaction was refluxed for 60min. The solvent was evaporated and the crude product purified by column chromatography on silica gel, using CH_2Cl_2/MeOH (100:0 to 90:10) as eluent. The different product fractions were collected and evaporated to dryness. The product was dissolved in a minimal amount of CH_2Cl_2 and crushed out by addition of pentane (twice) to obtain 102mg (65.32 µmol, yield = 92%) of the target compound as a red-pink powder.

^{1}H NMR (500 MHz, DMSO-D6) δ (ppm)= 1.91, 1.94, 2.00, 2.01 (4s, 12H, H_a), 3.10 (dt, J = 11.0, 6.9 Hz, 2H, H_z), 3.18 – 3.13 (m, 2H, H_{ag}), 3.58 (dt, J = 20.6, 6.7 Hz, 2H, H_y), 3.69 (dt, J = 15.3, 7.8 Hz, 2H, H_{af}), 4.06 (q, J = 5.1 Hz, 1H, H_d), 4.17 (q, J = 5.1 Hz, 2H, H_c), 4.95 (t, J = 9.7 Hz, 2H, H_g, H_e), 5.32 (d, J = 10.1 Hz, 1H, H_h), 5.40 (t, J = 9.4 Hz, 1H, H_f), 6.28 (d, J = 3.8 Hz, 1H, H_q), 6.44 (d, J = 3.8 Hz, 1H, H_p), 6.52 (d, J = 5.1 Hz, 1H, H_j), 6.91 (d, J = 5.1 Hz, 1H, H_k), 7.49 (d, J = 8.3 Hz, 2H, H_t), 7.63 – 7.53 (m, 12H, H_{ac}, H_{ad}), 7.84 – 7.77 (m, 8H, H_{ab}), 7.89 (d, J = 8.3 Hz, 2H, H_u), 8.47 (s, 1H, H_{ae}), 8.86 (t, J = 5.4 Hz, 1H, H_x).

^{13}C NMR (126 MHz, DMSO-D6) δ (ppm)= 20.23 (s, Ca), 20.3 (s, C_a), 20.4 (s, C_a), 20.5 (s, C_a), 26.4 (d, J = 37.8 Hz, C_y), 27.4 (d, J = 35.7 Hz, C_{af}), 35.8 (d, J = 5.4 Hz, C_z), 41.2 (d, J = 9.4 Hz, C_{ag}), 61.9 (s, C_c), 68.1 (s, C_e), 69.3 (s, C_f), 73.0 (s, C_g), 74.3 (s, C_d), 83.2 (s, C_h), 113.4 (s, C_q), 115.3 (s, C_j), 118.5 (s, C_p), 127.3 (s, C_k), 127.7 (s, C_o), 128.9 (dd, J = 60.7, 3.2 Hz, C_{aa}), 129.0 (s, C_m), 129.4 (dd, J = 11.6, 2.6 Hz, Ca_d), 129.5 (s, C_v), 129.9 (s, C_u), 132.0 (d, J = 16.9 Hz, C_{ac}), 132.5 (s, C_n), 133.1 (dd, J = 13.4, 1.6 Hz, C_{ab}), 133.2 (s, C_s), 134.3 (s, C_r), 135.0 (s, C_t), 136.5 (s, C_i), 161.2 (s, C_w), 169.0 (s, C_a), 169.3 (s, C_a), 169.4 (s, C_a), 169.9 (s, C_a).

^{11}B NMR (160 MHz, DMSO-D6) δ (ppm)= 1.04 – 0.40 (m).

^{19}F NMR (470 MHz, DMSO-D6) δ (ppm)= -142.79 – -143.80 (m).

^{31}P NMR (202 MHz, DMSO-D6) δ (ppm)= 24.62 – 24.15 (m, 1P), 25.32 – 24.77 (m, 1P).

^{31}P {1H} NMR (202 MHz, DMSO-D6) δ (ppm) = 24.42, 25.05.

HR-MS (ESI): *m/z* = calculated for $C_{58}H_{57}Au_2B_1Cl_2F_2N_4O_{10}P_2S_1Na_1$ $[M+Na]^+$ 1599.19321; found 1599.19617.

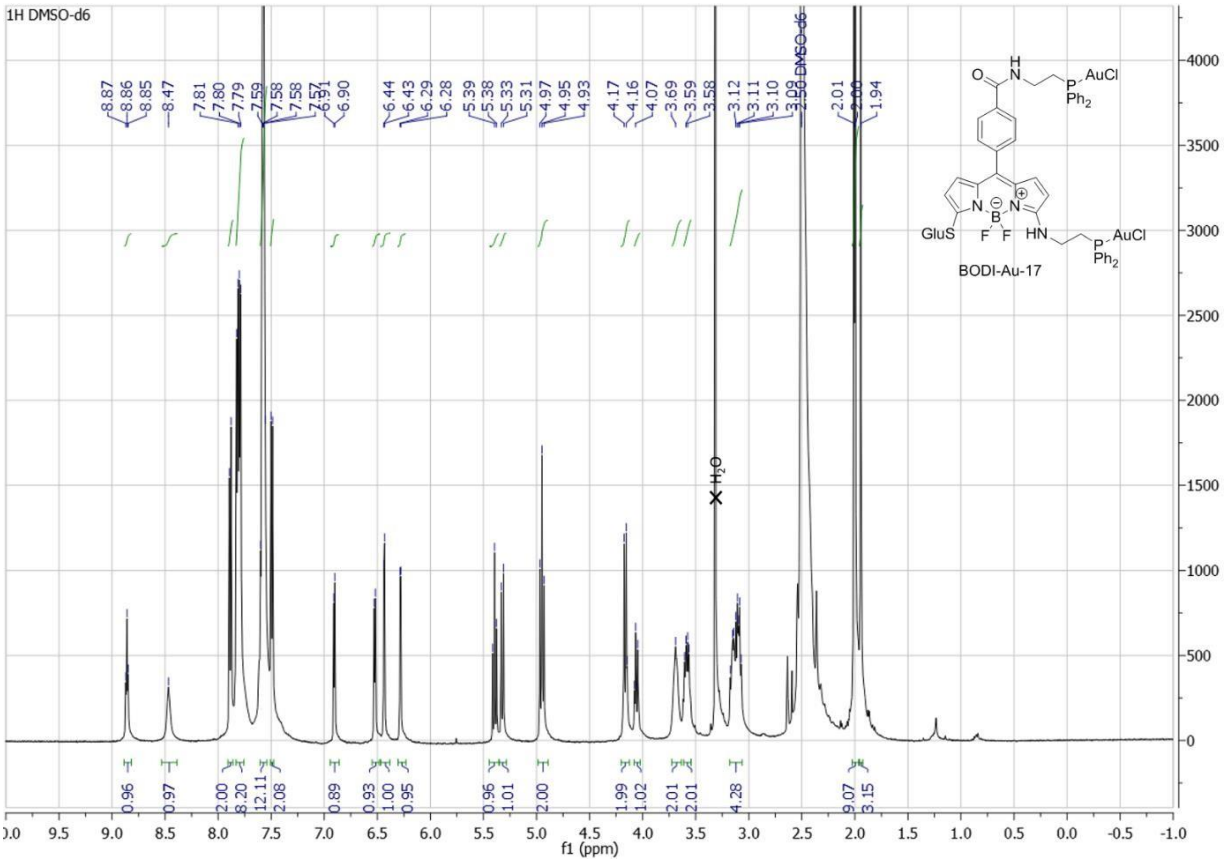

Figure S 95: ^{1}H NMR of **BODI-Au-17** (DMSO, 500 MHZ, 300K)

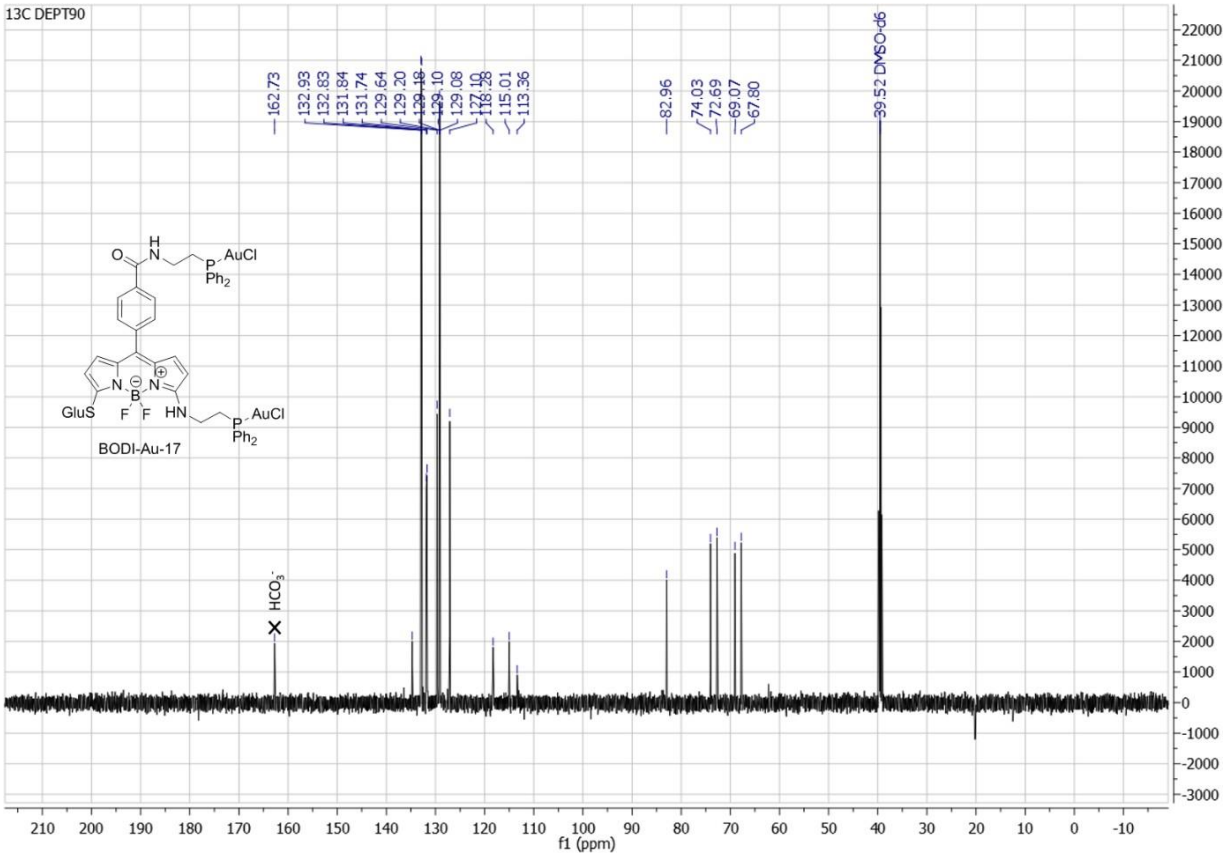

Figure S 96: ^{13}C NMR (DEPT90) of **BODI-Au-17** (DMSO, 126 MHZ, 300K)

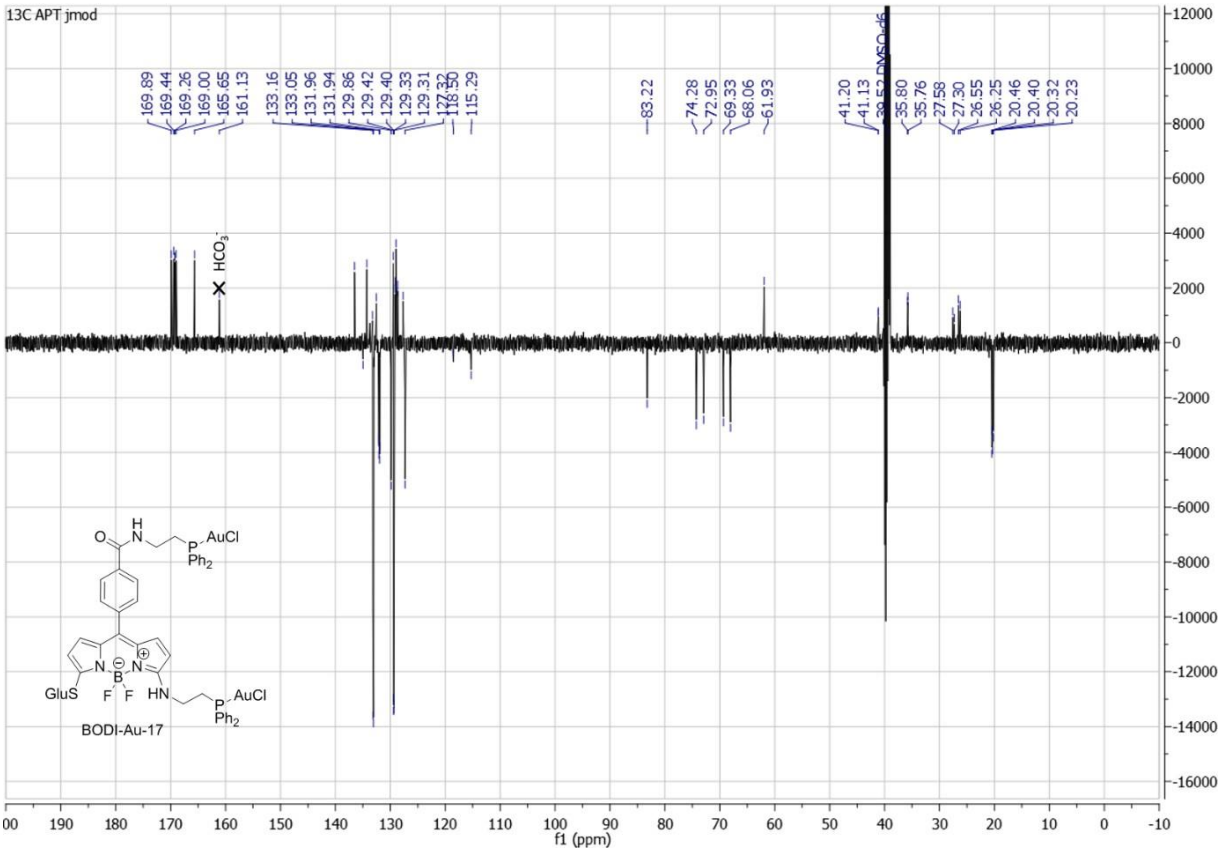

Figure S 97: ^{13}C NMR (APT jmod) of **BODI-Au-17** (DMSO, 126 MHZ, 300K)

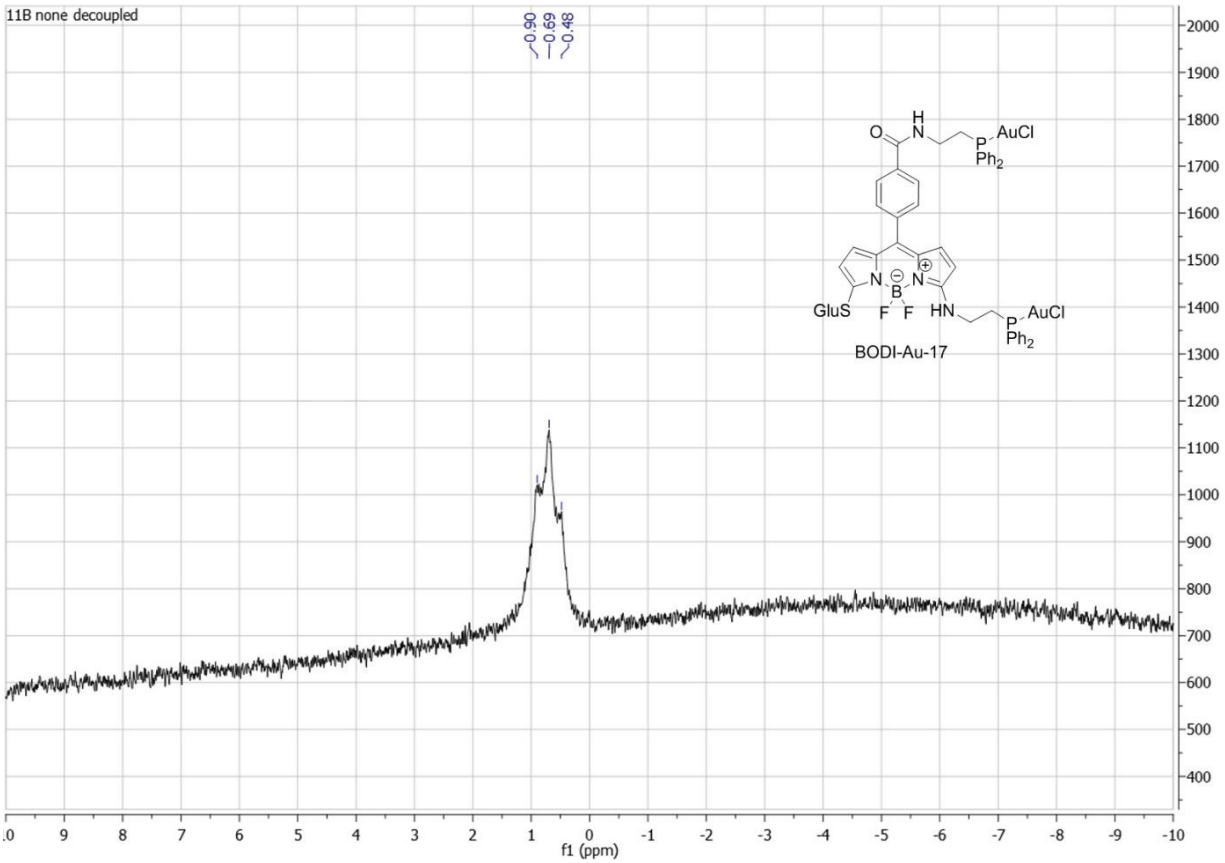

Figure S 98: ^{11}B NMR of **BODI-Au-17** (DMSO, 160 MHZ, 300K)

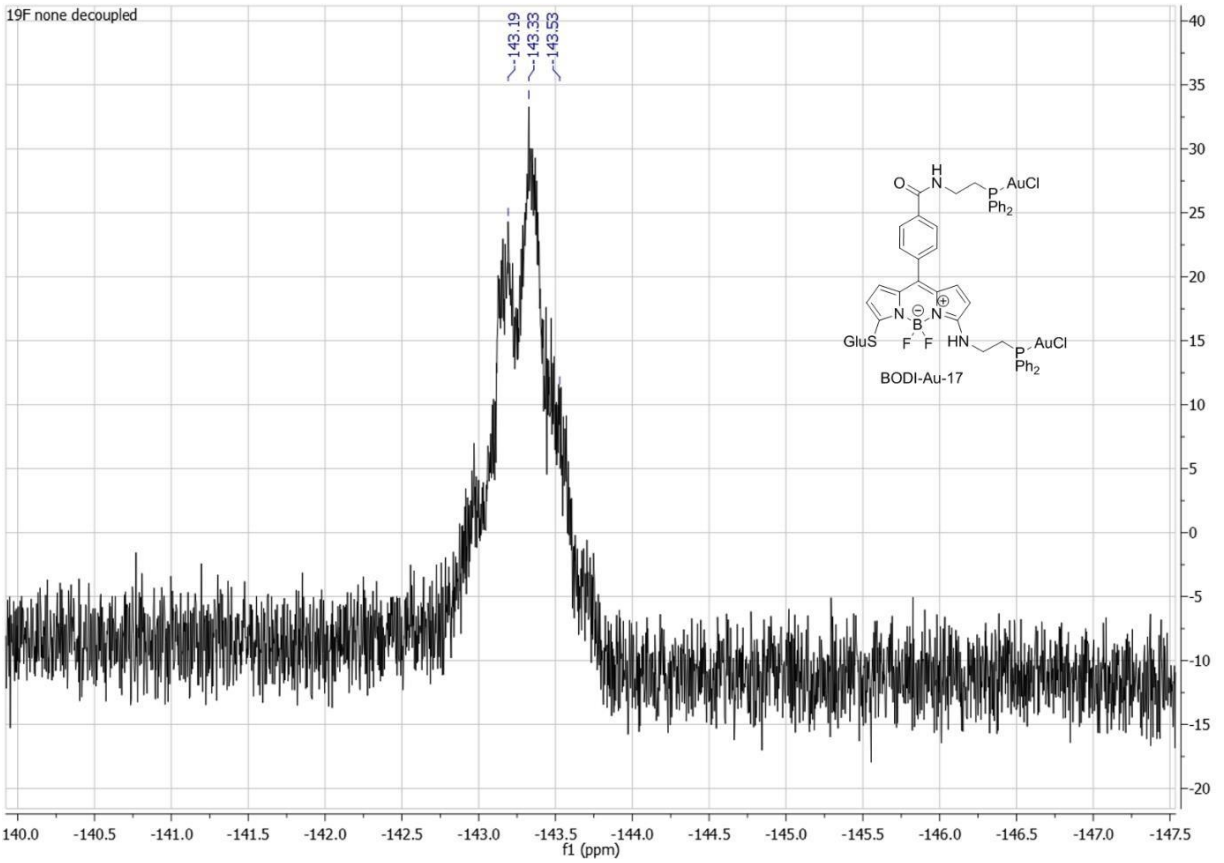

Figure S 99: ^{19}F NMR of **BODI-Au-17** (DMSO, 470 MHZ, 300K)

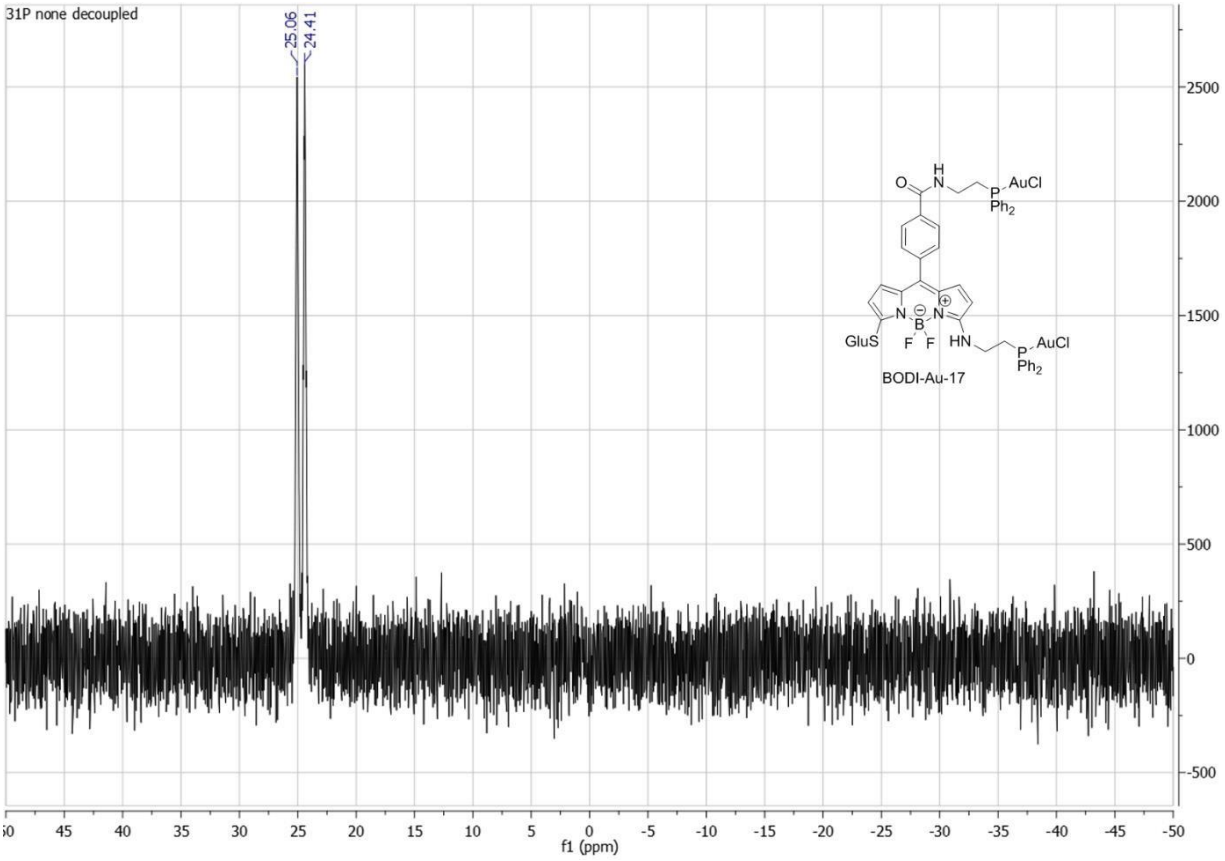

Figure S 100: ^{31}P NMR of **BODI-Au-17** (DMSO, 202 MHZ, 300K)

Photophysical data

UV-Visible absorption spectra were recorded on a JASCO V630BIO spectrometer. The steady-state fluorescence emission spectra were obtained by using a JASCO FP8560 spectrofluorometer instrument. All fluorescence spectra were corrected for instrument response. The fluorescence quantum yields (Φ_F) were calculated from equation:

$$\frac{\varphi_F}{\varphi_{FR}} = \frac{n^2}{n_R^2} \times \frac{\int_0^\infty I_F(\lambda_E, \lambda_F) d\lambda_F}{\int_0^\infty I_{FR}(\lambda_E, \lambda_F) d\lambda_F} \times \frac{1-10^{-A_R(\lambda_E)}}{1-10^{-A(\lambda_E)}}$$

Φ_F and Φ_{FR} are fluorescence quantum yields of the compound and the reference respectively. $A(\lambda_E)$ and $A_R(\lambda_E)$ are the absorbance at the excitation wavelength, and n is the refractive index of the medium. I_F and I_{FR} are fluorescent intensities of the compound and the reference respectively. Rhodamine 6G ($\Phi = 0.94$ in EtOH, λ_{ex} = 488 nm) was used as the standard.[4] In all Φ_F determinations, correction for the solvent refractive index (η) was applied.

Table S 1: Photophysical data and spectra of the different BODIPY derivatives in DMSO at 293K.

Compound	Structure	λ_{abs} (nm)	λ_{em} (nm)[a]	ε ($M^{-1}.cm^{-1}$)	Φ_f (%)[b]
1		514	530	76,000	13
2		518	538	69,000	5
3		517	537	66,000	6
4		538	553	73,000	39
5		516	531	125,000	8
6		541	559	48,000	23
7		540	555	75,000	26
8		525	567	29,000	21
BODI-Au-7		476	538	33,000	24
BODI-Au-8		476	538	35,000	23
BODI-Au-9		508	565	31,000	28
BODI-Au-10		516	533	81,000	8
BODI-Au-11		479	544	31,000	21
BODI-Au-12		479	543	34,000	24
BODI-Au-13		480	546	30,000	15
BODI-Au-14		480	546	26,000	18
BODI-Au-15		523	569	16,000	21
BODI-Au-16		513	570	24,000	15
BODI-Au-17		511	569	31,000	24

[a]: λ_{ex} = 488 nm; [b]: Rhodamine 6G ($\Phi = 0.94$ in EtOH, λ_{ex} = 488 nm) was used as the standard.[4]

BODIPY **1**

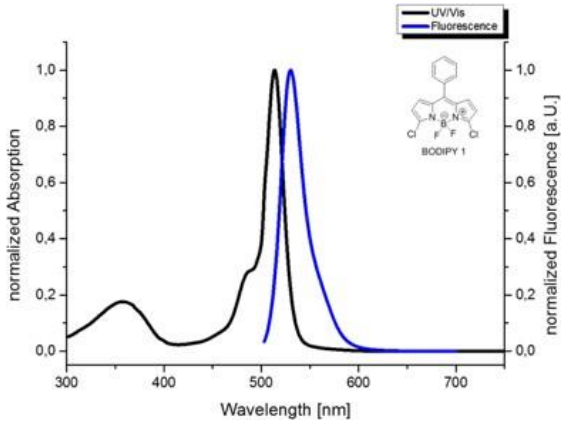

BODIPY **2**

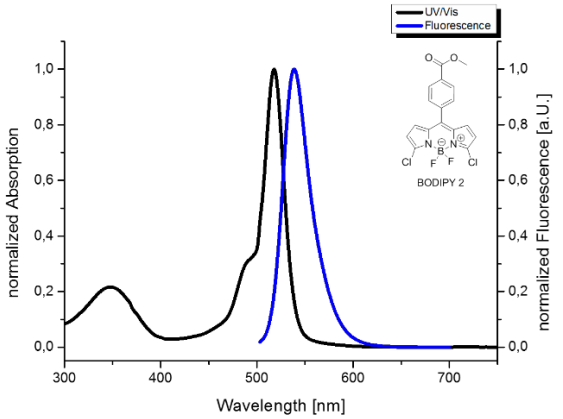

BODIPY **3**

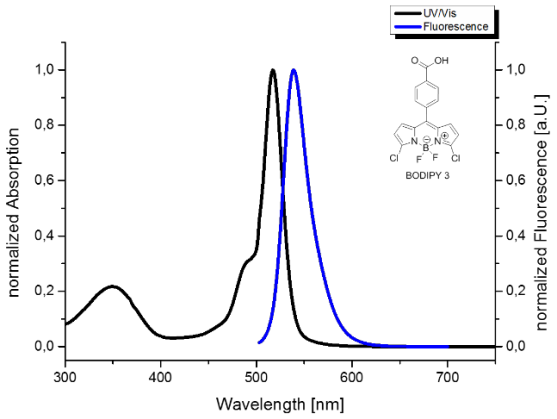

BODIPY **4**

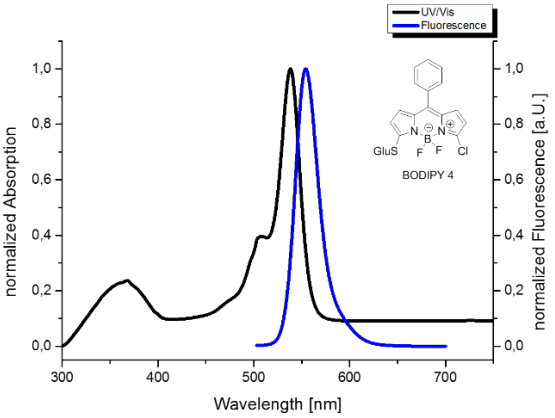

BODIPY **5**

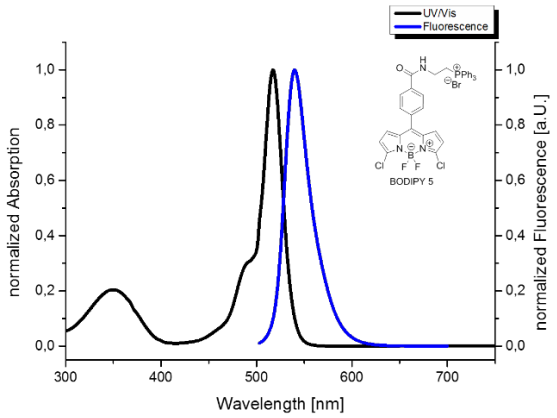

BODIPY **6**

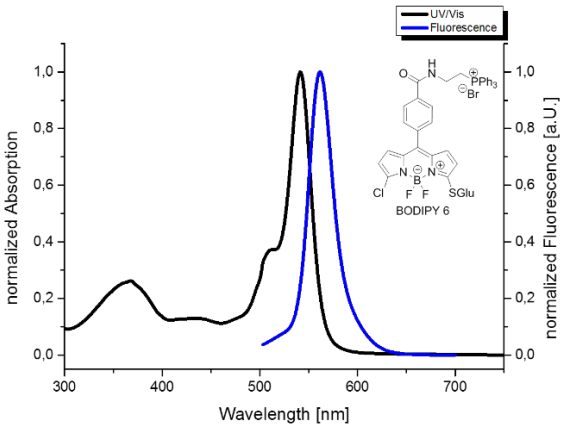

BODIPY **7**

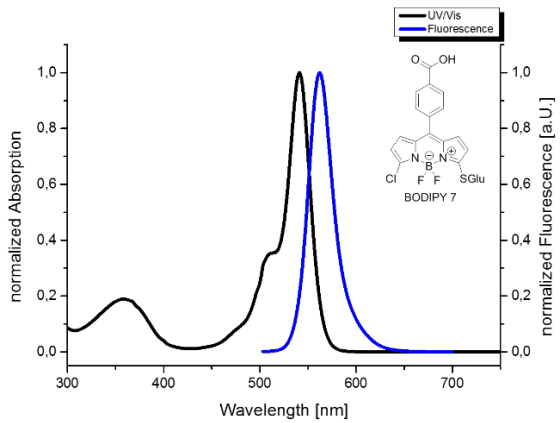

BODIPY **8**

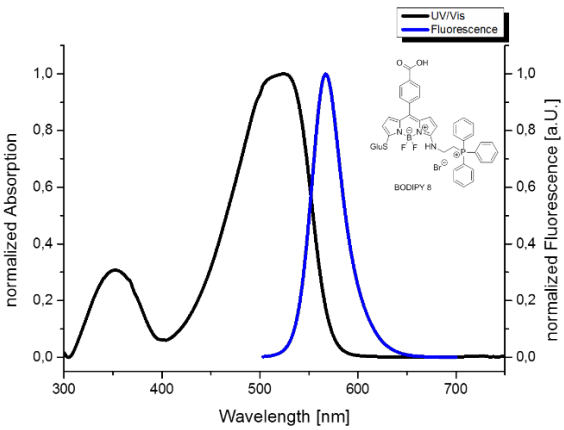

BODI-Au-7

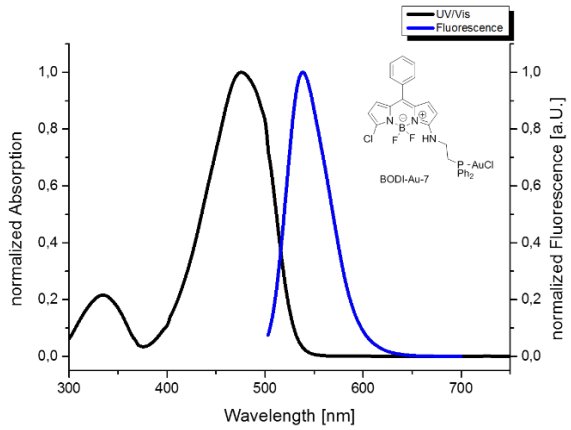

BODI-Au-8

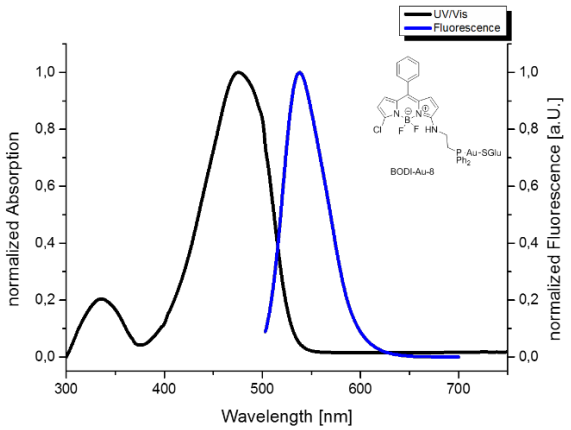

BODI-Au-9

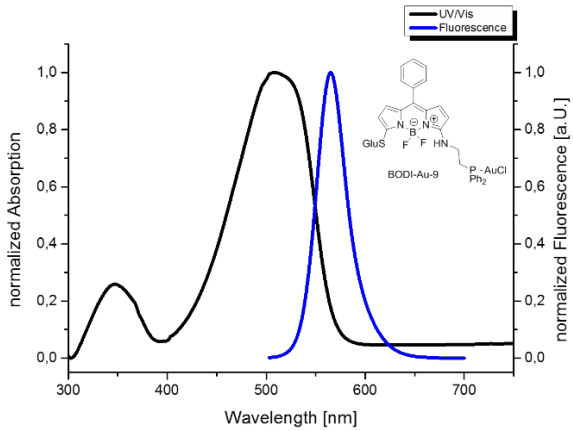

BODI-Au-10

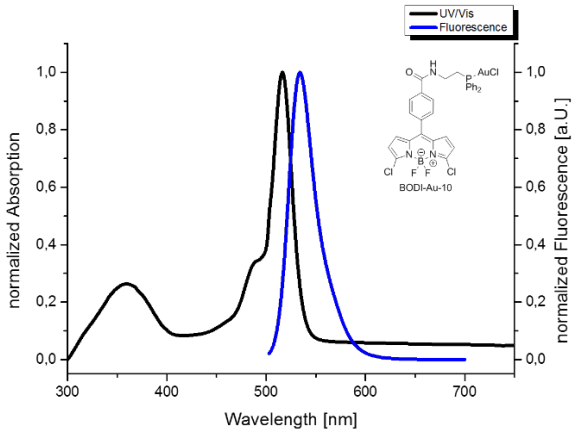

BODI-Au-11

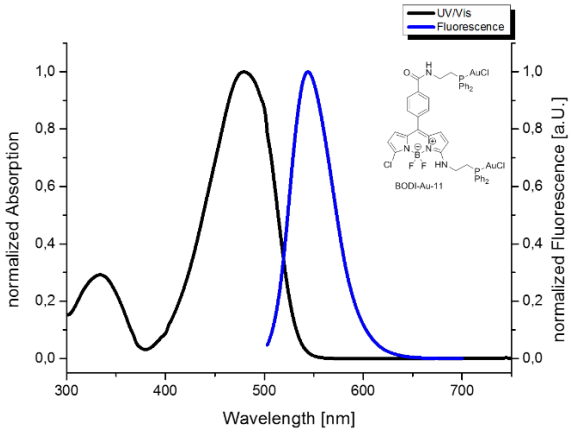

BODI-Au-12

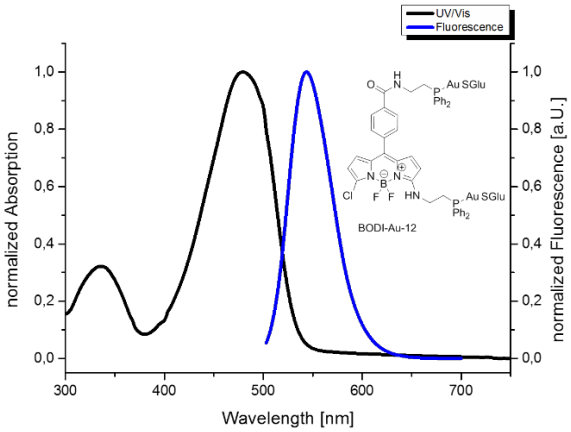

BODI-Au-13

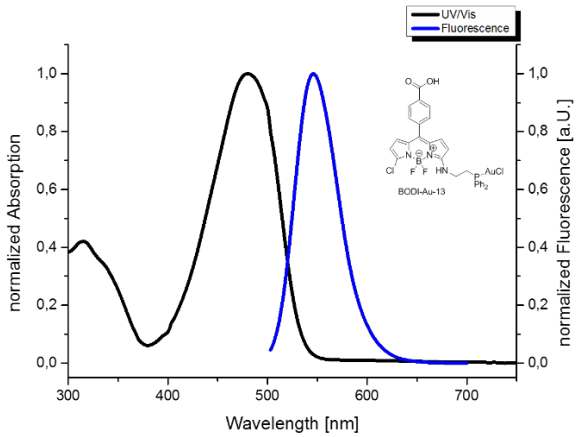

BODI-Au-14

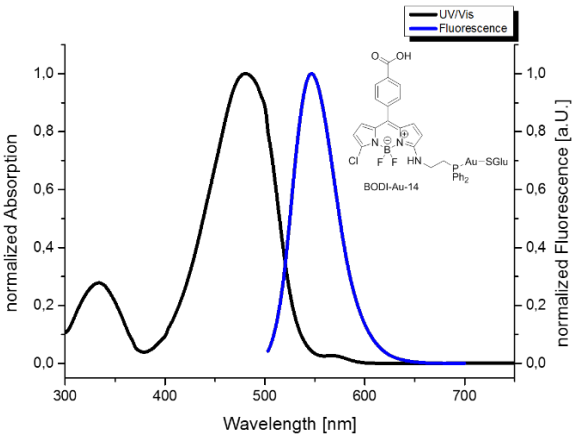

BODI-Au-15

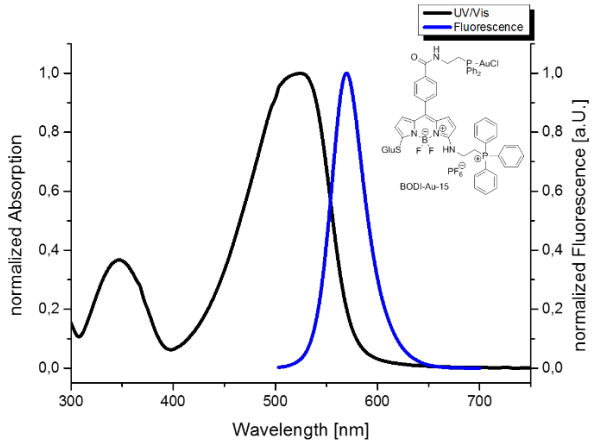

BODI-Au-16

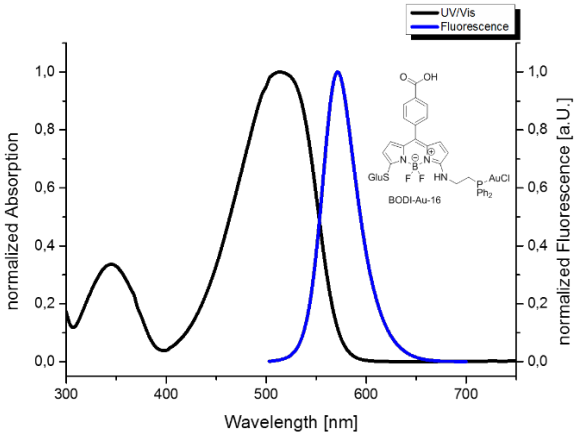

BODI-Au-17

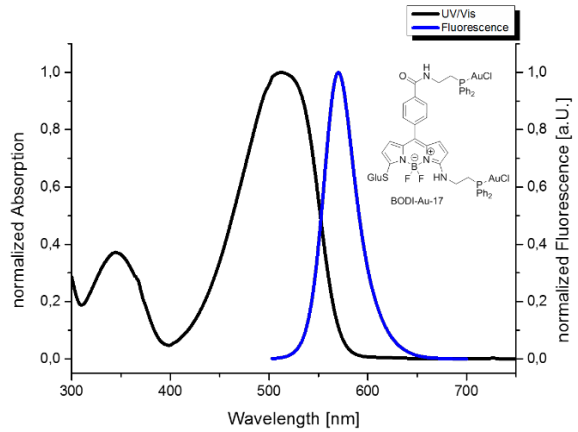

Figure S101: Normalized absorption (black) and emission ($\lambda_{ex} = 488$ nm) (blue) of BODIPY derivatives in DMSO at room temperature.

Theoretical calculation

Computational details

All DFT calculations were carried out Gaussian 09 (*Gaussian 09, Revision D.01, M. J. Frisch, G. W. Trucks, H. B. Schlegel, G. E. Scuseria, M. A. Robb, J. R. Cheeseman, G. Scalmani, V. Barone, G. A. Petersson, H. Nakatsuji, I. Li, M. Caricato, A. Marenich, J. Bloino, B. G. Janesko, R. Gomperts, B. Mennucci, H. P. Hratchian, J. V. Ortiz, A. F. Izmaylov, J. L. Sonnenberg, D. Williams-Young, F. Ding, F. Lipparini, F. Egidi, J. Goings, B. Peng, A. Petrone, T. Henderson, D. Ranasinghe, V. G. Zakrzewski, J. Gao, N. Rega, G. Zheng, W. Liang, M. Hada, M. Ehara, K. Toyota, R. Fukuda, J. Hasegawa, M. Ishida, T. Nakajima, Y. Honda, O. Kitao, H. Nakai, T. Vreven, K. Throssell, J. A. Montgomery, Jr., J. E. Peralta, F. Ogliaro, M. Bearpark, J. J. Heyd, E. Brothers, K. N. Kudin, V. N. Staroverov, T. Keith, R. Kobayashi, J. Normand, K. Raghavachari, A. Rendell, J. C. Burant, S. S. Iyengar, J. Tomasi, M. Cossi, J. M. Millam, M. Klene, C. Adamo, R. Cammi, J. W. Ochterski, R. L. Martin, K. Morokuma, O. Farkas, J. B. Foresman, and D. J. Fox, Gaussian, Inc., Wallingford CT, 2016.*), tightening self-consistent field convergence thresholds (10^{-10} a.u.). A 6-31G(d) basis set and the hybrid functional M06-2X[6] were employed given the good performance of such scheme in other studies.[7,8] The DMSO solvent effects were included according to the Polarizable Continuum Model.[9,10] The LUMO isosurfaces have been plotted with the Chemcraft code[11] considering a contour threshold of 0.05 a.u.

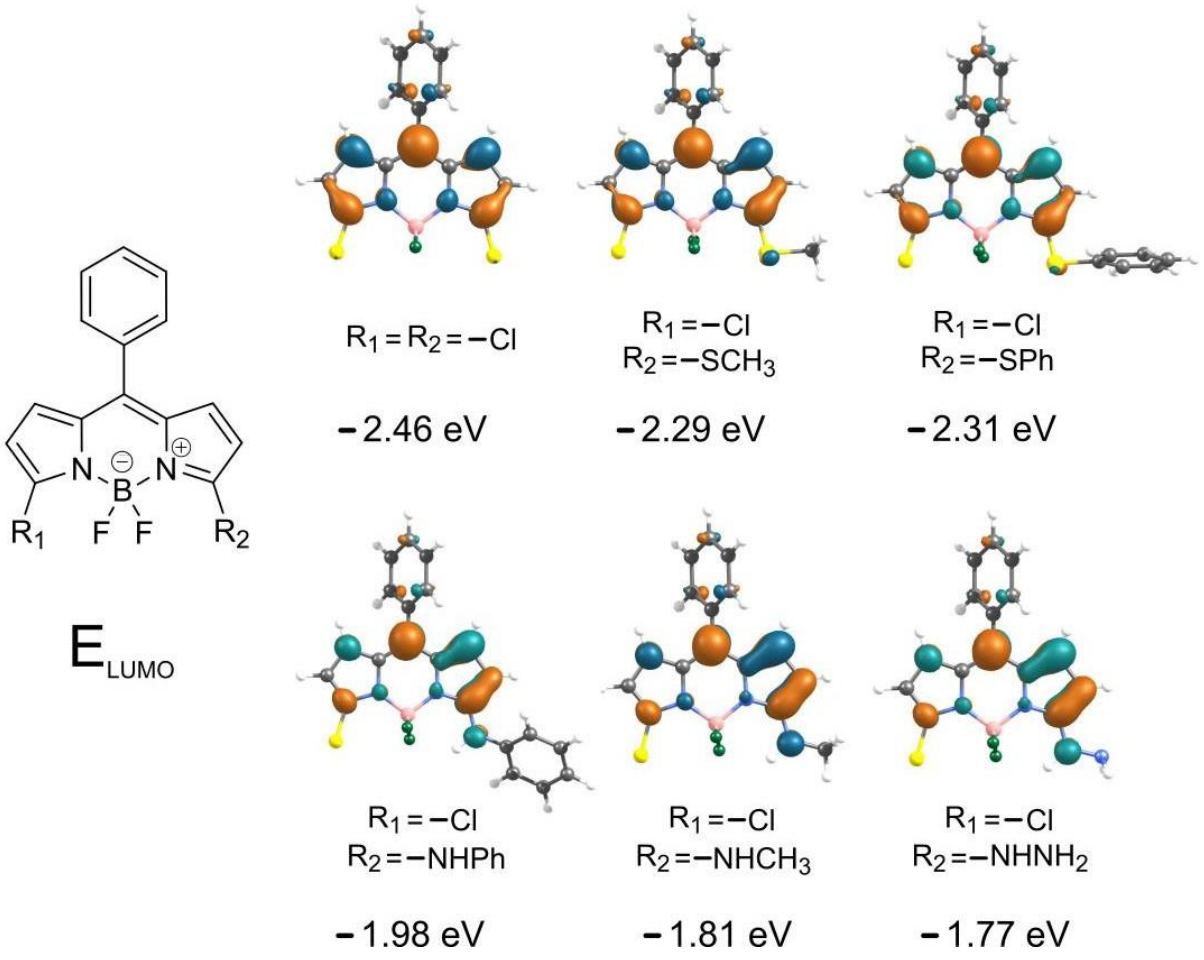

Figure S 102: LUMO energies (eV) for some model systems

Results and Discussion

We conducted DFT calculations at the M06-2X/6-31G(d) level to determine the lowest unoccupied molecular orbital energy (E_{LUMO}) for some model systems containing amino- and thio-groups, bearing in mind that this value can be associated to the electrophilicity of the

molecule.[12,13] Then, the higher E_{LUMO}, the lower the probability of the molecule to experience a nucleophilic attack.

In Figure S 102 we can observe the graphical representation of the LUMO, which is mainly distributed over the dipyrromethene core in all systems. Remarkably, the small contribution of the phenyl ring at the *meso* position evidences the poor conjugation between this fragment and the boron-dipyrromethene moiety given the broad dihedral angle between them.

The replacement of a chlorine atom by an amino-/thio- substituent leads to an E_{LUMO} increase with respect to the dichloro- starting compound. This effect is more pronounced for the amino-substituted BODYPYs (ΔE_{LUMO} ~ 0.61 eV) than for their thio-substituted counterparts (ΔE_{LUMO} ~ 0.16 eV). These calculated values are in good agreement with experimental data related to the great difficulty to incorporate a second group to the amino-substituted BODIPYs.

In summary, our results evidence how the higher electron-donor behavior of the amino-substituents increases the LUMO energy in a larger extent than the thio- groups, resulting in a minor reactivity of the BODIPY toward a nucleophilic substitution.

Additionally, we have estimated the reaction energies for (a) the incorporation of an aminomethyl group in the thio-substituted BODIPY and (b) the incorporation of a thiomethyl in the amino-substituted BODIPY, both process leading to the same products. We found that reaction (a) is the more exothermic process releasing more than three times the energy of (b).

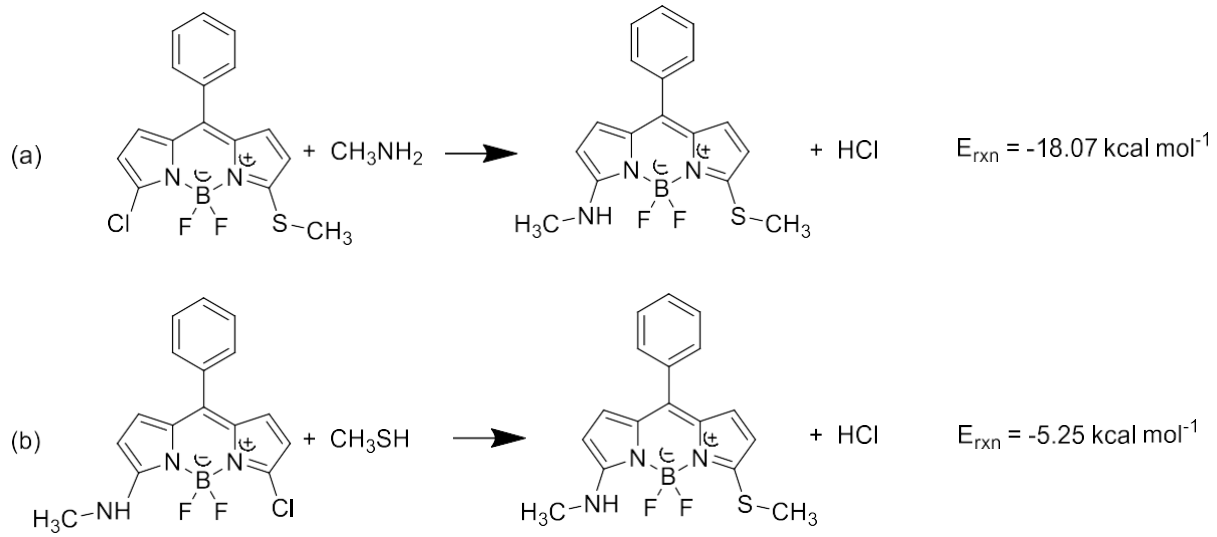

Scheme S 1: Some hypothetical reactions involving the model systems.

The energy release associated to the substituents incorporation is calculated, resulting in a more exothermic process when the thiomethyl is first added to the BODIPY, followed by the aminomethyl.

Determination of cytotoxic properties

5 mM stock solutions were prepared by dissolving the compounds in DMSO. 10^5 cells were seeded in 96-well flat-bottomed microplates (final volume 100 µL per well) and incubated for 24h to allow for cell adherence. The medium was then replenished with 100 µL fresh medium containing the compounds to be tested at increasing concentrations (ranging from 0.5 to 150 µM) at 37°C for 48 h. The cytotoxic activity of compounds and drug references was determined using the MTS assay (Promega®). The assay is based on the reduction of a tetrazolium compound to a colored formazan in the presence of an electron coupling reagent (phenazine ethosulfate; PES) and NADH/NADPH produced by metabolically active cells. Thereafter, 10 µL of MTS (3-(4,5-dimethylthiazol-2-yl)-5-(3-carboxymethoxyphenyl)-2-(4-sulfophenyl)-2H-tetrazolium, Promega, Charbonnieres, France) was added in 200 µL of medium and absorbance at 490 nm was measured after 3h incubation at 37°C. The resulting IC_{50} values were calculated using GraphPad Prism 5.0 software. Each treatment was performed in three independent experiments.

Table S 2: Determination of the IC_{50} values (µM) of the different BODIPY derivatives on MDA-MB-231, EMT6, and B16F10 cell lines by MTS assay (Promega®) at 48 h and comparison to auranofin (Results are the mean SD of 3 independent experiments).

Compound	MDA-MB-231		EMT6		B16-F10	
1	75.05	±0,2212	50.21	± 0,4385	74.87	±0,16
3	74.83	±0,3037	49.76	±0,3957	50.12	±0,123
4	19.76	±0,2150	19.75	±0,1521	19.89	±0,1193
5	25.19	±0,0897	24.94	±0,1404	25.02	±0,0907
6	74.92	±0,2841	50.2	±0,2056	100	±0,1109
7	74.96	±0,1629	49.61	±0,2509	74.9	±0,1949
BODI-Au-7	25.24	±0,1194	10.58	± 0,0947	49.97	±0,13
BODI-Au-8	29.79	±0,1279	19.73	±0,1815	20.16	±0,3106
BODI-Au-9	75	±0,1866	49.88	±0,1834	74.94	±0,168
BODI-Au-10	75.23	±0,2125	74.93	±0,3894	75.05	±0,1981
BODI-Au-11	49.97	±0,1875	74.78	±0,3134	74.93	±0,18
BODI-Au-12	50.03	±0,1793	49.91	±0,1913	49.8	±0,1672
BODI-Au-13	25.17	±0,1532	19.96	±0,1204	49.9	±0,14
BODI-Au-14	10.07	±0,1932	9.908	±0,0980	10.32	±0,2128
BODI-Au-15	75	±0,1935	40.4	±0,2409	100.2	±0,1390
BODI-Au-16	50.1	±0,1516	50.13	±0,1378	24.88	±0,2729
BODI-Au-17	100.2	±0,1991	49.92	±0,1705	100.1	±0,1343
Auranofin	5.225	±0,0942	4.865	±0,1154	4.683	±0,1573

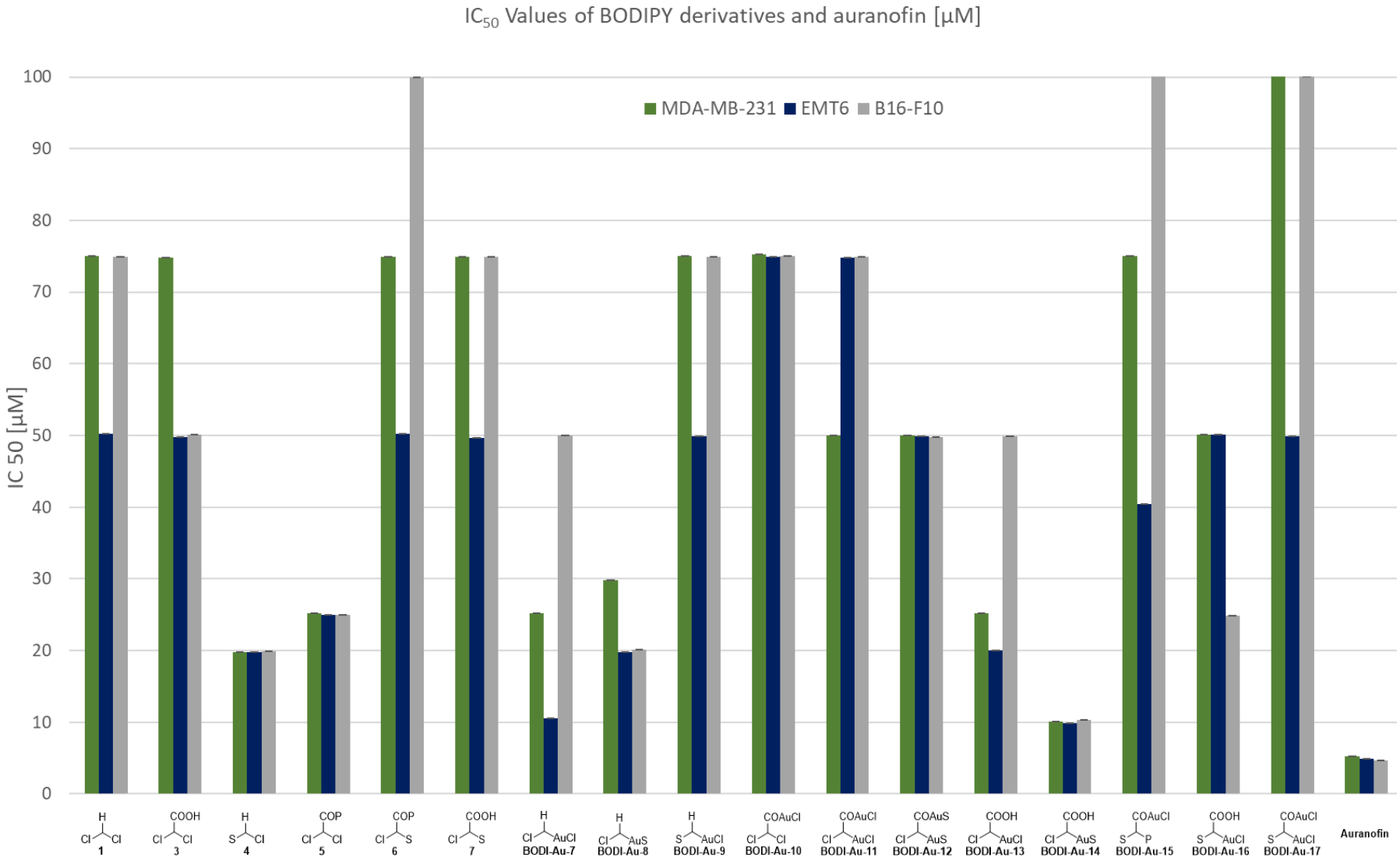

Figure S 103: Determination of the IC_{50} values (µM) of the different BODIPY derivatives on MDA-MB-231, EMT6, and B16F10 cell lines by MTS assay (Promega®) at 48 h and comparison to auranofin (Results are the mean SD of 3 independent experiments).

In vitro confocal microscopy experiments

MDA-MB-231 cells were seeded on chambered coverglasses (24 well-plate) and allowed to recover. Cells were incubated with 10 µM of each compound at 37°C. After 1, 4 and 24 hours the cells were fixed and permeabilized with iced methanol for 10 min at room temperature. Cells were then washed 3 times with PBS (5 min each), counterstained with 5 µM DRAQ5 (or 1µg.mL^{-1} DAPI) during 5-10 min, washed with PBS and mounted with Fluoromount-G® (Southern Biotech). Confocal imaging was performed using a confocal laser-scanning microscope (Leica TCS SP8) with a × 63 HCX PL APO oil immersion (ON 1.4) objective lens that allowed to simultaneously obtain DIC (Differential Interference Contrast) and fluorescent images (1024 pixels × 1024 pixels), and LASX software (Leica Microsystems, Ltd). The samples were excited using internal microscope lasers and emission intensity was recorded at the appropriate emission wavelength. Fluorescence images were sequentially acquired. For co-localization experiments, BODIPY compounds (green) were excited at 488 nm and their emission was recorded from 493 to 600 nm (BODIPY-Fl), whereas the nuclear probe, the DRAQ5 (red), was excited at 638 nm and its emission was recorded from 661nm to 778 nm (DRAQ5). Image processing and analyses were carried out using Fiji/ImageJ.

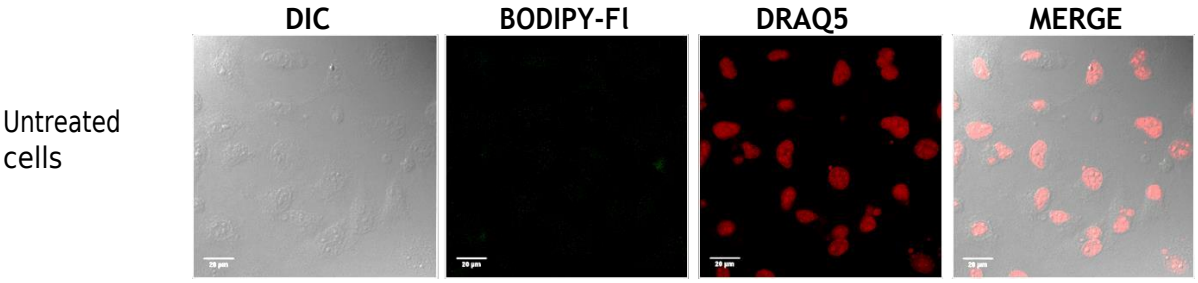

Figure S 104: Confocal immunofluorescent analysis of MDA-MB-231 labelled only with DRAQ5 (DIC: bright field, BODIPY-Fl: BODIPY fluorescence canal, DRAQ5: DRAQ5 canal). Cells are incubated with 10 µM BODIPY derivatives (green) for 4h at 37°C then fixed, permeabilized with iced methanol. The nuclei are counterstained with DRAQ5 (red, fluorescent DNA dye). Compounds localization (in green) and IC_{50} (in red) have been indicated to facilitate the comparison between the compounds.

BODIPY 1

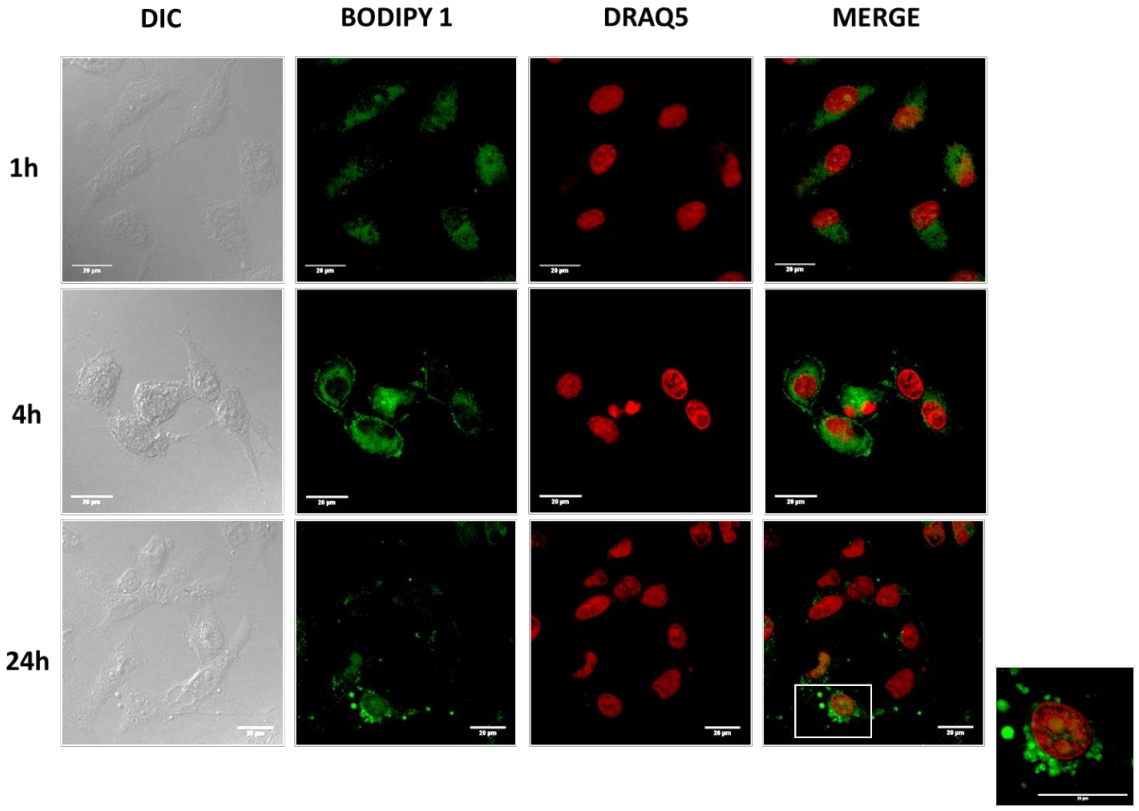

*Figure S 105: Confocal immunofluorescent analysis of MDA-MB-231 labelled with BODIPY **1** (DIC: bright field, BODIPY-Fl: BODIPY fluorescence canal, DRAQ5: DRAQ5 canal). Cells are incubated with 10 µM BODIPY derivatives (green) for 4h at 37°C then fixed, permeabilized with iced methanol. The nuclei are counterstained with DRAQ5 (red, fluorescent DNA dye). Compounds localization (in green) and IC_{50} (in red) have been indicated to facilitate the comparison between the compounds.*

BODIPY 3

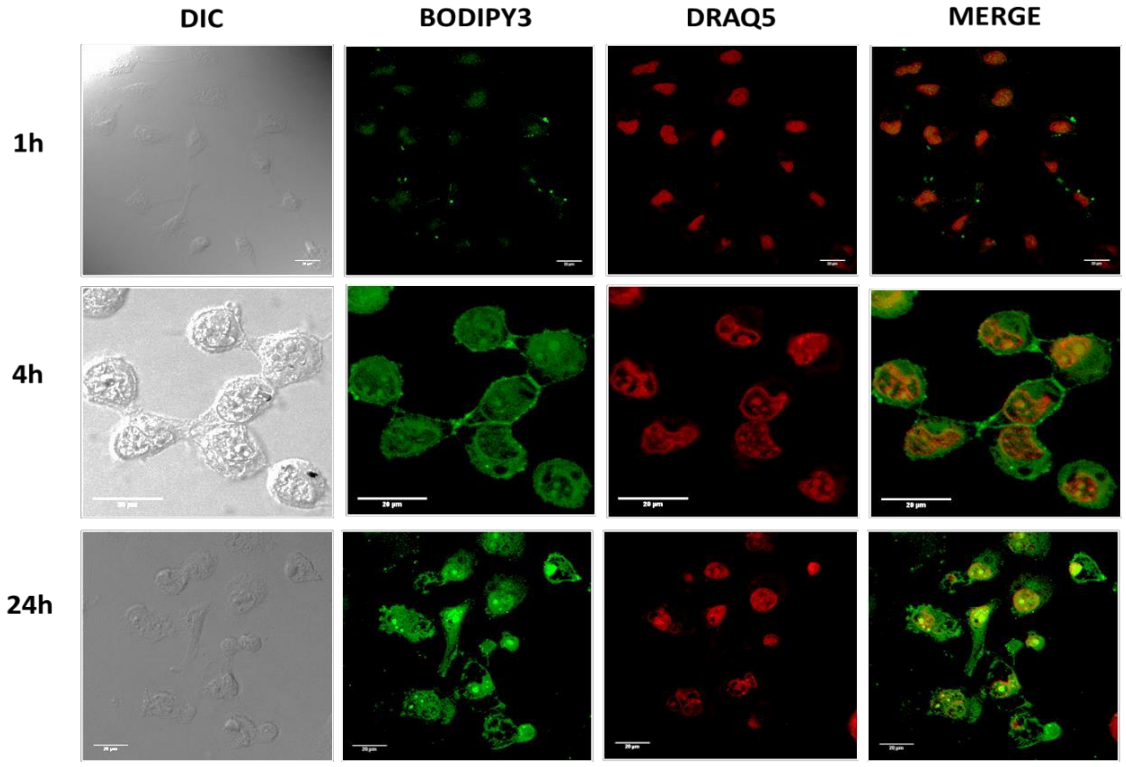

*Figure S 106: Confocal immunofluorescent analysis of MDA-MB-231 labelled with BODIPY **3** (DIC: bright field, BODIPY-Fl: BODIPY fluorescence canal, DRAQ5: DRAQ5 canal). Cells are incubated with 10 µM BODIPY derivatives (green) for 4h at 37°C then fixed, permeabilized with iced methanol. The nuclei are counterstained with DRAQ5 (red, fluorescent DNA dye). Compounds localization (in green) and IC_{50} (in red) have been indicated to facilitate the comparison between the compounds.*

BODIPY 4

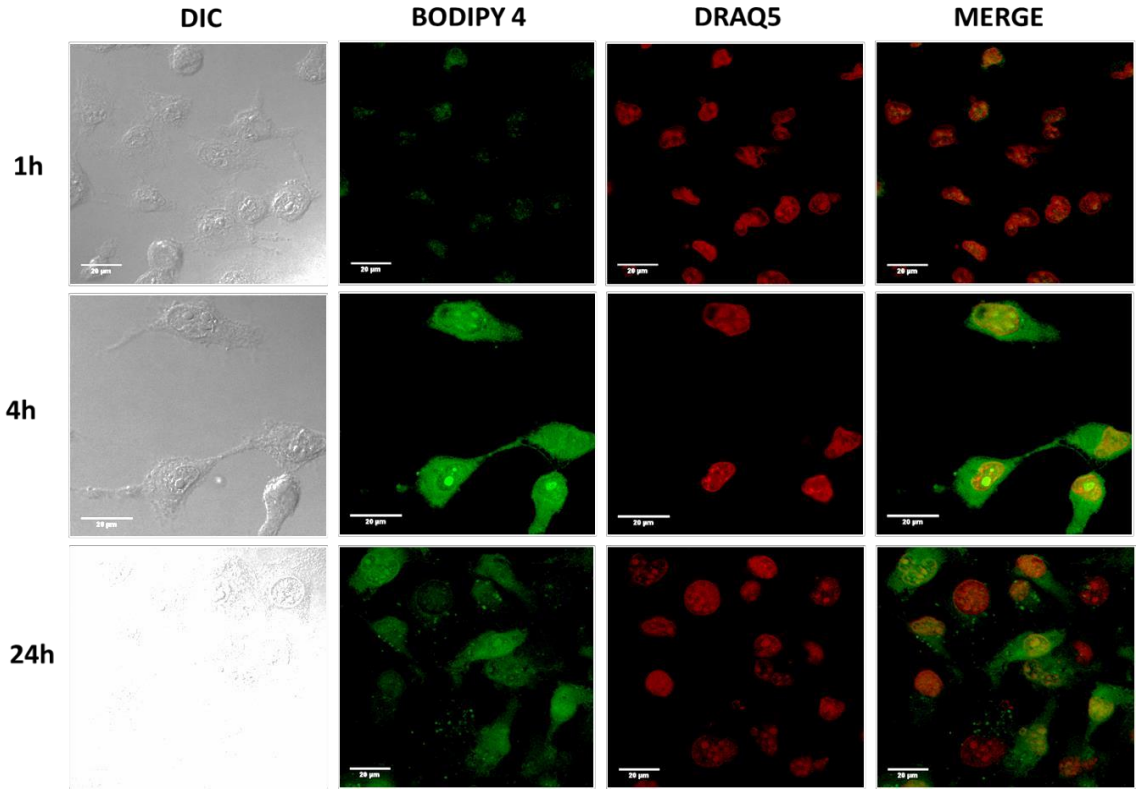

*Figure S 107: Confocal immunofluorescent analysis of MDA-MB-231 labelled with BODIPY **4** (DIC: bright field, BODIPY-Fl: BODIPY fluorescence canal, DRAQ5: DRAQ5 canal). Cells are incubated with 10 µM BODIPY derivatives (green) for 4h at 37°C then fixed, permeabilized with iced methanol. The nuclei are counterstained with DRAQ5 (red, fluorescent DNA dye). Compounds localization (in green) and IC_{50} (in red) have been indicated to facilitate the comparison between the compounds.*

BODIPY 5

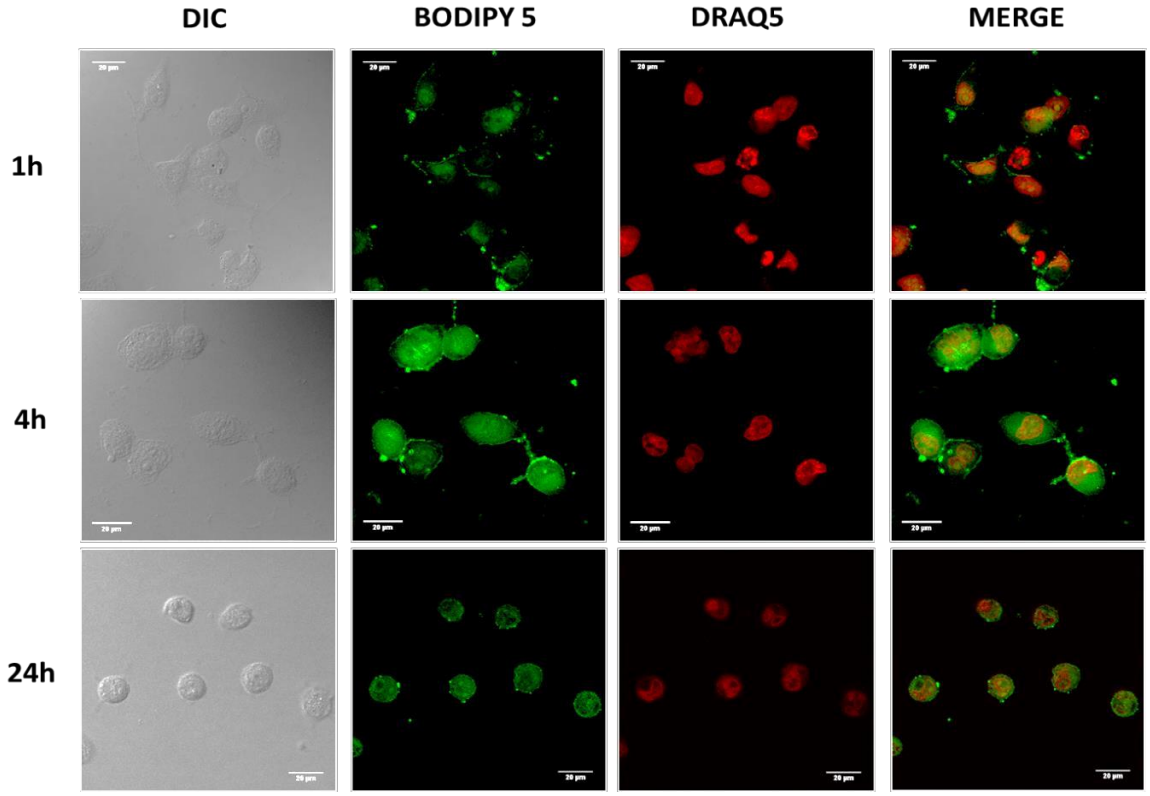

*Figure S 108: Confocal immunofluorescent analysis of MDA-MB-231 labelled with BODIPY **5** (DIC: bright field, BODIPY-Fl: BODIPY fluorescence canal, DRAQ5: DRAQ5 canal). Cells are incubated with 10 µM BODIPY derivatives (green) for 4h at 37°C then fixed, permeabilized with iced methanol. The nuclei are counterstained with DRAQ5 (red, fluorescent DNA dye). Compounds localization (in green) and IC_{50} (in red) have been indicated to facilitate the comparison between the compounds.*

BODIPY 6

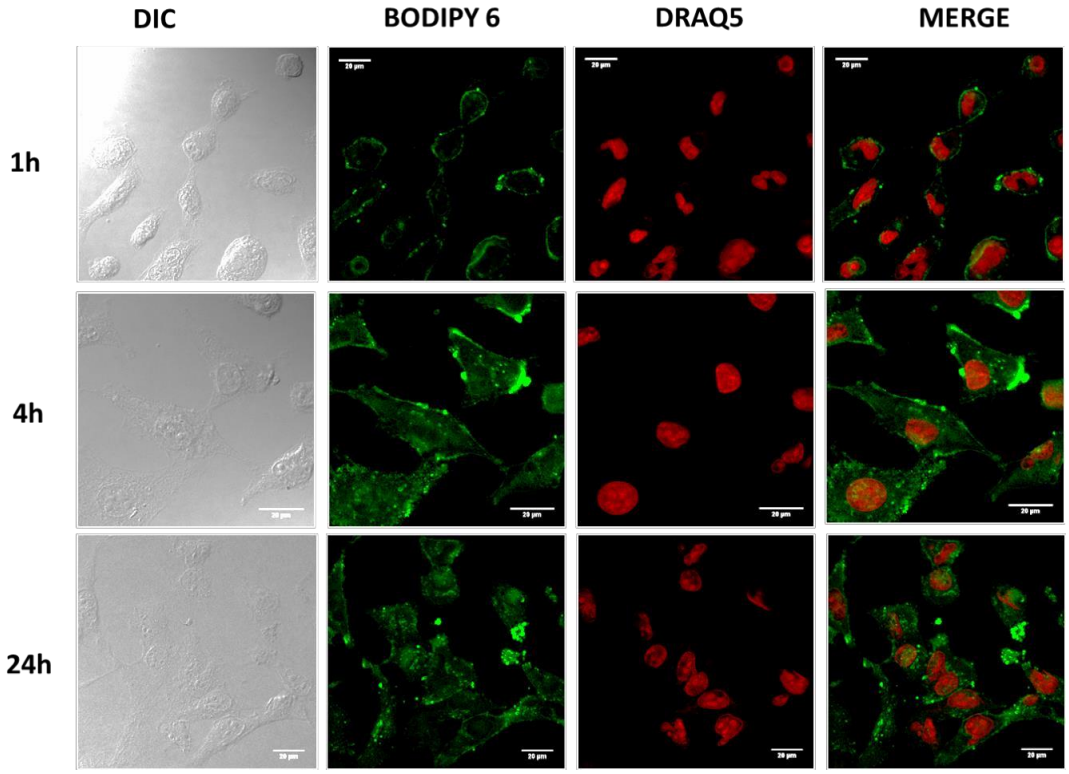

*Figure S 109: Confocal immunofluorescent analysis of MDA-MB-231 labelled with BODIPY **6** (DIC: bright field, BODIPY-Fl: BODIPY fluorescence canal, DRAQ5: DRAQ5 canal). Cells are incubated with 10 µM BODIPY derivatives (green) for 4h at 37°C then fixed, permeabilized with iced methanol. The nuclei are counterstained with DRAQ5 (red, fluorescent DNA dye). Compounds localization (in green) and IC_{50} (in red) have been indicated to facilitate the comparison between the compounds.*

BODIPY 7

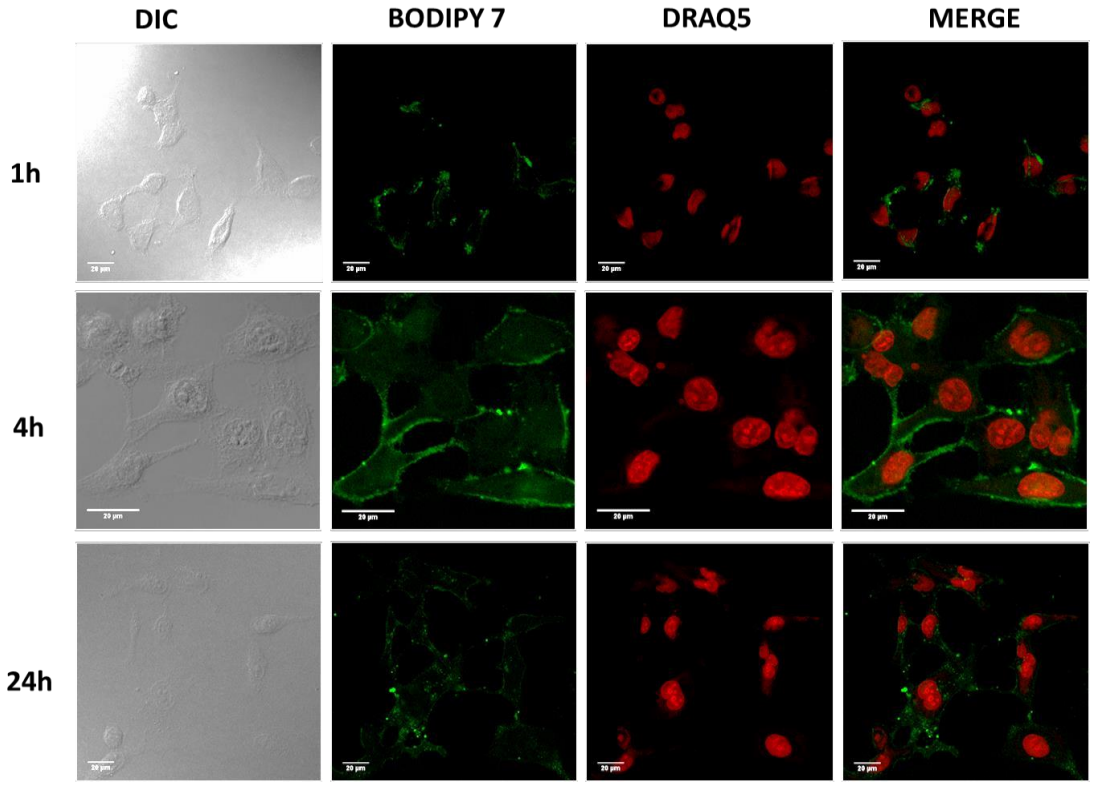

*Figure S 110: Confocal immunofluorescent analysis of MDA-MB-231 labelled with BODIPY **7** (DIC: bright field, BODIPY-Fl: BODIPY fluorescence canal, DRAQ5: DRAQ5 canal). Cells are incubated with 10 µM BODIPY derivatives (green) for 4h at 37°C then fixed, permeabilized with iced methanol. The nuclei are counterstained with DRAQ5 (red, fluorescent DNA dye). Compounds localization (in green) and IC_{50} (in red) have been indicated to facilitate the comparison between the compounds.*

BODIPY 8

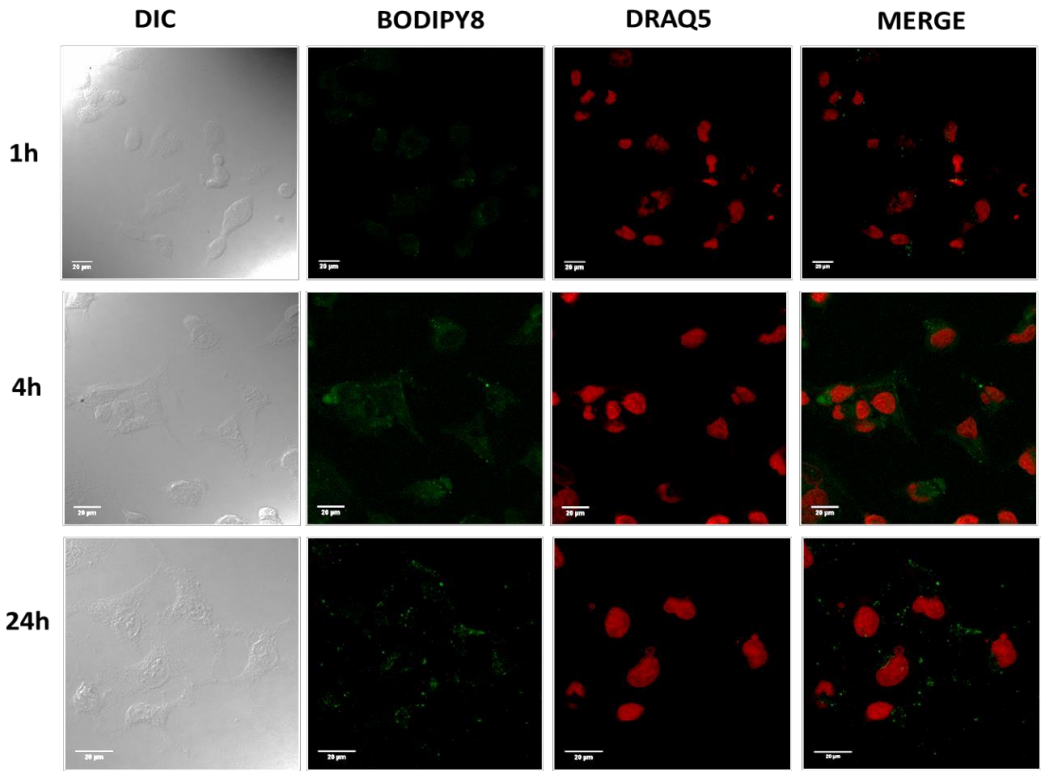

*Figure S 111: Confocal immunofluorescent analysis of MDA-MB-231 labelled with BODIPY **8** (DIC: bright field, BODIPY-Fl: BODIPY fluorescence canal, DRAQ5: DRAQ5 canal). Cells are incubated with 10 µM BODIPY derivatives (green) for 4h at 37°C then fixed, permeabilized with iced methanol. The nuclei are counterstained with DRAQ5 (red, fluorescent DNA dye). Compounds localization (in green) and IC_{50} (in red) have been indicated to facilitate the comparison between the compounds.*

BODI-Au-7

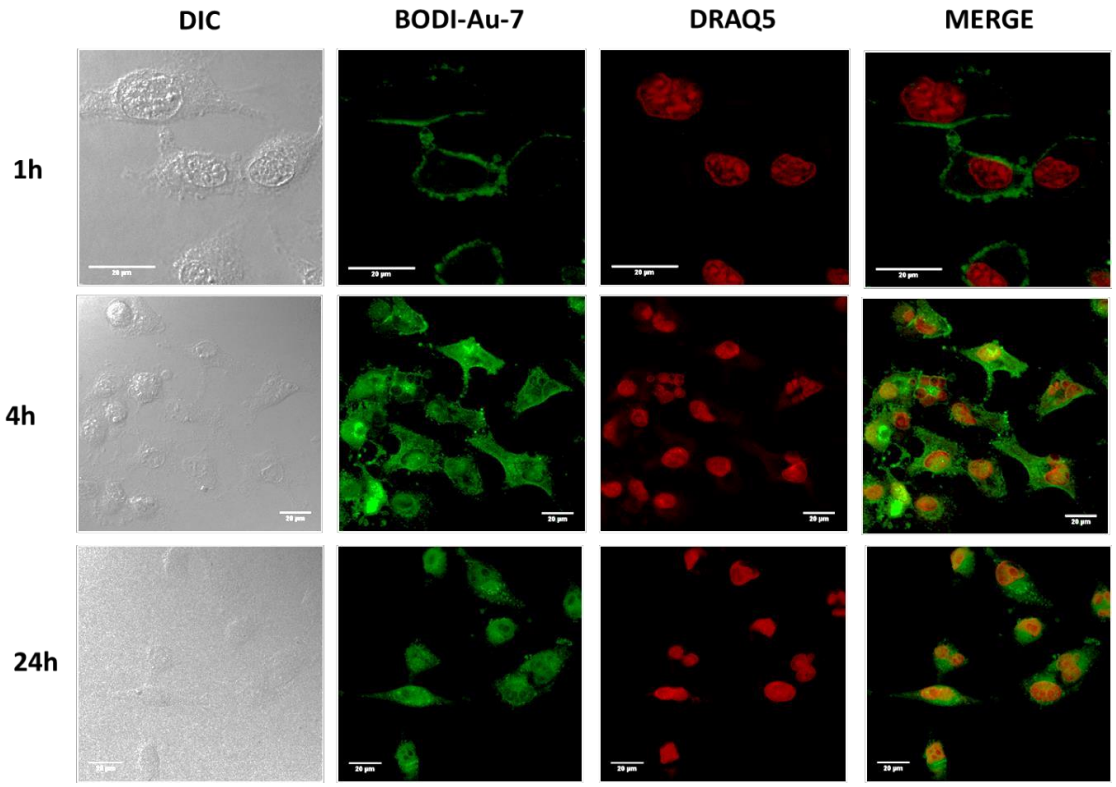

*Figure S 112: Confocal immunofluorescent analysis of MDA-MB-231 labelled with **BODI-Au-7** (DIC: bright field, BODIPY-Fl: BODIPY fluorescence canal, DRAQ5: DRAQ5 canal). Cells are incubated with 10 µM BODIPY derivatives (green) for 4h at 37°C then fixed, permeabilized with iced methanol. The nuclei are counterstained with DRAQ5 (red, fluorescent DNA dye). Compounds localization (in green) and IC_{50} (in red) have been indicated to facilitate the comparison between the compounds.*

BODI-Au-8

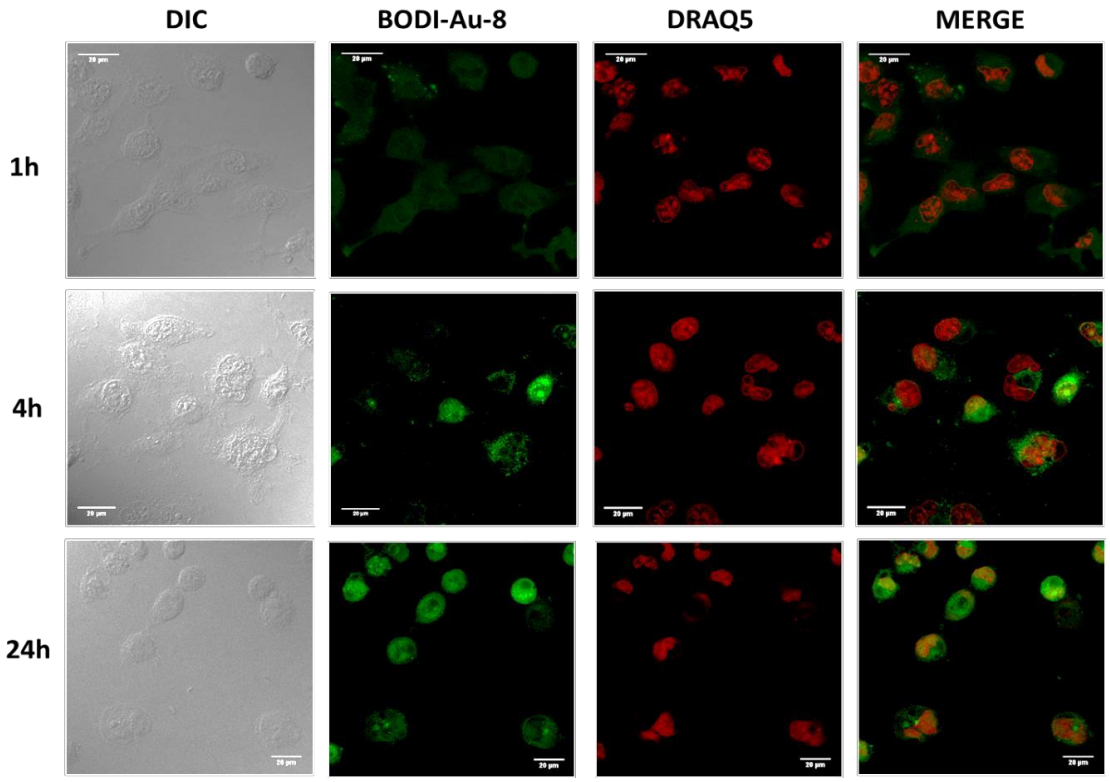

*Figure S 113: Confocal immunofluorescent analysis of MDA-MB-231 labelled with **BODI-Au-8** (DIC: bright field, BODIPY-Fl: BODIPY fluorescence canal, DRAQ5: DRAQ5 canal). Cells are incubated with 10 µM BODIPY derivatives (green) for 4h at 37°C then fixed, permeabilized with iced methanol. The nuclei are counterstained with DRAQ5 (red, fluorescent DNA dye). Compounds localization (in green) and IC_{50} (in red) have been indicated to facilitate the comparison between the compounds.*

BODI-Au-9

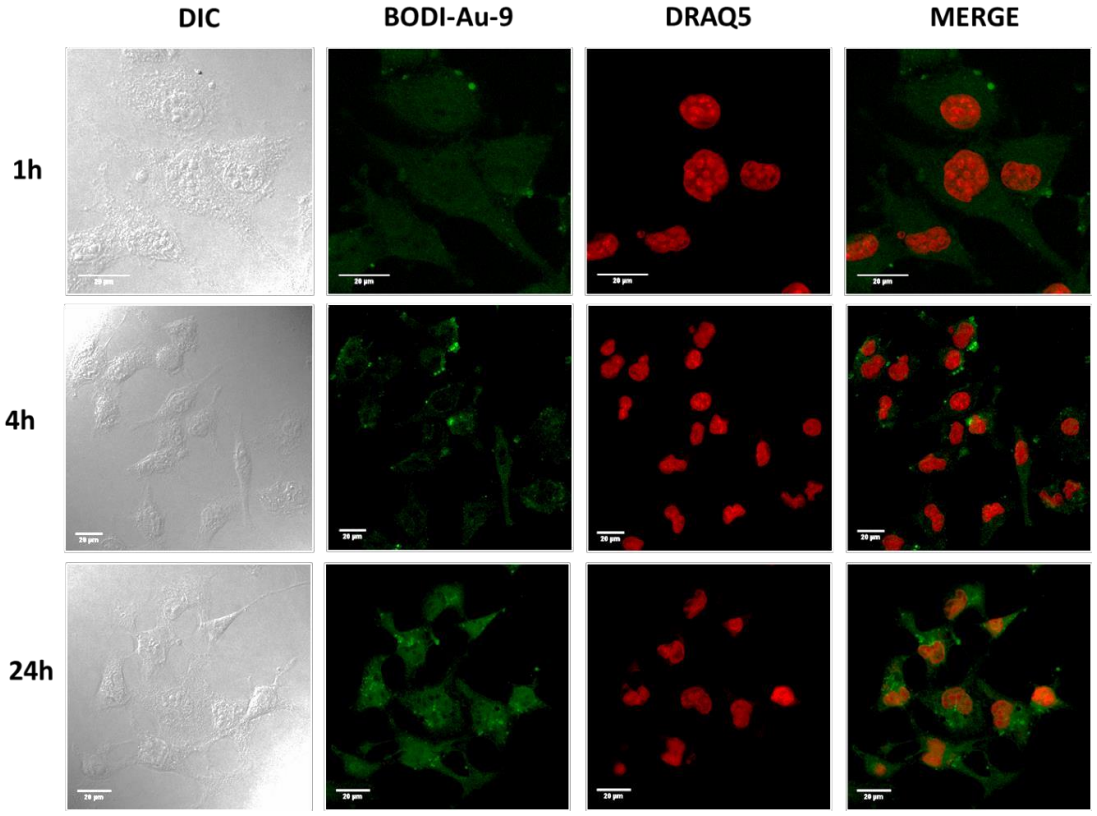

*Figure S 114: Confocal immunofluorescent analysis of MDA-MB-231 labelled with **BODI-Au-9** (DIC: bright field, BODIPY-Fl: BODIPY fluorescence canal, DRAQ5: DRAQ5 canal). Cells are incubated with 10 µM BODIPY derivatives (green) for 4h at 37°C then fixed, permeabilized with iced methanol. The nuclei are counterstained with DRAQ5 (red, fluorescent DNA dye). Compounds localization (in green) and IC_{50} (in red) have been indicated to facilitate the comparison between the compounds.*

BODI-Au-10

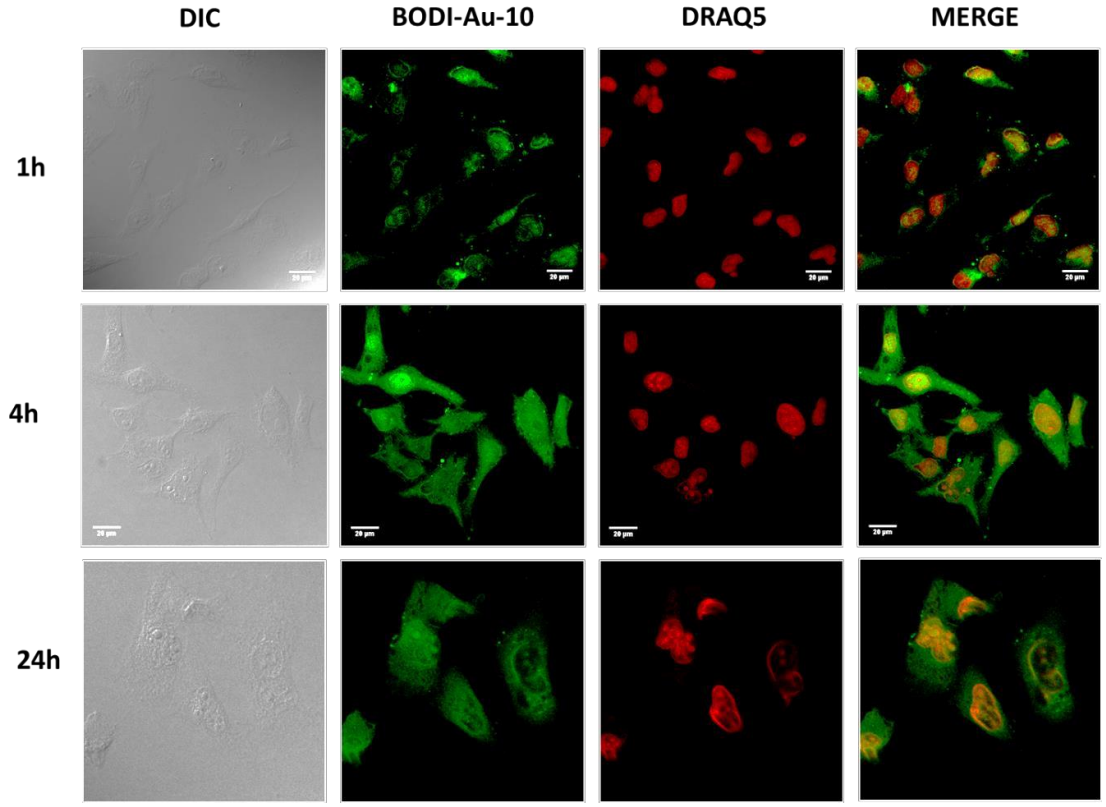

*Figure S 115: Confocal immunofluorescent analysis of MDA-MB-231 labelled with **BODI-Au-10** (DIC: bright field, BODIPY-Fl: BODIPY fluorescence canal, DRAQ5: DRAQ5 canal). Cells are incubated with 10 µM BODIPY derivatives (green) for 4h at 37°C then fixed, permeabilized with iced methanol. The nuclei are counterstained with DRAQ5 (red, fluorescent DNA dye). Compounds localization (in green) and IC_{50} (in red) have been indicated to facilitate the comparison between the compounds.*

BODI-Au-11

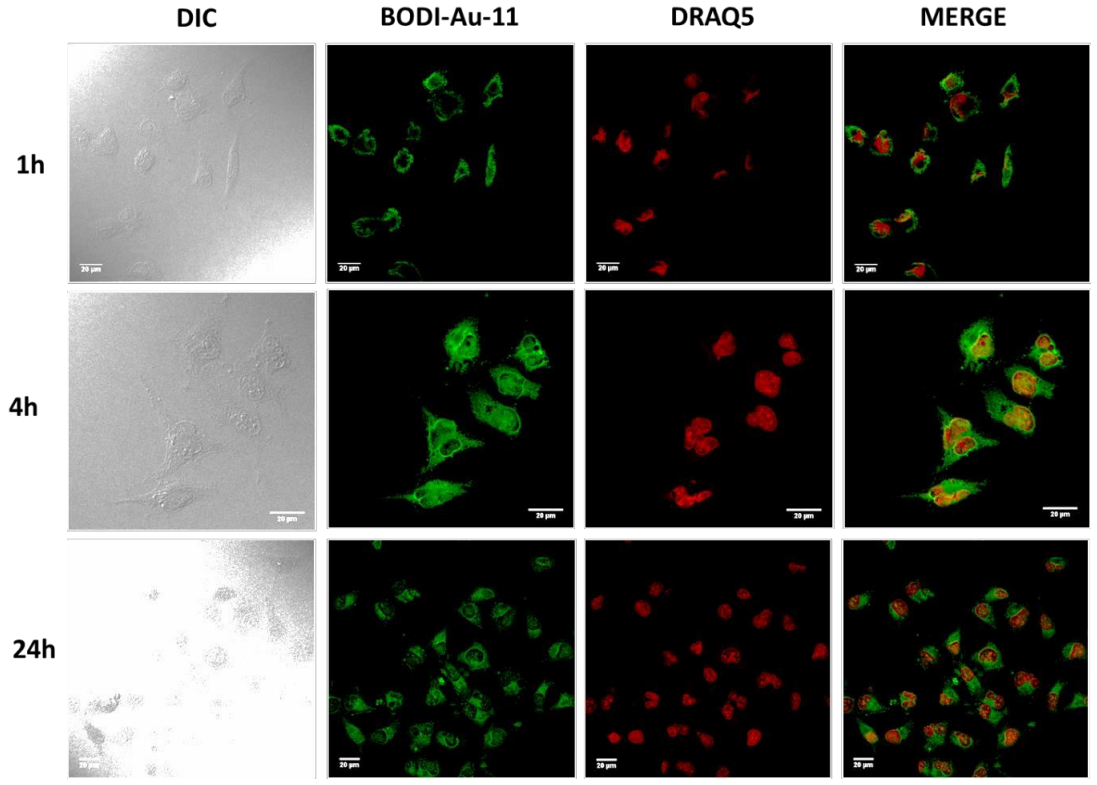

*Figure S 116: Confocal immunofluorescent analysis of MDA-MB-231 labelled with **BODI-Au-11** (DIC: bright field, BODIPY-Fl: BODIPY fluorescence canal, DRAQ5: DRAQ5 canal). Cells are incubated with 10 µM BODIPY derivatives (green) for 4h at 37°C then fixed, permeabilized with iced methanol. The nuclei are counterstained with DRAQ5 (red, fluorescent DNA dye). Compounds localization (in green) and IC_{50} (in red) have been indicated to facilitate the comparison between the compounds.*

BODI-Au-12

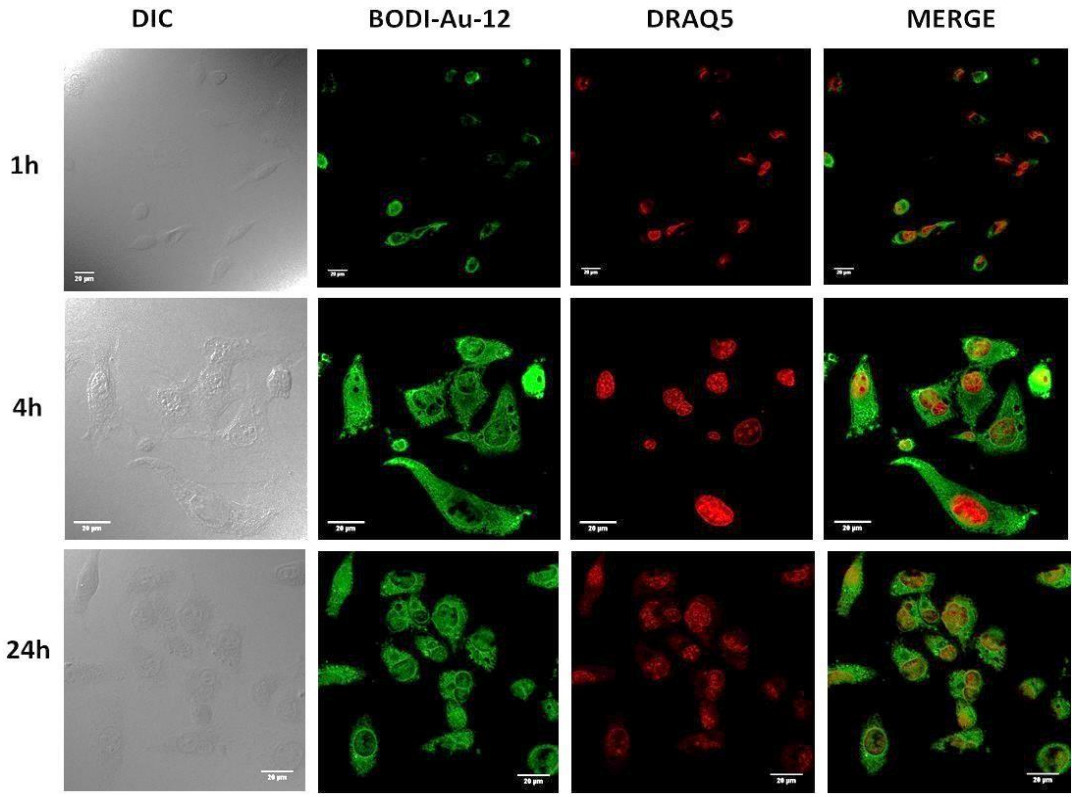

*Figure S 117: Confocal immunofluorescent analysis of MDA-MB-231 labelled with **BODI-Au-12** (DIC: bright field, BODIPY-Fl: BODIPY fluorescence canal, DRAQ5: DRAQ5 canal). Cells are incubated with 10 µM BODIPY derivatives (green) for 4h at 37°C then fixed, permeabilized with iced methanol. The nuclei are counterstained with DRAQ5 (red, fluorescent DNA dye). Compounds localization (in green) and IC_{50} (in red) have been indicated to facilitate the comparison between the compounds.*

BODI-Au-13

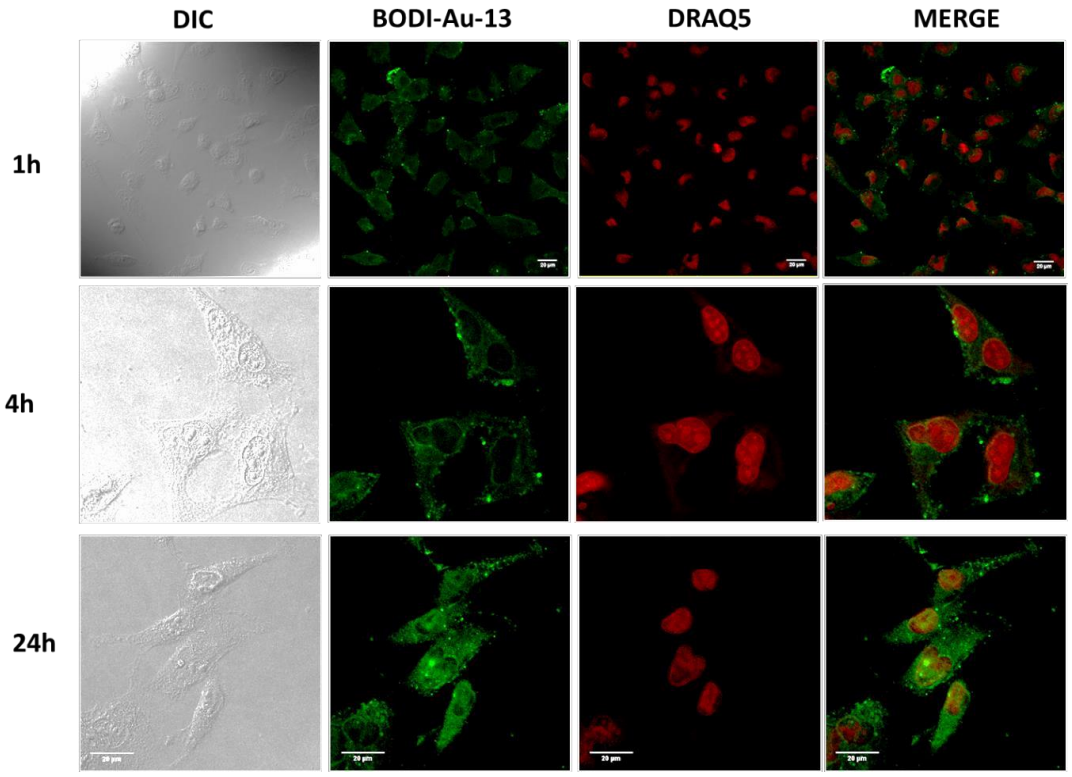

*Figure S 118: Confocal immunofluorescent analysis of MDA-MB-231 labelled with **BODI-Au-13** (DIC: bright field, BODIPY-Fl: BODIPY fluorescence canal, DRAQ5: DRAQ5 canal). Cells are incubated with 10 µM BODIPY derivatives (green) for 4h at 37°C then fixed, permeabilized with iced methanol. The nuclei are counterstained with DRAQ5 (red, fluorescent DNA dye). Compounds localization (in green) and IC_{50} (in red) have been indicated to facilitate the comparison between the compounds.*

BODI-Au-14

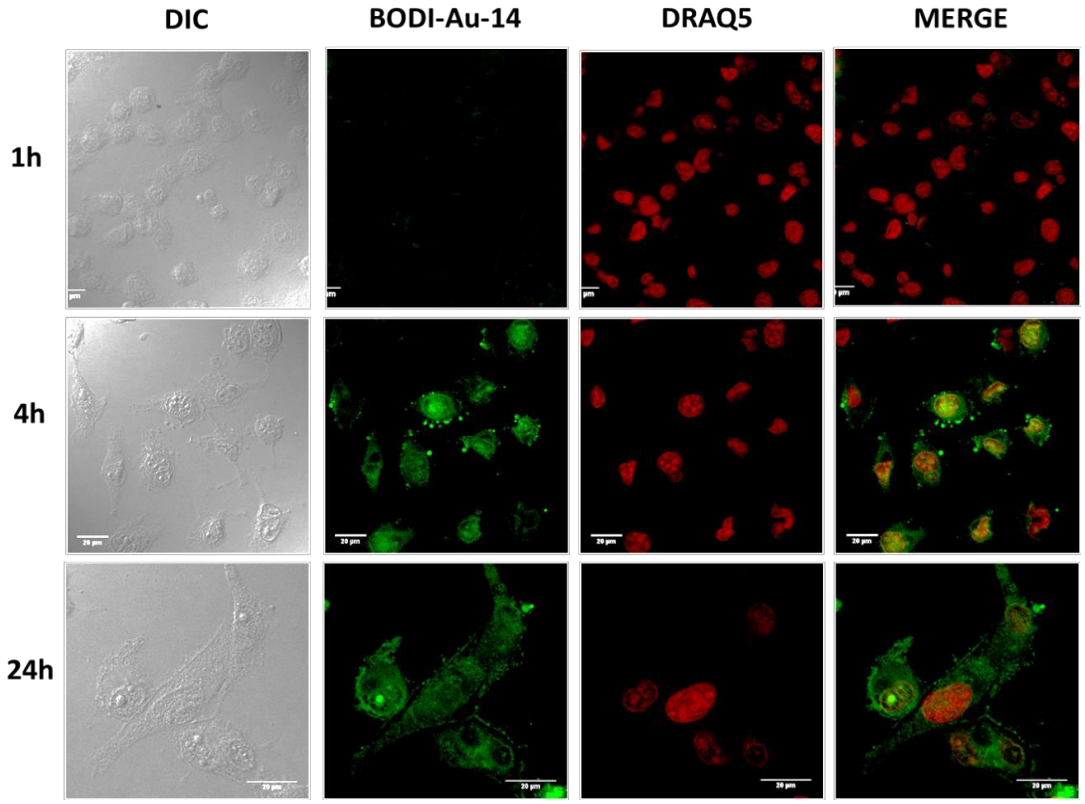

*Figure S 119: Confocal immunofluorescent analysis of MDA-MB-231 labelled with **BODI-Au-14** (DIC: bright field, BODIPY-Fl: BODIPY fluorescence canal, DRAQ5: DRAQ5 canal). Cells are incubated with 10 µM BODIPY derivatives (green) for 4h at 37°C then fixed, permeabilized with iced methanol. The nuclei are counterstained with DRAQ5 (red, fluorescent DNA dye). Compounds localization (in green) and IC_{50} (in red) have been indicated to facilitate the comparison between the compounds.*

BODI-Au-15

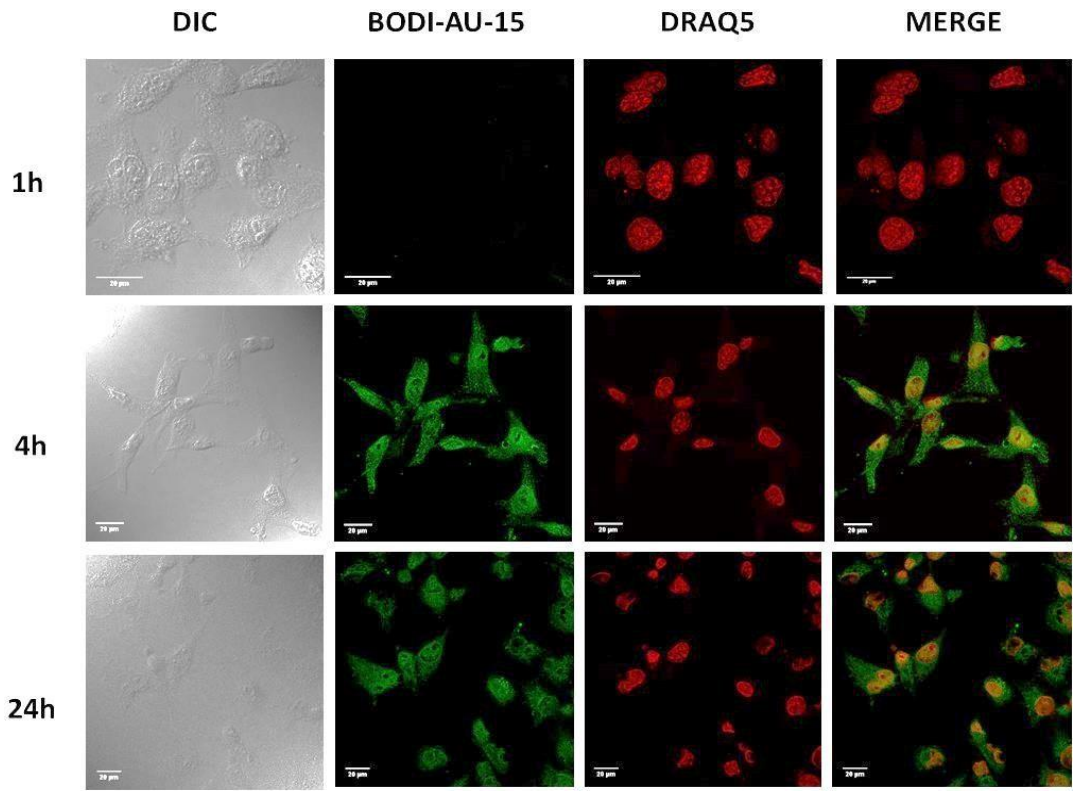

*Figure S 120: Confocal immunofluorescent analysis of MDA-MB-231 labelled with **BODI-Au-15** (DIC: bright field, BODIPY-Fl: BODIPY fluorescence canal, DRAQ5: DRAQ5 canal). Cells are incubated with 10 µM BODIPY derivatives (green) for 4h at 37°C then fixed, permeabilized with iced methanol. The nuclei are counterstained with DRAQ5 (red, fluorescent DNA dye). Compounds localization (in green) and IC_{50} (in red) have been indicated to facilitate the comparison between the compounds.*

BODI-Au-16

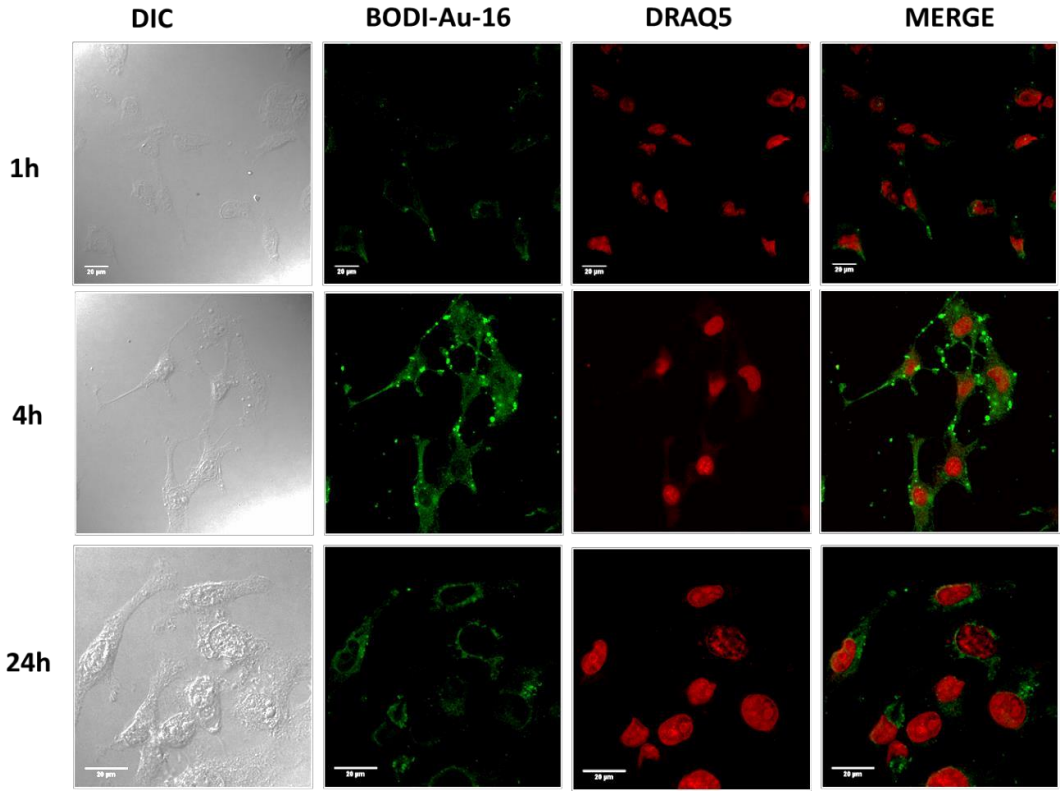

*Figure S 121: Confocal immunofluorescent analysis of MDA-MB-231 labelled with **BODI-Au-16** (DIC: bright field, BODIPY-Fl: BODIPY fluorescence canal, DRAQ5: DRAQ5 canal). Cells are incubated with 10 µM BODIPY derivatives (green) for 4h at 37°C then fixed, permeabilized with iced methanol. The nuclei are counterstained with DRAQ5 (red, fluorescent DNA dye). Compounds localization (in green) and IC_{50} (in red) have been indicated to facilitate the comparison between the compounds.*

BODI-Au-17

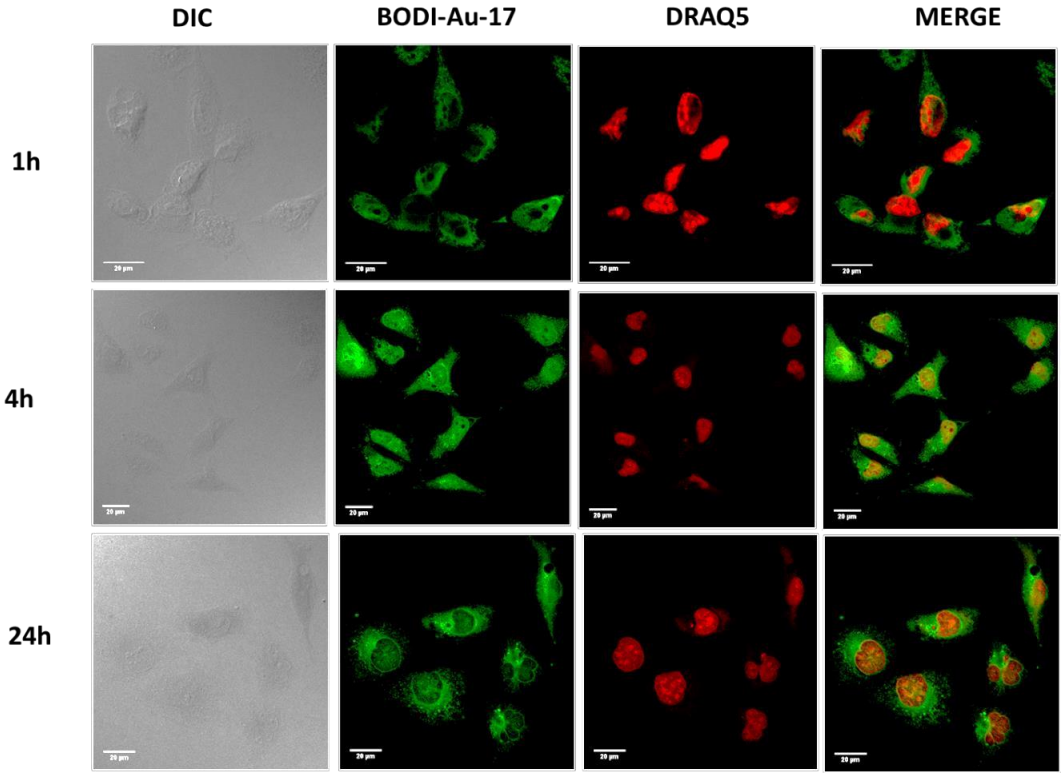

*Figure S 122: Confocal immunofluorescent analysis of MDA-MB-231 labelled with **BODI-Au-17** (DIC: bright field, BODIPY-Fl: BODIPY fluorescence canal, DRAQ5: DRAQ5 canal). Cells are incubated with 10 µM BODIPY derivatives (green) for 4h at 37°C then fixed, permeabilized with iced methanol. The nuclei are counterstained with DRAQ5 (red, fluorescent DNA dye). Compounds localization (in green) and IC_{50} (in red) have been indicated to facilitate the comparison between the compounds.*

Compound 2

Report created with **ReportPlus**

Submitted by: **Jacques Pliquett**

Solved by: **Yoann Rousselin**

Sample ID: **15JPL191**

Crystal Data and Experimental

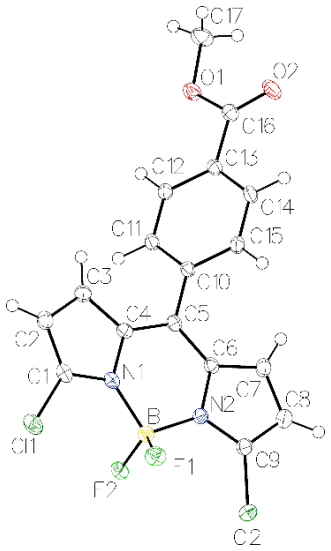

Experimental. Single clear light orange plate-shaped crystals of (**Compound 2**) were recrystallised from DCM by slow evaporation. A suitable crystal (0.46x0.40x0.21) mm^3 was selected and mounted on a MITIGEN holder oil on a Bruker D8 VENTURE diffractometer. The crystal was kept at T = 100(1) K during data collection. Using **Olex2** (Dolomanov et al., 2009), the structure was solved with the **ShelXT** (Sheldrick, 2015) structure solution program, using the Intrinsic Phasing solution method. The model was refined with version 2018/1 of **ShelXL** (Sheldrick, 2015) using Least Squares minimisation.

Crystal Data. $C_{17}H_{11}BCl_2F_2N_2O_2$, M_r = 394.99, triclinic, P-1 (No. 2), a = 7.8312(3) Å, b = 10.3013(5) Å, c = 10.4618(4) Å, α = 96.577(2)°, β = 101.739(2)°, γ = 97.026(2)°, V = 811.63(6) $Å^3$, T = 100(1) K, Z = 2, Z' = 1, $\mu(MoK_\alpha)$ = 0.437, 28837 reflections measured, 3731 unique (R_{int} = 0.0303) which were used in all calculations. The final wR_2 was 0.0902 (all data) and R_1 was 0.0361 (I > 2(I)).

Table S3: X-ray structure data of BODIPY ***2****.*

Compound	**Compound 2**
CCDC	**1825949**
Formula	$C_{17}H_{11}BCl_2F_2N_2O_2$
$D_{calc.}$/ g cm^{-3}	1.616
μ/mm^{-1}	0.437
Formula Weight	394.99
Colour	clear light orange
Shape	plate
Size/mm^3	0.46x0.40x0.21
T/K	100(1)
Crystal System	triclinic
Space Group	P-1
a/Å	7.8312(3)
b/Å	10.3013(5)
c/Å	10.4618(4)
α/°	96.577(2)
β/°	101.739(2)
γ/°	97.026(2)
V/$Å^3$	811.63(6)
Z	2
Z'	1
Wavelength/Å	0.71073
Radiation type	MoK_α
Θ_{min}/°	2.979
Θ_{max}/°	27.560
Measured Refl.	28837
Independent Refl.	3731
Reflections Used	3256
R_{int}	0.0303
Parameters	236
Restraints	0
Largest Peak	0.485
Deepest Hole	-0.284
GooF	1.046
wR_2 (all data)	0.0902
wR_2	0.0831
R_1 (all data)	0.0439
R_1	0.0361

*Table S 4: BODIPY **2** structure Quality Indicators.*

Reflections:	d min (Mo)	0.77	I/σ	37.5	Rint	3.03%	complete	100%
Refinement:	Shift	0.000	Max Peak	0.5	Min Peak	-0.3	GooF	1.046

A clear light orange plate-shaped crystal with dimensions 0.46x0.40x0.21 mm^3 was mounted on a MITIGEN holder oil. X-ray diffraction data were collected using a Bruker D8 VENTURE diffractometer equipped with a Oxford Cryosystems low-temperature device, operating at T = 100(1) K. Data were measured using ϕ and ω scans of 2° per frame for 10s using MoK_α radiation (X-ray tube, 50 kV, 32 mA). The total number of runs and images was based on the strategy calculation from the program APEX3 (Bruker, 2015).The maximum resolution achieved was Θ = 27.560°. Cell parameters were retrieved using the **SAINT** (Bruker, V8.34A, after 2013) software and refined using **SAINT** (Bruker, V8.34A, after 2013) on 9970 reflections, 35 % of the observed reflections. Data reduction was performed using the **SAINT** (Bruker, V8.34A, after 2013) software which corrects for Lorentz polarisation. The final completeness is 99.90 % out to 27.560° in Θ. A multi-scan absorption correction was performed using SADABS-2014/5 (Bruker,2014) was used for absorption correction. wR_2(int) was 0.0603 before and 0.0502 after correction. The Ratio of minimum to maximum transmission is 0.9179. The λ/2 correction factor is 0.00150. The absorption coefficient μ of this material is 0.437 mm^{-1} at this wavelength (λ = 0.71073Å) and the minimum and maximum transmissions are 0.6844 and 0.7456. The structure was solved in the space group P-1 (# 2) by Intrinsic Phasing using the **ShelXT** (Sheldrick, 2015) structure solution program and refined by Least Squares using version 2018/1 of **ShelXL** (Sheldrick, 2015). All non-hydrogen atoms were refined anisotropically. Hydrogen atom positions were calculated geometrically and refined using the riding model. SADABS-2014/5 (Bruker, 2014) was used for absorption correction. wR_2(int) was 0.0603 before and 0.0502 after correction. The Ratio of minimum to maximum transmission is 0.9179. The λ/2 correction factor is 0.00150. There is a single molecule in the asymmetric unit, which is represented by the reported sum formula. In other words: Z is 2 and Z' is 1.

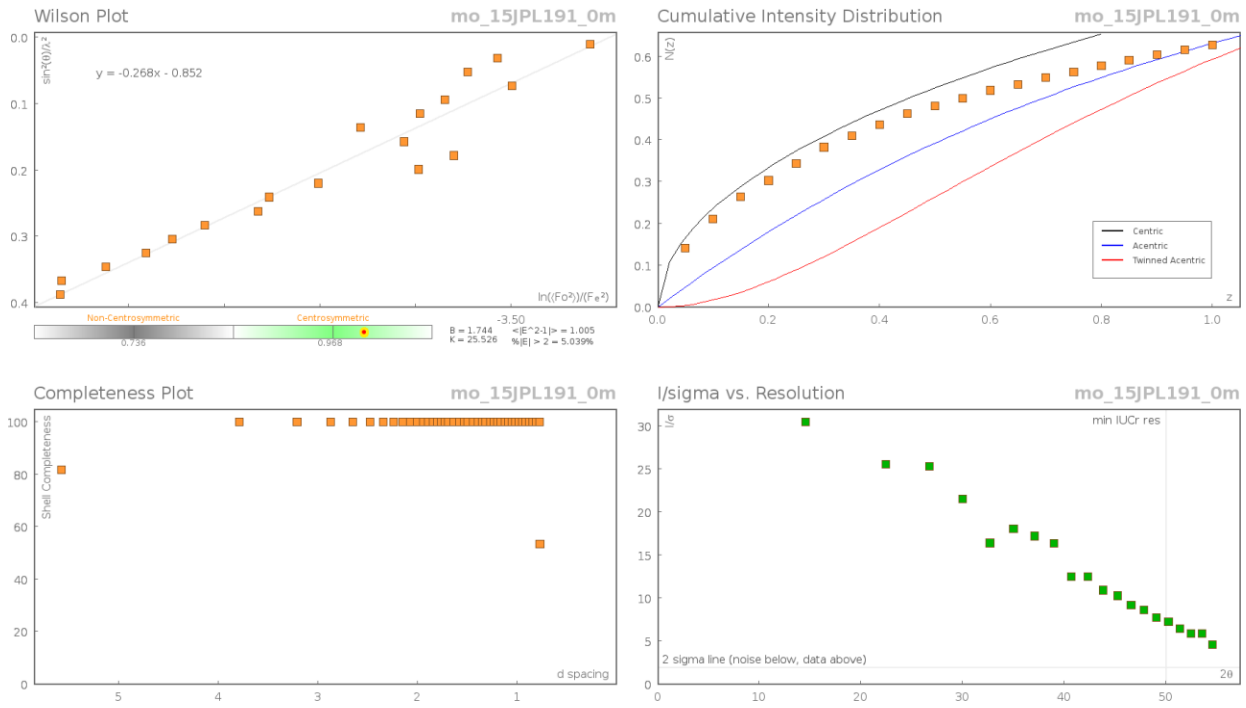

*Figure S 123: Data Plots: Diffraction Data of BODIPY **2** structure.*

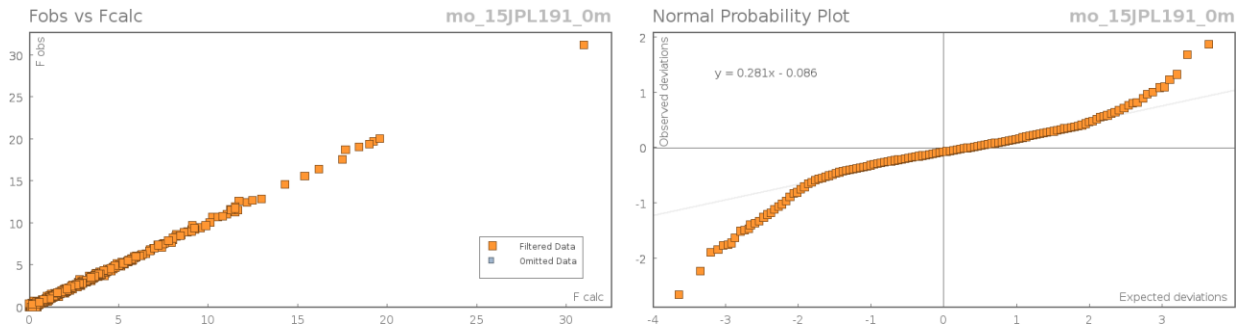

*Figure S 124: Data Plots: refinement and Data of BODIPY **2** structure.*

*Table S 5: reflection statistics of BODIPY **2** structure.*

Total reflections (after filtering)	28837	Unique reflections	3731
Completeness	0.998	Mean I/σ	37.48
hkl_{max} collected	(10, 13, 13)	hkl_{min} collected	(-10, -13, -13)
hkl_{max} used	(9, 13, 13)	hkl_{min} used	(-10, -13, 0)
Lim d_{max} collected	100.0	Lim d_{min} collected	0.36
d_{max} used	6.84	d_{min} used	0.77
Friedel pairs	3682	Friedel pairs merged	1
Inconsistent equivalents	0	R_{int}	0.0303
R_{sigma}	0.0165	Intensity transformed	0
Omitted reflections	0	Omitted by user (OMIT hkl)	0
Multiplicity	(348, 290, 1401, 3353, 1832, 189)	Maximum multiplicity	12
Removed systematic absences	0	Filtered off (Shel/OMIT)	0

*Table S 6: Fractional Atomic Coordinates ($x10^4$) and Equivalent Isotropic Displacement Parameters ($Å^2x10^3$) for BODIPY **2**. U_{eq} is defined as 1/3 of the trace of the orthogonalised U_{ij}.*

Atom	x	y	z	U_{eq}
Cl1	14603.7(6)	2109.6(5)	4125.4(4)	25.14(12)
Cl2	11604.2(6)	-2049.7(4)	7066.5(5)	26.37(12)
F1	12251.3(14)	-158.1(10)	5016.4(10)	23.4(2)
F2	14239.5(13)	745.1(10)	6920.7(10)	21.1(2)
O1	6802.8(16)	7422.6(12)	9542.5(12)	21.3(3)
O2	4326.4(16)	5956.4(13)	8781.9(14)	27.1(3)
N1	12418.8(18)	2178.9(14)	5778.4(13)	15.9(3)
N2	11155.1(18)	468.1(14)	6963.9(14)	16.1(3)
C1	13229(2)	2821.1(17)	4963.9(16)	18.2(3)
C2	12813(2)	4105.1(18)	4938.6(17)	19.5(3)
C3	11685(2)	4252.9(17)	5780.0(16)	17.7(3)
C4	11425(2)	3057.4(16)	6302.6(16)	15.3(3)
C5	10314(2)	2663.9(16)	7125.8(15)	14.8(3)
C6	10190(2)	1384.8(16)	7456.1(16)	15.5(3)
C7	9158(2)	761.1(17)	8237.6(17)	19.4(3)

Atom	x	y	z	U_{eq}
C8	9473(2)	-529.1(18)	8204.3(18)	22.3(4)
C9	10700(2)	-662.5(17)	7416.0(18)	19.5(3)
C10	9206(2)	3598.8(16)	7608.3(15)	14.6(3)
C11	9957(2)	4871.2(16)	8239.0(16)	15.7(3)
C12	8905(2)	5730.4(16)	8686.1(16)	15.9(3)
C13	7089(2)	5335.4(16)	8507.4(16)	15.5(3)
C14	6341(2)	4067.6(16)	7879.6(16)	17.0(3)
C15	7382(2)	3199.4(16)	7429.8(16)	16.9(3)
C16	5905(2)	6239.3(17)	8948.8(16)	17.7(3)
C17	5743(3)	8397.4(19)	9916(2)	27.0(4)
B	12581(2)	752.9(18)	6135.9(19)	16.6(4)

*Table S 7: Anisotropic Displacement Parameters (x10⁴) BODIPY **2**. The anisotropic displacement factor exponent takes the form: $-2\pi^2[h^2a^{*2} \times U_{11} + \ldots + 2hka^* \times b^* \times U_{12}]$*

Atom	U_{11}	U_{22}	U_{33}	U_{23}	U_{13}	U_{12}
Cl1	22.6(2)	32.4(2)	24.3(2)	3.29(17)	12.74(17)	7.03(17)
Cl2	22.6(2)	16.3(2)	42.3(3)	6.26(18)	10.08(19)	4.10(16)
F1	25.9(5)	21.0(5)	21.9(5)	-2.8(4)	5.1(4)	4.2(4)
F2	14.3(5)	23.6(5)	25.0(5)	5.0(4)	2.3(4)	3.1(4)
O1	17.2(6)	20.0(6)	25.9(6)	-3.0(5)	6.1(5)	3.3(5)
O2	14.8(6)	28.0(7)	38.4(8)	-1.4(6)	9.0(5)	3.5(5)
N1	13.5(6)	19.3(7)	15.4(6)	1.7(5)	4.1(5)	2.7(5)
N2	12.9(6)	15.2(6)	19.1(7)	2.2(5)	1.4(5)	1.1(5)
C1	14.0(7)	24.2(8)	16.3(7)	2.4(6)	4.1(6)	1.7(6)
C2	16.6(8)	23.4(8)	19.0(8)	6.8(6)	3.8(6)	1.9(6)
C3	16.3(7)	18.8(8)	18.0(8)	4.5(6)	2.4(6)	3.0(6)
C4	13.5(7)	16.7(7)	15.4(7)	1.5(6)	2.3(6)	3.1(6)
C5	12.2(7)	16.7(7)	13.9(7)	0.7(6)	0.6(6)	0.5(6)
C6	12.7(7)	16.2(7)	16.7(7)	0.9(6)	2.4(6)	0.7(6)
C7	18.3(8)	20.2(8)	20.6(8)	5.6(6)	6.3(6)	0.5(6)
C8	20.3(8)	19.9(8)	26.9(9)	5.8(7)	6.1(7)	0.5(7)
C9	15.2(7)	16.4(8)	25.0(9)	3.4(6)	0.9(6)	0.7(6)
C10	13.5(7)	17.0(7)	14.4(7)	4.9(6)	3.7(6)	2.6(6)
C11	12.0(7)	17.9(8)	17.2(7)	4.0(6)	2.9(6)	1.0(6)
C12	14.5(7)	16.1(7)	16.7(7)	2.7(6)	3.1(6)	0.6(6)
C13	13.9(7)	18.5(8)	15.3(7)	3.5(6)	4.8(6)	3.1(6)

Atom	U_{11}	U_{22}	U_{33}	U_{23}	U_{13}	U_{12}
C14	11.3(7)	20.6(8)	19.1(8)	4.0(6)	3.4(6)	0.7(6)
C15	15.1(7)	16.4(8)	18.5(8)	3.4(6)	3.4(6)	-0.6(6)
C16	16.8(8)	20.9(8)	15.9(7)	2.9(6)	4.6(6)	2.9(6)
C17	24.4(9)	25.6(9)	29.9(10)	-6.2(7)	7.1(8)	7.6(7)
B	14.6(8)	16.4(8)	18.1(9)	0.7(7)	3.1(7)	1.8(7)

*Table S 8: Bond Lengths in Å for BODIPY **2**.*

Atom	Atom	Length/Å	Atom	Atom	Length/Å
Cl1	C1	1.7019(17)	C3	C4	1.413(2)
Cl2	C9	1.7062(18)	C4	C5	1.401(2)
F1	B	1.373(2)	C5	C6	1.397(2)
F2	B	1.390(2)	C5	C10	1.485(2)
O1	C16	1.344(2)	C6	C7	1.413(2)
O1	C17	1.448(2)	C7	C8	1.379(2)
O2	C16	1.207(2)	C8	C9	1.397(2)
N1	C1	1.346(2)	C10	C11	1.398(2)
N1	C4	1.399(2)	C10	C15	1.405(2)
N1	B	1.570(2)	C11	C12	1.386(2)
N2	C6	1.396(2)	C12	C13	1.399(2)
N2	C9	1.342(2)	C13	C14	1.393(2)
N2	B	1.567(2)	C13	C16	1.492(2)
C1	C2	1.402(2)	C14	C15	1.387(2)
C2	C3	1.378(2)			

*Table S 9: Bond Angles in ° for BODIPY **2**.*

Atom	Atom	Atom	Angle/°	Atom	Atom	Atom	Angle/°
C16	O1	C17	115.70(14)	C2	C1	Cl1	126.57(13)
C1	N1	C4	106.29(14)	C3	C2	C1	106.09(15)
C1	N1	B	128.09(14)	C2	C3	C4	107.77(15)
C4	N1	B	125.59(13)	N1	C4	C3	108.31(14)
C6	N2	B	126.08(14)	N1	C4	C5	121.02(15)
C9	N2	C6	106.29(14)	C5	C4	C3	130.52(15)
C9	N2	B	127.49(14)	C4	C5	C10	119.62(14)
N1	C1	Cl1	121.88(13)	C6	C5	C4	120.57(15)
N1	C1	C2	111.54(15)	C6	C5	C10	119.77(14)

Atom	Atom	Atom	Angle/°
N2	C6	C5	120.85(14)
N2	C6	C7	108.28(14)
C5	C6	C7	130.84(16)
C8	C7	C6	107.59(15)
C7	C8	C9	106.00(15)
N2	C9	Cl2	121.94(14)
N2	C9	C8	111.83(15)
C8	C9	Cl2	126.21(14)
C11	C10	C5	120.80(14)
C11	C10	C15	119.60(15)
C15	C10	C5	119.60(14)
C12	C11	C10	120.06(15)
C11	C12	C13	120.42(15)
C12	C13	C16	122.11(15)
C14	C13	C12	119.53(15)
C14	C13	C16	118.35(14)
C15	C14	C13	120.50(15)
C14	C15	C10	119.88(15)
O1	C16	C13	111.92(14)
O2	C16	O1	123.60(16)
O2	C16	C13	124.48(16)
F1	B	F2	111.55(14)
F1	B	N1	110.90(14)
F1	B	N2	110.55(14)
F2	B	N1	109.71(13)
F2	B	N2	108.90(14)
N2	B	N1	105.02(13)

*Table S 10: Torsion Angles in ° for BODIPY **2**.*

Atom	Atom	Atom	Atom	Angle/°
Cl1	C1	C2	C3	-178.93(13)
N1	C1	C2	C3	-0.2(2)
N1	C4	C5	C6	0.8(2)
N1	C4	C5	C10	-176.80(14)
N2	C6	C7	C8	-0.87(19)
C1	N1	C4	C3	-0.55(18)
C1	N1	C4	C5	175.51(15)
C1	N1	B	F1	-53.0(2)
C1	N1	B	F2	70.6(2)
C1	N1	B	N2	-172.47(15)
C1	C2	C3	C4	-0.17(19)
C2	C3	C4	N1	0.45(19)
C2	C3	C4	C5	-175.11(17)
C3	C4	C5	C6	175.88(17)
C3	C4	C5	C10	-1.7(3)
C4	N1	C1	Cl1	179.27(12)
C4	N1	C1	C2	0.46(19)
C4	N1	B	F1	129.52(16)
C4	N1	B	F2	-106.80(17)
C4	N1	B	N2	10.1(2)
C4	C5	C6	N2	-0.7(2)
C4	C5	C6	C7	-178.81(17)
C4	C5	C10	C11	-52.7(2)
C4	C5	C10	C15	127.37(17)
C5	C6	C7	C8	177.47(17)
C5	C10	C11	C12	-179.84(15)
C5	C10	C15	C14	179.93(15)
C6	N2	C9	Cl2	-178.98(12)
C6	N2	C9	C8	-0.53(19)
C6	N2	B	F1	-129.66(16)
C6	N2	B	F2	107.45(17)
C6	N2	B	N1	-10.0(2)
C6	C5	C10	C11	129.68(17)
C6	C5	C10	C15	-50.3(2)

Atom	Atom	Atom	Atom	Angle/°
C6	C7	C8	C9	0.5(2)
C7	C8	C9	Cl2	178.36(13)
C7	C8	C9	N2	0.0(2)
C9	N2	C6	C5	-177.69(15)
C9	N2	C6	C7	0.85(18)
C9	N2	B	F1	55.2(2)
C9	N2	B	F2	-67.7(2)
C9	N2	B	N1	174.85(15)
C10	C5	C6	N2	176.96(14)
C10	C5	C6	C7	-1.2(3)
C10	C11	C12	C13	-0.2(2)
C11	C10	C15	C14	0.0(2)
C11	C12	C13	C14	0.2(2)
C11	C12	C13	C16	-178.70(15)
C12	C13	C14	C15	-0.1(2)
C12	C13	C16	O1	-1.4(2)
C12	C13	C16	O2	177.73(17)
C13	C14	C15	C10	0.0(2)
C14	C13	C16	O1	179.69(14)
C14	C13	C16	O2	-1.2(3)
C15	C10	C11	C12	0.1(2)
C16	C13	C14	C15	178.82(15)
C17	O1	C16	O2	-3.5(2)
C17	O1	C16	C13	175.59(14)
B	N1	C1	Cl1	1.4(2)
B	N1	C1	C2	-177.38(15)
B	N1	C4	C3	177.35(14)
B	N1	C4	C5	-6.6(2)
B	N2	C6	C5	6.3(2)
B	N2	C6	C7	-175.14(14)
B	N2	C9	Cl2	-3.1(2)
B	N2	C9	C8	175.40(15)

Table S11: Hydrogen Fractional Atomic Coordinates ($x10^4$) and Equivalent Isotropic Displacement Parameters ($Å^2x10^3$) for BODIPY **2**. U_{eq} is defined as 1/3 of the trace of the orthogonalised U_{ij}.

Atom	x	y	z	U_{eq}
H2	13226.21	4743.83	4441.68	23
H3	11173.17	5021.46	5974.06	21
H7	8386.56	1158.54	8701.77	23
H8	8960.02	-1192.17	8630.74	27
H11	11189.14	5147.15	8361.14	19
H12	9421.5	6593.19	9116.74	19
H14	5108.37	3795.39	7758.47	20
H15	6863.3	2336.26	7001.97	20
H17A	4981.76	8604.71	9122.65	40
H17B	6517.65	9202.44	10387.36	40
H17C	5012.35	8044.87	10491.02	40

Submitted by: **Jacques Pliquett**

Solved by: **Yoann Rousselin**

Sample ID: **16jpl23_2**

Crystal Data and Experimental

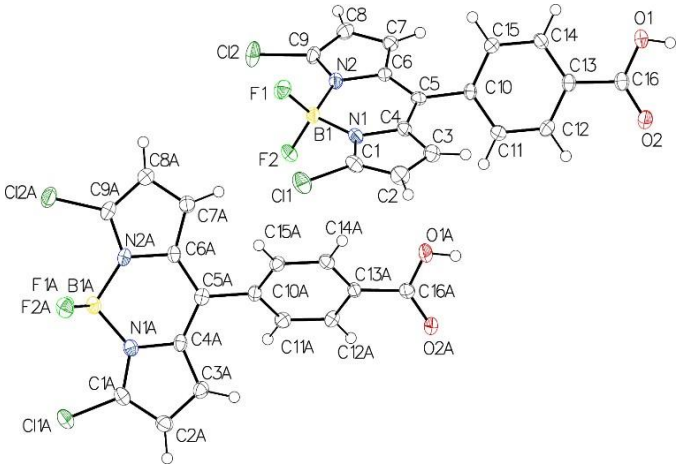

Experimental. Single clear light pink needle-shaped crystals of (**Compound 3**) were recrystallised from a mixture of DCM and methanol by slow evaporation. A suitable crystal (0.60x0.41x0.27) mm^3 was selected and mounted on a MITIGEN holder oil on a Nonius Kappa APEX-II diffractometer. The crystal was kept at T = 115(1) K during data collection. Using **Olex2** (Dolomanov et al., 2009), the structure was solved with the **ShelXT** (Sheldrick, 2015) structure solution program, using the Direct Methods solution method. The model was refined with version 2018/1 of **ShelXL** (Sheldrick, 2015) using Least Squares minimisation.

Crystal Data. $C_{16}H_9BCl_2F_2N_2O_2$, M_r = 380.96, triclinic, P-1 (No. 2), a = 10.9208(5) Å, b = 11.1413(5) Å, c = 14.0873(6) Å, α = 69.876(3)°, β = 75.945(3)°, γ = 75.941(3)°, V = 1537.13(12) $Å^3$, T = 115(1) K, Z = 4, Z' = 2, μ(MoK$_\alpha$) = 0.458, 37815 reflections measured, 7063 unique (R_{int} = 0.0455) which were used in all calculations. The final wR_2 was 0.0950 (all data) and R_1 was 0.0368 (I > 2(I)).

*Table S12: X-ray structure data of BODIPY **3**.*

Compound	**Compound 3**
CCDC	**1825950**
Formula	$C_{16}H_9BCl_2F_2N_2O_2$
$D_{calc.}$/ g cm^{-3}	1.646
μ/mm^{-1}	0.458
Formula Weight	380.96
Colour	clear light pink
Shape	needle
Size/mm^3	0.60x0.41x0.27
T/K	115(1)
Crystal System	triclinic
Space Group	P-1
a/Å	10.9208(5)
b/Å	11.1413(5)
c/Å	14.0873(6)
α/°	69.876(3)
β/°	75.945(3)
γ/°	75.941(3)
V/$Å^3$	1537.13(12)
Z	4
Z'	2
Wavelength/Å	0.71073
Radiation type	MoK$_\alpha$
Θ_{min}/°	1.564
Θ_{max}/°	27.499
Measured Refl.	37815
Independent Refl.	7063
Reflections Used	5037
R_{int}	0.0455
Parameters	453
Restraints	0
Largest Peak	0.365
Deepest Hole	-0.348
GooF	1.017
wR_2 (all data)	0.0950
wR_2	0.0820
R_1 (all data)	0.0653
R_1	0.0368

*Table S 13: BODIPY **3** structure Quality Indicators.*

Reflections:	d min (Mo) 0.77	I/σ 18.9	Rint 4.55%	complete 100%
Refinement:	Shift -0.001	Max Peak 0.4	Min Peak -0.3	GooF 1.017

A clear light pink needle-shaped crystal with dimensions 0.60x0.41x0.27 mm^3 was mounted on a MITIGEN holder oil. X-ray diffraction data were collected using a Nonius Kappa APEX-II diffractometer equipped with a Oxford Cryosystems low-temperature device, operating at T = 115(1) K. Data were measured using ϕ and ω scans of 2° per frame for 10s using MoK_α radiation (X-ray tube, 50 kV, 32 mA). The total number of runs and images was based on the strategy calculation from the program APEX3 (Bruker, 2015).The maximum resolution achieved was Θ = 27.499°. Cell parameters were retrieved using the **SAINT** (Bruker, V8.34A, after 2013) software and refined using **SAINT** (Bruker, V8.34A, after 2013) on 9455 reflections, 25 % of the observed reflections. Data reduction was performed using the **SAINT** (Bruker, V8.34A, after 2013) software which corrects for Lorentz polarisation. The final completeness is 99.90 % out to 27.499° in Θ. A multi-scan absorption correction was performed using SADABS-2014/5 (Bruker,2014) was used for absorption correction. wR_2(int) was 0.0541 before and 0.0473 after correction. The Ratio of minimum to maximum transmission is 0.9065. The λ/2 correction factor is 0.00150. The absorption coefficient μ of this material is 0.458 mm^{-1} at this wavelength (λ = 0.71073Å) and the minimum and maximum transmissions are 0.6759 and 0.7456. The structure was solved in the space group P-1 (# 2) by Direct Methods using the **ShelXT** (Sheldrick, 2015) structure solution program and refined by Least Squares using version 2018/1 of **ShelXL** (Sheldrick, 2015). All non-hydrogen atoms were refined anisotropically. Hydrogen atom positions were calculated geometrically and refined using the riding model. SADABS-2014/5 (Bruker,2014) was used for absorption correction. wR_2(int) was 0.0541 before and 0.0473 after correction. The Ratio of minimum to maximum transmission is 0.9065. The λ/2 correction factor is 0.00150. The value of Z' is 2. This means that there are two independent molecules in the asymmetric unit.

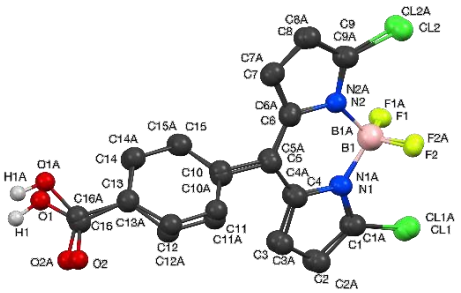

Figure S 125: Overlay view of both molecules present in asymmetric unit (RMSD = 0.24 Å).

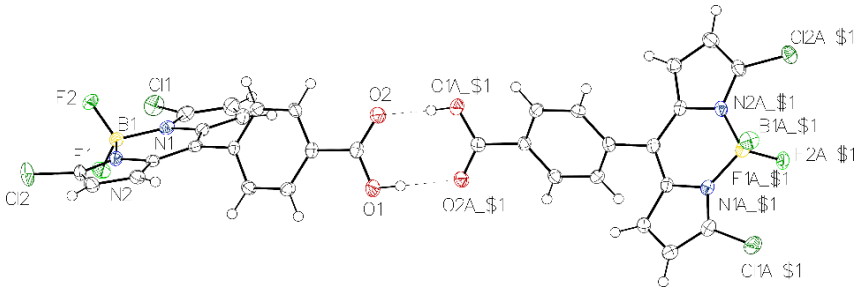

Figure S 126: ORTEP view of hydrogen bonds. Thermal ellipsoids are draw at 50% probability level.

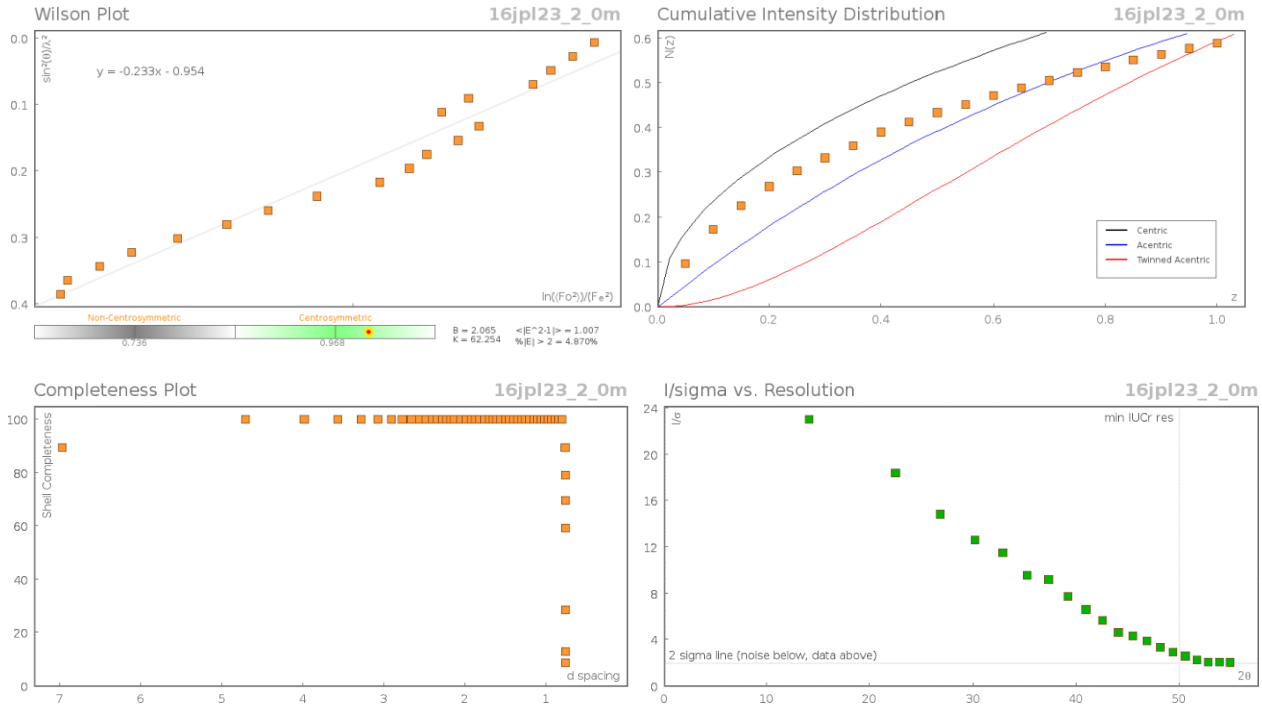

*Figure S 127: Data Plots: Diffraction Data of BODIPY **3** structure.*

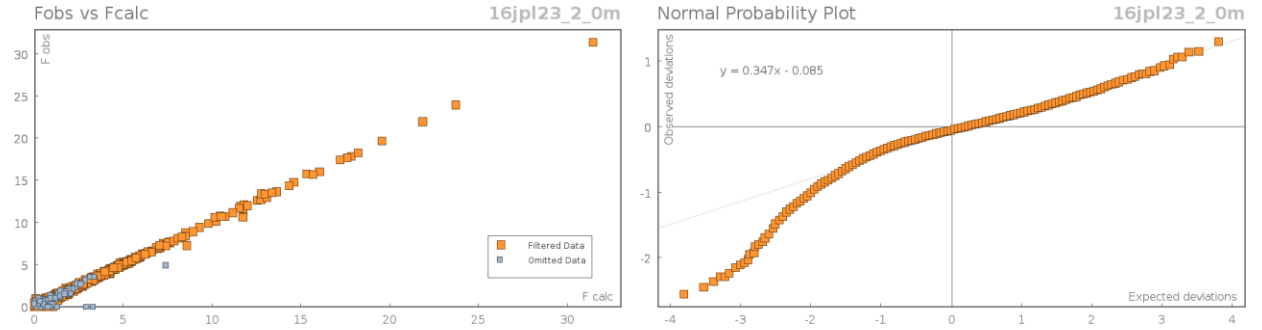

*Figure S 128: Data Plots: refinement and Data of BODIPY **3** structure.*

*Table S 14: reflection statistics of BODIPY **3** structure.*

Total reflections (after filtering)	37834	Unique reflections	7063
Completeness	0.999	Mean I/σ	18.87
hkl_{max} collected	(14, 14, 18)	hkl_{min} collected	(-14, -14, -18)
hkl_{max} used	(14, 14, 18)	hkl_{min} used	(-13, -13, 0)
Lim d_{max} collected	100.0	Lim d_{min} collected	0.77
d_{max} used	13.02	d_{min} used	0.77
Friedel pairs	6968	Friedel pairs merged	1
Inconsistent equivalents	0	R_{int}	0.0455
R_{sigma}	0.0404	Intensity transformed	0
Omitted reflections	0	Omitted by user (OMIT hkl)	19
Multiplicity	(2285, 5067, 3479, 1749, 1245, 279, 31, 3)	Maximum multiplicity	13
Removed systematic absences	0	Filtered off (Shel/OMIT)	158

*Table S 15: Fractional Atomic Coordinates (x10^4) and Equivalent Isotropic Displacement Parameters (Å^{2}x10^3) for BODIPY **3**. U_{eq} is defined as 1/3 of the trace of the orthogonalised U_{ij}.*

Atom	x	y	z	U_{eq}
Cl1	2868.0(6)	9837.2(6)	6303.2(4)	31.88(14)
Cl2	-580.7(6)	6135.4(6)	6594.9(4)	34.20(15)
F1	422.7(12)	8732.6(12)	6359.6(9)	26.7(3)
F2	2119.5(11)	7149.8(11)	6155.6(9)	24.5(3)
O1	1573.6(14)	11872.1(16)	-1487.5(11)	28.3(4)
O2	3651.1(15)	11047.9(16)	-1481.7(11)	32.8(4)
N1	2091.1(16)	9252.8(16)	4883.2(12)	18.4(4)
N2	616.4(16)	7805.1(16)	5001.4(12)	18.1(4)
C1	2758(2)	9978(2)	5081.7(16)	23.2(5)
C2	3338(2)	10802(2)	4185.4(17)	27.7(5)
C3	3016(2)	10575(2)	3382.9(16)	23.2(5)
C4	2239.7(19)	9611.2(19)	3812.5(15)	18.0(4)
C5	1585.9(18)	9104.7(19)	3346.6(15)	17.1(4)
C6	775.3(18)	8217.8(19)	3931.0(14)	16.9(4)
C7	64.1(19)	7553(2)	3635.5(15)	20.0(4)
C8	-527(2)	6737(2)	4516.4(16)	23.1(5)
C9	-159(2)	6917(2)	5327.4(15)	20.9(4)
C10	1771.2(19)	9521.1(18)	2210.3(14)	16.2(4)
C11	3004.4(19)	9328.5(19)	1651.7(15)	18.9(4)
C12	3218.5(19)	9799.6(19)	597.6(15)	19.5(4)
C13	2205(2)	10500.1(19)	84.1(15)	18.9(4)
C14	960(2)	10648(2)	632.9(15)	20.7(4)
C15	742.8(19)	10148(2)	1692.1(15)	20.1(4)
C16	2529(2)	11157(2)	-1033.9(15)	20.8(4)
B1	1303(2)	8215(2)	5662.2(17)	18.8(5)
Cl1A	7386.9(6)	2067.3(6)	11226.0(4)	30.42(14)
Cl2A	1667.3(5)	3289.2(6)	11205.1(4)	29.57(14)
F1A	4541.3(12)	3617.5(12)	11161.8(9)	27.7(3)
F2A	4591.9(12)	1730.1(11)	10870.0(9)	25.6(3)
O1A	5555.8(14)	7879.2(15)	3413.1(11)	26.3(3)
O2A	7465.7(14)	6575.4(14)	3302.1(10)	23.8(3)
N1A	6029.3(16)	3156.1(16)	9709.1(12)	19.0(4)
N2A	3685.1(16)	3720.0(16)	9703.5(12)	18.8(4)

Atom	x	y	z	U_{eq}
C1A	7191(2)	2813(2)	9979.8(16)	22.6(4)
C2A	8162(2)	3143(2)	9137.1(16)	24.3(5)
C3A	7554(2)	3728(2)	8300.9(16)	22.2(4)
C4A	6231.2(19)	3730.3(19)	8646.5(15)	18.3(4)
C5A	5204.6(19)	4283.9(18)	8117.7(15)	17.5(4)
C6A	3943.2(19)	4285.9(19)	8639.3(15)	18.0(4)
C7A	2765(2)	4765(2)	8284.8(16)	21.9(4)
C8A	1796(2)	4511(2)	9118.6(16)	25.2(5)
C9A	2405(2)	3864(2)	9968.7(16)	22.4(4)
C10A	5465.8(19)	4934.0(19)	6993.3(15)	17.9(4)
C11A	6356.6(19)	4298(2)	6342.7(15)	20.1(4)
C12A	6654.0(19)	4929(2)	5306.4(15)	19.6(4)
C13A	6040.2(19)	6190.8(19)	4899.2(14)	17.4(4)
C14A	5119.2(19)	6809(2)	5531.6(15)	18.7(4)
C15A	4846.1(19)	6195.8(19)	6576.6(15)	18.8(4)
C16A	6404.0(19)	6898(2)	3798.0(15)	18.8(4)
B1A	4700(2)	3021(2)	10423.5(17)	19.8(5)

*Table S 16: Anisotropic Displacement Parameters (x10⁴) BODIPY **3**. The anisotropic displacement factor exponent takes the form: $-2\pi^2[h^2a^{*2} \times U_{11} + \ldots + 2hka^* \times b^* \times U_{12}]$*

Atom	U_{11}	U_{22}	U_{33}	U_{23}	U_{13}	U_{12}
Cl1	40.5(3)	36.2(3)	26.5(3)	-12.9(2)	-13.0(2)	-8.5(3)
Cl2	46.8(4)	34.5(3)	18.9(3)	-2.8(2)	4.0(2)	-20.4(3)
F1	25.7(7)	31.8(7)	23.6(6)	-14.6(6)	0.4(5)	-2.5(5)
F2	26.1(7)	22.0(6)	21.8(6)	-1.2(5)	-9.4(5)	-0.1(5)
O1	27.0(9)	35.5(9)	15.8(8)	0.9(7)	-3.7(6)	-6.3(7)
O2	25.3(9)	40(1)	20.0(8)	0.6(7)	0.3(6)	-0.3(7)
N1	19.7(9)	19.1(9)	16.9(8)	-5.6(7)	-6.2(7)	-0.7(7)
N2	20.4(9)	16.6(9)	15.0(8)	-3.0(7)	-2.0(7)	-2.7(7)
C1	26.6(12)	21.9(11)	24.4(11)	-8.5(9)	-11.1(9)	-1.4(9)
C2	30.2(13)	24.5(12)	30.9(12)	-6.8(10)	-8(1)	-9.1(10)
C3	24.4(11)	19.4(11)	24.4(11)	-2.3(9)	-5.3(9)	-6.3(9)
C4	18.5(10)	16.3(10)	17.4(10)	-3.3(8)	-4.7(8)	-0.9(8)
C5	14.8(10)	16(1)	18.7(10)	-4.9(8)	-4.1(8)	1.5(8)
C6	14.8(10)	17.4(10)	16.1(10)	-4.7(8)	-2.2(8)	0.5(8)
C7	18.8(10)	23.6(11)	18.8(10)	-7.4(8)	-4.7(8)	-3.0(8)

Atom	U_{11}	U_{22}	U_{33}	U_{23}	U_{13}	U_{12}
C8	20.5(11)	23.1(11)	25.9(11)	-6.8(9)	-2.3(9)	-6.9(9)
C9	22.6(11)	18.8(10)	17.1(10)	-1.0(8)	0.6(8)	-6.3(8)
C10	20.2(10)	12.8(9)	14.2(9)	-2.4(7)	-1.6(8)	-4.5(8)
C11	18.6(10)	17.7(10)	20.5(10)	-5.2(8)	-5.2(8)	-2.2(8)
C12	18.6(10)	17.8(10)	20.6(10)	-5.4(8)	1.0(8)	-5.4(8)
C13	24.0(11)	16.2(10)	16.4(10)	-4.6(8)	-2.0(8)	-5.6(8)
C14	20.7(11)	23.1(11)	17.3(10)	-5.4(8)	-5.8(8)	-0.5(9)
C15	17.3(10)	23.4(11)	18.6(10)	-6.4(8)	-1.8(8)	-3.2(8)
C16	26.0(12)	17.4(10)	18.5(10)	-4.7(8)	-3.3(9)	-4.3(9)
B1	20.1(12)	19.8(12)	14.0(11)	-4.5(9)	-1.9(9)	-1.1(9)
Cl1A	32.8(3)	33.7(3)	22.0(3)	-3.2(2)	-11.2(2)	-2.0(2)
Cl2A	28.5(3)	33.0(3)	21.0(3)	-5.6(2)	4.6(2)	-6.9(2)
F1A	32.3(7)	31.4(7)	23.4(6)	-15.6(6)	-5.4(5)	-1.7(6)
F2A	29.9(7)	17.9(6)	22.9(6)	-0.2(5)	0.3(5)	-6.4(5)
O1A	27.4(9)	26.6(8)	16.9(7)	1.2(6)	-3.5(6)	-2.0(7)
O2A	22.8(8)	29.6(8)	15.5(7)	-4.7(6)	-1.0(6)	-3.4(6)
N1A	22.0(9)	15.6(9)	18.5(9)	-3.7(7)	-4.3(7)	-3.2(7)
N2A	21.6(9)	18.1(9)	15.2(8)	-4.1(7)	0.7(7)	-5.8(7)
C1A	27.7(12)	19.2(11)	21.0(11)	-3.6(9)	-8.0(9)	-3.9(9)
C2A	21.7(11)	22.7(11)	26.3(11)	-3.8(9)	-6.7(9)	-2.5(9)
C3A	22.1(11)	19.1(11)	21.7(11)	-2.9(8)	-0.6(8)	-4.8(8)
C4A	22.3(11)	14.9(10)	16.1(10)	-3.5(8)	-1.5(8)	-3.6(8)
C5A	21.8(11)	12.5(9)	18.5(10)	-6.2(8)	-1.8(8)	-3.1(8)
C6A	22.7(11)	15.2(10)	15.1(10)	-3.6(8)	-2.5(8)	-4.0(8)
C7A	22.6(11)	22.3(11)	20.5(10)	-5.6(9)	-4.0(8)	-4.6(9)
C8A	21.1(11)	29.9(12)	23.7(11)	-7.7(9)	-1.9(9)	-5.4(9)
C9A	23.7(11)	21.8(11)	19.9(10)	-7.4(9)	3.2(8)	-6.3(9)
C10A	19.3(10)	19.7(10)	15.2(10)	-4.5(8)	-2.0(8)	-6.1(8)
C11A	19.9(11)	15.7(10)	22.7(11)	-4.6(8)	-3.5(8)	-1.5(8)
C12A	19.1(10)	19.9(11)	18.9(10)	-6.8(8)	0.2(8)	-4.3(8)
C13A	17.9(10)	19.2(10)	15(1)	-3.0(8)	-4.0(8)	-5.1(8)
C14A	19.6(10)	16.5(10)	20(1)	-3.8(8)	-6.2(8)	-2.7(8)
C15A	17.3(10)	18.9(10)	19.2(10)	-6.5(8)	-1.4(8)	-2.0(8)
C16A	19.8(10)	19.8(11)	18.9(10)	-5.8(8)	-5.1(8)	-5.8(8)
B1A	24.4(13)	17.2(11)	17.1(11)	-5.3(9)	-3.3(9)	-2.8(9)

*Table S 17: Bond Lengths in Å for BODIPY **3**.*

Atom	Atom	Length/Å	Atom	Atom	Length/Å
Cl1	C1	1.704(2)	Cl1A	C1A	1.706(2)
Cl2	C9	1.698(2)	Cl2A	C9A	1.701(2)
F1	B1	1.373(2)	F1A	B1A	1.373(2)
F2	B1	1.380(3)	F2A	B1A	1.380(3)
O1	C16	1.304(3)	O1A	C16A	1.301(2)
O2	C16	1.233(3)	O2A	C16A	1.240(2)
N1	C1	1.343(3)	N1A	C1A	1.341(3)
N1	C4	1.400(2)	N1A	C4A	1.396(3)
N1	B1	1.560(3)	N1A	B1A	1.561(3)
N2	C6	1.396(2)	N2A	C6A	1.398(2)
N2	C9	1.346(3)	N2A	C9A	1.341(3)
N2	B1	1.561(3)	N2A	B1A	1.564(3)
C1	C2	1.391(3)	C1A	C2A	1.395(3)
C2	C3	1.378(3)	C2A	C3A	1.376(3)
C3	C4	1.408(3)	C3A	C4A	1.408(3)
C4	C5	1.392(3)	C4A	C5A	1.395(3)
C5	C6	1.396(3)	C5A	C6A	1.395(3)
C5	C10	1.482(3)	C5A	C10A	1.485(3)
C6	C7	1.405(3)	C6A	C7A	1.409(3)
C7	C8	1.379(3)	C7A	C8A	1.376(3)
C8	C9	1.388(3)	C8A	C9A	1.399(3)
C10	C11	1.393(3)	C10A	C11A	1.403(3)
C10	C15	1.396(3)	C10A	C15A	1.393(3)
C11	C12	1.375(3)	C11A	C12A	1.380(3)
C12	C13	1.392(3)	C12A	C13A	1.389(3)
C13	C14	1.393(3)	C13A	C14A	1.389(3)
C13	C16	1.484(3)	C13A	C16A	1.482(3)
C14	C15	1.383(3)	C14A	C15A	1.384(3)

*Table S 18: Bond Angles in ° for BODIPY **3**.*

Atom	Atom	Atom	Angle/°
C1	N1	C4	105.92(17)
C1	N1	B1	128.30(17)
C4	N1	B1	125.78(16)
C6	N2	B1	126.15(16)
C9	N2	C6	105.90(16)
C9	N2	B1	127.76(17)
N1	C1	Cl1	122.02(16)
N1	C1	C2	111.80(18)
C2	C1	Cl1	126.17(17)
C3	C2	C1	106.43(19)
C2	C3	C4	107.25(19)
N1	C4	C3	108.61(17)
C5	C4	N1	120.74(18)
C5	C4	C3	130.44(19)
C4	C5	C6	121.11(18)
C4	C5	C10	118.61(17)
C6	C5	C10	120.29(17)
N2	C6	C7	108.41(17)
C5	C6	N2	120.44(17)
C5	C6	C7	131.07(18)
C8	C7	C6	107.73(18)
C7	C8	C9	105.97(18)
N2	C9	Cl2	121.60(16)
N2	C9	C8	111.97(18)
C8	C9	Cl2	126.42(16)
C11	C10	C5	119.11(17)
C11	C10	C15	119.59(18)
C15	C10	C5	121.24(17)
C12	C11	C10	120.35(19)
C11	C12	C13	120.00(18)
C12	C13	C14	119.99(18)
C12	C13	C16	117.22(18)
C14	C13	C16	122.58(19)
C15	C14	C13	119.83(19)
C14	C15	C10	120.03(19)
O1	C16	C13	116.22(18)
O2	C16	O1	123.22(19)
O2	C16	C13	120.52(19)
F1	B1	F2	110.69(17)
F1	B1	N1	110.63(17)
F1	B1	N2	110.63(17)
F2	B1	N1	109.93(17)
F2	B1	N2	109.32(17)
N1	B1	N2	105.50(15)
C1A	N1A	C4A	106.09(17)
C1A	N1A	B1A	127.98(17)
C4A	N1A	B1A	125.85(17)
C6A	N2A	B1A	126.31(17)
C9A	N2A	C6A	106.21(17)
C9A	N2A	B1A	127.45(17)
N1A	C1A	Cl1A	121.73(16)
N1A	C1A	C2A	112.08(18)
C2A	C1A	Cl1A	126.19(17)
C3A	C2A	C1A	105.57(19)
C2A	C3A	C4A	108.07(18)
N1A	C4A	C3A	108.18(17)
C5A	C4A	N1A	121.16(18)
C5A	C4A	C3A	130.41(19)
C4A	C5A	C10A	119.18(18)
C6A	C5A	C4A	120.79(18)
C6A	C5A	C10A	119.96(18)
N2A	C6A	C7A	108.12(17)
C5A	C6A	N2A	120.48(18)
C5A	C6A	C7A	131.39(19)
C8A	C7A	C6A	108.05(19)
C7A	C8A	C9A	105.71(19)
N2A	C9A	Cl2A	122.03(16)
N2A	C9A	C8A	111.90(18)

Atom	Atom	Atom	Angle/°
C8A	C9A	Cl2A	126.06(17)
C11A	C10A	C5A	120.52(18)
C15A	C10A	C5A	120.18(17)
C15A	C10A	C11A	119.29(18)
C12A	C11A	C10A	120.50(19)
C11A	C12A	C13A	119.78(18)
C12A	C13A	C14A	120.05(18)
C12A	C13A	C16A	120.01(18)
C14A	C13A	C16A	119.90(18)
C15A	C14A	C13A	120.39(19)

Atom	Atom	Atom	Angle/°
C14A	C15A	C10A	119.91(18)
O1A	C16A	C13A	115.46(18)
O2A	C16A	O1A	123.51(18)
O2A	C16A	C13A	121.01(18)
F1A	B1A	F2A	110.61(17)
F1A	B1A	N1A	110.14(17)
F1A	B1A	N2A	110.39(17)
F2A	B1A	N1A	110.41(17)
F2A	B1A	N2A	109.82(17)
N1A	B1A	N2A	105.34(16)

*Table S 19: Torsion Angles in ° for BODIPY **3**.*

Atom	Atom	Atom	Atom	Angle/°
Cl1	C1	C2	C3	178.68(17)
N1	C1	C2	C3	-0.1(3)
N1	C4	C5	C6	-0.6(3)
N1	C4	C5	C10	179.67(17)
N2	C6	C7	C8	0.0(2)
C1	N1	C4	C3	-0.1(2)
C1	N1	C4	C5	-175.24(18)
C1	N1	B1	F1	54.1(3)
C1	N1	B1	F2	-68.4(3)
C1	N1	B1	N2	173.82(18)
C1	C2	C3	C4	0.0(2)
C2	C3	C4	N1	0.0(2)
C2	C3	C4	C5	174.6(2)
C3	C4	C5	C6	-174.6(2)
C3	C4	C5	C10	5.7(3)
C4	N1	C1	Cl1	-178.72(15)
C4	N1	C1	C2	0.1(2)
C4	N1	B1	F1	-125.92(19)
C4	N1	B1	F2	111.5(2)
C4	N1	B1	N2	-6.2(3)
C4	C5	C6	N2	-0.9(3)
C4	C5	C6	C7	-177.4(2)

Atom	Atom	Atom	Atom	Angle/°
C4	C5	C10	C11	57.5(3)
C4	C5	C10	C15	-119.9(2)
C5	C6	C7	C8	176.9(2)
C5	C10	C11	C12	-174.68(18)
C5	C10	C15	C14	173.15(18)
C6	N2	C9	Cl2	178.72(15)
C6	N2	C9	C8	-0.6(2)
C6	N2	B1	F1	124.4(2)
C6	N2	B1	F2	-113.5(2)
C6	N2	B1	N1	4.7(3)
C6	C5	C10	C11	-122.2(2)
C6	C5	C10	C15	60.4(3)
C6	C7	C8	C9	-0.3(2)
C7	C8	C9	Cl2	-178.69(17)
C7	C8	C9	N2	0.6(2)
C9	N2	C6	C5	-176.94(18)
C9	N2	C6	C7	0.3(2)
C9	N2	B1	F1	-61.4(3)
C9	N2	B1	F2	60.7(3)
C9	N2	B1	N1	178.92(18)
C10	C5	C6	N2	178.83(17)
C10	C5	C6	C7	2.2(3)
C10	C11	C12	C13	1.5(3)
C11	C10	C15	C14	-4.2(3)
C11	C12	C13	C14	-4.3(3)
C11	C12	C13	C16	170.55(18)
C12	C13	C14	C15	2.9(3)
C12	C13	C16	O1	-175.96(18)
C12	C13	C16	O2	1.9(3)
C13	C14	C15	C10	1.4(3)
C14	C13	C16	O1	-1.2(3)
C14	C13	C16	O2	176.6(2)
C15	C10	C11	C12	2.7(3)
C16	C13	C14	C15	-171.75(19)
B1	N1	C1	Cl1	1.2(3)

Atom	Atom	Atom	Atom	Angle/°
B1	N1	C1	C2	-179.97(19)
B1	N1	C4	C3	179.97(18)
B1	N1	C4	C5	4.8(3)
B1	N2	C6	C5	-1.7(3)
B1	N2	C6	C7	175.59(18)
B1	N2	C9	Cl2	3.6(3)
B1	N2	C9	C8	-175.70(19)
Cl1A	C1A	C2A	C3A	-179.54(16)
N1A	C1A	C2A	C3A	0.2(2)
N1A	C4A	C5A	C6A	0.4(3)
N1A	C4A	C5A	C10A	177.38(17)
N2A	C6A	C7A	C8A	0.6(2)
C1A	N1A	C4A	C3A	-0.7(2)
C1A	N1A	C4A	C5A	-175.51(18)
C1A	N1A	B1A	F1A	54.6(3)
C1A	N1A	B1A	F2A	-67.8(3)
C1A	N1A	B1A	N2A	173.69(18)
C1A	C2A	C3A	C4A	-0.6(2)
C2A	C3A	C4A	N1A	0.9(2)
C2A	C3A	C4A	C5A	175.0(2)
C3A	C4A	C5A	C6A	-173.1(2)
C3A	C4A	C5A	C10A	3.9(3)
C4A	N1A	C1A	Cl1A	-179.92(15)
C4A	N1A	C1A	C2A	0.3(2)
C4A	N1A	B1A	F1A	-121.9(2)
C4A	N1A	B1A	F2A	115.7(2)
C4A	N1A	B1A	N2A	-2.8(2)
C4A	C5A	C6A	N2A	-0.6(3)
C4A	C5A	C6A	C7A	-179.4(2)
C4A	C5A	C10A	C11A	50.8(3)
C4A	C5A	C10A	C15A	-127.8(2)
C5A	C6A	C7A	C8A	179.5(2)
C5A	C10A	C11A	C12A	-176.24(18)
C5A	C10A	C15A	C14A	178.27(18)
C6A	N2A	C9A	Cl2A	179.15(15)

Atom	Atom	Atom	Atom	Angle/°
C6A	N2A	C9A	C8A	-0.2(2)
C6A	N2A	B1A	F1A	121.5(2)
C6A	N2A	B1A	F2A	-116.3(2)
C6A	N2A	B1A	N1A	2.6(3)
C6A	C5A	C10A	C11A	-132.2(2)
C6A	C5A	C10A	C15A	49.2(3)
C6A	C7A	C8A	C9A	-0.7(2)
C7A	C8A	C9A	Cl2A	-178.74(16)
C7A	C8A	C9A	N2A	0.6(2)
C9A	N2A	C6A	C5A	-179.29(18)
C9A	N2A	C6A	C7A	-0.3(2)
C9A	N2A	B1A	F1A	-60.8(3)
C9A	N2A	B1A	F2A	61.4(3)
C9A	N2A	B1A	N1A	-179.66(18)
C10A	C5A	C6A	N2A	-177.58(17)
C10A	C5A	C6A	C7A	3.7(3)
C10A	C11A	C12A	C13A	-1.8(3)
C11A	C10A	C15A	C14A	-0.4(3)
C11A	C12A	C13A	C14A	-0.8(3)
C11A	C12A	C13A	C16A	176.79(18)
C12A	C13A	C14A	C15A	2.8(3)
C12A	C13A	C16A	O1A	159.84(18)
C12A	C13A	C16A	O2A	-22.0(3)
C13A	C14A	C15A	C10A	-2.2(3)
C14A	C13A	C16A	O1A	-22.6(3)
C14A	C13A	C16A	O2A	155.58(19)
C15A	C10A	C11A	C12A	2.4(3)
C16A	C13A	C14A	C15A	-174.77(18)
B1A	N1A	C1A	Cl1A	3.0(3)
B1A	N1A	C1A	C2A	-176.72(19)
B1A	N1A	C4A	C3A	176.42(18)
B1A	N1A	C4A	C5A	1.6(3)
B1A	N2A	C6A	C5A	-1.2(3)
B1A	N2A	C6A	C7A	177.88(18)
B1A	N2A	C9A	Cl2A	1.0(3)

Atom	Atom	Atom	Atom	Angle/°
B1A	N2A	C9A	C8A	-178.31(19)

*Table S 20: Hydrogen Fractional Atomic Coordinates (x10⁴) and Equivalent Isotropic Displacement Parameters (Å²x10³) for BODIPY **3**. U_{eq} is defined as 1/3 of the trace of the orthogonalised U_{ij}.*

Atom	x	y	z	U_{eq}
H1	1858.45	12340.5	-2071.86	42
H2	3855.14	11401.53	4136.03	33
H3	3269.49	10991.22	2672.23	28
H7	1.67	7647.35	2951.57	24
H8	-1074.33	6168.65	4559.51	28
H11	3701.23	8869.21	2000.98	23
H12	4058.08	9647.31	219.56	23
H14	263.02	11091.99	280.66	25
H15	-106.95	10230.74	2067.01	24
H1A	5832.66	8221.63	2789.27	39
H2A	9055.18	2995.43	9139.94	29
H3A	7956.85	4070.49	7610.95	27
H7A	2658.27	5189.65	7591.22	26
H8A	899.73	4729.12	9117.16	30
H11A	6758.3	3425.95	6617.35	24
H12A	7276.43	4501.65	4873.11	23
H14A	4674.16	7657.83	5245.22	22
H15A	4237.06	6634.57	7008.98	23

*Table S 21: Hydrogen Bond information for BODIPY **3**.*

D	H	A	d(D-H)/Å	d(H-A)/Å	d(D-A)/Å	D-H-A/deg
O1	H1	O2A[1]	0.84	1.84	2.676(2)	175.7
O1A	H1A	O2[1]	0.84	1.75	2.589(2)	177.8

[1]1-x,2-y,-z

Submitted by: Jacques Pliquett

Solved by: **Yoann Rousselin**

Sample ID: **15JPL223**

Crystal Data and Experimental

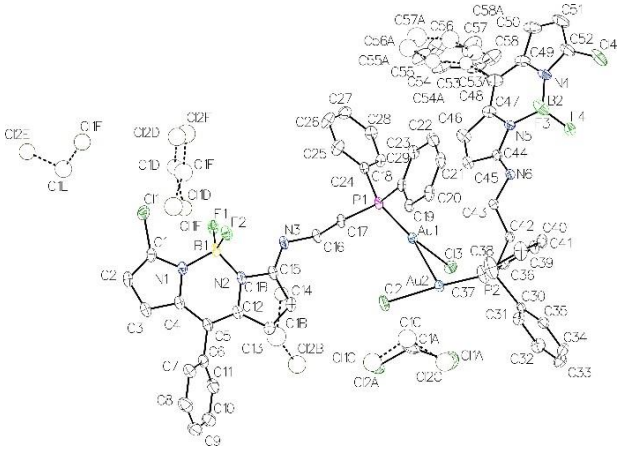

Experimental. Single clear light orange prism-shaped crystals of (**BODI-Au-7**) were recrystallised from a mixture of DCM and hexane by slow evaporation. A suitable crystal (0.39x0.25x0.18) mm^3 was selected and mounted on a MITIGEN holder oil on a Nonius Kappa Apex II diffractometer. The crystal was kept at T = 115(1) K during data collection. Using **Olex2** (Dolomanov et al., 2009), the structure was solved with the **ShelXT** (Sheldrick, 2015) structure solution program, using the Direct Methods solution method. The model was refined with version 2018/1 of **ShelXL** (Sheldrick, 2015) using Least Squares minimisation.

Crystal Data. $C_{30}H_{26}AuBCl_4F_2N_3P$, M_r = 847.08, monoclinic, $P2_1/c$ (No. 14), a = 13.9927(4) Å, b = 29.9994(8) Å, c = 15.2788(5) Å, β = 95.500(2)°, $\alpha = \gamma$ = 90°, V = 6384.1(3) $Å^3$, T = 115(1) K, Z = 8, Z' = 2, $\mu(MoK_\alpha)$ = 5.031, 113257 reflections measured, 14774 unique (R_{int} = 0.0503) which were used in all calculations. The final wR_2 was 0.0542 (all data) and R_1 was 0.0252 (I > 2(I)).

*Table S22: X-ray structure data of **BODI-AU-7**.*

Compound	**BODI-Au-7**
CCDC	**1825951**
Formula	$C_{30}H_{26}AuBCl_4F_2N_3P$
$D_{calc.}$/ g cm^{-3}	1.763
μ/mm^{-1}	5.031
Formula Weight	847.08
Colour	clear light orange
Shape	prism
Size/mm^3	0.39x0.25x0.18
T/K	115(1)
Crystal System	monoclinic
Space Group	$P2_1/c$
a/Å	13.9927(4)
b/Å	29.9994(8)
c/Å	15.2788(5)
α/°	90
β/°	95.500(2)
γ/°	90
V/$Å^3$	6384.1(3)
Z	8
Z'	2
Wavelength/Å	0.71073
Radiation type	MoK_α
Θ_{min}/°	2.438
Θ_{max}/°	27.617
Measured Refl.	113257
Independent Refl.	14774
Reflections Used	12297
R_{int}	0.0503
Parameters	774
Restraints	38
Largest Peak	1.312
Deepest Hole	-0.877
GooF	1.031
wR_2 (all data)	0.0542
wR_2	0.0489
R_1 (all data)	0.0396
R_1	0.0252

Table S 23: ***BODI-AU-7*** *structure Quality Indicators.*

Reflections:	d min (Mo) 0.77	I/σ 22.9	Rint 5.03%	complete 100%
Refinement:	Shift 0.005	Max Peak 1.3	Min Peak -0.9	GooF 1.031

A clear light orange prism-shaped crystal with dimensions 0.39x0.25x0.18 mm^3 was mounted on a MITIGEN holder oil. X-ray diffraction data were collected using a Nonius Kappa Apex II diffractometer equipped with a Oxford Cryosystems low-temperature device, operating at T = 115(1) K. Data were measured using ϕ and ω scans of 0.6° per frame for 7s using MoK_α radiation (X-ray tube, 50 kV, 32 mA). The total number of runs and images was based on the strategy calculation from the program APEX3 (Bruker, 2015).The maximum resolution achieved was Θ = 27.617°. Cell parameters were retrieved using the **SAINT** (Bruker, V8.34A, after 2013) software and refined using **SAINT** (Bruker, V8.34A, after 2013) on 9812 reflections, 9 % of the observed reflections. Data reduction was performed using the **SAINT** (Bruker, V8.34A, after 2013) software which corrects for Lorentz polarisation. The final completeness is 99.90 % out to 27.617° in Θ. A multi-scan absorption correction was performed using SADABS-2014/5 (Bruker, 2014) was used for absorption correction. wR_2(int) was 0.1361 before and 0.0534 after correction. The Ratio of minimum to maximum transmission is 0.6090. The λ/2 correction factor is 0.00150. The absorption coefficient μ of this material is 5.031 mm^{-1} at this wavelength (λ = 0.71073Å) and the minimum and maximum transmissions are 0.4541 and 0.7456. The structure was solved in the space group $P2_1/c$ (# 14) by Direct Methods using the **ShelXT** (Sheldrick, 2015) structure solution program and refined by Least Squares using version 2018/1 of **ShelXL** (Sheldrick, 2015). All non-hydrogen atoms were refined anisotropically, excepted minor disordered part. Hydrogen atom positions were calculated geometrically and refined using the riding model. Two DCM molecules and one phenyl group from main complex were found disordered over three or two positions respectively. Some SHELXL restraints (RIGU) were employed to maintain a reasonable model. For DCM molecules some rigid groups were employed with AFIX 6. For more detail, see res file incluse in cif file. SADABS-2014/5 (Bruker,2014) was used for absorption correction. wR_2(int) was 0.1361 before and 0.0534 after correction. The Ratio of minimum to maximum transmission is 0.6090. The λ/2 correction factor is 0.00150. The value of Z' is 2. This means that there are two independent molecules in the asymmetric unit.

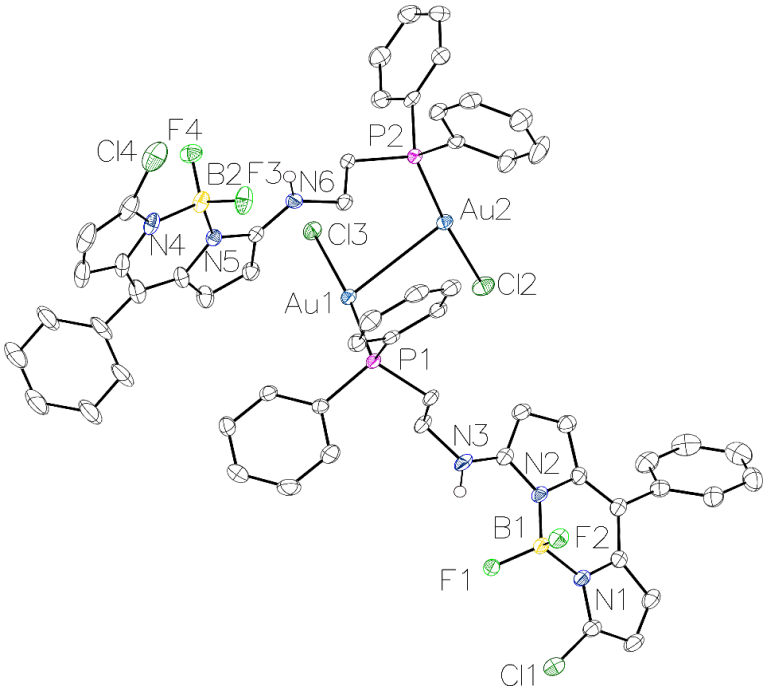

*Figure S 129: ORTEP view of **BODI-Au-7**. Thermal ellipsoids are draw at 50% probability plot. H-atoms on carbon atoms, disordered phenyl group and solvent are omitted for clarity.*

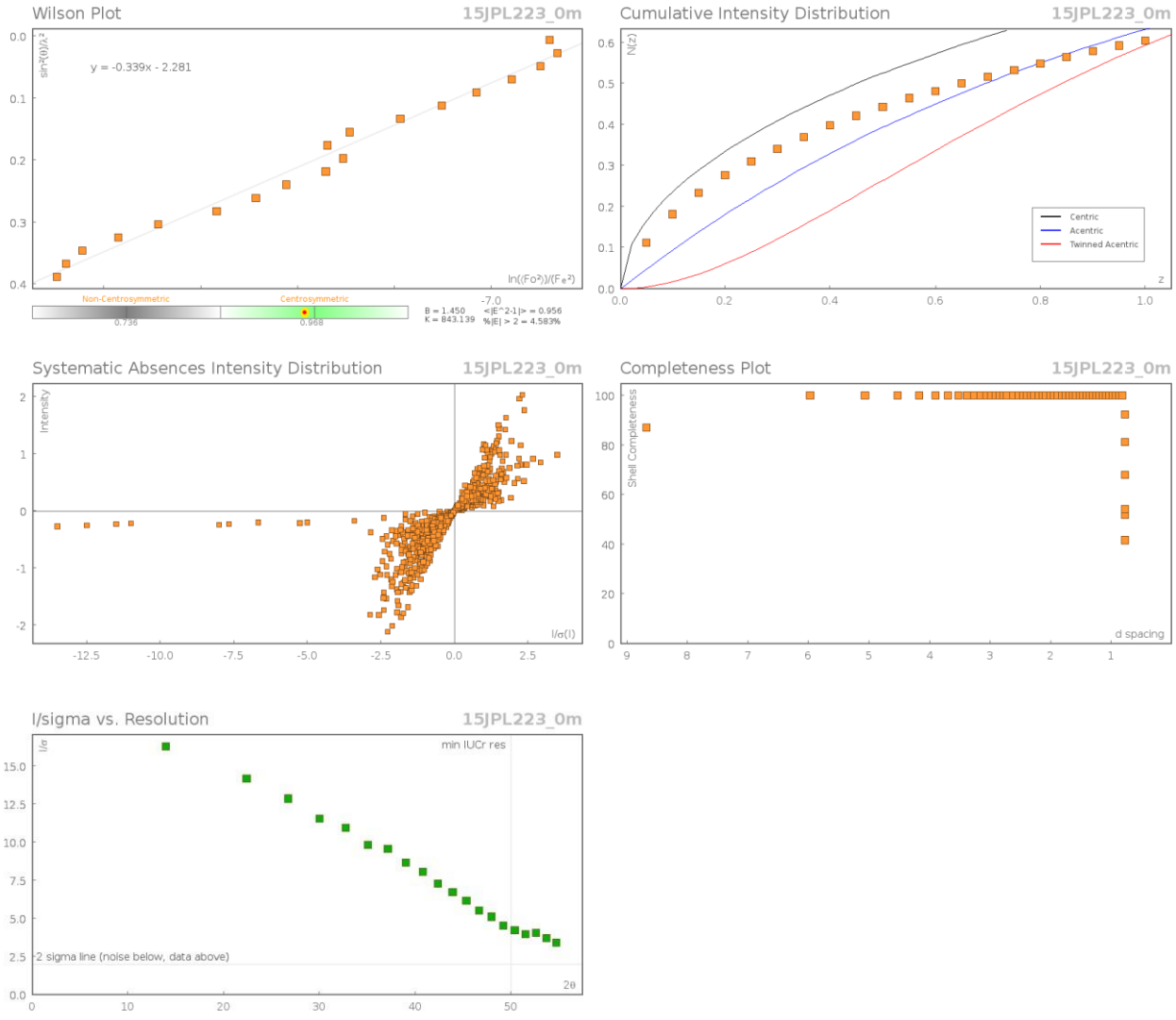

*Figure S 130: Data Plots: Diffraction Data of **BODI-Au-7** structure.*

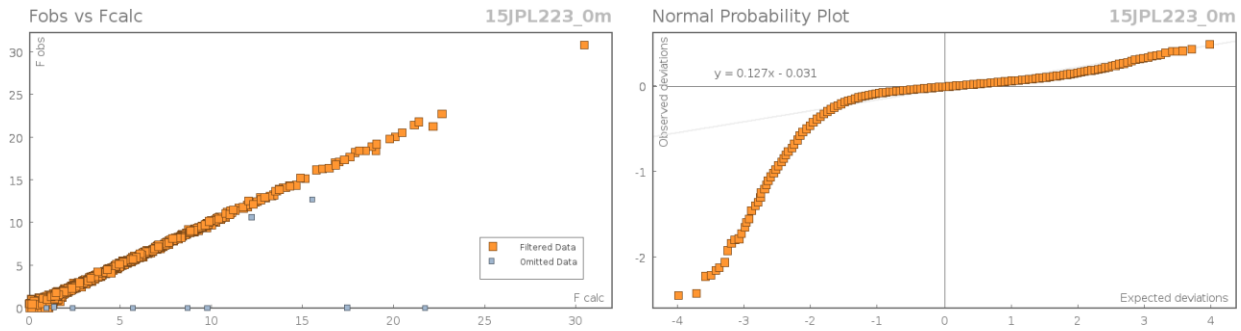

*Figure S 131: Data Plots: refinement and Data of **BODI-Au-7** structure.*

*Table S 24: reflection statistics of **BODI-Au-7** structure.*

Total reflections (after filtering)	114708	Unique reflections	14774
Completeness	0.996	Mean I/σ	22.91
hkl_{max} collected	(18, 39, 19)	hkl_{min} collected	(-18, -38, -18)
hkl_{max} used	(18, 39, 19)	hkl_{min} used	(-18, 0, 0)
Lim d_{max} collected	100.0	Lim d_{min} collected	0.36
d_{max} used	15.21	d_{min} used	0.77
Friedel pairs	24662	Friedel pairs merged	1
Inconsistent equivalents	0	R_{int}	0.0503
R_{sigma}	0.0323	Intensity transformed	0
Omitted reflections	0	Omitted by user (OMIT hkl)	103
Multiplicity	(19232, 17510, 10918, 5008, 1372, 135)	Maximum multiplicity	19
Removed systematic absences	1348	Filtered off (Shel/OMIT)	0

Table S 25: Fractional Atomic Coordinates ($x10^4$) and Equivalent Isotropic Displacement Parameters ($Å^2x10^3$) for **BODI-Au-7**. U_{eq} is defined as 1/3 of the trace of the orthogonalised U_{ij}.

Atom	**x**	**y**	**z**	U_{eq}
Au1	5318.7(2)	7043.3(2)	2545.8(2)	16.41(3)
Au2	6839.6(2)	7623.6(2)	3680.5(2)	18.48(3)
Cl1	3519.7(7)	4493.2(3)	7380.4(6)	29.94(19)
Cl2	7079.7(7)	6942.9(3)	4362.0(6)	34.1(2)
Cl3	6270.9(6)	7213.1(3)	1448.9(5)	24.13(17)
Cl4	1087.5(8)	9766.2(3)	452.2(7)	44.6(3)
P1	4221.9(6)	6914.0(3)	3484.8(5)	16.59(16)
P2	6720.8(6)	8309.6(3)	3111.1(5)	15.51(16)
F1	4196.7(14)	5056.8(6)	5869.6(12)	23.9(4)
F2	4471.7(14)	5554.1(6)	6985.8(12)	24.7(4)
F3	2258.1(16)	9108.9(7)	1695.6(12)	33.1(5)
F4	2947.4(14)	9104.9(6)	409.3(13)	27.8(4)

Atom	x	y	z	U_{eq}
N1	5251(2)	4839.4(8)	7153.1(16)	19.1(6)
N2	5755(2)	5391.0(8)	6098.3(17)	18.9(6)
N3	4933(2)	5807.1(9)	4971.5(17)	21.7(6)
N4	1291(2)	8884.8(10)	373.8(17)	23.7(6)
N5	2571.5(18)	8405.4(8)	1046.7(16)	17.3(5)
N6	3991.4(19)	8525.8(9)	1964.6(17)	19.4(6)
C1	4744(3)	4535.6(10)	7581(2)	22.4(7)
C2	5338(3)	4277.7(11)	8140(2)	27.6(8)
C3	6267(3)	4430.0(11)	8065(2)	25.0(7)
C4	6210(2)	4777.3(10)	7455(2)	19.6(7)
C5	6952(2)	5034.8(10)	7111(2)	19.5(7)
C6	7958(3)	4969.2(10)	7481(2)	23.7(7)
C7	8203(3)	4990.9(11)	8388(2)	27.7(8)
C8	9146(3)	4927.9(13)	8736(3)	35.5(9)
C9	9852(3)	4842.8(13)	8186(3)	39.8(10)
C10	9620(3)	4821.4(12)	7292(3)	38(1)
C11	8680(3)	4881.8(12)	6940(3)	31.6(8)
C12	6717(2)	5331.1(10)	6442(2)	20.8(7)
C13	7290(3)	5616.6(11)	5949(2)	23.3(7)
C14	6708(3)	5827.4(11)	5322(2)	23.5(7)
C15	5744(3)	5682.7(10)	5426(2)	20.2(7)
C16	4873(3)	6102.7(10)	4208(2)	21.1(7)
C17	4578(3)	6574.5(10)	4447.1(19)	19.9(7)
C18	3843(2)	7437.7(10)	3942(2)	18.6(7)
C19	4482(3)	7664.1(10)	4542(2)	21.4(7)
C20	4243(3)	8081.9(11)	4852(2)	26.1(8)
C21	3369(3)	8271.9(11)	4560(2)	28.5(8)
C22	2733(3)	8049.3(12)	3966(2)	30.5(8)
C23	2966(3)	7631.7(11)	3654(2)	24.1(7)
C24	3147(2)	6656.8(10)	2953(2)	18.0(6)
C25	2469(3)	6459.2(12)	3439(2)	31.1(8)
C26	1644(3)	6275.7(13)	3018(2)	34.2(9)
C27	1474(3)	6293.3(11)	2123(2)	27.2(8)
C28	2141(3)	6484.3(11)	1628(2)	26.2(8)
C29	2978(2)	6660.9(10)	2042(2)	21.6(7)
C30	7789(2)	8468.4(10)	2602(2)	17.9(6)

Atom	x	y	z	U_{eq}
C31	8069(3)	8203.4(11)	1919(2)	24.8(7)
C32	8897(3)	8306.9(12)	1538(2)	30.1(8)
C33	9450(3)	8669.4(12)	1835(2)	30.7(8)
C34	9171(3)	8934.5(12)	2502(2)	27.2(8)
C35	8338(2)	8835.5(11)	2884(2)	21.2(7)
C36	6557(2)	8731(1)	3933(2)	17.2(6)
C37	6771(3)	8629.9(12)	4814(2)	32.6(9)
C38	6655(4)	8949.5(13)	5446(2)	46.1(12)
C39	6321(3)	9369.9(12)	5208(2)	36.4(9)
C40	6106(3)	9473.2(11)	4337(2)	25.2(7)
C41	6218(2)	9155.7(10)	3703(2)	22.4(7)
C42	5750(2)	8405.6(10)	2243.1(19)	17.4(6)
C43	4768(2)	8369.5(11)	2596(2)	20.1(7)
C44	3378(2)	8257.4(10)	1518.4(19)	17.9(6)
C45	3435(2)	7781.1(11)	1432(2)	22.4(7)
C46	2645(3)	7651.9(12)	912(2)	26.8(8)
C47	2079(2)	8035.0(11)	674(2)	23.0(7)
C48	1210(3)	8079.6(13)	197(2)	29.6(8)
C49	793(2)	8508.0(13)	54(2)	28.0(8)
C50	-99(3)	8643.1(16)	-340(2)	38.4(10)
C51	-150(3)	9103.1(16)	-271(2)	41.7(11)
C52	708(3)	9239.7(13)	165(2)	33.0(9)
C53	749(3)	7712.6(13)	-260(3)	35.8(13)
C58	498(4)	7712.0(14)	-1163(3)	46.3(16)
C57	89(4)	7334.3(17)	-1571(2)	59(2)
C56	-70(4)	6957.3(14)	-1076(3)	56(2)
C55	180(4)	6957.8(13)	-174(3)	48.2(17)
C54	590(3)	7335.5(15)	234(2)	38.9(14)
C53A	584(6)	7635(2)	-17(4)	31(3)
C58A	286(6)	7548(2)	-895(4)	39(3)
C57A	-207(6)	7157(3)	-1127(4)	53(4)
C56A	-401(6)	6853(2)	-482(6)	63(4)
C55A	-103(6)	6939(2)	395(5)	51(3)
C54A	389(6)	7330(2)	628(4)	35(3)
B1	4873(3)	5209.4(11)	6512(2)	19.0(8)
B2	2279(3)	8897.3(13)	895(2)	21.3(8)

Atom	x	y	z	U_{eq}
Cl1D	3648.6(19)	5557.5(11)	8950(2)	39.3(9)
Cl2D	1634.2(19)	5736.1(13)	9214(3)	51.2(9)
C1D	2437(2)	5441(3)	8610(5)	38(3)
Cl1F	3569(3)	5527.4(17)	9393(4)	54.4(9)
Cl2F	1574(3)	5784.0(18)	8863(4)	54.4(9)
C1F	2627(7)	5536(9)	8543(6)	54.4(9)
Cl1A	8893.8(18)	6957.6(7)	1583(2)	59.9(7)
Cl2A	8752(2)	6096.2(6)	2469.8(18)	35.9(6)
C1A	8370(6)	6655.2(11)	2401(5)	45(2)
Cl1C	8611(11)	6116(3)	2677(9)	54.4(9)
Cl2C	8932(6)	7036(3)	2126(8)	54.4(9)
C1C	8106(11)	6647(5)	2480(30)	54.4(9)
Cl1E	1259(4)	3923.4(11)	7838(3)	44.0(16)
Cl2E	1251(3)	2964.9(10)	7457(3)	42.8(9)
C1E	1912(6)	3464.5(19)	7492(15)	47(5)
Cl1B	6182(3)	4447.6(15)	853(4)	31.1(11)
Cl2B	8217(3)	4385.0(17)	553(3)	51.1(12)
C1B	7369(3)	4382(8)	1332(3)	60(5)

*Table S 26: Anisotropic Displacement Parameters ($x10^4$) **BODI-Au-7**. The anisotropic displacement factor exponent takes the form: $-2\pi^2[h^2a^{*2} \times U_{11} + ... + 2hka^* \times b^* \times U_{12}]$*

Atom	U_{11}	U_{22}	U_{33}	U_{23}	U_{13}	U_{12}
Au1	20.80(6)	14.74(6)	13.65(6)	1.09(4)	1.54(4)	1.22(5)
Au2	22.54(7)	14.36(6)	18.08(6)	2.72(4)	-0.44(5)	0.22(5)
Cl1	33.0(5)	31.7(5)	25.7(4)	5.8(3)	5.9(4)	-4.2(4)
Cl2	45.4(6)	18.5(4)	36.7(5)	10.7(3)	-5.3(4)	0.6(4)
Cl3	25.4(4)	30.1(4)	17.6(4)	-0.8(3)	6.2(3)	-1.2(4)
Cl4	53.5(7)	38.9(5)	41.0(6)	10.1(4)	2.3(5)	25.6(5)
P1	23.7(4)	13.2(4)	12.8(4)	1.7(3)	1.4(3)	-0.2(3)
P2	16.1(4)	15.8(4)	14.4(4)	1.6(3)	0.8(3)	0.2(3)
F1	32.8(11)	20.1(9)	18.0(9)	1.7(7)	-2.0(8)	-5.0(8)
F2	36.5(12)	16.2(9)	21.9(10)	-2.0(7)	5.3(8)	5.3(8)
F3	45.4(13)	31.7(11)	20.9(10)	-5.7(8)	-3.9(9)	18.1(10)
F4	27.8(11)	22.7(10)	33.0(11)	6.2(8)	3.6(9)	2.7(9)
N1	28.7(16)	13.9(12)	14.8(13)	-0.3(10)	3.7(11)	-0.1(12)
N2	28.3(16)	12.9(12)	15.4(13)	1.7(10)	1.0(11)	0.9(11)

Atom	U_{11}	U_{22}	U_{33}	U_{23}	U_{13}	U_{12}
N3	30.0(16)	17.5(13)	17.9(14)	6.7(11)	3.9(12)	2.9(12)
N4	20.4(15)	35.0(16)	15.5(13)	4.4(12)	1.6(11)	10.3(13)
N5	15.9(14)	19.8(13)	16.1(13)	1.4(10)	1.3(10)	2.6(11)
N6	17.9(14)	16.2(13)	23.3(14)	4.7(11)	-2.0(11)	-0.7(11)
C1	31.3(19)	18.2(16)	18.4(16)	0.1(12)	5.6(14)	-1.0(14)
C2	42(2)	20.4(17)	21.3(17)	6.1(13)	4.9(16)	-0.5(16)
C3	36(2)	19.5(16)	19.7(17)	3.3(13)	1.3(15)	4.9(15)
C4	29.4(19)	12.8(14)	16.6(15)	-3.5(12)	1.4(13)	1.4(13)
C5	28.8(19)	13.4(14)	16.3(15)	-2.5(12)	2.0(13)	3.5(13)
C6	28.8(19)	15.5(15)	26.6(18)	1.5(13)	1.0(15)	1.0(14)
C7	32(2)	22.0(17)	28.2(19)	0.7(14)	-0.2(15)	3.8(15)
C8	36(2)	33(2)	35(2)	0.0(16)	-8.9(17)	2.6(18)
C9	30(2)	28(2)	60(3)	3.0(19)	-3(2)	4.8(17)
C10	35(2)	27(2)	54(3)	3.3(18)	15(2)	8.6(17)
C11	39(2)	24.3(18)	32(2)	3.6(15)	6.3(17)	6.6(17)
C12	29.2(19)	16.5(15)	16.3(15)	-3.1(12)	0.7(13)	0.5(14)
C13	28.3(19)	21.2(16)	20.8(17)	-0.4(13)	5.2(14)	-0.3(14)
C14	34(2)	18.5(16)	19.0(16)	1.1(13)	5.0(14)	-2.9(15)
C15	34(2)	10.8(14)	15.9(15)	-1.9(11)	3.0(14)	3.3(14)
C16	32.8(19)	16.7(15)	14.3(15)	3.3(12)	4.3(13)	4.7(14)
C17	30.8(19)	16.7(15)	12.4(15)	2.9(12)	2.4(13)	-0.5(14)
C18	28.4(18)	13.7(14)	14.7(15)	2.7(11)	6.6(13)	-1.4(13)
C19	26.8(18)	19.8(16)	18.0(16)	3.7(12)	4.6(13)	-1.3(14)
C20	42(2)	17.7(16)	19.8(17)	-1.4(13)	8.4(15)	-3.7(15)
C21	45(2)	15.2(16)	27.6(19)	1.6(14)	14.8(17)	3.4(16)
C22	37(2)	26.3(18)	29.3(19)	5.3(15)	7.3(16)	9.1(16)
C23	29.7(19)	20.9(16)	21.7(17)	1.2(13)	1.8(14)	-0.3(15)
C24	22.5(17)	13.0(14)	18.4(15)	1.1(12)	1.1(13)	-0.5(13)
C25	39(2)	37(2)	18.2(17)	-0.1(15)	7.8(15)	-9.4(18)
C26	37(2)	37(2)	31(2)	-1.6(16)	13.6(17)	-14.7(18)
C27	24.2(19)	23.6(17)	34(2)	-5.5(15)	1.3(15)	-4.3(15)
C28	32(2)	24.9(17)	20.2(17)	-2.8(13)	-3.4(14)	-3.6(15)
C29	28.2(19)	17.9(16)	19.0(16)	2.1(12)	3.4(14)	-3.4(14)
C30	20.3(17)	18.4(15)	15.3(15)	6.5(12)	3.0(12)	4.9(13)
C31	26.9(19)	23.8(17)	24.0(17)	1.2(14)	4.0(14)	-1.7(15)
C32	35(2)	33(2)	24.3(18)	-2.1(15)	10.4(16)	2.3(17)

Atom	U_{11}	U_{22}	U_{33}	U_{23}	U_{13}	U_{12}
C33	24.9(19)	38(2)	31(2)	7.0(16)	10.0(16)	-1.5(16)
C34	24.8(19)	26.4(18)	30.7(19)	4.3(15)	4.0(15)	-7.0(15)
C35	22.1(17)	19.8(16)	21.9(17)	1.3(13)	3.6(13)	2.9(14)
C36	16.3(16)	19.6(15)	16.6(15)	0.4(12)	6.2(12)	-1.8(13)
C37	55(3)	21.8(17)	20.9(18)	1.6(14)	0.4(17)	7.1(17)
C38	89(4)	32(2)	17.2(18)	0.3(15)	3(2)	8(2)
C39	59(3)	26.3(19)	24.9(19)	-5.9(15)	11.6(18)	-0.1(19)
C40	32(2)	15.3(16)	29.0(19)	1.1(13)	8.5(15)	1.2(14)
C41	28.8(19)	18.6(16)	19.9(16)	3.4(13)	3.4(14)	1.0(14)
C42	18.9(16)	17.8(15)	14.9(15)	3.2(12)	-1.0(12)	-1.4(13)
C43	18.5(17)	22.1(16)	19.2(16)	5.8(13)	-0.2(13)	0.6(13)
C44	20.6(17)	18.4(15)	14.6(15)	2.8(12)	1.5(12)	1.0(13)
C45	27.4(19)	19.0(16)	20.2(16)	0.8(13)	-0.8(14)	2.6(14)
C46	32(2)	25.1(18)	22.2(17)	-6.7(14)	-2.3(15)	4.0(16)
C47	22.4(18)	28.0(18)	17.8(16)	-7.1(13)	-1.7(13)	1.0(14)
C48	26(2)	40(2)	22.3(18)	-8.2(15)	-2.7(15)	1.5(16)
C49	19.9(18)	50(2)	14.1(16)	-1.0(15)	-1.1(13)	4.7(17)
C50	23(2)	72(3)	19.4(18)	4.1(18)	-3.4(15)	8(2)
C51	32(2)	65(3)	27(2)	14.2(19)	-0.2(17)	23(2)
C52	31(2)	45(2)	23.4(18)	9.9(16)	4.8(16)	17.8(18)
C53	15(3)	53.5(19)	38.6(18)	-20.0(14)	1.2(16)	-13.7(17)
C58	40(4)	58(2)	39.3(18)	-19.1(15)	-3.2(17)	-23(2)
C57	70(5)	63(2)	43.1(19)	-18.9(14)	-8.2(16)	-34(3)
C56	61(5)	61(2)	44.1(19)	-19.7(14)	-6.8(19)	-32(2)
C55	42(4)	57.4(19)	43.5(19)	-19.9(15)	-3.3(18)	-24.1(19)
C54	22(3)	54(2)	39.6(19)	-19.7(13)	0.2(15)	-16.7(18)
B1	30(2)	13.2(16)	13.9(17)	-0.1(13)	1.7(15)	-0.5(15)
B2	22(2)	25.4(19)	17.0(17)	1.2(14)	1.8(15)	10.1(16)
Cl1A	55.1(15)	62.3(15)	65.8(18)	6.5(12)	24.1(12)	2.7(11)
Cl2A	33.5(14)	46.6(12)	27.2(17)	-0.3(10)	0.9(11)	13.1(8)
C1A	33(5)	53(5)	50(5)	6(4)	13(4)	24(5)

*Table S 27: Bond Lengths in Å for **BODI-Au-7**.*

Atom	Atom	Length/Å
Au1	Au2	3.13975(19)

Atom	Atom	Length/Å
Au1	Cl3	2.2961(8)

Atom	Atom	Length/Å
Au1	P1	2.2330(8)
Au2	Cl2	2.3021(8)
Au2	P2	2.2344(8)
Cl1	C1	1.716(4)
Cl4	C52	1.710(4)
P1	C17	1.818(3)
P1	C18	1.819(3)
P1	C24	1.813(3)
P2	C30	1.813(3)
P2	C36	1.812(3)
P2	C42	1.828(3)
F1	B1	1.374(4)
F2	B1	1.410(4)
F3	B2	1.380(4)
F4	B2	1.396(4)
N1	C1	1.360(4)
N1	C4	1.389(4)
N1	B1	1.540(4)
N2	C12	1.408(4)
N2	C15	1.348(4)
N2	B1	1.539(5)
N3	C15	1.325(4)
N3	C16	1.461(4)
N4	C49	1.392(5)
N4	C52	1.361(4)
N4	B2	1.528(5)
N5	C44	1.354(4)
N5	C47	1.400(4)
N5	B2	1.543(4)
N6	C43	1.460(4)
N6	C44	1.318(4)
C1	C2	1.372(5)
C2	C3	1.393(5)
C3	C4	1.395(4)
C4	C5	1.433(5)
C5	C6	1.479(5)
C5	C12	1.371(4)
C6	C7	1.397(5)
C6	C11	1.389(5)
C7	C8	1.387(5)
C8	C9	1.381(6)
C9	C10	1.376(6)
C10	C11	1.384(6)
C12	C13	1.436(5)
C13	C14	1.353(5)
C14	C15	1.441(5)
C16	C17	1.528(4)
C18	C19	1.393(5)
C18	C23	1.392(5)
C19	C20	1.392(4)
C20	C21	1.383(5)
C21	C22	1.381(5)
C22	C23	1.390(5)
C24	C25	1.392(5)
C24	C29	1.389(4)
C25	C26	1.380(5)
C26	C27	1.367(5)
C27	C28	1.381(5)
C28	C29	1.383(5)
C30	C31	1.397(4)
C30	C35	1.388(5)
C31	C32	1.381(5)
C32	C33	1.385(5)
C33	C34	1.379(5)
C34	C35	1.384(5)
C36	C37	1.384(4)
C36	C41	1.393(4)
C37	C38	1.381(5)
C38	C39	1.382(5)
C39	C40	1.371(5)
C40	C41	1.379(4)
C42	C43	1.527(4)

Atom	Atom	Length/Å
C44	C45	1.438(4)
C45	C46	1.355(5)
C46	C47	1.423(5)
C47	C48	1.363(5)
C48	C49	1.419(5)
C48	C53	1.425(4)
C48	C53A	1.612(6)
C49	C50	1.393(5)
C50	C51	1.386(6)
C51	C52	1.378(6)
C53	C58	1.3900
C53	C54	1.3900
C58	C57	1.3900
C57	C56	1.3900
C56	C55	1.3900
C55	C54	1.3900
C53A	C58A	1.3900

Atom	Atom	Length/Å
C53A	C54A	1.3900
C58A	C57A	1.3900
C57A	C56A	1.3900
C56A	C55A	1.3900
C55A	C54A	1.3900
Cl1D	C1D	1.7598
Cl2D	C1D	1.7604
Cl1F	C1F	1.7598
Cl2F	C1F	1.7599
Cl1A	C1A	1.7599
Cl2A	C1A	1.7601
Cl1C	C1C	1.7578
Cl2C	C1C	1.7606
Cl1E	C1E	1.7614
Cl2E	C1E	1.7596
Cl1B	C1B	1.7608
Cl2B	C1B	1.7595

*Table S 28: Bond Angles in ° for **BODI-Au-7**.*

Atom	Atom	Atom	Angle/°
Cl3	Au1	Au2	82.53(2)
P1	Au1	Au2	102.29(2)
P1	Au1	Cl3	171.97(3)
Cl2	Au2	Au1	79.62(2)
P2	Au2	Au1	105.93(2)
P2	Au2	Cl2	174.45(3)
C17	P1	Au1	117.70(12)
C17	P1	C18	103.91(14)
C18	P1	Au1	109.88(10)
C24	P1	Au1	112.21(10)
C24	P1	C17	106.00(15)
C24	P1	C18	106.27(15)
C30	P2	Au2	112.06(10)

Atom	Atom	Atom	Angle/°
C30	P2	C42	103.48(14)
C36	P2	Au2	112.47(10)
C36	P2	C30	106.17(14)
C36	P2	C42	104.96(15)
C42	P2	Au2	116.74(10)
C1	N1	C4	106.4(3)
C1	N1	B1	128.7(3)
C4	N1	B1	124.7(3)
C12	N2	B1	125.2(3)
C15	N2	C12	108.0(3)
C15	N2	B1	126.2(3)
C15	N3	C16	124.8(3)
C49	N4	B2	126.9(3)

Atom	Atom	Atom	Angle/°
C52	N4	C49	106.5(3)
C52	N4	B2	126.5(3)
C44	N5	C47	108.0(3)
C44	N5	B2	126.1(3)
C47	N5	B2	125.8(3)
C44	N6	C43	123.5(3)
N1	C1	Cl1	121.4(2)
N1	C1	C2	111.4(3)
C2	C1	Cl1	127.2(3)
C1	C2	C3	106.1(3)
C2	C3	C4	107.8(3)
N1	C4	C3	108.2(3)
N1	C4	C5	121.1(3)
C3	C4	C5	130.5(3)
C4	C5	C6	119.0(3)
C12	C5	C4	119.5(3)
C12	C5	C6	121.5(3)
C7	C6	C5	120.4(3)
C11	C6	C5	121.2(3)
C11	C6	C7	118.4(3)
C8	C7	C6	120.5(4)
C9	C8	C7	120.2(4)
C10	C9	C8	119.9(4)
C9	C10	C11	120.3(4)
C10	C11	C6	120.8(4)
N2	C12	C13	106.9(3)
C5	C12	N2	120.9(3)
C5	C12	C13	132.2(3)
C14	C13	C12	108.7(3)
C13	C14	C15	106.7(3)
N2	C15	C14	109.6(3)
N3	C15	N2	122.0(3)
N3	C15	C14	128.4(3)
N3	C16	C17	111.6(2)
C16	C17	P1	112.6(2)

Atom	Atom	Atom	Angle/°
C19	C18	P1	118.8(3)
C23	C18	P1	121.3(2)
C23	C18	C19	119.6(3)
C20	C19	C18	120.2(3)
C21	C20	C19	119.7(3)
C22	C21	C20	120.4(3)
C21	C22	C23	120.2(3)
C22	C23	C18	119.8(3)
C25	C24	P1	121.4(2)
C29	C24	P1	119.9(2)
C29	C24	C25	118.7(3)
C26	C25	C24	120.1(3)
C27	C26	C25	120.6(3)
C26	C27	C28	120.1(3)
C27	C28	C29	119.8(3)
C28	C29	C24	120.6(3)
C31	C30	P2	118.2(3)
C35	C30	P2	122.0(2)
C35	C30	C31	119.8(3)
C32	C31	C30	119.6(3)
C31	C32	C33	120.2(3)
C34	C33	C32	120.4(3)
C33	C34	C35	119.8(3)
C34	C35	C30	120.2(3)
C37	C36	P2	119.4(2)
C37	C36	C41	118.9(3)
C41	C36	P2	121.7(2)
C38	C37	C36	119.9(3)
C37	C38	C39	120.6(4)
C40	C39	C38	119.9(3)
C39	C40	C41	119.8(3)
C40	C41	C36	120.9(3)
C43	C42	P2	111.3(2)
N6	C43	C42	112.4(3)
N5	C44	C45	109.1(3)

Atom	Atom	Atom	Angle/°
N6	C44	N5	122.9(3)
N6	C44	C45	128.0(3)
C46	C45	C44	106.8(3)
C45	C46	C47	108.7(3)
N5	C47	C46	107.3(3)
C48	C47	N5	121.3(3)
C48	C47	C46	131.4(3)
C47	C48	C49	120.2(3)
C47	C48	C53	121.7(4)
C47	C48	C53A	117.8(4)
C49	C48	C53	117.7(4)
C49	C48	C53A	120.7(4)
N4	C49	C48	119.8(3)
N4	C49	C50	108.2(3)
C50	C49	C48	131.9(4)
C51	C50	C49	107.9(4)
C52	C51	C50	106.5(3)
N4	C52	Cl4	119.8(3)
N4	C52	C51	110.8(4)
C51	C52	Cl4	129.3(3)
C58	C53	C48	123.1(3)
C58	C53	C54	120.0
C54	C53	C48	116.8(3)
C57	C58	C53	120.0
C58	C57	C56	120.0
C55	C56	C57	120.0
C56	C55	C54	120.0
C55	C54	C53	120.0
C58A	C53A	C48	117.2(4)
C58A	C53A	C54A	120.0
C54A	C53A	C48	122.7(4)
C53A	C58A	C57A	120.0
C56A	C57A	C58A	120.0
C55A	C56A	C57A	120.0
C56A	C55A	C54A	120.0
C55A	C54A	C53A	120.0
F1	B1	F2	109.3(3)
F1	B1	N1	112.6(3)
F1	B1	N2	110.5(3)
F2	B1	N1	109.3(3)
F2	B1	N2	109.0(3)
N2	B1	N1	106.0(3)
F3	B2	F4	109.8(3)
F3	B2	N4	112.2(3)
F3	B2	N5	109.6(3)
F4	B2	N4	110.6(3)
F4	B2	N5	108.9(3)
N4	B2	N5	105.6(3)
Cl1D	C1D	Cl2D	113.0
Cl1F	C1F	Cl2F	112.9
Cl1A	C1A	Cl2A	112.9
Cl1C	C1C	Cl2C	112.9
Cl2E	C1E	Cl1E	112.9
Cl2B	C1B	Cl1B	112.9

*Table S 29: Torsion Angles in ° for **BODI-Au-7**.*

Atom	Atom	Atom	Atom	Angle/°
Au1	P1	C17	C16	-61.6(3)
Au1	P1	C18	C19	-71.4(2)
Au1	P1	C18	C23	103.5(3)
Au1	P1	C24	C25	165.6(3)

Atom	Atom	Atom	Atom	Angle/°
Au1	P1	C24	C29	-15.5(3)
Au2	P2	C30	C31	58.5(3)
Au2	P2	C30	C35	-119.9(2)
Au2	P2	C36	C37	17.1(3)
Au2	P2	C36	C41	-162.8(2)
Au2	P2	C42	C43	66.6(2)
Cl1	C1	C2	C3	178.6(3)
P1	C18	C19	C20	175.0(2)
P1	C18	C23	C22	-174.8(3)
P1	C24	C25	C26	178.4(3)
P1	C24	C29	C28	-177.0(3)
P2	C30	C31	C32	-177.8(3)
P2	C30	C35	C34	177.3(3)
P2	C36	C37	C38	179.5(3)
P2	C36	C41	C40	-179.4(3)
P2	C42	C43	N6	169.2(2)
N1	C1	C2	C3	0.5(4)
N1	C4	C5	C6	177.4(3)
N1	C4	C5	C12	-3.5(4)
N2	C12	C13	C14	-1.8(4)
N3	C16	C17	P1	-166.4(2)
N4	C49	C50	C51	0.5(4)
N5	C44	C45	C46	-0.7(4)
N5	C47	C48	C49	1.2(5)
N5	C47	C48	C53	173.5(4)
N5	C47	C48	C53A	-166.2(4)
N6	C44	C45	C46	-179.9(3)
C1	N1	C4	C3	0.3(3)
C1	N1	C4	C5	177.7(3)
C1	N1	B1	F1	-48.6(4)
C1	N1	B1	F2	73.1(4)
C1	N1	B1	N2	-169.5(3)
C1	C2	C3	C4	-0.3(4)
C2	C3	C4	N1	0.0(4)
C2	C3	C4	C5	-177.1(3)

Atom	Atom	Atom	Atom	Angle/°
C3	C4	C5	C6	-5.8(5)
C3	C4	C5	C12	173.3(3)
C4	N1	C1	Cl1	-178.8(2)
C4	N1	C1	C2	-0.5(4)
C4	N1	B1	F1	136.4(3)
C4	N1	B1	F2	-101.9(3)
C4	N1	B1	N2	15.5(4)
C4	C5	C6	C7	-51.8(4)
C4	C5	C6	C11	127.7(3)
C4	C5	C12	N2	1.1(4)
C4	C5	C12	C13	-177.2(3)
C5	C6	C7	C8	179.8(3)
C5	C6	C11	C10	179.9(3)
C5	C12	C13	C14	176.7(3)
C6	C5	C12	N2	-179.8(3)
C6	C5	C12	C13	1.9(5)
C6	C7	C8	C9	0.0(5)
C7	C6	C11	C10	-0.6(5)
C7	C8	C9	C10	0.2(6)
C8	C9	C10	C11	-0.5(6)
C9	C10	C11	C6	0.7(6)
C11	C6	C7	C8	0.2(5)
C12	N2	C15	N3	-179.8(3)
C12	N2	C15	C14	-0.9(3)
C12	N2	B1	F1	-140.4(3)
C12	N2	B1	F2	99.5(3)
C12	N2	B1	N1	-18.1(4)
C12	C5	C6	C7	129.1(3)
C12	C5	C6	C11	-51.4(4)
C12	C13	C14	C15	1.2(4)
C13	C14	C15	N2	-0.2(4)
C13	C14	C15	N3	178.6(3)
C15	N2	C12	C5	-177.0(3)
C15	N2	C12	C13	1.6(3)
C15	N2	B1	F1	49.5(4)

Atom	Atom	Atom	Atom	Angle/°
C15	N2	B1	F2	-70.6(4)
C15	N2	B1	N1	171.8(3)
C15	N3	C16	C17	-102.3(4)
C16	N3	C15	N2	-176.6(3)
C16	N3	C15	C14	4.7(5)
C17	P1	C18	C19	55.4(3)
C17	P1	C18	C23	-129.8(3)
C17	P1	C24	C25	35.8(3)
C17	P1	C24	C29	-145.3(3)
C18	P1	C17	C16	176.7(2)
C18	P1	C24	C25	-74.3(3)
C18	P1	C24	C29	104.6(3)
C18	C19	C20	C21	-0.1(5)
C19	C18	C23	C22	0.0(5)
C19	C20	C21	C22	0.1(5)
C20	C21	C22	C23	-0.1(5)
C21	C22	C23	C18	0.0(5)
C23	C18	C19	C20	0.1(5)
C24	P1	C17	C16	64.9(3)
C24	P1	C18	C19	167.0(2)
C24	P1	C18	C23	-18.2(3)
C24	C25	C26	C27	-1.3(6)
C25	C24	C29	C28	1.9(5)
C25	C26	C27	C28	1.9(6)
C26	C27	C28	C29	-0.6(5)
C27	C28	C29	C24	-1.4(5)
C29	C24	C25	C26	-0.6(5)
C30	P2	C36	C37	-105.8(3)
C30	P2	C36	C41	74.3(3)
C30	P2	C42	C43	-169.8(2)
C30	C31	C32	C33	0.4(5)
C31	C30	C35	C34	-1.2(5)
C31	C32	C33	C34	-1.1(6)
C32	C33	C34	C35	0.6(5)
C33	C34	C35	C30	0.5(5)

Atom	Atom	Atom	Atom	Angle/°
C35	C30	C31	C32	0.7(5)
C36	P2	C30	C31	-178.3(2)
C36	P2	C30	C35	3.2(3)
C36	P2	C42	C43	-58.7(2)
C36	C37	C38	C39	0.4(7)
C37	C36	C41	C40	0.7(5)
C37	C38	C39	C40	-0.3(7)
C38	C39	C40	C41	0.4(6)
C39	C40	C41	C36	-0.6(5)
C41	C36	C37	C38	-0.6(6)
C42	P2	C30	C31	-68.1(3)
C42	P2	C30	C35	113.4(3)
C42	P2	C36	C37	145.0(3)
C42	P2	C36	C41	-34.9(3)
C43	N6	C44	N5	168.8(3)
C43	N6	C44	C45	-12.0(5)
C44	N5	C47	C46	-2.3(4)
C44	N5	C47	C48	176.6(3)
C44	N5	B2	F3	-55.5(4)
C44	N5	B2	F4	64.5(4)
C44	N5	B2	N4	-176.6(3)
C44	N6	C43	C42	106.1(3)
C44	C45	C46	C47	-0.8(4)
C45	C46	C47	N5	1.9(4)
C45	C46	C47	C48	-176.9(4)
C46	C47	C48	C49	179.8(4)
C46	C47	C48	C53	-7.9(7)
C46	C47	C48	C53A	12.4(6)
C47	N5	C44	N6	-178.8(3)
C47	N5	C44	C45	1.9(3)
C47	N5	B2	F3	128.8(3)
C47	N5	B2	F4	-111.2(3)
C47	N5	B2	N4	7.7(4)
C47	C48	C49	N4	2.5(5)
C47	C48	C49	C50	-174.3(4)

Atom	Atom	Atom	Atom	Angle/°
C47	C48	C53	C58	-121.3(4)
C47	C48	C53	C54	55.8(5)
C47	C48	C53A	C58A	-125.2(5)
C47	C48	C53A	C54A	50.9(6)
C48	C49	C50	C51	177.6(4)
C48	C53	C58	C57	177.1(5)
C48	C53	C54	C55	-177.3(4)
C48	C53A	C58A	C57A	176.2(7)
C48	C53A	C54A	C55A	-176.0(7)
C49	N4	C52	Cl4	-179.7(2)
C49	N4	C52	C51	0.5(4)
C49	N4	B2	F3	-123.1(3)
C49	N4	B2	F4	113.9(3)
C49	N4	B2	N5	-3.8(4)
C49	C48	C53	C58	51.1(5)
C49	C48	C53	C54	-131.7(3)
C49	C48	C53A	C58A	67.4(6)
C49	C48	C53A	C54A	-116.5(5)
C49	C50	C51	C52	-0.2(4)
C50	C51	C52	Cl4	180.0(3)
C50	C51	C52	N4	-0.2(4)
C52	N4	C49	C48	-178.1(3)
C52	N4	C49	C50	-0.6(4)
C52	N4	B2	F3	53.7(4)
C52	N4	B2	F4	-69.3(4)
C52	N4	B2	N5	173.0(3)
C53	C48	C49	N4	-170.0(4)
C53	C48	C49	C50	13.1(6)
C53	C58	C57	C56	0.0
C58	C53	C54	C55	0.0
C58	C57	C56	C55	0.0
C57	C56	C55	C54	0.0
C56	C55	C54	C53	0.0
C54	C53	C58	C57	0.0
C53A	C48	C49	N4	169.5(4)

Atom	Atom	Atom	Atom	Angle/°
C53A	C48	C49	C50	-7.3(6)
C53A	C58A	C57A	C56A	0.0
C58A	C53A	C54A	C55A	0.0
C58A	C57A	C56A	C55A	0.0
C57A	C56A	C55A	C54A	0.0
C56A	C55A	C54A	C53A	0.0
C54A	C53A	C58A	C57A	0.0
B1	N1	C1	Cl1	5.6(4)
B1	N1	C1	C2	-176.2(3)
B1	N1	C4	C3	176.2(3)
B1	N1	C4	C5	-6.4(4)
B1	N2	C12	C5	11.4(5)
B1	N2	C12	C13	-170.0(3)
B1	N2	C15	N3	-8.3(5)
B1	N2	C15	C14	170.6(3)
B2	N4	C49	C48	-0.7(5)
B2	N4	C49	C50	176.8(3)
B2	N4	C52	Cl4	3.0(5)
B2	N4	C52	C51	-176.9(3)
B2	N5	C44	N6	4.8(5)
B2	N5	C44	C45	-174.5(3)
B2	N5	C47	C46	174.0(3)
B2	N5	C47	C48	-7.0(5)

Table S30: Hydrogen Fractional Atomic Coordinates (x10^4) and Equivalent Isotropic Displacement Parameters (Å^{2}x10^3) for ***BODI-Au-7***. U_{eq} is defined as 1/3 of the trace of the orthogonalised U_{ij}.

Atom	x	y	z	U_{eq}
H3	4392.27	5704.04	5141.68	26
H6	3929.44	8814.67	1877.08	23
H2	5152.67	4042.56	8504.17	33
H3A	6837.57	4317.54	8374.07	30
H7	7719.83	5049.13	8769.6	33
H8	9305.67	4943.42	9353.39	43
H9	10497.18	4799.03	8425.47	48
H10	10107	4765.01	6913.46	46
H11	8526.02	4863.26	6322.28	38
H13	7966.98	5651.7	6046.5	28
H14	6898.34	6031.43	4896.15	28
H16A	4397.93	5982.12	3746.57	25
H16B	5504.28	6113.13	3967.07	25
H17A	5122.8	6720.26	4797.21	24
H17B	4036.52	6557.1	4817.9	24
H19	5081.67	7532.89	4739.87	26
H20	4677.58	8235.88	5261.59	31
H21	3205.61	8557.38	4769.91	34
H22	2134.08	8181.97	3769.42	37
H23	2527.42	7479.15	3245.44	29
H25	2573.75	6450.73	4062.83	37
H26	1191.55	6135.88	3353.56	41
H27	895.02	6174.07	1840.53	33
H28	2025.51	6494.22	1005.37	31
H29	3443.28	6786.37	1700.33	26
H31	7692.19	7953.64	1718.27	30
H32	9088.39	8128.83	1071.47	36
H33	10024.96	8735.66	1576.86	37
H34	9549	9184.43	2699.6	33
H35	8142.6	9019.33	3340.95	25
H37	6996.48	8341.06	4984.14	39
H38	6806.48	8879.71	6049.59	55
H39	6240.07	9587.22	5646.92	44

Atom	x	y	z	U_{eq}
H40	5879.67	9762.63	4171.56	30
H41	6062.26	9227.6	3100.45	27
H42A	5821.56	8705.97	1989.02	21
H42B	5793.37	8183.85	1768.67	21
H43A	4648.68	8054.6	2746.28	24
H43B	4772.14	8547.32	3142.48	24
H45	3930.44	7593.19	1690.54	27
H46	2493.46	7354.61	734.69	32
H50	-585.44	8453.55	-608.99	46
H51	-673.66	9287.77	-483.28	50
H58	606.8	7969.71	-1500.69	56
H57	-82.25	7333.92	-2187.8	71
H56	-349.85	6699.14	-1355.36	67
H55	71.6	6700.13	164.18	58
H54	760.64	7335.92	851.31	47
H58A	419.11	7756.58	-1335.75	47
H57A	-410.29	7097.95	-1727.21	63
H56A	-738.11	6585.16	-641.3	76
H55A	-236.52	6731	836.09	61
H54A	592.88	7389.63	1227.57	42
H1DA	2323.5	5117.26	8673.05	45
H1DB	2305.85	5517.32	7979.51	45
H1FA	2480.87	5226.66	8348.83	65
H1FB	2838.36	5702.15	8036.09	65
H1AA	7662.83	6662.84	2274.3	54
H1AB	8533.8	6801.35	2976.78	54
H1CA	7858.25	6758.35	3021.57	65
H1CB	7555.56	6622.04	2021.08	65
H1EA	2110.06	3526.91	6898.9	56
H1EB	2501.58	3426.85	7897.8	56
H1BA	7520.88	4625.6	1759.19	73
H1BB	7419.47	4096.48	1658.68	73

*Table S 31: Hydrogen Bond information for **BODI-Au-7**.*

D	H	A	d(D-H)/Å	d(H-A)/Å	d(D-A)/Å	D-H-A/deg
N3	H3	F4[1]	0.88	2.18	2.932(4)	143.5
N6	H6	F2[2]	0.88	2.04	2.841(3)	150.6

[1]+x,3/2-y,1/2+z; [2]+x,3/2-y,-1/2+z

*Table S 32: Atomic Occupancies for all atoms that are not fully occupied in **BODI-Au-7**.*

Atom	Occupancy	Atom	Occupancy
C53	0.612(7)	Cl2F	0.262(3)
C58	0.612(7)	C1F	0.262(3)
H58	0.612(7)	H1FA	0.262(3)
C57	0.612(7)	H1FB	0.262(3)
H57	0.612(7)	Cl1A	0.547(3)
C56	0.612(7)	Cl2A	0.547(3)
H56	0.612(7)	C1A	0.547(3)
C55	0.612(7)	H1AA	0.547(3)
H55	0.612(7)	H1AB	0.547(3)
C54	0.612(7)	Cl1C	0.165(3)
H54	0.612(7)	Cl2C	0.165(3)
C53A	0.388(7)	C1C	0.165(3)
C58A	0.388(7)	H1CA	0.165(3)
H58A	0.388(7)	H1CB	0.165(3)
C57A	0.388(7)	Cl1E	0.307(2)
H57A	0.388(7)	Cl2E	0.307(2)
C56A	0.388(7)	C1E	0.307(2)
H56A	0.388(7)	H1EA	0.307(2)
C55A	0.388(7)	H1EB	0.307(2)
H55A	0.388(7)	Cl1B	0.288(2)
C54A	0.388(7)	Cl2B	0.288(2)
H54A	0.388(7)	C1B	0.288(2)
Cl1D	0.430(3)	H1BA	0.288(2)
Cl2D	0.430(3)	H1BB	0.288(2)
C1D	0.430(3)		
H1DA	0.430(3)		
H1DB	0.430(3)		
Cl1F	0.262(3)		

Submitted by: **Jacques Pliquett**

Solved by: **Yoann Rousselin**

SampleID: **17jpl382**

Crystal Data and Experimental

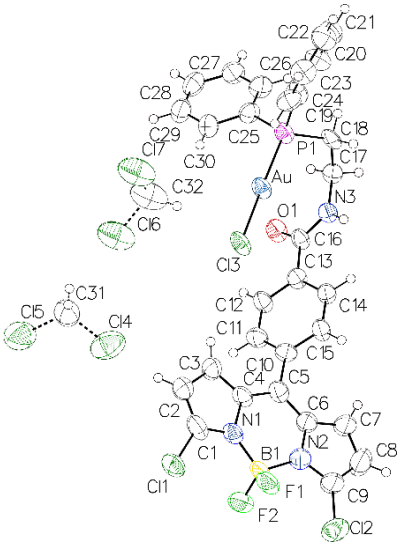

Experimental. Single clear light pink plate-shaped crystals of (**BODI-Au-10**) were recrystallised from DCM by slow evaporation. A suitable crystal (0.51x0.13x0.05) mm³ was selected and mounted on a MITIGEN holder oil on a Nonius Kappa Apex II diffractometer. The crystal was kept at T = 115(1) K during data collection. Using **Olex2** (Dolomanov et al., 2009), the structure was solved with the **ShelXT** (Sheldrick, 2015) structure solution program, using the Intrinsic Phasing solution method. The model was refined with version 2018/1 of **ShelXL** (Sheldrick, 2015) using Least Squares minimisation.

Crystal Data. $C_{127}H_{106}Au_4B_4Cl_{26}F_8N_{12}O_4P_4$, M_r = 3892.92, orthorhombic, Pbca (No. 61), a = 25.643(4) Å, b = 9.4006(16) Å, c = 30.308(5) Å, $\alpha = \beta = \gamma = 90^\circ$, V = 7306(2) Å^3, T = 115(1) K, Z = 2, Z' = 0.25, μ(MoK$_\alpha$) = 4.588, 151102 reflections measured, 6424 unique (R_{int} = 0.0918) which were used in all calculations. The final wR_2 was 0.1979 (all data) and R_1 was 0.0732 (I > 2(I)).

*Table S33: X-ray structure data of **BODI-Au-10**.*

Compound	**BODI-Au-10**
CCDC	**1825952**
Formula	$C_{127}H_{106}Au_4B_4Cl_{26}F_8N_{12}O_4P_4$
$D_{calc.}$/ g cm^{-3}	1.770
μ/mm^{-1}	4.588
Formula Weight	3892.92
Colour	clear light pink
Shape	plate
Size/mm³	0.51x0.13x0.05
T/K	115(1)
Crystal System	orthorhombic
Space Group	Pbca
a/Å	25.643(4)
b/Å	9.4006(16)
c/Å	30.308(5)
α/°	90
β/°	90
γ/°	90
V/Å³	7306(2)
Z	2
Z'	0.25
Wavelength/Å	0.71073
Radiation type	MoK$_\alpha$
Θ_{min}/°	2.671
Θ_{max}/°	25.000
Measured Refl.	151102
Independent Refl.	6424
Reflections Used	4993
R_{int}	0.0918
Parameters	415
Restraints	0
Largest Peak	2.462
Deepest Hole	-2.994
GooF	1.168
wR_2 (all data)	0.1979
wR_2	0.1845
R_1 (all data)	0.0907
R_1	0.0732

Table S 34: ***BODI-Au-10*** *structure Quality Indicators.*

Reflections:	d min (Mo) 0.84	I/σ 20.4	Rint 9.18%	complete 100%
Refinement:	Shift -0.001	Max Peak 2.5	Min Peak -3.0	GooF 1.168

A clear light pink plate-shaped crystal with dimensions 0.51x0.13x0.05 mm^3 was mounted on a MITIGEN holder oil. X-ray diffraction data were collected using a Nonius Kappa Apex II diffractometer equipped with a Oxford Cryosystems low-temperature device, operating at T = 115(1) K. Data were measured using ϕ and ω scans of 0.6° per frame for 120s using MoK_α radiation (X-ray tube, 50 kV, 32 mA). The total number of runs and images was based on the strategy calculation from the program APEX3 (Bruker, 2015).The maximum resolution achieved was Θ = 25.000°. Cell parameters were retrieved using the **SAINT** (Bruker, V8.38A, after 2013) software and refined using **SAINT** (Bruker, V8.38A, after 2013) on 9817 reflections, 6 % of the observed reflections. Data reduction was performed using the **SAINT** (Bruker, V8.38A, after 2013) software which corrects for Lorentz polarisation. The final completeness is 99.90 % out to 25.000° in Θ. A multi-scan absorption correction was performed using SADABS-2016/2 (Bruker,2016/2) was used for absorption correction. wR_2(int) was 0.1173 before and 0.0831 after correction. The Ratio of minimum to maximum transmission is 0.1990. The λ/2 correction factor is Not present. The absorption coefficient μ of this material is 4.588 mm^{-1} at this wavelength (λ = 0.71073Å) and the minimum and maximum transmissions are 0.0041 and 0.0206. The structure was solved in the space group *P*bca (# 61) by Intrinsic Phasing using the **ShelXT** (Sheldrick, 2015) structure solution program and refined by Least Squares using version 2018/1 of **ShelXL** (Sheldrick, 2015). All non-hydrogen atoms were refined anisotropically. Hydrogen atom positions were calculated geometrically and refined using the riding model. SADABS-2016/2 (Bruker, 2016/2) was used for absorption correction. wR_2(int) was 0.1173 before and 0.0831 after correction. The Ratio of minimum to maximum transmission is 0.1990. The value of Z' is 0.25.

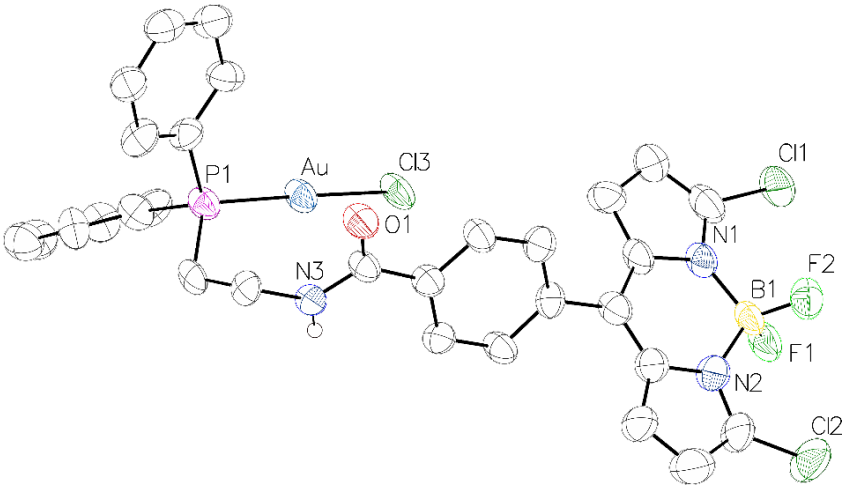

Figure S 132: ORTEP view of ***BODI-Au-10****. Thermal ellipsoids are draw at 50% probability level. Solvent molecules and H-atoms on carbon atom are omitted for clarity.*

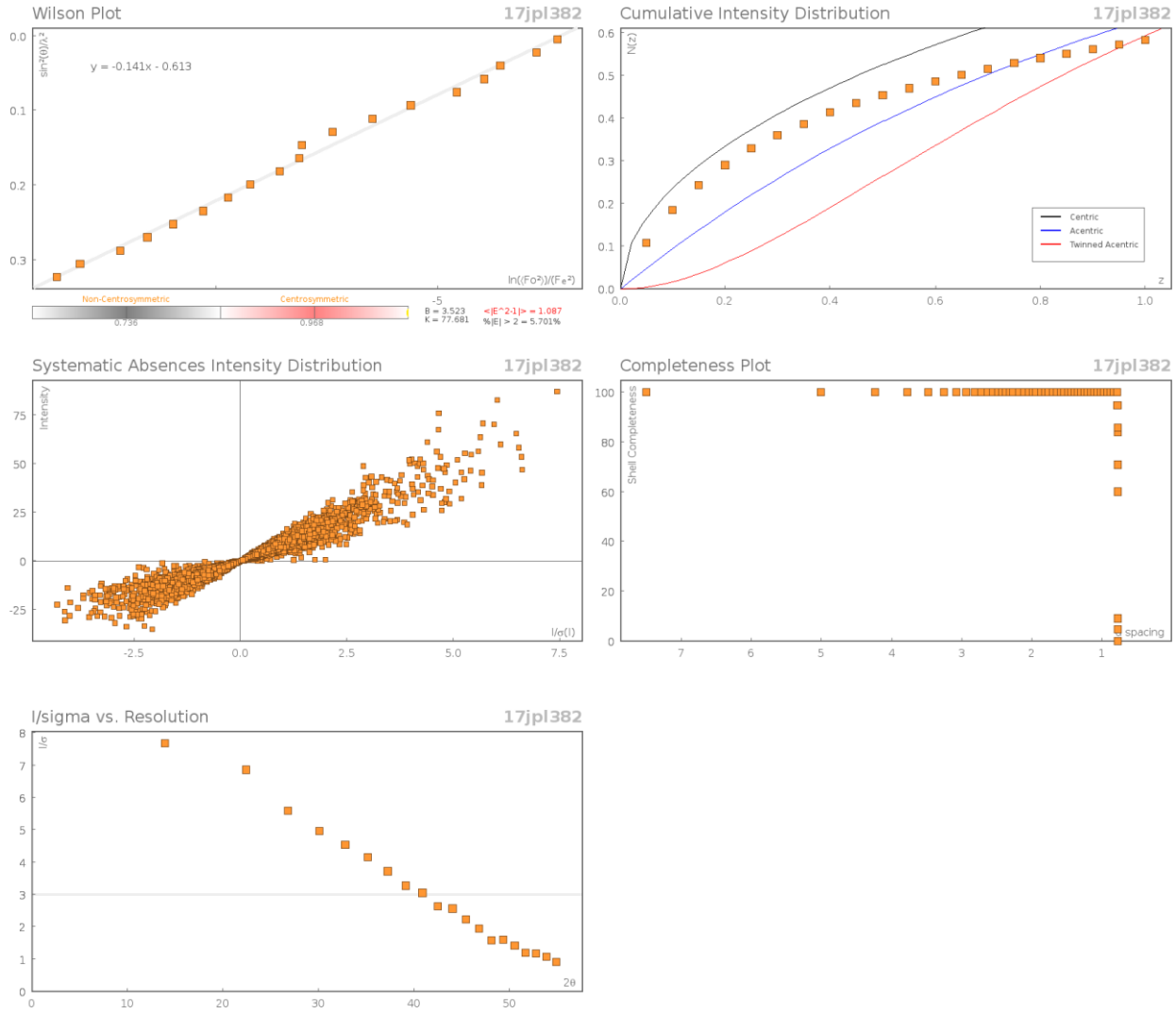

*Figure S 133: Data Plots: Diffraction Data of **BODI-Au-10** structure.*

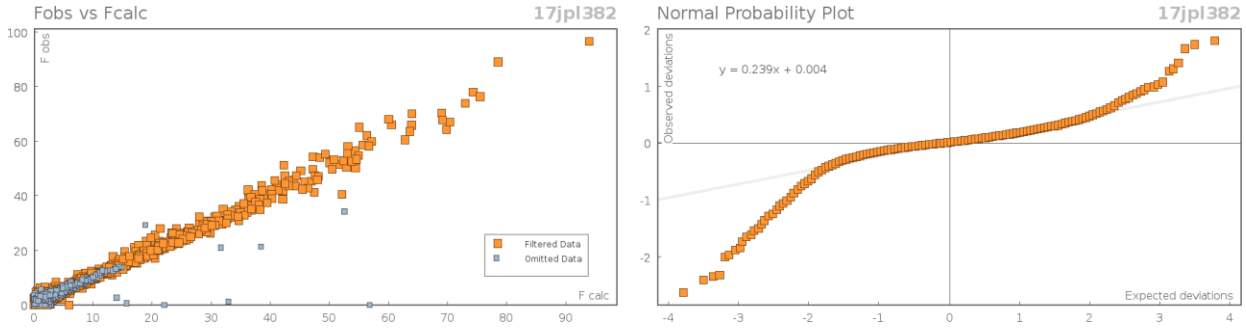

*Figure S 134: Data Plots: refinement and Data of **BODI-Au-10** structure.*

*Table S 35: reflection statistics of **BODI-Au-10** structure.*

Total reflections (after filtering)	161317	Unique reflections	6424
Completeness	0.999	Mean I/σ	20.37
hkl_{max} collected	(33, 10, 39)	hkl_{min} collected	(-33, -12, -39)
hkl_{max} used	(30, 11, 36)	hkl_{min} used	(0, 0, 0)
Lim d_{max} collected	100.0	Lim d_{min} collected	0.84

d_{max} used	25.64	d_{min} used	0.84
Friedel pairs	25777	Friedel pairs merged	1
Inconsistent equivalents	0	R_{int}	0.0918
R_{sigma}	0.0282	Intensity transformed	0
Omitted reflections	0	Omitted by user (OMIT hkl)	44
Multiplicity	(6368, 12582, 14535, 15028, 9624, 763, 216, 127, 54, 23, 78)	Maximum multiplicity	41
Removed systematic absences	10171	Filtered off (Shel/OMIT)	30732

Table S 36: Fractional Atomic Coordinates ($x10^4$) and Equivalent Isotropic Displacement Parameters ($Å^2x10^3$) for ***BODI-Au-10****. U_{eq} is defined as 1/3 of the trace of the orthogonalised U_{ij}.*

Atom	**x**	**y**	**z**	U_{eq}
Au	6446.1(2)	3749.6(5)	2959.0(2)	46.59(19)
Cl1	7750.5(16)	2732(4)	6052.1(10)	72.2(10)
Cl2	9581(2)	6483(6)	5602.5(13)	104.4(18)
Cl3	6526.8(15)	3833(3)	3712.2(9)	56.6(8)
P1	6343.1(13)	3786(3)	2226(1)	44.8(7)
F1	8431(3)	5431(8)	5789(2)	62(2)
F2	8942(3)	3478(8)	5689(2)	63(2)
O1	7799(4)	2016(9)	2558(3)	56(2)
N1	8141(4)	3627(11)	5285(3)	50(2)
N2	8881(5)	5202(12)	5092(3)	57(3)
N3	7583(4)	4313(10)	2452(3)	43(2)
C1	7749(6)	2941(15)	5493(4)	65(4)
C2	7382(6)	2398(17)	5202(4)	70(4)
C3	7547(6)	2799(15)	4785(4)	61(4)
C4	8008(5)	3567(13)	4839(4)	52(3)
C5	8331(5)	4207(13)	4520(4)	49(3)
C6	8751(5)	5020(14)	4650(4)	53(3)
C7	9135(6)	5768(18)	4402(4)	75(5)
C8	9475(8)	6380(20)	4685(6)	97(6)
C9	9317(7)	6004(19)	5114(4)	78(5)
C10	8197(5)	4014(13)	4047(4)	45(3)
C11	8135(5)	2639(14)	3877(4)	53(3)
C12	8010(5)	2440(13)	3447(4)	49(3)
C13	7925(5)	3580(12)	3163(4)	45(3)
C14	8001(5)	4962(12)	3326(4)	43(3)
C15	8135(5)	5176(13)	3762(4)	49(3)

Atom	x	y	z	U_{eq}
C16	7774(5)	3258(12)	2700(3)	42(3)
C17	7412(5)	4096(13)	2003(3)	43(3)
C18	6860(5)	4659(13)	1920(3)	45(3)
C19	5772(5)	4867(14)	2076(4)	52(3)
C20	5684(6)	5252(16)	1645(4)	61(3)
C21	5284(6)	6176(16)	1540(5)	64(4)
C22	4976(6)	6750(16)	1861(5)	66(4)
C23	5069(6)	6369(16)	2291(5)	65(4)
C24	5466(5)	5421(15)	2408(5)	58(3)
C25	6286(5)	2030(13)	1974(4)	49(3)
C26	6361(5)	1775(16)	1536(4)	56(3)
C27	6321(5)	436(15)	1359(4)	58(3)
C28	6197(5)	-697(15)	1626(5)	59(3)
C29	6130(6)	-507(16)	2067(5)	66(4)
C30	6175(5)	864(14)	2255(5)	54(3)
B1	8601(6)	4442(15)	5487(4)	50(3)
Cl4	4955.9(19)	4177(6)	6407.3(17)	111.2(18)
Cl5	4405(2)	1605(5)	6695(2)	121(2)
C31	4380(3)	3167(11)	6375(5)	95(6)
Cl6	4435(3)	3478(9)	5192(3)	119.2(18)
Cl7	3523(3)	5185(9)	4941(3)	119.2(18)
C32	4163(5)	4670(30)	4806(5)	119.2(18)

Table S 37: Anisotropic Displacement Parameters (x10⁴) ***BODI-Au-10****. The anisotropic displacement factor exponent takes the form: $-2\pi^2[h^2a^{*2} \times U_{11} + \ldots + 2hka^* \times b^* \times U_{12}]$.*

Atom	U_{11}	U_{22}	U_{33}	U_{23}	U_{13}	U_{12}
Au	64.1(3)	43.4(3)	32.3(3)	2.90(19)	5.58(19)	1.6(2)
Cl1	99(3)	83(3)	34.5(15)	10.1(16)	2.1(16)	-15(2)
Cl2	122(4)	142(4)	49(2)	-5(2)	-14(2)	-65(3)
Cl3	99(2)	40.5(16)	30.6(14)	4.5(12)	5.6(14)	4.0(16)
P1	59.8(18)	39.6(16)	34.9(15)	2.4(13)	3.6(13)	2.5(15)
F1	93(5)	61(5)	33(4)	7(3)	-1(3)	0(4)
F2	76(5)	65(5)	49(4)	0(4)	-13(4)	8(4)
O1	90(7)	37(5)	41(4)	-6(4)	-1(4)	2(4)
N1	74(7)	49(6)	29(5)	1(4)	2(5)	-3(5)
N2	78(8)	57(7)	36(5)	-8(5)	-1(5)	-13(6)

Atom	U_{11}	U_{22}	U_{33}	U_{23}	U_{13}	U_{12}
N3	69(6)	34(5)	27(4)	-8(4)	1(4)	-3(5)
C1	96(11)	55(8)	43(7)	13(6)	5(7)	0(8)
C2	82(10)	76(10)	51(8)	12(7)	-4(7)	-24(9)
C3	73(9)	67(9)	43(7)	5(7)	3(6)	-23(7)
C4	80(9)	48(7)	27(5)	1(5)	0(5)	-4(7)
C5	66(8)	42(7)	40(6)	-1(5)	4(6)	1(6)
C6	64(8)	56(8)	39(6)	0(6)	1(6)	-9(7)
C7	95(11)	92(11)	38(7)	1(7)	-8(7)	-39(9)
C8	126(15)	97(14)	68(11)	-1(9)	-2(10)	-61(12)
C9	95(11)	100(13)	38(7)	4(7)	-11(7)	-37(10)
C10	52(7)	51(7)	31(5)	-7(5)	-2(5)	4(6)
C11	71(8)	52(7)	37(6)	-2(6)	-5(6)	-4(7)
C12	75(8)	35(6)	38(6)	1(5)	-1(6)	1(6)
C13	56(7)	38(6)	42(6)	-4(5)	2(5)	2(5)
C14	56(7)	38(6)	36(6)	-1(5)	2(5)	-3(5)
C15	78(9)	35(6)	34(6)	-2(5)	4(6)	-5(6)
C16	56(7)	39(6)	31(5)	3(5)	7(5)	1(5)
C17	54(7)	45(7)	30(5)	-8(5)	7(5)	-3(5)
C18	77(8)	41(6)	17(5)	0(4)	4(5)	6(6)
C19	58(7)	54(7)	44(7)	1(6)	11(6)	6(6)
C20	68(8)	68(9)	45(7)	2(6)	-3(6)	15(8)
C21	76(9)	66(9)	51(8)	4(7)	3(7)	-3(8)
C22	75(9)	56(8)	67(9)	-3(7)	-1(8)	12(7)
C23	63(8)	65(9)	66(9)	-11(7)	8(7)	7(7)
C24	46(7)	69(9)	57(8)	-13(7)	2(6)	-2(7)
C25	55(7)	41(7)	50(7)	-10(6)	-5(6)	-1(6)
C26	68(8)	56(8)	43(7)	-14(6)	4(6)	-5(7)
C27	73(9)	51(8)	49(7)	-8(6)	-5(6)	-2(7)
C28	58(8)	43(7)	76(10)	-11(7)	-1(7)	-5(6)
C29	62(9)	51(8)	84(11)	8(8)	-8(7)	-12(7)
C30	59(8)	44(7)	59(8)	2(6)	2(6)	-2(6)
B1	81(10)	39(7)	29(6)	5(6)	-4(6)	1(7)
Cl4	89(3)	159(5)	85(3)	-29(3)	6(2)	-20(3)
Cl5	125(4)	92(4)	145(5)	-1(3)	-45(4)	5(3)
C31	128(16)	89(12)	69(11)	8(10)	-11(11)	-26(12)
Cl6	133(4)	128(4)	96(3)	-1(3)	-22(3)	40(4)

Atom	U_{11}	U_{22}	U_{33}	U_{23}	U_{13}	U_{12}
Cl7	133(4)	128(4)	96(3)	-1(3)	-22(3)	40(4)
C32	133(4)	128(4)	96(3)	-1(3)	-22(3)	40(4)

*Table S 38: Bond Lengths in Å for **BODI-Au-10**.*

Atom	Atom	Length/Å
Au	Cl3	2.293(3)
Au	P1	2.238(3)
Cl1	C1	1.707(13)
Cl2	C9	1.689(14)
P1	C18	1.814(12)
P1	C19	1.840(13)
P1	C25	1.825(12)
F1	B1	1.375(16)
F2	B1	1.401(16)
O1	C16	1.247(14)
N1	C1	1.351(17)
N1	C4	1.395(15)
N1	B1	1.534(18)
N2	C6	1.391(15)
N2	C9	1.352(18)
N2	B1	1.567(17)
N3	C16	1.338(15)
N3	C17	1.442(13)
C1	C2	1.39(2)
C2	C3	1.382(18)
C3	C4	1.396(18)
C4	C5	1.408(17)
C5	C6	1.378(18)
C5	C10	1.486(16)
C6	C7	1.423(19)
C7	C8	1.35(2)
C8	C9	1.41(2)
C10	C11	1.400(17)
C10	C15	1.402(16)
C11	C12	1.355(16)
C12	C13	1.392(16)
C13	C14	1.404(16)
C13	C16	1.485(16)
C14	C15	1.379(16)
C17	C18	1.533(17)
C19	C20	1.374(17)
C19	C24	1.378(17)
C20	C21	1.380(19)
C21	C22	1.36(2)
C22	C23	1.37(2)
C23	C24	1.399(19)
C25	C26	1.362(17)
C25	C30	1.419(18)
C26	C27	1.371(19)
C27	C28	1.374(19)
C28	C29	1.36(2)
C29	C30	1.413(19)
Cl4	C31	1.7586
Cl5	C31	1.7596
Cl6	C32	1.7613
Cl7	C32	1.7596

*Table S 39: Bond Angles in ° for **BODI-Au-10**.*

Atom	Atom	Atom	Angle/°
P1	Au	Cl3	176.75(12)
C18	P1	Au	115.4(4)
C18	P1	C19	101.8(6)
C18	P1	C25	104.6(6)
C19	P1	Au	110.3(4)
C25	P1	Au	114.3(4)
C25	P1	C19	109.4(6)
C1	N1	C4	104.6(11)
C1	N1	B1	128.7(10)
C4	N1	B1	126.5(10)
C6	N2	B1	124.7(11)
C9	N2	C6	108.2(11)
C9	N2	B1	126.7(11)
C16	N3	C17	122.4(10)
N1	C1	Cl1	121.1(11)
N1	C1	C2	112.5(11)
C2	C1	Cl1	126.3(12)
C3	C2	C1	105.9(13)
C2	C3	C4	107.1(12)
N1	C4	C3	109.9(11)
N1	C4	C5	120.3(12)
C3	C4	C5	129.8(11)
C4	C5	C10	118.3(11)
C6	C5	C4	120.1(11)
C6	C5	C10	121.6(11)
N2	C6	C7	106.4(11)
C5	C6	N2	122.0(11)
C5	C6	C7	131.6(12)
C8	C7	C6	108.9(13)
C7	C8	C9	107.0(15)
N2	C9	Cl2	121.5(11)
N2	C9	C8	109.5(13)
C8	C9	Cl2	129.0(13)
C11	C10	C5	119.6(11)
C11	C10	C15	118.7(10)
C15	C10	C5	121.7(11)
C12	C11	C10	120.5(12)
C11	C12	C13	121.8(12)
C12	C13	C14	118.2(11)
C12	C13	C16	117.9(10)
C14	C13	C16	123.9(11)
C15	C14	C13	120.5(11)
C14	C15	C10	120.3(11)
O1	C16	N3	121.2(10)
O1	C16	C13	120.3(10)
N3	C16	C13	118.4(10)
N3	C17	C18	112.8(9)
C17	C18	P1	115.7(8)
C20	C19	P1	120.7(10)
C20	C19	C24	120.1(13)
C24	C19	P1	118.8(10)
C19	C20	C21	120.4(13)
C22	C21	C20	121.0(14)
C21	C22	C23	118.2(14)
C22	C23	C24	122.3(13)
C19	C24	C23	118.0(13)
C26	C25	P1	123.8(11)
C26	C25	C30	118.6(12)
C30	C25	P1	117.6(10)
C25	C26	C27	122.1(14)
C26	C27	C28	120.0(13)
C29	C28	C27	120.3(13)
C28	C29	C30	120.4(14)
C29	C30	C25	118.6(13)
F1	B1	F2	110.1(10)
F1	B1	N1	111.1(12)

Atom	Atom	Atom	Angle/°
F1	B1	N2	110.2(10)
F2	B1	N1	109.4(11)
F2	B1	N2	110.0(12)
N1	B1	N2	106.0(9)
Cl4	C31	Cl5	112.9
Cl7	C32	Cl6	112.9

*Table S 40: Hydrogen Fractional Atomic Coordinates (x10⁴) and Equivalent Isotropic Displacement Parameters (Å²x10³) for **BODI-Au-10**. U_{eq} is defined as 1/3 of the trace of the orthogonalised U_{ij}.*

Atom	x	y	z	U_{eq}
H3	7559.87	5170.87	2566.45	52
H2	7080.28	1860.47	5273.4	84
H3A	7377.13	2591.8	4514.26	73
H7	9148.84	5827.86	4089.69	90
H8	9766.36	6953.04	4607.97	117
H11	8182.12	1839.41	4064.56	64
H12	7977.89	1498.06	3337.11	59
H14	7959.85	5755.35	3135.16	52
H15	8184.53	6115.54	3869.13	59
H17A	7421.39	3065.51	1935.94	52
H17B	7657.55	4579.47	1801.03	52
H18A	6782.94	4566.12	1600.71	54
H18B	6853.24	5685.45	1992.19	54
H20	5899.51	4879.55	1417.74	73
H21	5222.71	6415	1240.34	77
H22	4704.23	7396.3	1789.02	79
H23	4856.57	6762.09	2516.81	77
H24	5523.65	5167.6	2707.85	69
H26	6442.74	2549.46	1346.77	67
H27	6378.79	292.78	1052.93	69
H28	6157.69	-1617.99	1500.87	71
H29	6052.72	-1299.86	2250.21	79
H30	6130.74	1000.73	2563.52	65
H31A	4315.72	2906.85	6063.33	115
H31B	4083.26	3756.85	6476.11	115
H32A	4386.11	5526.76	4788.58	143
H32B	4162.12	4213.57	4511.5	143

*Table S 41: Hydrogen Bond information for **BODI-Au-10**.*

D	H	A	d(D-H)/Å	d(H-A)/Å	d(D-A)/Å	D-H-A/deg
N3	H3	O1[1]	0.88	1.96	2.742(13)	146.6

———

[1]3/2-x,1/2+y,+z

*Table S 42: Atomic Occupancies for all atoms that are not fully occupied in **BODI-Au-10**.*

Atom	Occupancy
Cl6	0.75
Cl7	0.75
C32	0.75
H32A	0.75
H32B	0.75

SHAPE Analysis

The corresponding coordination polyhedra are generally described in terms of four idealized geometries with equal distances between the center and all vertices: the trigonal planar (TP-3), the pyramid (vacant tetrahedron) (vT3), the fac-trivacant octahedron (fac-vOC-3), and the mer-trivacant octahedron (T-shape) (mer-vOC-3). As a general approach, shape analysis of coordination polyhedra provides a quantitative mean for evaluating the departure of an experimental (*Q*) from an ideal archetypal stereochemistry (*P*). The Continuous Shape Measure (CShM) criterion $S_Q(P)$ [Equation (1)] introduced by Avnir and coworkers reflects the minimal normalized square deviation between the Cartesian coordinates of each vertex belonging to the actual coordination polyhedron *Q* and a perfect reference geometry *P*. Accordingly, $S_Q(P)$ ranges between 0 and 100, a closer structural match giving a lower $S_Q(P)$ value. Casanova and coworkers reported shape maps and reference polyhedral.

$$S_Q(P) = \frac{\sum_{k=1}^{N} \left| \vec{Q}_k - \vec{P}_k \right|^2}{\sum_{k=1}^{N} \left| \vec{Q}_k - \vec{Q}_0 \right|^2} \times 100 \qquad \text{with} \qquad \vec{Q}_0 = \frac{1}{N} \sum_{k=1}^{N} \vec{Q}_k \qquad (1)$$

The lowest values of $S_Q(P)$, as determined by continuous shape measure calculations using the SHAPE 2.1 program (M. Llunell, D. Casanova, J. Cirera, P. Alemany, S. Alvarez, *SHAPE, v. 2.1*, University of Barcelona, Spain, **2013**, **Erreur ! Source du renvoi introuvable.**9), correspond systematically to the four ideal geometries TP-3, vT3, fac-vOC-3 and mer-vOC-3. According to **Erreur ! Source du renvoi introuvable.**9, the metal centers are found in an T-shape (mer-vOC-3) environment.

*Table S 43: Continuous Shape Measure values $S_Q(P)$ calculated for the coordination polyhedra found in the crystal structures of complexes **BODI-Au-7** and **BODI-Au-10**. Limiting values corresponding to the ideal reference geometries are also included.[a]*

Polyhedron (*Q*)	S_Q(TP-3)	S_Q(vT3)	S_Q(fac-vOC-3)	S_Q(mer-vOC-3)	Geometry
BODI-Au-7	5.567	7.322	13.548	**3.373**	mer-vOC-3
BODI-Au-10	5.930	8.500	15.391	**3.764**	mer-vOC-3

[a] Bold-faced numbers correspond to the lowest $S_Q(P)$ values calculated according to Equation (1) by the Shape 2.1 program. The considered ideal reference geometries (*P*) are the trigonal planar (TP-3), the pyramid (vacant tetrahedron) (vT3), the fac-trivacant octahedron (fac-vOC-3), and the mer-trivacant octahedron (T-shape) (mer-vOC-3).

References

1 Dupré Nathalie, Brazel Christian, Fensterbank Louis, Malacria Max, Thorimbert Serge, Hasenknopf Bernold and Lacôte Emmanuel, *Chem. – Eur. J.*, 2012, **18**, 12962–12965.

2 T. Rohand, M. Baruah, W. Qin, N. Boens and W. Dehaen, *Chem. Commun.*, 2006, 266–268.

3 M. Laine, N. A. Barbosa, A. Kochel, B. Osiecka, G. Szewczyk, T. Sarna, P. Ziółkowski, R. Wieczorek and A. Filarowski, *Sens. Actuators B Chem.*, 2017, **238**, 548–555.

4 M. Fischer and J. Georges, *Chem. Phys. Lett.*, 1996, **260**, 115–118.

5 M. J. Frisch, Gaussian 09. Revision D. 01., Gaussian. Inc., Wallingford CT, 2009.

6 Y. Zhao and D. G. Truhlar, *Theor. Chem. Acc.*, 2008, **120**, 215–241.

7 N. Chéron, D. Jacquemin and P. Fleurat-Lessard, *Phys. Chem. Chem. Phys.*, 2012, **14**, 7170–7175.

8 N. Chéron, R. Ramozzi, L. E. Kaïm, L. Grimaud and P. Fleurat-Lessard, *J. Org. Chem.*, 2012, **77**, 1361–1366.

9 J. Tomasi, B. Mennucci and R. Cammi, *Chem. Rev.*, 2005, **105**, 2999–3094.

10 B. Mennucci, J. Tomasi, R. Cammi, J. R. Cheeseman, M. J. Frisch, F. J. Devlin, S. Gabriel and P. J. Stephens, *J. Phys. Chem. A*, 2002, **106**, 6102–6113.

11 G. Andrienko, http://www.chemcraftprog.com.

12 K. Fukui, T. Yonezawa and H. Shingu, *J. Chem. Phys.*, 1952, **20**, 722–725.

13 L.-G. Zhuo, W. Liao and Z.-X. Yu, *Asian J. Org. Chem.*, 2012, **1**, 336–345.

References XRD

O.V. Dolomanov and L.J. Bourhis and R.J. Gildea and J.A.K. Howard and H. Puschmann, Olex2: A complete structure solution, refinement and analysis program, *J. Appl. Cryst.*, 2009, **42**, 339-341.

Sheldrick, G.M., Crystal structure refinement with ShelXL, *Acta Cryst.*, 2015, **C27**, 3-8.

Sheldrick, G.M., ShelXT-Integrated space-group and crystal-structure determination, *Acta Cryst.*, 2015, **A71**, 3-8.

Software for the Integration of CCD Detector System Bruker Analytical X-ray Systems, Bruker axs, Madison, WI (after 2013).